Effects of Fiber Type, Contraction, Exercise, and Diet on

Skeletal Muscle Signaling Proteins and Glucose Transport

by

Carlos Michel Castorena

A dissertation submitted in partial fulfillment
of the requirements for the degree of
Doctoral of Philosophy
(Kinesiology)
in The University of Michigan
2013

Doctoral Committee:

Professor Gregory D. Cartee, Chair
Professor Charles F. Burant
Professor Jeffrey F. Horowitz
Assistant Professor Peter F. Bodary

I dedicate this thesis to my grandparents. You are all extraordinary people and I want you all to know that I would not have been able to do this without each of you. I frequently think of the sacrifices that you have all made in order to provide your families with opportunities that were not afforded to you. As a result, I strive to be the best possible person that I can be to ensure that those sacrifices were worthwhile. I love you all very much and thank you for all that you have done for me.

Acknowledgements

The work presented in the upcoming chapters only represents a portion of the events that have brought me to this point. Therefore, I would like to take some time to acknowledge some influential individuals that if it were not for them I would not be in the position that I am today. Putting my feelings into written words is definitely not one of my strengths, so I am going to keep it short and sweet.

Dr. Cartee thank you. I honestly do not believe that I could not have received better mentorship than I have from you than I could have from anybody else. The time and dedication that you put into your graduate students is second to none and I am very grateful you were my doctoral advisor. Thank you for taking a chance on me and thank you for providing an amazing environment for me to grow as a scientist and a person. I wish you the best in all of your future endeavors.

Katherine, you are an amazing woman, mother and wife and although you do not like to when I tell you, because you do not like the "pressure," but I have and will continue to strive to be as successful as I can for you. You have made numerous sacrifices to help us get to where we are and I appreciate every one of them. Because you are such an amazing mother and wife, you have allowed me to be able to focus on my work and not worry about anything else. We have come a long way together and I am excited to see what our future holds. I know that you always think that I am joking, but you truly are my primary motivation and I love you.

Kevin and Casen, I could not have asked for better kids than you two. It is funny because when ever other people around school first find out that I am your Dad, the first question they ask is how do I manage having two kids with graduate school? Luckily your Mom is awesome,

and makes it easy for me. The reality is, I do not think that I would be able to stay motivated if it was not for you two and your mom. Whenever I am feeling tired, burnt out, and just having doubts about what I am doing, I just have to think about you two and it all goes away. Thank you.

Mom, thank you for instilling the values of being a good husband and father. You have always been there when I needed you, and you continue to be there for the boys. I love you and appreciated everything you have done for me.

Dad, thanks for teaching that if I am going to do something, I do it right and I go all out, or as I have put a more modern twist on it "go big or go home." You have shown me that if I am going to put the time into something then I might as well do it right, as you used said growing up "it takes just as much to do something half assed and make it seem like you did it right, than to just do it right in the first place.

To my in-laws, I really feel that I am lucky to have all four of you. You all have been extremely supportive of me ever since we met and I thank you for that. Claire, hopefully I will one day fulfill your dream and publish something that gets picked up the mainstream media and get a page in Discover Magazine. Tim, hopefully soon I will be able to get my "Man Card" and successfully hunt some form of game with you, and I know "rodents don't count." Greg, it is always good to hear from you and know that I have someone that can share in the misery of being a fan of teams that do not feel the need to win championships, or to just consistently win in general. Diana, thanks for always being positive and giving us thoughtful advice. All four of you are amazing grandparents to the boys. And the generosity from all of you is amazing and I am extremely grateful for all of you. I know that there is no official scorecard/competition, but I am definitely leading in the in-laws department.

Tia Norma, thank for being one of the few positive role models growing up. As I have grown you have always been there for me. I cannot tell you how comforting it is to have someone in the family that I can go to and that understands what I have gone through and where my career is taking me. You are an awesome person and you continue to amaze me. I still have a long way to go, but one of my goals always has been, and continues to be, that I want to be a similar positive influence for the younger generations that you have been for me.

To all of my nieces, nephews, and cousins, you all have been one of my major motivations, and I think about you all often. You are all capable individuals and I would like to tell you all to not be intimidated by the work necessary to attain your goals. Also, I know San Diego is a great city and our family is very tight night, but to not be afraid get out, travel and try new things. San Diego is not going anywhere and will always be our home. Although I have been in school for a long time (feels like forever), I feel that I have learned just as much from the new people that I have met and cities I have visited than I have from the classes that I have attended. Even though it is great to get to see you all when I visit, it would make me even happier if you were not there and out experiencing the world.

Jesse and Vanessa, you guys have been great siblings. Jesse you have always been very positive and have always put my best interests before yours. You looked out for me when I was young and taught me more than you realize. Vanessa thanks for looking out for me as well. And even though you are my younger sister you took on the older sister role to help keep me in line. I love both of you.

Leo and Josh, you guys seriously are like brothers to me. I know I can always count on you two and it is awesome. Whenever I need to unwind you both are there. When I need to talk to someone, you guys are there. From coming from where we did, it made it easy knowing that you two were always had and continue to have my back.

Dr. Edward Belisario Arias, you have been great. You have a way of lightening the mood and keeping things in perspective. I was not joking when I said you are like an uncle to me. You have been a great resource and mentor. I also appreciate how you and Susana accepted my family with open arms. You two have been extremely helpful and generous with us. You two are great parents to your kids and I always looked forward to spending time with your family. Also, I apologize, I know that you wanted a paragraph all to yourself, but it did not feel right to not mention Susana. Thank you both for everything.

Sharma, Donel and Sean, I am going to end with you guys, well because this was supposed to be short and sweet and it feels like it may be getting out of control. You guys are great friends and colleagues. Although grad school was tough, I could not imagine how difficult it would have been without you guys. Sharma, you seriously are the most knowledgeable person

of irrelevant subjects that I have ever met. Donel, your heated couch is amazing and I would like to believe that I have absorbed some of your island ways, although Katherine would disagree. Sean, thanks for dropping all of the ex phys knowledge on me and being the most dependable golf partner. We have had some great times together and I look forward to many more. All three of you are awesome and I wish all of you the best in the future.

Table of Contents

List of Tables

Apendix II: Tables

List of Figures

Appendix I: Figures

Appendix II: Figures

List of Appendices

Abstract

This thesis focused on the regulation of glucose uptake in rat skeletal muscle. Skeletal muscle plays a central role in the regulation of whole body glucose homeostasis. Because skeletal muscle is a heterogeneous tissue, muscles are often categorized by fiber type (myosin heavy chain, MHC, expression). MHC expression was determined at both the muscle tissue and single fiber levels, along with measurement of the abundance of multiple proteins relevant to glucose uptake, including the GLUT4 glucose transporter and Akt substrate of 160kDa (AS160). Key measurements included contraction-stimulated glucose uptake by single fibers from epitrochlearis muscles, and insulin-stimulated glucose uptake by whole epitrochlearis muscles from both normal rats fed low fat diet (LFD) and insulin-resistant rats (fed high fat diet, HFD, for 2 weeks). Novel results included: 1) MHC-related differences in GLUT4, but not AS160, protein abundance were found in whole muscles and single fibers; 2) despite a four-fold range of GLUT4 abundance among fiber types, contraction-stimulated glucose uptake did not differ by MHC-expression; 3) immediately post-exercise, insulin-independent glucose uptake and phosphorylation of AMP-associated protein kinase and AS160 were not different for LFD versus HFD groups; 4) improved insulin-stimulated glucose uptake 3 hours post-exercise in both LFD and HFD groups was associated with greater pAS160 (phosphorylated AS160) with unaltered GLUT4 abundance and MHC-expression; and 5) values for both insulin-stimulated glucose uptake and pAS160 post-exercise were greater for LFD versus HFD rats. Earlier studies suggested that muscle insulin resistance with HFD results from increased insulin receptor substrate-1 serine phosphorylation (pIRS-1^{Ser}), thereby inhibiting proximal insulin signaling (including tyrosine phosphorylation of the insulin receptor, IRS-1-associated phosphatidyl-3-kinase, and Akt activity), but exercise did not increase these proximal signaling steps in either diet-group. Greater pIRS-1^{Ser} is believed to result from elevated diacylglycerol and ceramides leading to activation of serine kinases, including JNK, but exercise did not attenuate pIRS-1^{Ser},

diacylglycerol, ceramides or pJNK. Results of this thesis indicate that exercise did not appear to act on several processes that are commonly linked to insulin resistance, suggesting that future experiments seeking to identify mechanisms for improved insulin-simulated glucose uptake post-exercise should focus on distal signaling steps regulating pAS160.

Chapter I

Introduction

Insulin resistance, a subnormal response to a physiological dose of insulin, is an essential precursor for developing type 2 dependent diabetes mellitus (T2DM) and a risk factor for other prevalent diseases, including cardiovascular disease and some forms of cancer (20). Skeletal muscle accounts for approximately 85 percent of insulin-stimulated glucose disposal, thus making skeletal muscle a prime target for combating insulin resistance (16-18). Because glucose transport into the cell is a rate-limiting step for glucose disposal in skeletal muscle (27), understanding the regulation of glucose transport has great significance.

Glucose transport in skeletal muscle can be modified by various physiologic interventions, including exercise and diet. During and immediately after exercise, skeletal muscle glucose transport is increased independent of insulin (24, 28). Additionally, a single bout of exercise can result in a subsequent increase in skeletal muscle insulin sensitivity (3, 12, 14, 22). The increased insulin sensitivity can be observed 3 to 4 hours following the exercise bout, once insulin-independent glucose transport has returned to baseline levels, and can last up to 48 hours (14, 22, 35). Although a high fat diet (HFD) can lead to insulin resistance in the skeletal muscle of rats, several studies have demonstrated that rats consuming a HFD can also respond to acute exercise with improved glucose uptake by insulin-stimulated glucose transport (36-37, 41, 44). The specific underlying mechanisms that account for improved insulin sensitivity after exercise by either normal or insulin resistant individuals remain to be clearly identified.

Skeletal muscle is a heterogeneous tissue, and different muscles in the same individual can vary greatly with regard to metabolic characteristics. Evidence suggests that the variability in insulin-stimulated glucose uptake observed among skeletal muscles may be in part attributable to differences in muscle fiber type composition and the level of expression of the insulin responsive glucose transporter known as GLUT4 (26, 34). Furthermore, it has been suggested that muscles with differing fiber type compositions may differ with regard to the extent of increased insulin-independent glucose uptake that occurs during and immediately after a muscular contraction (9, 19, 26, 32-33, 38-39).

The research in this dissertation focuses on: 1) elucidating the relationship between muscle fiber type and the abundance of several key proteins that are implicated in the regulation of glucose transport; 2) identifying the relationship between muscle fiber type and contraction-stimulated glucose transport; and 3) probing the potential mechanisms that underlie the benefits of acute exercise on insulin-stimulated glucose transport in muscle from both normal and insulin resistant rats.

Study 1: *Clustering of GLUT4, TUG, and RUVBL2 Protein Levels Correlate with Myosin Heavy Chain Isoform Pattern in Skeletal Muscles, but AS160 and TBC1D1 Levels Do Not*

The relative expression of GLUT4 has been reported to differ in skeletal muscles of varying fiber type (26, 34), but the earlier studies that assessed the relationship between fiber type and GLUT4 abundance in more than three skeletal muscles failed to determine fiber type using the method that is widely acknowledged as the gold standard (myosin heavy chain, MHC, expression). Furthermore, although GLUT4 is the ultimate mediator of muscle glucose transport capacity, a number of other proteins participate in insulin's regulation of GLUT4 function. Among the proteins that are recognized or proposed to regulate GLUT4-mediated glucose transport are: the Tethering protein containing an UBX-domain for GLUT4 (TUG) which is a putative GLUT4 tethering protein that functions as part of the system that retains GLUT4 intracellularly in the absence of insulin (5-6, 52-53); two paralog Rab GTPase proteins (Akt substrate of 160 kDa, AS160 also known as TBC1D4, and TBC1D1) that are recognized as key signaling proteins that control GLUT4 trafficking and glucose transport (11, 13, 15, 42); and RuvB-like protein two (RUVBL2) that was found to physically associate with AS160, and

genetic depletion of RUVBL2 in cells resulted in reduced phosphorylated AS160 and insulin-stimulated glucose uptake (51). Data are currently lacking with regard to the relative protein abundance of AS160, TBC1D1, RUVBL2 and TUG in rat skeletal muscles of varying fiber type composition. Therefore, the first major goal of Study 1 was to extend knowledge about the relationship between MHC isoform composition and the abundance of GLUT4 and four proteins (GLUT4, AS160, TBC1D1, RUVBL2 and TUG) that are either established or putative regulators of glucose transport in rat skeletal muscle. In addition, because all of these proteins are proposed to participate in a common function (regulation of glucose transport), characterizing how their expression patterns converge or diverge with each other would provide useful information. The second major goal of Study 1 was to determine if the abundance of any of these proteins are significantly associated with each other.

Study 2: *Myosin Heavy Chain Isoform Expression, Contraction-stimulated Glucose Uptake and Abundance of Proteins that Regulate Glucose Uptake and Metabolism in Single Skeletal Muscle Fibers*

Glucose transport into skeletal muscle is increased independent of insulin during and immediately following exercise or electrical stimulation. Evidence suggests that the responsiveness of contraction-stimulated glucose uptake may be related to skeletal muscle fiber type. Although extensive research has been performed in an effort to elucidate this relationship, the results are inconsistent. The most conclusive data comes from ex vivo experiments in which isolated intact muscles of varying fiber type were electrically stimulated to contract (1-2, 26, 30-31). The major limitation of these studies is muscle differences (epitrochlearis versus soleus versus flexor digitorum brevis) versus fiber type differences (myosin heavy chain, MHC, expression) with respect to insulin-independent glucose uptake cannot be separated. Therefore, Study 2 used our novel method for measuring glucose uptake by isolated single muscle fibers of known MHC fiber type to address these limitations. The first major goal of Study 2 was to make direct fiber type comparisons for contraction-stimulated glucose uptake within the same intact rat epitrochlearis muscles (fiber type representative of the entire rat hindlimb), which were incubated *ex vivo* and electrically stimulated to contract prior to single fiber isolation and glucose uptake measurements. The second major goal of Study 2 was to further investigate the fiber type

and protein co-expression patterns for GLUT4, TUG, AS160, TBC1D1 and RUVBL2 at the single fiber level. The third major goal of Study 2 was to determine if the abundance of any of these proteins are significantly correlated with each other or with other metabolically relevant proteins (Cytochrome C oxidase IV, COX IV; glycogen phosphorylase; glyceraldehyde-3-phosphate dehydrogenase, GAPDH; and filamin C).

Study 3: *Acute Exercise Effects on Insulin Signaling and Insulin-Stimulated Glucose Uptake in Isolated Skeletal Muscle from Rats Fed either Low Fat or High Fat Diet*

A single exercise bout is an effective stimulus for increasing insulin-stimulated glucose transport in skeletal muscle of humans (35, 46, 48, 50) or rodents (12, 14, 22, 35, 40) with normal insulin sensitivity prior to exercise. A single bout of exercise can also improve insulin-stimulated glucose uptake in skeletal muscle of insulin resistant humans (10, 43) or rats (4, 23, 36, 41, 44). Available data suggest that improvements in insulin-stimulated glucose transport following a single session of exercise in both insulin sensitive and insulin resistant individuals may occur via distinct mechanisms. In insulin sensitive rats or humans, the improved insulin-stimulated glucose uptake following an acute exercise bout is apparently not due to improved proximal signaling (7-8, 25, 29, 45, 47, 49-50, 54), but may be associated with the sustained increase in phosphorylation of AS160 (pAS160) (3, 11, 21-22, 48). In insulin resistant rats fed a HFD (an intervention that leads to increases in both caloric and dietary fat intake), limited data suggest that the improved insulin sensitivity following acute exercise may occur by reducing serine phosphorylation of insulin receptor substrate-1 (pIRS-1^{Ser}) (36, 41) and restoring proximal signaling steps (36-37, 41), thereby reversing the inhibition induced by high fat feeding. However, in these studies on skeletal muscle from HFD fed rats, the effects of exercise on pAS160 were not determined, and most of the proximal insulin signaling measurements were made using a supraphysiologic insulin dose. Therefore, Study 3 used LFD fed and HFD fed rats that either remained sedentary or performed acute exercise to investigate potential mechanisms that may be important for the post-exercise increase in insulin-stimulated glucose transport by skeletal muscle using a physiologic insulin dose. The first major goal for Study 3 was to investigate the mechanism (measurements of proximal insulin signaling and AS160) for the exercise induced improvements for insulin-stimulated glucose uptake by skeletal muscle from

insulin sensitive and insulin resistant rats. The second major goal of Study 3 was to identify possible changes in GLUT4, AS160, TBC1D1, TUG, RUVBL2 and muscle fiber type following 2 weeks of high fat feeding. The third major goal of Study 3 was to determine the effects of acute exercise on putative mediators of insulin resistance: lipid metabolites (acyl-CoA; diacylglycerol, DAG; ceramide), phosphorylation of the serine kinase c-Jun N-terminal (pJNK) and pIRS-1^{Ser}.

References

1. **Ai H, Ihlemann J, Hellsten Y, Lauritzen HP, Hardie DG, Galbo H, and Ploug T.** Effect of fiber type and nutritional state on AICAR- and contraction-stimulated glucose transport in rat muscle. *Am J Physiol Endocrinol Metab* 282: E1291-1300, 2002.
2. **Ai H, Ralston E, Lauritzen HP, Galbo H, and Ploug T.** Disruption of microtubules in rat skeletal muscle does not inhibit insulin- or contraction-stimulated glucose transport. *Am J Physiol Endocrinol Metab* 285: E836-844, 2003.
3. **Arias EB, Kim J, Funai K, and Cartee GD.** Prior exercise increases phosphorylation of Akt substrate of 160 kDa (AS160) in rat skeletal muscle. *Am J Physiol Endocrinol Metab* 292: E1191-1200, 2007.
4. **Betts JJ, Sherman WM, Reed MJ, and Gao JP.** Duration of improved muscle glucose uptake after acute exercise in obese Zucker rats. *Obes Res* 1: 295-302, 1993.
5. **Bogan JS, Hendon N, McKee AE, Tsao TS, and Lodish HF.** Functional cloning of TUG as a regulator of GLUT4 glucose transporter trafficking. *Nature* 425: 727-733, 2003.
6. **Bogan JS, Rubin BR, Yu C, Loffler MG, Orme CM, Belman JP, McNally LJ, Hao M, and Cresswell JA.** Endoproteolytic cleavage of TUG protein regulates GLUT4 glucose transporter translocation. *J Biol Chem* 287: 23932-23947, 2012.
7. **Bonen A, Tan MH, Clune P, and Kirby RL.** Effects of exercise on insulin binding to human muscle. *Am J Physiol* 248: E403-408, 1985.
8. **Bonen A, Tan MH, and Watson-Wright WM.** Effects of exercise on insulin binding and glucose metabolism in muscle. *Can J Physiol Pharmacol* 62: 1500-1504, 1984.
9. **Brozinick JT, Jr., Etgen GJ, Jr., Yaspelkis BB, 3rd, and Ivy JL.** Contraction-activated glucose uptake is normal in insulin-resistant muscle of the obese Zucker rat. *J Appl Physiol* 73: 382-387, 1992.
10. **Burstein R, Epstein Y, Shapiro Y, Charuzi I, and Karnieli E.** Effect of an acute bout of exercise on glucose disposal in human obesity. *J Appl Physiol* 69: 299-304, 1990.
11. **Cartee GD and Funai K.** Exercise and Insulin: Convergence or Divergence at AS160 and TBC1D1? *Exercise and Sport Sciences Reviews* 37: 188-195, 2009.
12. **Cartee GD and Holloszy JO.** Exercise increases susceptibility of muscle glucose transport to activation by various stimuli. *Am J Physiol* 258: E390-393, 1990.
13. **Cartee GD and Wojtaszewski JF.** Role of Akt substrate of 160 kDa in insulin-stimulated and contraction-stimulated glucose transport. *Appl Physiol Nutr Metab* 32: 557-566, 2007.

14. **Cartee GD, Young DA, Sleeper MD, Zierath J, Wallberg-Henriksson H, and Holloszy JO.** Prolonged increase in insulin-stimulated glucose transport in muscle after exercise. *Am J Physiol* 256: E494-499, 1989.
15. **Chavez JA, Roach WG, Keller SR, Lane WS, and Lienhard GE.** Inhibition of GLUT4 Translocation by Tbc1d1, a Rab GTPase-activating Protein Abundant in Skeletal Muscle, Is Partially Relieved by AMP-activated Protein Kinase Activation. *J Biol Chem* 283: 9187-9195, 2008.
16. **DeFronzo RA.** Lilly lecture 1987. The triumvirate: beta-cell, muscle, liver. A collusion responsible for NIDDM. *Diabetes* 37: 667-687, 1988.
17. **DeFronzo RA, Gunnarsson R, Bjorkman O, Olsson M, and Wahren J.** Effects of insulin on peripheral and splanchnic glucose metabolism in noninsulin-dependent (type II) diabetes mellitus. *J Clin Invest* 76: 149-155, 1985.
18. **DeFronzo RA and Tripathy D.** Skeletal muscle insulin resistance is the primary defect in type 2 diabetes. *Diabetes Care* 32 Suppl 2: S157-163, 2009.
19. **Derave W, Lund S, Holman GD, Wojtaszewski J, Pedersen O, and Richter EA.** Contraction-stimulated muscle glucose transport and GLUT-4 surface content are dependent on glycogen content. *Am J Physiol* 277: E1103-1110, 1999.
20. **Facchini FS, Hua N, Abbasi F, and Reaven GM.** Insulin resistance as a predictor of age-related diseases. *J Clin Endocrinol Metab* 86: 3574-3578, 2001.
21. **Funai K, Schweitzer GG, Castorena CM, Kanzaki M, and Cartee GD.** In vivo exercise followed by in vitro contraction additively elevates subsequent insulin-stimulated glucose transport by rat skeletal muscle. *Am J Physiol Endocrinol Metab* 298: E999-1010, 2010.
22. **Funai K, Schweitzer GG, Sharma N, Kanzaki M, and Cartee GD.** Increased AS160 phosphorylation, but not TBC1D1 phosphorylation, with increased postexercise insulin sensitivity in rat skeletal muscle. *Am J Physiol Endocrinol Metab* 297: E242-251, 2009.
23. **Gao J, Sherman WM, McCune SA, and Osei K.** Effects of acute running exercise on whole body insulin action in obese male SHHF/Mcc-facp rats. *J Appl Physiol* 77: 534-541, 1994.
24. **Garetto LP, Richter EA, Goodman MN, and Ruderman NB.** Enhanced muscle glucose metabolism after exercise in the rat: the two phases. *Am J Physiol Endocrinol Metab* 246: E471-475, 1984.
25. **Hansen PA, Nolte LA, Chen MM, and Holloszy JO.** Increased GLUT-4 translocation mediates enhanced insulin sensitivity of muscle glucose transport after exercise. *J Appl Physiol* 85: 1218-1222, 1998.
26. **Henriksen EJ, Bourey RE, Rodnick KJ, Koranyi L, Permutt MA, and Holloszy JO.** Glucose transporter protein content and glucose transport capacity in rat skeletal muscles. *Am J Physiol* 259: E593-598, 1990.
27. **Herman MA and Kahn BB.** Glucose transport and sensing in the maintenance of glucose homeostasis and metabolic harmony. *J Clin Invest* 116: 1767-1775, 2006.
28. **Holloszy JO.** Muscle metabolism during exercise. *Arch Phys Med Rehabil* 63: 231-234, 1982.
29. **Howlett KF, Sakamoto K, Hirshman MF, Aschenbach WG, Dow M, White MF, and Goodyear LJ.** Insulin signaling after exercise in insulin receptor substrate-2-deficient mice. *Diabetes* 51: 479-483, 2002.
30. **Ihlemann J, Ploug T, and Galbo H.** Effect of force development on contraction induced glucose transport in fast twitch rat muscle. *Acta Physiol Scand* 171: 439-444, 2001.

31. **Ihlemann J, Ploug T, Hellsten Y, and Galbo H.** Effect of stimulation frequency on contraction-induced glucose transport in rat skeletal muscle. *Am J Physiol Endocrinol Metab* 279: E862-867, 2000.
32. **James DE, Kraegen EW, and Chisholm DJ.** Muscle glucose metabolism in exercising rats: comparison with insulin stimulation. *Am J Physiol* 248: E575-580, 1985.
33. **Johannsson E, Jensen J, Gundersen K, Dahl HA, and Bonen A.** Effect of electrical stimulation patterns on glucose transport in rat muscles. *Am J Physiol* 271: R426-431, 1996.
34. **Megeney LA, Neufer PD, Dohm GL, Tan MH, Blewett CA, Elder GC, and Bonen A.** Effects of muscle activity and fiber composition on glucose transport and GLUT-4. *Am J Physiol* 264: E583-593, 1993.
35. **Mikines KJ, Sonne B, Farrell PA, Tronier B, and Galbo H.** Effect of physical exercise on sensitivity and responsiveness to insulin in humans. *Am J Physiol* 254: E248-259, 1988.
36. **Oliveira AG, Carvalho BM, Tobar N, Ropelle ER, Pauli JR, Bagarolli RA, Guadagnini D, Carvalheira JB, and Saad MJ.** Physical exercise reduces circulating lipopolysaccharide and TLR4 activation and improves insulin signaling in tissues of DIO rats. *Diabetes* 60: 784-796, 2011.
37. **Pauli JR, Ropelle ER, Cintra DE, Carvalho-Filho MA, Moraes JC, De Souza CT, Velloso LA, Carvalheira JB, and Saad MJ.** Acute physical exercise reverses S-nitrosation of the insulin receptor, insulin receptor substrate 1 and protein kinase B/Akt in diet-induced obese Wistar rats. *J Physiol* 586: 659-671, 2008.
38. **Rattigan S, Dora KA, Tong AC, and Clark MG.** Perfused skeletal muscle contraction and metabolism improved by angiotensin II-mediated vasoconstriction. *Am J Physiol* 271: E96-103, 1996.
39. **Richter EA, Garetto LP, Goodman MN, and Ruderman NB.** Enhanced muscle glucose metabolism after exercise: modulation by local factors. *Am J Physiol* 246: E476-482, 1984.
40. **Richter EA, Garetto LP, Goodman MN, and Ruderman NB.** Muscle glucose metabolism following exercise in the rat: increased sensitivity to insulin. *J Clin Invest* 69: 785-793, 1982.
41. **Ropelle ER, Pauli JR, Prada PO, de Souza CT, Picardi PK, Faria MC, Cintra DE, Fernandes MF, Flores MB, Velloso LA, Saad MJ, and Carvalheira JB.** Reversal of diet-induced insulin resistance with a single bout of exercise in the rat: the role of PTP1B and IRS-1 serine phosphorylation. *J Physiol* 577: 997-1007, 2006.
42. **Sano H, Kane S, Sano E, Miinea CP, Asara JM, Lane WS, Garner CW, and Lienhard GE.** Insulin-stimulated phosphorylation of a Rab GTPase-activating protein regulates GLUT4 translocation. *J Biol Chem* 278: 14599-14602, 2003.
43. **Sharoff CG, Hagobian TA, Malin SK, Chipkin SR, Yu H, Hirshman MF, Goodyear LJ, and Braun B.** Combining short-term metformin treatment and one bout of exercise does not increase insulin action in insulin-resistant individuals. *Am J Physiol Endocrinol Metab* 298: E815-823, 2010.
44. **Tanaka S, Hayashi T, Toyoda T, Hamada T, Shimizu Y, Hirata M, Ebihara K, Masuzaki H, Hosoda K, Fushiki T, and Nakao K.** High-fat diet impairs the effects of a single bout of endurance exercise on glucose transport and insulin sensitivity in rat skeletal muscle. *Metabolism* 56: 1719-1728, 2007.

45. **Thong FS and Graham TE.** The putative roles of adenosine in insulin- and exercise-mediated regulation of glucose transport and glycogen metabolism in skeletal muscle. *Can J Appl Physiol* 27: 152-178, 2002.
46. **Thorell A, Hirshman MF, Nygren J, Jorfeldt L, Wojtaszewski JF, Dufresne SD, Horton ES, Ljungqvist O, and Goodyear LJ.** Exercise and insulin cause GLUT-4 translocation in human skeletal muscle. *Am J Physiol* 277: E733-741, 1999.
47. **Treadway JL, James DE, Burcel E, and Ruderman NB.** Effect of exercise on insulin receptor binding and kinase activity in skeletal muscle. *Am J Physiol* 256: E138-144, 1989.
48. **Treebak JT, Frosig C, Pehmoller C, Chen S, Maarbjerg SJ, Brandt N, MacKintosh C, Zierath JR, Hardie DG, Kiens B, Richter EA, Pilegaard H, and Wojtaszewski JF.** Potential role of TBC1D4 in enhanced post-exercise insulin action in human skeletal muscle. *Diabetologia* 52: 891-900, 2009.
49. **Wojtaszewski JF, Hansen BF, Gade, Kiens B, Markuns JF, Goodyear LJ, and Richter EA.** Insulin signaling and insulin sensitivity after exercise in human skeletal muscle. *Diabetes* 49: 325-331, 2000.
50. **Wojtaszewski JF, Nielsen JN, and Richter EA.** Invited review: effect of acute exercise on insulin signaling and action in humans. *J Appl Physiol* 93: 384-392, 2002.
51. **Xie X, Chen Y, Xue P, Fan Y, Deng Y, Peng G, Yang F, and Xu T.** RUVBL2, a novel AS160-binding protein, regulates insulin-stimulated GLUT4 translocation. *Cell Res,* 2009.
52. **Xu Y, Rubin BR, Orme CM, Karpikov A, Yu C, Bogan JS, and Toomre DK.** Dual-mode of insulin action controls GLUT4 vesicle exocytosis. *J Cell Biol*, 2011.
53. **Yu CF, Cresswell J, Loffler MG, and Bogan JS.** The glucose transporter 4-regulating protein TUG is essential for highly insulin-responsive glucose uptake in 3T3-L1 adipocytes. *Journal of Biological Chemistry* 282: 7710-7722, 2007.
54. **Zorzano A, Balon TW, Garetto LP, Goodman MN, and Ruderman NB.** Muscle alpha-aminoisobutyric acid transport after exercise: enhanced stimulation by insulin. *Am J Physiol* 248: E546-552, 1985.

Chapter II

Review of Literature

Importance of Skeletal Muscle Glucose Transport

It has been estimated that greater than 30 percent of the United States population will develop diabetes in their lifetime (119), with Type 2 diabetes mellitus (T2DM, also known as Non-Insulin Dependent Diabetes Mellitus) accounting for 90-95 percent of all individuals with diabetes (1). Insulin resistance, a subnormal response to a physiological dose of insulin, is an essential precursor for developing T2DM, as well as a predictor of numerous other diseases (e.g., atherosclerosis, stroke, hypertension and some types of cancer) (46). Skeletal muscle accounts for approximately 85 percent of insulin-stimulated glucose disposal, thus making skeletal muscle a prime target for combating insulin resistance (38-40). Skeletal muscle is a heterogeneous tissue that is composed of different fiber types, and previous studies have reported differences in metabolic properties for muscles with differing fiber type composition.

Glucose transport into the cell is a rate-limiting step for glucose disposal by skeletal muscle (65). Glucose is a hydrophilic molecule and cannot freely pass through the plasma membrane (the hydrophobic lipid bilayer) to enter the cell. Therefore, glucose transporter proteins (GLUTs) fuse with the plasma membrane in order to allow for glucose to enter the cell. In skeletal muscle, GLUT4 is the major glucose transporter that is regulated by both insulin and contraction. In response to either stimulus, GLUT4 translocates from intracellular vesicles to cell surface membranes (sarcolemma and t-tubules) to allow for greater diffusion of glucose into

the cell (15, 52, 81, 98, 136-137, 189). However, insulin- and contraction-mediated GLUT4 translocation appear to occur via distinct mechanisms (30, 32, 35, 53, 120). In addition to increased insulin-independent glucose uptake being elevated during and immediately after exercise, a single bout of exercise can result in subsequently increased skeletal muscle insulin sensitivity (8, 31, 33, 52, 55, 68). The increased insulin sensitivity can be observed 3 to 4 hours following the exercise bout, once insulin independent glucose transport has returned to baseline levels, and can last up to 48 hours (33, 52, 112). For insulin resistant individuals, improving insulin sensitivity with exercise can be very beneficial for regulating circulating glucose levels (93, 169). Therefore, it is important to understand the mechanisms for the exercise induced improvements in insulin sensitivity to aid in the development of new therapies for insulin resistance and diabetes.

The exercise effects on skeletal muscle glucose transport and improved insulin sensitivity are also beneficial for healthy individuals. Following strenuous exercise when muscle energy stores are low (depleted muscle glycogen), increased insulin-independent glucose transport facilitates greater glucose clearance from the blood to replete muscle glycogen. In addition, the increased insulin sensitivity following exercise will increase postprandial glycogen storage. Quickly replenishing energy stores is important for athletes to maintain performance, or for individuals with labor intensive jobs (36, 77). Improved insulin sensitivity, resulting in decreased circulating insulin concentrations, has also been associated with improved health and longevity (12, 21).

Insulin-stimulated Glucose Transport

Insulin increases the translocation of GLUT4 from intracellular vesicles to cell surface membranes allowing for glucose to enter the cell (15, 98, 189). While the entire mechanism for this process is not fully understood, the proximal signaling steps have been well characterized. The binding of insulin to its receptor initiates a signaling cascade beginning with conformational changes of the receptors cytosolic domain, resulting in autophosphorylation of the insulin receptor on multiple tyrosine residues (28, 163, 179, 190). Insulin receptor tyrosine phosphorylation activates its kinase activity and promotes docking and tyrosine phosphorylation

on Insulin Receptor Substrate-1 (pIRS-1^{Tyr}), as well as other proteins (118, 144, 161, 178). Activated IRS-1 then allows for phosphatidylinositol 3-kinase (PI3K) binding, resulting in conformational changes in PI3K thereby increasing its kinase activity (29). PI3K, in turn, phosphorylates membrane-associated phosphatidylinositol-(4, 5)-bisphosphate converting it to phosphatidylinositol-(3,4,5)-trisphosphate (PIP3) (172-173). PIP3 then binds proteins containing pleckstrin homology (PH) domains, namely phosphoinositide-dependent kinases-1 (PDK1) and Akt (7, 99). Akt is a key signaling protein, and its activation mediates a number of cellular functions including glucose transport, cell proliferation, proteins synthesis and apoptosis (142, 147, 153, 160). Although Akt has been well established for regulating glucose transport, the link between Akt and GLUT4 translocation was unknown until the relatively recent discovery of distal signaling proteins involved in regulating GLUT4 translocation.

TBC1D4 (Tre-2/USP6, BUB2, cdc16 domain family, member 4), often referred to as AS160 (Akt Substrate at 160 kDa), is a Rab-GTPase protein that is phosphorylated on multiple residues in response to insulin and has been shown be important for glucose transport (83). Rab-GTPase proteins regulate membrane trafficking including vesicle formation, vesicle translocation and membrane fusion (70, 72). When not phosphorylated, AS160 retains its target Rabs in their inactive GDP-bound form. Phosphorylation of AS160, inhibits its GTPase activity and allows for the conversion of Rabs to their active GTP-bound form, thereby enabling GLUT4 vesicles to translocate to the cell surface and increase glucose transport (83, 146).

Gustav Lienhard's group identified AS160 in adipocytes as an insulin responsive Akt substrate by immunoprecipitating with the PAS antibody (Phosphor-Akt Substrate antibody that recognizes Akt phospho-motifs, RXRXXpT/S) followed by tandem mass spectrometry (83). Site-specific mutations of the four insulin-responsive phosphor-Ser/Thr residues on AS160 (4P-AS160) in 3T3-L1 adipocytes, thereby inhibiting the insulin-stimulated phosphorylation of AS160 and deactivation of its GAP domain, resulted in an ~80% decrease of insulin-stimulated GLUT4 translocation to the plasma membrane (146). Insulin-stimulated GLUT4 translocation was reduced by ~60% when only the Thr^{642} phospho-site was mutated, ~25% when only the Ser^{588} phospho-site was mutated on AS160, and the double mutant (2P-AS160 both Thr^{642} and Ser^{588} are mutated) resulted in similar reductions (~80%) in insulin-stimulated GLUT4 translocation observed with the 4P-AS160. These data suggest that Thr^{642} and Ser^{588} on AS160

are the primary regulatory residues for insulin-stimulated GLUT4 translocation recognized by the PAS antibody. The attenuated GLUT4 translocation associated with 4P-AS160 was rescued with the overexpression of a mutant AS160 that had the 4P mutation in addition to an inactivated GAP domain (due to the mutation of a key arginine site Arg^{973}, to a Lys; 4P + R/K-AS160; where R = Arg and K = Lys). These data demonstrate the importance of a functional GAP domain for AS160's restraint of GLUT4, and AS160's importance for insulin-stimulated glucose uptake in adipocytes.

AS160 has also been shown to be important for both *ex vivo* and *in vivo* insulin-stimulated glucose transport in skeletal muscle (30). For insulin-stimulated phosphorylation of AS160 to be physiologically relevant, the kinetics for the phosphorylation and dephosphorylation of AS160 must coincide with the rapid changes in glucose transport in the presence and absence of insulin. Thus, kinetics experiments were performed *ex vivo* using isolated rat epitrochlearis muscles in order to test this hypothesis. These experiments revealed that insulin rapidly increases AS160's phosphorylation (within 10 minutes of exposure to insulin) in a dose-dependent manner, which was consistent with insulin-stimulated increases in glucose transport and Akt phosphorylation (24). When incubated muscles were pre-treated with insulin and subsequently transferred to a secondary vial containing media without insulin, the phosphorylation of AS160 was essentially fully reversed within 20 minutes, in coordination with reduced glucose uptake and Akt phosphorylation (154). Additionally, when muscles were incubated with insulin and the PI3K inhibitor wortmannin, both AS160 phosphorylation and glucose transport were eliminated (24, 50). *In vivo* experiments found that an 8-fold increase in the expression of wild-type (WT) AS160 in the mouse tibialas anterior compared with the control muscles had no effect on insulin-stimulated glucose uptake (96). Overexpression of 4P-AS160 mutant in the TA, thereby eliminating the ability of AS160 to be phosphorylated on four Akt responsive phosphomotifs, versus the control muscle resulted in a 50% reduction in insulin-stimulated glucose uptake. Insulin-stimulated glucose uptake was restored to control levels when the 4P + R/K-AS160 double mutant (mutated 4 Akt phosphor-motifs by substitution of alanine for serine or threonine and lacking a functional GAP domain) was over expressed, suggesting that the phosphorylation of the four Akt motifs are important for regulating AS160's GAP activity in response to insulin. These data provide evidence that AS160 is pertinent for regulation of insulin-stimulated glucose transport in skeletal muscle.

RuvB-Like Protein 2 (RUVBL2), also known as Reptin or Tip48, an ATP-binding protein that belongs to the AAA+ (ATPase Associated with diverse cellular Activities) family of ATPases (6), was identified as a protein that physically associates with AS160 in 3T3-L1 adipocytes. RUVBL2 complexes with Pontin to form a double hexamer complex. Based on the structure of this complex, it is believed to act as a DNA helicase and play a role in DNA repair (56, 75, 84). Often studied for its role in the development of cancer, RUVBL2 expression is greatly increased in tumors, has been shown to repress β-catenin-T-Cell Factor transcriptional activity and possibly regulate *Wnt* signaling (known for its role in embryogenesis and cancer) (13, 130, 177). It was previously revealed that RUVBL2 expression and cellular localization in testicular germ cells was altered by media differing in glucose concentration, suggesting a possible relationship between glucose metabolism and RUVBL2 (113). In 3T3-L1 adipocytes, genetic depletion of RUVBL2 was associated with both a decrease in insulin-stimulated AS160 phosphorylation and glucose uptake (187). This study also showed that epididymal fat pads from obese diabetic KKAy mice had dramatically reduced RUVBL2 expression compared to normal controls, but they did not measure insulin-stimulated glucose uptake in the fat pads from the KKay mice. The available data suggest that the abundance of RUVBL2 may be related to insulin signaling and action in adipocytes, but data for RUVBL2 in skeletal muscle is lacking.

The Tethering protein containing an UBX-domain for GLUT4 (TUG) has also been suggested as a possible regulator of insulin-stimulated glucose transport. Bogan et al. identified TUG as a putative GLUT4 binding protein while performing a functional screen for insulin responsive proteins in Chinese Hamster Ovary cells (17). They found that GLUT4 can be co-immunoprecipitated with TUG, and results from immunohistochemistry experiments suggest that the two proteins are colocalized intracellularly. It was determined that the UBX-C terminus fragment of TUG can bind GLUT4, but the UBX-C terminus fragment lacks the region of TUG that sequesters the TUG-GLUT4 complex intracellularly. When the UBX-C terminus fragment is overexpressed it acts as a dominant negative regulator of full length TUG, binding with GLUT4 but not allowing GLUT4 to be retained intracellularly, resulting in increased GLUT4 localized near the plasma membrane. They determined that the UBX domain is necessary for the binding of GLUT4 and TUG does not bind GLUT1. In addition, structural comparisons of TUG's UBX domain with other proteins that have the ability to bind GLUT4 suggest that TUG binds GLUT4's large cytoplasmic loop between the sixth and seventh transmembrane domains.

In the absence of insulin, TUG has been shown to bind and retain GLUT4 intracellularly in 3T3-L1 cells, and the addition of insulin results in a reduction of TUG's intracellular retention of GLUT4 (17). The shRNA knockdown of TUG expression resulted in an increase in both basal and insulin-stimulated glucose uptake in adipocytes compared to control cells, and the overexpression of wild-type TUG in combination with shRNA knockdown was able to rescue both basal and insulin-stimulated glucose uptake to similar levels as control cells (192). Consistent with the data from adipocytes, in both L6 myotubes and mouse skeletal muscle overexpressing a *myc*-tagged GLUT4 (GLUT4*myc*), TUG associates with GLUT4 without the addition of insulin determined by co-immunoprecipitation (151). When insulin was added to the L6 myotubes or injected into transgenic mice, there was a rapid decrease in the amount of TUG that co-immunoprecipitated with GLUT4*myc* in comparison to the non-insulin treated cells or mice. A recent study using adipocytes expressing GLUT4-GFP confirmed previous studies in 3T3-L1 cells, shRNA knockdown of TUG increased GLUT4-GFP near the plasma membrane and decreased the amount of intracellular bound GLUT4-GFP in the absence of insulin compared to control cells, and overexpression of TUG rescued the control phenotype (188). These data support the hypothesis that in the absence or low insulin concentration TUG restrains GLUT4 intracellularly, and addition of insulin result in the disassociation of GLUT4 from TUG allowing for increased GLUT4 translocation to the plasma membrane.

To summarize, the proximal insulin signaling steps that regulate glucose transport have been relatively well characterized. However, distal insulin signaling steps are not as well understood. Evidence suggests that the phosphorylation of AS160 on key phospho-motifs in response to insulin is important for regulating GLUT4 translocation in both adipocytes and skeletal muscle. In adipocytes the level of insulin-stimulated AS160 phosphorylation may be dependent on the total protein abundance of RUVBL2, but it is not known if this relationship holds true in skeletal muscle. The GLUT4 binding protein TUG has been shown to physically associate with GLUT4 in both adipocytes and skeletal muscle, and evidence suggests that TUGs intracellular restraint of GLUT4 is insulin dependent. However, the mechanism for the insulin-stimulated release of GLUT4 from TUG is not known.

Contraction-stimulated Glucose Transport

It has been repeatedly shown that a muscular contraction can increase glucose transport into the muscle cell independent of insulin, and contraction and insulin-mediated glucose transport have been shown to occur via distinct mechanisms (16, 49, 52, 81, 97, 136-137, 186). It is generally well accepted that contraction-mediated glucose transport results from increased intracellular calcium concentrations and the activation of the AMP activated protein kinase (AMPK), independent of the activation of the IRS-1/PI3K pathway observed with insulin stimulation. However, evidence suggests that the activation of the distinct insulin and contraction pathways may converge at AS160 and its paralog protein TBC1D1 (Tre-2/USP6, BUB2, cdc16 domain family, member 1).

Muscle contraction (during *in vivo* exercise, *in situ* electrical stimulation, or *ex vivo* electrical stimulation) results in an increase in calcium release from the sarcoplasmic reticulum, increasing the concentration of calcium around the myofibrils. Calcium then binds troponin, exposing myosin binding sites on actin, allowing for the myosin head to bind actin. When adenosine triphosphate (ATP) binds to the myosin head it is hydrolyzed to adenosine diphosphate (ADP) and inorganic phosphate (Pi). The energy released from the hydrolysis of ATP results in the disassociation of the myosin head from actin, "cocking" it in preparation for the "power stroke," which results in muscle contraction. Once the power stroke is complete, ADP is released from the myosin head and if calcium concentration remains elevated, then additional muscle contractions will occur. With muscle contractions (during exercise or electrical stimulation), cellular adenosine monophosphate (AMP) concentrations can increase, leading to the activation of the AMP-activated protein kinase (AMPK). AMPK is often described as an "energy sensing protein," and is activated when the energy balance is disrupted (decreased ATP and increased AMP concentrations) (63, 139, 141). Activation of AMPK is widely believed to play a key role in contraction-stimulated GLUT4 translocation, allowing for increased glucose uptake into the cell. Although the exact mechanism is not known, AMPK may regulate glucose uptake independent of insulin by regulating the phosphorylation of AS160 and/or TBC1D1 allowing for greater GLUT4 translocation (30, 32, 52, 63, 79). AS160 and TBC1D1 are approximately 41 percent identical over the length of the entire proteins, and their GAP domains 79% identical (138). TBC1D1, like AS160, retains its target Rabs in their inactive

GDP-bound form. Phosphorylation of specific sites inhibit TBC1D1's GTPase activity, allows for the conversion of Rabs to their active GTP-bound form and enables GLUT4 vesicles to translocate.

Due to the structural similarity of AS160 and TBC1D1 and the fact that phosphorylation of both proteins is elevated in response insulin and contraction, it is has been suggested that AS160 and TBC1D1 may each participate in both insulin- and contraction-stimulated glucose uptake in skeletal muscle. However, multiple lines of evidence suggest that increased AS160 phosphorylation is not essential for contraction-mediated glucose transport. In humans muscle, AS160 phosphorylation was not increased following 10 or 30 min of endurance exercise at 67% VO_{2Peak}, when increase glucose uptake would be expected (167). When isolated rat epitrochlearis muscles were electrically stimulated to contract *ex vivo*, glucose transport was increased in association with greater TBC1D1 and AS160 phosphorylation (24, 50). However, in muscles that were incubated with wortmannin (an inhibitor of PI3K), contraction-mediated glucose uptake and TBC1D1 phosporylation were unaltered (50), but AS160 phosphorylation was eliminated (24, 50). When muscles were incubated with Compound C (an AMPK inhibitor), contraction-induced increases in both TBC1D1 phosphorylation and glucose transport were eliminated, while AS160 phosphorylation remained elevated (50). Similarly, incubation with N-benzyl-p-toluenesulfonamide (BTS; a highly specific myosin type II inhibitor) resulted in a 57% reduction in contraction-stimulated glucose transport and eliminated TBC1D1 phosphorylation (16). These data suggest that although both AS160 and TBC1D1 can both be phosphorylated in response to contraction, TBC1D1 phosphorylation may be required, but AS160 phosphorylation is not (30).

Regulation of insulin-independent glucose uptake in response to muscle contraction is complex, with multiple signaling pathways likely being important. The elevated calcium levels that initiate muscle contraction can activate the signaling proteins calmodulin activated protein kinase II (CaMKII) and calmodulin activated protein kinase kinase (CaMKK) via calmodulin, a calcium sensing protein, resulting in increased glucose transport independent of AMPK activation (16, 30, 79, 139, 141). Both TBC1D1 and AS160 have calmodulin binding domains that may participate in their restraint on the GLUT4 vesicle in response to elevated calcium concentrations (30). It should be noted that although calcium-calmodulin dependent processes

may be important for contraction-stimulated glucose uptake, it remains controversial whether increased calcium concentration alone is sufficient to increase skeletal muscle glucose transport (69, 79-80, 186).

Although calcium and AMPK are generally considered to be key stimuli for contraction-stimulated glucose transport, other factors may also be important. For example, reactive oxygen species, specific Protein Kinase C isoforms (PKC: α, β_1, β_2 and γ) and Sucrose Nonfermenting AMPK-Related Kinase (SNARK) have been implicated in possibly contributing to the complex regulation of contraction-mediated glucose uptake by skeletal muscle (10, 79, 94, 107-111, 139, 141, 145).

Increased Insulin Sensitivity Following Exercise in Insulin Sensitive Individuals

Immediately after an acute exercise bout, insulin-independent glucose transport is increased in skeletal muscle of healthy, insulin sensitive rats (8, 45, 137). Within approximately 1-3 hours after the cessation of exercise, most of the insulin-independent glucose transport by isolated muscles has returned to baseline levels. At approximately 3-4 hours post-exercise skeletal muscle insulin sensitivity is increased compared to sedentary controls. This increase in insulin sensitivity can be observed up to 48 hours following a single bout of exercise (33, 52, 112). The improved insulin sensitivity is the result of greater insulin-stimulated GLUT4 at the cell surface, rather than an increase in total GLUT4 abundance (62).

Extensive research has been performed in insulin sensitive humans or rats to determine possible mechanisms that may account for the increased cell surface GLUT4 recruited by insulin following a single exercise bout. Many studies have indicated that the improved insulin sensitivity is not due to amplification of proximal insulin signaling steps including: 1) the affinity of insulin binding to its receptor (18-19, 193), 2) IR tyrosine phosphorylation or kinase activity (164, 166, 181), 3) IRS-1 tyrosine phosphorylation (pTyr-IRS-1) (62, 71), 4) PI3K associated with IRS-1 (37, 44, 182-183) and 5) Akt activation (8, 47, 52, 58, 181). Unlike proximal insulin signaling steps, AS160 has been shown to remain phosphorylated hours after a single session of exercise in insulin sensitive rats. Arias and colleagues found that in rat epitrochlearis muscle taken 3-4 hours after acute exercise had increased basal (absence of insulin) AS160

phosphorylation, measured with the PAS antibody (PAS-AS160), compared to sedentary controls (8). This sustained increase in basal PAS-AS160 was apparent despite both insulin-independent glucose transport and the phosphorylation of upstream signaling proteins (pAkt, pGSK3 and pAMPK) having returned to baseline (unexercised) levels. With added insulin, muscles from exercise versus muscles from non-exercised rats had greater PAS-AS160 and increased glucose transport. It should be noted that the greater PAS-AS160 phosphorylation observed with insulin in muscles from exercised rats could be at least partly accounted for by a sustained increase in basal PAS-AS160 observed in the contralateral non-insulin treated muscle. In other words, if the basal PAS-AS160 was subtracted from the contralateral muscle's PAS-AS160 with insulin, there was no difference in delta PAS-160 [delta PAS-AS160 = (PAS-AS160 with insulin) – (PAS-AS160 without insulin)] among the muscles from the exercised and sedentary rat. This was the first evidence to show that elevated PAS-AS160 in the hours following exercise in muscle was associated with increased insulin sensitivity.

In lean humans, Sriwijitkamol et al. found that in skeletal muscle PAS-AS160 was sustained 40 and 150 minutes following cycling exercise, but they did not measure glucose uptake (158). Therefore, they were unable to determine if the increased PAS-AS160 was associated with increased insulin-stimulated glucose disposal or if the residual insulin-independent glucose uptake was still present. A subsequent study found a sustained increase in AS160 phosphorylation in skeletal muscle samples taken from healthy men four hours after performing one-legged knee extensor exercise compared to the muscle sampled from the contralateral resting leg (168). Non-insulin-stimulated AS160 phosphorylation (pAS160) was increased in the exercised leg versus the non-exercised leg on four phospho-serine sites of AS160 (Ser-318, Ser-341, Ser-588 and Ser-751). However, they did not observe a sustained increase on AS160 phosphorylation for PAS-AS160, Thr-642, or Ser-666. Insulin increased AS160 phosphorylation measurements in both the sedentary and exercised leg for all of the separate phosphosites measured (Thr-642, Ser-666, Ser-318, Ser-341, Ser-588, Ser-751) and also using the PAS antibody. In the exercised versus non-exercised leg, there was greater insulin phosphorylation observed on the Ser-318, Ser-341, Ser-588 and Ser-751 residues (sites that had sustained phosphorylation without insulin). Consistent with the data from rats, the increased phosphorylation of AS160 with insulin in the exercised leg was due to the increased residual

phosphorylation, without greater sensitivity of AS160 phosphorylation to insulin (delta pAS160 was not altered by exercise) (8, 168).

The increased insulin sensitivity post-exercise can last as long as 48 hours (33, 52, 112), and the time-course of the reversal for the increased insulin sensitivity can be accelerated by post-exercise carbohydrate intake (33, 52). Three hours after acute exercise rat epitrochlearis muscles had increased insulin sensitivity, measured by glucose transport (33). However, 18 hours after the exercise bout, muscles from rats that were fed either rat chow (~60% carbohydrate) or 100% carbohydrates no longer had increased insulin sensitivity. On the other hand, muscles from rat that were not fed carbohydrate (fed lard or fasted) for the 18 hours following exercise retained the increased insulin sensitivity. This phenomenon was revisited by Funai et al. to determine if the carbohydrate induced reversal of improved insulin sensitivity following exercise also reversed the sustained increase in pAS160 (52). They observed in rats that were fasted following exercise, both insulin-stimulated glucose transport and pAS160 (pThr642 and PAS) were elevated at 3 hours and 27 hours after exercise. However, when rats were allowed free access to chow after exercise, both improved insulin sensitivity and AS160 phosphorylation reversed to non-exercise levels. Although these data did not prove that greater AS160 phosphorylation is necessary for increased insulin-stimulated glucose transport, they are consistent with this idea.

TBC1D1 has also been assessed for its possible role in the post-exercise increase in insulin sensitivity using the PAS antibody. Despite the evidence suggesting TBC1D1 importance for contraction-stimulated glucose uptake and TBC1D1's structural similarities to AS160, there was no sustained TBC1D1 phosphorylation without insulin nor was there elevated TBC1D1 phosphorylation with insulin 3-4 hours following exercise. Therefore, it does not appear that TBC1D1 phosphorylation, at least not on sites recognized by PAS, is important for the improved insulin sensitivity following exercise.

To summarize, skeletal muscle insulin sensitivity is improved in the hours following a single session of exercise. Many studies have demonstrated the increased insulin sensitivity does not appear to be due to enhanced proximal insulin signaling or greater TBC1D1 phosphorylation. Interestingly, AS160 phosphorylation has been shown to be increased hours after the exercise bout. AS160 is the only insulin signaling protein that has been identified to have greater

phosphorylation with insulin hours after the exercise bout. However, the mechanism for the sustained increase in AS160 phosphorylation after exercise has not been identified.

Possible Mechanism for High Fat Diet-induced Insulin Resistance

High fat diet-induced obesity is accompanied by insulin resistance, but the mechanism is not fully understood (114). Both obesity and insulin resistance are prevailing risk factors for developing T2DM (48, 132). In the obese state, fatty acid availability is increased due to increased fatty acid flux (greater breakdown and uptake) compared to lean insulin sensitive individuals. The greater fatty acid availability is associated with increased fatty acid storage in ectopic tissue (i.e., skeletal muscle, liver and pancreas). In skeletal muscle the accumulation of fatty acids either induced by diet or lipid infusion is associated with insulin resistance (67, 86, 148, 156, 191). The decrease in insulin-stimulated glucose transport is believed to result from impaired insulin signaling leading to reduced translocation of GLUT4 to the cell's surface. A commonly cited model for fatty acid induced insulin resistance in skeletal muscle is that fatty acid accumulation results in increased fatty acid intermediates, primarily diacylglycerol (DAG) and/or ceramides. Elevated DAG levels then activate serine kinases (Protein Kinase C-Theta, PKC-θ, and c-Jun N-terminal Kinase, JNK), which phosphorylate IRS-1 on inhibitory serine sites (pIRS-1^{Ser}), thereby reducing subsequent steps of insulin signaling (decreased PI3K activity and association with IRS-1 and decreased Akt activation), resulting in less GLUT4 translocation and glucose transport. Ceramides, on the other hand, appear to act downstream of IRS-1 and may increase the activity of Ser/Thr protein phosphatases responsible for dephosphorylating Akt.

Although obesity results from chronic (months to years) energy surplus resulting from excessive caloric intake and/or inadequate physical activity leading to increased adiposity, insulin resistance can be observed with short term (days or weeks) high calorie feeding (typically via high fat diet; HFD) or acute lipid infusion (hours) (22, 91, 95, 102, 159, 170, 176, 191). A study from Gerald Shulman's group demonstrated that the insulin resistance observed with a lipid infusion was associated with increased DAG in skeletal muscle of rats (191). They postulated that fatty acid accumulation was necessary for the lipid induced insulin resistance because reductions in insulin signaling (decreased pIRS-1^{Tyr}, decreased PI3K associated with

IRS-1, and increased pIRS-1^{Ser}) and glucose uptake were not apparent until five hours of lipid infusion. Concomitant with the reduced insulin signaling they observed an increase in acyl-CoA, DAG and membrane associated PKC-θ, but no increases in ceramides or triacylglycerol (TG) in skeletal muscle. They proposed that the rise in DAG was responsible for the activation of the serine kinase PKC-θ, leading to the increased pIRS-1^{Ser} [which was previously shown to inhibit insulin signaling (2)] and fatty acid-induced insulin resistance. In support of this hypothesis, in obese humans intramyocellular DAG concentrations obtained from skeletal muscle was shown to be a predictor of insulin resistance (116). Additionally, insulin resistance in high fat fed mice was associated with the increased levels of DAG, PKC-θ and JNK (101).

DAG is a fatty acid intermediate that is composed of a glyceride backbone attached to two fatty acid chains and is produced through multiple mechanisms: 1) the addition of a fatty acid group from fatty acyl-CoA by the enzyme monoacylglycerol acyltransferase to monoacylglycerol to form DAG, 2) the hydrolysis of TG by lipases to form DAG and acylglycerol, 3) the hydrolysis of phosphatidylinositol-4,5-bisphosphate by phospholipase C to form DAG and inositol-1,4,5-triphospate (IP3) and 4) during the formation TG when lysophosphatidic acid is converted to phosphatidic acid by 1-acylglycerol-3-phosphate acyltransferase and either becomes a phospholipid or is converted to DAG by phosphatidic acid phosphatase to TG by DAG acyltransferase. When fatty acids are available in excess, which occurs with HFD and obesity, it is hypothesized that the accumulation of DAG is attributable to incomplete fatty acid oxidation or incomplete conversion of fatty acids to TG for storage (11, 88, 115, 117, 149-150). Once formed, DAG can become embedded in the plasma membrane, thereby increasing the affinity of PKC-θ to the membrane and stabilizing PKC-θ in its active conformation (148, 156).

PKC-θ is a novel isoform (characterized by a lack of a calcium-binding site in the C2 domain of the regulatory N-terminal region) that can be maximally activated by DAG independent of calcium. Because PKC-θ is a serine kinase that can increase pIRS-1^{Ser} and PKC-θ is activated by DAG, numerous studies have investigated PKC-θ role in diet induced insulin resistance (57, 100). Oakes et al. found that high fat fed rats that had been treated with the thiazolidinedione BRL-49653 had improved insulin-stimulated glucose uptake and reduced circulating fatty acids compared to the control group (121). It was later found that BRL-49653

reduces the amount of membrane associated PKC-θ (152). Muscle PKC-θ activity was approximately 5-fold greater in type 2 diabetic patients compared to non-diabetic controls (76), and PKC-θ knockout mice were protected against insulin resistance induced by lipid infusion (90).

JNK is a serine kinase that represents a subfamily of mitogen-activated protein kinases (MAPK) that are activated by specific MAPK kinases (MAPKK). JNK activity is also believed to be increased by non-esterified fatty acids (57, 87) and it has been suggested that PKC-θ may also increase JNK activity (100) based on findings in T-cells (5). However, the mechanism for this is not fully understood. Several studies have shown that in conditions of increased fatty acid availability (high fat feeding, lipid infusion and genetic models of obesity), activation of JNK is increased along with elevated pIRS-1^{Ser}, and these changes are accompanied by reduced insulin signaling (57, 66, 87). Hirosumi et al. showed that both high fat fed and ob/ob (a genetic model of obesity) mice had significantly increased JNK activity in skeletal muscle, liver and adipose tissue, with reduced glucose and insulin tolerance and increased pSer-IRS-1 (66). Heterozygote ($JNK^{+/-}$) and homozygote JNK knockout ($JNK^{-/-}$) were protected against insulin resistance associated with HFD, and ob/ob mice with $JNK^{-/-}$ had improved insulin tolerance (66). However, recent studies have demonstrated varying results with respect of muscle specific deletion of JNK. Sabio and colleagues found that skeletal muscle specific ablation of JNK in mice protected skeletal muscle insulin-mediated glucose uptake in response to HFD (143). On the other hand, results from Pal et al. show that skeletal muscle specific deletion of JNK did not improve glucose metabolism and insulin sensitivity in mice fed a HFD (124).

In summary, skeletal muscle insulin resistance associated with excess dietary fat intake is believed to result from muscle lipid accumulation. Particularly, increased concentrations of the fatty acid intermediates DAG and ceramides in muscle are believed to facilitate the activation of inhibitory serine kinases (JNK and PKC-θ). These inhibitory kinases can lead to increased pIRS-1^{Ser}, thereby reducing downstream insulin-mediated GLUT4 translocation and glucose uptake.

Increased Insulin Sensitivity following Acute Exercise in Insulin Resistant Individuals

Several studies have shown that acute exercise can improve insulin sensitivity in insulin resistant humans. These studies demonstrated that different modes of acute exercise [cycle ergometer (43, 155), treadmill walking (27), and stair climbing (127)] can increase whole body glucose disposal measured by the hyperinsulinemic-euglycemic clamp. However, none of these studies examined possible mechanisms that may account for improved insulin sensitivity. Apparently the only study to perform insulin signaling measurements in insulin-stimulated skeletal muscle following acute exercise in insulin resistant humans was performed by Cusi and colleagues (37). Following a single session of exercise on a cycle ergometer, they found improved insulin-stimulated tyrosine phosphorylation of both the insulin receptor and IRS-1, but they did not observe a statistically significant improvement in insulin-stimulated glucose disposal. However, there was a non-significant trend for an ~50% greater glucose disposal post-exercise versus pre-exercise. In summary, several studies show that acute exercise can improve insulin sensitivity in insulin resistant humans, but the mechanism for this phenomenon has not been identified.

Numerous studies have investigated the improved insulin sensitivity after exercise in insulin resistant and diabetic rats, but much is still unknown about the underlying mechanisms. Insulin-stimulated glucose uptake, measured by hindlimb perfusion with maximally effective insulin, was improved up to 48 hours after exercise in Obese Zucker rats (a genetic model of obesity and T2DM that have a defective leptin receptor) versus lean sedentary controls (14). Similarly, SHHF/Mcc-Facp rats [obese spontaneously hypertensive heart failure rats with similar metabolic characteristics as humans with T2DM (105)] had improved whole body glucose disposal during a hyperinsulinemic-euglycemic clamp (using supraphysiologic insulin concentration) 2.5 hours after acute exercise (54). Tanaka et al. showed that rats fed a high fat diet (HFD) had improved insulin-stimulated glucose transport (physiologic insulin dose) in the isolated soleus 2 hours after acute exercise (162). They reported that isolated soleus muscle from exercised versus sedentary HFD rats had improved glucose transport and was not due to greater Akt phosphorylation. Recently Mario Saad's laboratory has investigated the improvements in insulin signaling and insulin-stimulated glucose disposal after acute exercise in insulin resistant rats that had been fed a HFD for 3 months (123, 126, 140). With a hyperinsulinemic-euglycemic

clamp (physiologic insulin dose) following exercise (6 hour swim bout), both whole body and skeletal muscle glucose uptake in insulin resistant rats were restored to levels similar to chow fed sedentary rats (123, 140). They observed that in previously exercised HFD rats versus sedentary HFD rats, insulin-stimulation (supraphysiologic dose) resulted in increased: insulin receptor tyrosine phosphorylation, pIRS-1^{Tyr}, IRS-1-PI3K association and Akt phosphorylation (123, 126, 140). Interestingly, two studies from Saad's group attributed improvements in insulin signaling observed in the HFD rats after exercise to be partially explained by reduced pJNK and reduced pSer-IRS-1 on the 307 site (pJNK can phosphorylate IRS-1 on the Ser307 site) (123, 140). However, a third study from the same group observed similar improvements in insulin signaling (increased insulin receptor tyrosine phosphorylation, pIRS-1^{Tyr}, IRS-1-PI3K association and Akt phosphorylation) in HFD rats after acute exercise (126), but they did not observe reductions in pJNK or pIRS-1^{Ser} on the 307 site as reported in the other two studies (123, 140). It is notable that the Saad group measured insulin-stimulated glucose disposal with a physiologic insulin dose, but all of the insulin signaling measurements were performed using a supraphysiologic insulin dose. Therefore, it is not clear if the post-exercise induced improvements in insulin signaling were relevant to the observed improvements in glucose disposal.

To summarize, multiple studies in insulin resistant rats (14, 54, 123, 126, 140, 162) or humans (27, 43, 127, 155) have shown that different modes of acute exercise can improve insulin sensitivity. The only study that performed insulin signaling measurements in insulin resistant humans found that proximal insulin signaling was improved in biopsies from the vastus lateralis after exercise, but whole body glucose disposal was not significantly increased (37). In gastrocnemius muscles from insulin resistant rats, two studies found that improved insulin-stimulated glucose uptake (physiologic insulin dose) following acute exercise was associated with reduced pJNK and improved proximal signaling (supraphysiologic insulin dose) (123, 140). A third study from this group also observed improved proximal insulin signaling (supraphysiologic insulin dose) in the gastrocnemius following exercise, but they did not find a reduction in pJNK (126). However, with a physiologic insulin concentration, Tanaka et al. found that after acute exercise insulin-stimulated glucose uptake was improved in the soleus muscle from insulin resistant rats without improved Akt phosphorylation (162). To date, no study of insulin resistant individuals has evaluated the effect of acute exercise on muscle glucose uptake

and the signaling at key proximal (insulin receptor and Akt) and distal (AS160) steps with a physiologic insulin dose.

Differences in Exercise Effects on Insulin Signaling of Insulin Sensitive versus Insulin Resistant Muscle

Available data suggest that improvements in insulin-stimulated glucose transport following a single session of exercise in both insulin sensitive and insulin resistant individuals may occur via distinct mechanisms. A large amount of data on insulin sensitive rats or humans reveals that the improved insulin sensitivity following an acute exercise bout is apparently not due to increased affinity of insulin to its receptor (18-19, 185, 193), insulin receptor tyrosine kinase activity (165-166, 181, 185), pIRS-1^{Tyr} (62, 71, 185), PI3K associated with IRS-1 (165, 181, 185), or Akt activation (71, 181, 185). Instead, in insulin sensitive rats, improved insulin-stimulated glucose transport is accompanied by a sustained increase in pAS160 (8, 30, 51-52, 168). In high fat fed rats, limited data suggest that the improved insulin sensitivity following acute exercise may occur by reducing pIRS-1^{Ser} (123, 140) and restoring proximal signaling steps by increasing pIRS-1^{Tyr} (123, 126, 140), thereby reversing the inhibition induced by high fat feeding. In these studies a supraphysiological dose of insulin was used for the insulin signaling measurements. Therefore, it is not known if these results will be observed at a physiologically relevant insulin concentration. It would be valuable for a study to investigate the mechanism for improved skeletal muscle insulin sensitivity following acute exercise in both insulin sensitive rats and high fat fed insulin resistant rats using a physiologic insulin concentration and the inclusion of sedentary and exercise rats from both diet groups (i.e., chow fed sedentary, HFD fed sedentary, chow fed exercise, and HFD fed exercise).

Heterogeneity of Skeletal Muscle

The capacity for contraction-mediated and insulin-mediated glucose uptake, as well as other metabolic characteristics, can vary greatly in different skeletal muscles. This variability appears to be related to differences in muscle fiber type composition. Prior to the identification

of myosin heavy chain (MHC) isoforms, muscles were often classified by color (red or white), contractile speed (slow- or fast-twitch), or by contractile speed and oxidative capacity [Slow Oxidative (SO), Fast Oxidative Glycolytic (FOG), or Fast Glycolytic (FG)]. SO muscles are rich in MHC-I fibers, FOG muscles are rich in MHC-IIa fibers, and FG muscles are rich in MHC-IIb. The histochemical staining and MHC schemes for fiber type classification do not coincide perfectly with each other. Often there appears to be a high level of correspondence between SO and MHC-I fibers, and a moderate, but more variable level of correspondence for FOG with MHC-IIa and FG with MHC-IIb fibers (41). One source of disparity between these schemes is that rat skeletal muscle also expresses MHC-IIx, and the subjectivity of earlier fiber typing techniques often results in inconsistency with IIx fibers being identified as either MHC-IIa or MHC-IIb, depending on the method used. As a result, fiber typing via the MHC isoform expression is considered the "gold-standard" for determining muscle fiber type. Identification of the correct fiber type is important because MHC isoforms have been associated with differences in metabolic phenotypes observed among various muscles.

Glucose Uptake in Response to In Vivo Exercise without Insulin Infusion

Few studies have measured the effects of *in vivo* exercise on insulin-independent glucose transport in different muscles of varying fiber type. In these studies the insulin-independent glucose uptake immediately after a single session of exercise was greatest in the soleus (SOL: a muscle rich in SO fibers), followed by the deep red region of the gastrocnemius (Gas R: muscle region rich in FOG fibers) and the white region of the gastrocnemius (Gas W: a muscle region rich in FG fibers) (SO > FOG > FG) (78, 137). However, these results should be interpreted with caution. For *in vivo* measurements for insulin-independent glucose uptake, although no exogenous insulin is infused, endogenous levels of insulin are still present. Non-uniform recruitment during *in vivo* exercise of the muscles studied and differences in blood flow to the various muscles are additional factors that complicate the interpretation of these results. Additionally, the muscles or regions of muscles used to represent a given fiber type are not pure representations of any one fiber type.

Contraction-stimulated Glucose Uptake in Response to In Situ Electrical Stimulation

During *in vivo* exercise, muscle differences in glucose uptake depend in large part on the level of recruitment of the different muscles. To minimize recruitment differences between muscles, multiple studies have utilized *in situ* electrical stimulation of the sciatic nerve of anesthetized rats, in combination with the hindlimb perfusion technique, to assess the relationship between skeletal muscle fiber type and contraction-stimulated glucose uptake in the absence of insulin. However, several studies using this technique have reported divergent results for contraction-mediated glucose uptake with respect to muscle fiber type [FG > FOG > SO (128-129, 133), FOG > SO > FG (23, 60, 184), FG > FOG > FG > SO (131), FG > SO ≥ FOG > FG (82) or FOG > FG > SO (42)]. Although it is not clear what accounts for the diverse results, differences in glucose delivery to the various muscles studied and/or variations in electrical-stimulation protocols are potential factors.

Insulin-Independent Glucose Uptake in Response to Ex Vivo Electrical Stimulation

Another approach for investigating fiber type relationships with contraction induced glucose uptake has been the use of intact isolated skeletal muscles with different fiber type profiles. *Ex vivo* experiments on isolated skeletal muscles allow for a highly controlled environment in order to assess the intrinsic properties of the muscles, free from confounding influences related to humeral factors, nutrient delivery via vasculature and neuromuscular recruitment. In isolated intact skeletal muscles predominantly composed of a given fiber type electrically stimulated to contract *ex vivo*, the consensus for the relationship between fiber type and insulin-independent glucose uptake is that FOG > FG ≥ SO (3-4, 64, 73-74). Each of these 5 studies reported that contractions stimulated glucose uptake was greater for the FDB versus the soleus and/or epitrochlearis. There was variability in ranking the contraction-stimulated glucose uptake for the epitrochleairs and soleus: Henriksen et al. had soleus > epitrochlearis (64), 4 other studies had epitrochlearis > soleus (3-4, 73-74). Although *ex vivo* electrical stimulation of isolated skeletal muscles allows for the greatest control, the possibility cannot be ruled out that the differences reported in these various muscles are due to muscle differences (e.g. epitrochlearis versus soleus versus flexor digitorum brevis) that are not exclusively attributable to fiber type specific differences.

To summarize, the differences in contraction-stimulated glucose uptake among different skeletal muscles may be fiber type dependent. *In vivo* exercise appears to result in greater insulin-independent glucose uptake in muscles rich oxidative fibers versus muscles rich in glycolytic fibers (SO > FOG > FG). Experiments that measured glucose uptake following *in situ* contraction in the perfused hindlimb have not revealed a consistent fiber type relationship for insulin-independent glucose uptake. In isolated intact rat skeletal muscles electrically stimulated to contract *ex vivo*, multiple studies consistently show insulin-independent glucose uptake in different muscles of varying fiber type have the following rank order: FOG (flexor digitorum brevis) > FG (epitrochlearis) ≥ SO (soleus). *Ex vivo* experiments allow muscle to muscle (e.g., flexor digitorum brevis versus epitrochlearis) comparisons to be made free from exogenous factors that are present in both *in vivo* and *in situ* models. However, no muscle is a pure representation of one fiber type (or cell type). As a result, these findings do not allow for direct muscle fiber type comparisons (e.g., MHC-IIa versus MHC-IIb) in relation to contraction-stimulated glucose uptake.

Addressing Fiber Type Differences in Skeletal Muscle

Much is still not known about the fiber type specific characteristics for insulin-independent glucose uptake following muscle contraction. Recently our group has developed and validated a novel method for determining both glucose uptake and fiber type (via myosin heavy chain expression) for isolated single muscle fibers from rat epitrochlearis muscles (103). By using the isolated epitrochlearis electrically stimulated to contract *ex vivo*, the single fiber method allows for direct fiber type comparisons for insulin-independent glucose uptake for the first time.

Rationale for Research Models Used in this Thesis

Chow fed and high fat fed Wistar rats were evaluated for several potential mechanisms that may be important for the post-exercise increase in insulin-stimulated glucose transport by skeletal muscle. There is a large body of evidence showing that isolated epitrochlearis muscles from lean Wistar rats have improved insulin sensitivity following a single bout of exercise (8, 30-31, 44, 51-52, 62, 175). Metabolic impairments associated with high fat feeding in Wistar

rats are similar to those observed with in obese humans (22, 25-26, 92, 180). For example high fat feeding in rats: 1) induces skeletal muscle insulin resistance and impaired whole body glucose tolerance (89, 176), 2) increases plasma triglyceride and non-esterified fatty acids (122, 180), 3) increases body mass (34, 157, 171), 4) increases adiposity (26, 91, 157) and 5) induces insulin resistance without altering GLUT4 total abundance (59, 61).

Study 1 used 12 muscles or regions of muscles of varying fiber type composition (adductor longus, extensor digitorum longus, epitrochlearis, mixed gastrocnemius, red gastrocnemius, white gastrocnemius, plantaris, soleus, red tibialis anterior, white tibialis anterior, tensor fasciae latae and white vastus lateralis). These muscles or regions of muscles were chosen because they represent the spectrum of muscle fiber type composition that can be found in the rat, from muscle almost entirely composed of Type I fibers (soleus and adductor longus) to muscle that are almost entirely composed of Type IIb fibers (white vastus lateralis), as well as other muscles of mixed fiber type composition.

The epitrochlearis muscle was isolated and incubated *ex vivo* for Studies 2 and 3. For Study 2, the epitrochlearis was electrically stimulated to contract in order to investigate the relationship between skeletal muscle fiber type and insulin-independent glucose uptake. Study 3 used the epitrochlearis to investigate the signaling events associated with improved skeletal muscle insulin sensitivity in chow fed and high fat fed rats following acute exercise. The epitrochlearis was used because it is a thin muscle, approximately 25 fibers thick, located in the forelimb of the rat, and it is recruited during swim exercise (indicated by AMPK activation, glycogen depletion and increased glucose transport) (8, 85, 174). The epitrochlearis is ideal for *ex vivo* incubation experiments, because its geometry allows for adequate diffusion of nutrients into the muscle, it has been shown to be viable with *ex vivo* incubation (174), electrical stimulation increases insulin-independent glucose transport (174) and it can be used for single fiber isolation to measure glucose uptake and fiber type (103). Additionally, the fiber type composition of the epitrochlearis (15% MHC-I, 20% MHC-IIa, 65% MHC-IIb) is similar to the fiber type of the entire hindlimb muscle mass (5% MHC-I, 19 % MHC-IIa, 76% MHC-IIb) in the rat (9, 174).

For Study 3, swim exercise was chosen because a single bout of swimming has been shown to consistently increase skeletal muscle insulin stimulated-glucose uptake in lean (8, 33,

51-52) and obese rats (14, 123, 126, 140). The effects of a single bout of swim exercise on the epitrochlearis from normal rats are similar to those observed in normal humans following aerobic exercise (e.g., increased insulin-independent glucose uptake immediately following exercise, increased insulin-stimulated glucose uptake several hours after the completion of the exercise bout and a sustained AS160 phosphorylation without altered proximal signaling) (104, 135, 158, 181).

Gaps to Be Filled by this Research

In Study 1, twelve skeletal muscles of varying fiber type composition were used to extend knowledge about the relationship between MHC isoform composition and the abundance of five proteins (GLUT4, AS160, TBC1D1, RUVBL2 and TUG) that are either established or putative regulators of glucose transport in rat skeletal muscle. Skeletal muscle is a heterogeneous tissue, and different muscles can vary greatly in their capacity for insulin- and contraction- mediated glucose uptake. One of the most often cited studies regarding the association between skeletal muscle fiber type, and the capacity for insulin-stimulated glucose uptake was performed by Henriksen and colleagues (64). The capacity for glucose uptake was associated with GLUT4 protein abundance based on the analysis of four different rat skeletal muscles. They concluded that oxidative muscles (composed of primarily MHC-I and MHC-IIa fibers) compared with glycolytic muscles (composed of primarily MHC-IIb fibers) have greater capacity for glucose transport due to greater total GLUT4 protein abundance. It is important to note that they did not perform fiber type analysis on the muscles that they studied. Instead, fiber type data used were from previous publications that used different strains of rats than the rats that Henriksen et al. used. The most comprehensive study to measure both GLUT4 abundance and fiber type composition in rat skeletal muscles was performed by Megeney et al. who evaluated six different muscles or muscle regions and correlated percent fiber type composition of the muscles (determined by ATPase staining in the same six muscles from other rats) with GLUT4 abundance (106). They found a significant positive correlation with percent of oxidative fibers (SO + FOG) and a significant negative correlation with the percent of FG fibers. However, identification of the muscle's MHC isoform expression (MHC-I, MHC-IIa, MHC-IIb and MHC-IIx) is considered the gold standard of fiber typing muscle (20, 125). ATPase staining is not

ideal because of the subjectivity of the stain and the difficult in identifying all four MHC isoforms present in rat skeletal muscle (i.e. Henriksen and Megeney only report MHC-I, IIa and IIb, and fail to identify MHC-IIx muscle fibers in their analyses). Study 1 extended the knowledge from earlier studies by measuring total GLUT4 protein abundance and MHC expression in 12 different rat muscles or regions of muscles. These earlier studies were published prior to the discovery of many of the proteins that are known or putative regulators of GLUT4 and glucose transport (e.g., AS160, TBC1D1, TUG and RUVBL2). Prior to Study 1, there has only been one other study that examined the relationship between AS160 and TBC1D1 total protein abundance in different rodent muscles and in relation to MHC isoform expression. This previous study used mice rather than rats, and it only used three skeletal muscles. They did not quantitatively examine the relationship between MHC isoform expression and total abundance of either AS160 or TBC1D1. Study 1 was the first investigation of the relationships between RUVBL2, TUG and MHC isoform expression in multiple muscles, and the first investigation of their relationship with other established GLUT4 regulatory proteins. Current evidence indicates that the variability in glucose uptake observed in different muscles is associated with disparities in GLUT4 protein abundance of different fiber types. The first major goal of Study 1 was to extend knowledge about the relationship between MHC isoform composition and the abundance of GLUT4 and other proteins (AS160, TBC1D1, RUVBL2 and TUG) that are either established or putative regulators of glucose transport in rat skeletal muscle. The second major goal of Study 1 was to determine if the abundance of any of these proteins were significantly associated with each other.

In Study 2, a novel method for measuring glucose uptake by single muscle fibers from the isolated epitrochlearis muscles electrically stimulated to contract *ex vivo* was used to extend the knowledge on the relationship between skeletal muscle fiber type and insulin-independent glucose uptake. Previous findings suggest that contraction-mediated glucose uptake may vary based on fiber type composition. However, groups investigating this relationship have obtained conflicting results. The complexity of *in vivo* conditions or perfused hindlimb preparation confounds to the ability to understand the effects of fiber type per se on contraction-stimulated glucose uptake. Various groups utilizing a reductionist approach analyzed insulin-independent glucose uptake in isolated intact skeletal muscles of varying fiber type electrically stimulated to contract *ex vivo*. In these studies, there is a general consensus that muscles rich in fast oxidative

fibers (MHC-IIa) versus glycolytic (MHC-IIb) tend to have greater contraction-stimulated glucose uptake (3-4, 64, 73-74). However, it is unclear if the observed differences in contraction-mediated glucose uptake are due to skeletal muscle fiber type or if they are due to the intrinsic properties of the different muscles used. Study 2 avoided these issues by determining MHC expression and glucose uptake in the same muscle fiber from isolated rat epitrochlearis muscles that have been incubated *ex vivo* and electrically stimulated to contract. The first major goal of Study 2 was to use intact rat epitrochlearis muscles incubated *ex vivo* and electrically stimulated to contract prior to single fiber isolation and glucose uptake measurements, allowing for direct fiber type comparisons for contraction-stimulated glucose uptake within the same muscle. The second major goal of Study 2 was to further investigate the fiber type and protein co-expression patterns for GLUT4, TUG, AS160, TBC1D1 and RUVBL2 at the single fiber level. The third major goal of Study 2 was to determine if the abundance of any of these proteins are significantly correlated with each other or with other metabolically relevant proteins (Cytochrome C oxidase IV, COX IV; glycogen phosphorylase; glyceraldehyde-3-phosphate dehydrogenase, GAPDH; and filamin C).

In Study 3, chow (low fat) fed and high fat fed rats were evaluated for potential mechanisms that may be important for the post-exercise increase in insulin-stimulated glucose transport by skeletal muscle. It is well established that a single bout of exercise can increase insulin sensitivity in skeletal muscle of insulin sensitive (8, 33, 51-52, 134) and insulin resistant rats (14, 54, 123, 126, 140). However, it is not clear if the improved insulin sensitivity in both groups occurs via the same mechanism. For insulin sensitive rats, enhanced insulin sensitivity does not appear to be due to improved proximal insulin signaling steps that have been studied. This benefit of exercise appears to be associated with the sustained increase in AS160 phosphorylation. Limited data in three studies by Mario Saad's group suggest that improved insulin sensitivity in insulin resistant rats following acute exercise may occur by restoring proximal insulin signaling secondary to a decrease in pSer-IRS-1 (123, 140). However, in these studies a supraphysiological dose of insulin was used for the insulin signaling measurements. Therefore, it is not known if these results will be observed at a physiologically relevant insulin concentration. These earlier studies also did not include an insulin sensitive exercise control. Thus, although there is a consensus for improved insulin-stimulated glucose uptake after exercise by HFD fed rats, there is uncertainty about the effects on proximal insulin signaling.

Additionally, none of the studies that examined the mechanisms for improved insulin sensitive after acute exercise in insulin resistant rats include assessment of AS160 phosphorylation. Study 3 avoided these issues by using a physiologic insulin dose for glucose uptake and insulin signaling measurements, including a chow fed exercise control to be compared to the HFD exercise group, and measuring both proximal insulin signaling and AS160 phosphorylation. The first major goal for Study 3 was to investigate the mechanism (measurements of proximal insulin signaling and AS160) for the exercise induced improvements for insulin-stimulated glucose uptake by skeletal muscle from insulin sensitive and insulin resistant rats. The second major goal of Study 3 was to identify possible changes in GLUT4, AS160, TBC1D1, TUG, RUVBL2 and muscle fiber type following 2 weeks of high fat feeding. The third major goal of Study 3 was to determine the effects of acute exercise on putative mediators of insulin resistance: lipid metabolites (acyl-CoA, DAG and ceramide), phosphorylation of the serine JNK and pIRS-1^{Ser}.

References

1. **Centers for Disease Control and Prevention.** Diabetes Successes and Opportunities for Population-Based Prevention and Control At a Glance. 2011.
2. **Aguirre V, Uchida T, Yenush L, Davis R, and White MF.** The c-Jun NH(2)-terminal kinase promotes insulin resistance during association with insulin receptor substrate-1 and phosphorylation of Ser(307). *J Biol Chem* 275: 9047-9054, 2000.
3. **Ai H, Ihlemann J, Hellsten Y, Lauritzen HP, Hardie DG, Galbo H, and Ploug T.** Effect of fiber type and nutritional state on AICAR- and contraction-stimulated glucose transport in rat muscle. *Am J Physiol Endocrinol Metab* 282: E1291-1300, 2002.
4. **Ai H, Ralston E, Lauritzen HP, Galbo H, and Ploug T.** Disruption of microtubules in rat skeletal muscle does not inhibit insulin- or contraction-stimulated glucose transport. *Am J Physiol Endocrinol Metab* 285: E836-844, 2003.
5. **Altman A, Isakov N, and Baier G.** Protein kinase Ctheta: a new essential superstar on the T-cell stage. *Immunol Today* 21: 567-573, 2000.
6. **Ammelburg M, Frickey T, and Lupas AN.** Classification of AAA+ proteins. *J Struct Biol* 156: 2-11, 2006.
7. **Andjelkovic M, Alessi DR, Meier R, Fernandez A, Lamb NJ, Frech M, Cron P, Cohen P, Lucocq JM, and Hemmings BA.** Role of translocation in the activation and function of protein kinase B. *J Biol Chem* 272: 31515-31524, 1997.
8. **Arias EB, Kim J, Funai K, and Cartee GD.** Prior exercise increases phosphorylation of Akt substrate of 160 kDa (AS160) in rat skeletal muscle. *Am J Physiol Endocrinol Metab* 292: E1191-1200, 2007.
9. **Armstrong RB and Phelps RO.** Muscle fiber type composition of the rat hindlimb. *Am J Anat* 171: 259-272, 1984.

10. **Balon TW and Nadler JL.** Evidence that nitric oxide increases glucose transport in skeletal muscle. *J Appl Physiol* 82: 359-363, 1997.
11. **Bandyopadhyay GK, Yu JG, Ofrecio J, and Olefsky JM.** Increased malonyl-CoA levels in muscle from obese and type 2 diabetic subjects lead to decreased fatty acid oxidation and increased lipogenesis; thiazolidinedione treatment reverses these defects. *Diabetes* 55: 2277-2285, 2006.
12. **Bartke A.** Insulin and aging. *Cell Cycle* 7: 3338-3343, 2008.
13. **Bauer A, Chauvet S, Huber O, Usseglio F, Rothbacher U, Aragnol D, Kemler R, and Pradel J.** Pontin52 and reptin52 function as antagonistic regulators of beta-catenin signalling activity. *EMBO J* 19: 6121-6130, 2000.
14. **Betts JJ, Sherman WM, Reed MJ, and Gao JP.** Duration of improved muscle glucose uptake after acute exercise in obese Zucker rats. *Obes Res* 1: 295-302, 1993.
15. **Birnbaum MJ.** The insulin-sensitive glucose transporter. *Int Rev Cytol* 137: 239-297, 1992.
16. **Blair DR, Funai K, Schweitzer GG, and Cartee GD.** A myosin II ATPase inhibitor reduces force production, glucose transport, and phosphorylation of AMPK and TBC1D1 in electrically stimulated rat skeletal muscle. *Am J Physiol Endocrinol Metab* 296: E993-E1002, 2009.
17. **Bogan JS, Hendon N, McKee AE, Tsao TS, and Lodish HF.** Functional cloning of TUG as a regulator of GLUT4 glucose transporter trafficking. *Nature* 425: 727-733, 2003.
18. **Bonen A, Tan MH, Clune P, and Kirby RL.** Effects of exercise on insulin binding to human muscle. *Am J Physiol* 248: E403-408, 1985.
19. **Bonen A, Tan MH, and Watson-Wright WM.** Effects of exercise on insulin binding and glucose metabolism in muscle. *Can J Physiol Pharmacol* 62: 1500-1504, 1984.
20. **Booth FW, Laye MJ, and Spangenburg EE.** Gold standards for scientists who are conducting animal-based exercise studies. *J Appl Physiol* 108: 219-221, 2010.
21. **Bordone L and Guarente L.** Calorie restriction, SIRT1 and metabolism: understanding longevity. *Nat Rev Mol Cell Biol* 6: 298-305, 2005.
22. **Brons C, Jensen CB, Storgaard H, Hiscock NJ, White A, Appel JS, Jacobsen S, Nilsson E, Larsen CM, Astrup A, Quistorff B, and Vaag A.** Impact of short-term high-fat feeding on glucose and insulin metabolism in young healthy men. *J Physiol* 587: 2387-2397, 2009.
23. **Brozinick JT, Jr., Etgen GJ, Jr., Yaspelkis BB, 3rd, and Ivy JL.** Contraction-activated glucose uptake is normal in insulin-resistant muscle of the obese Zucker rat. *J Appl Physiol* 73: 382-387, 1992.
24. **Bruss MD, Arias EB, Lienhard GE, and Cartee GD.** Increased phosphorylation of Akt substrate of 160 kDa (AS160) in rat skeletal muscle in response to insulin or contractile activity. *Diabetes* 54: 41-50, 2005.
25. **Buettner R, Parhofer KG, Woenckhaus M, Wrede CE, Kunz-Schughart LA, Scholmerich J, and Bollheimer LC.** Defining high-fat-diet rat models: metabolic and molecular effects of different fat types. *J Mol Endocrinol* 36: 485-501, 2006.
26. **Buettner R, Scholmerich J, and Bollheimer LC.** High-fat diets: modeling the metabolic disorders of human obesity in rodents. *Obesity (Silver Spring)* 15: 798-808, 2007.
27. **Burstein R, Epstein Y, Shapiro Y, Charuzi I, and Karnieli E.** Effect of an acute bout of exercise on glucose disposal in human obesity. *J Appl Physiol* 69: 299-304, 1990.

28. **Cann AD and Kohanski RA.** Cis-autophosphorylation of juxtamembrane tyrosines in the insulin receptor kinase domain. *Biochemistry* 36: 7681-7689, 1997.
29. **Cantley LC.** The phosphoinositide 3-kinase pathway. *Science* 296: 1655-1657, 2002.
30. **Cartee GD and Funai K.** Exercise and Insulin: Convergence or Divergence at AS160 and TBC1D1? *Exercise and Sport Sciences Reviews* 37: 188-195, 2009.
31. **Cartee GD and Holloszy JO.** Exercise increases susceptibility of muscle glucose transport to activation by various stimuli. *Am J Physiol* 258: E390-393, 1990.
32. **Cartee GD and Wojtaszewski JF.** Role of Akt substrate of 160 kDa in insulin-stimulated and contraction-stimulated glucose transport. *Appl Physiol Nutr Metab* 32: 557-566, 2007.
33. **Cartee GD, Young DA, Sleeper MD, Zierath J, Wallberg-Henriksson H, and Holloszy JO.** Prolonged increase in insulin-stimulated glucose transport in muscle after exercise. *Am J Physiol* 256: E494-499, 1989.
34. **Ciapaite J, van den Broek NM, Te Brinke H, Nicolay K, Jeneson JA, Houten SM, and Prompers JJ.** Differential effects of short- and long-term high-fat diet feeding on hepatic fatty acid metabolism in rats. *Biochim Biophys Acta* 1811: 441-451, 2011.
35. **Constable SH, Favier RJ, Cartee GD, Young DA, and Holloszy JO.** Muscle glucose transport: interactions of in vitro contractions, insulin, and exercise. *J Appl Physiol* 64: 2329-2332, 1988.
36. **Coyle EF.** Timing and method of increased carbohydrate intake to cope with heavy training, competition and recovery. *J Sports Sci* 9 Spec No: 29-51; discussion 51-22, 1991.
37. **Cusi K, Maezono K, Osman A, Pendergrass M, Patti ME, Pratipanawatr T, DeFronzo RA, Kahn CR, and Mandarino LJ.** Insulin resistance differentially affects the PI 3-kinase- and MAP kinase-mediated signaling in human muscle. *J Clin Invest* 105: 311-320, 2000.
38. **DeFronzo RA.** Lilly lecture 1987. The triumvirate: beta-cell, muscle, liver. A collusion responsible for NIDDM. *Diabetes* 37: 667-687, 1988.
39. **DeFronzo RA, Gunnarsson R, Bjorkman O, Olsson M, and Wahren J.** Effects of insulin on peripheral and splanchnic glucose metabolism in noninsulin-dependent (type II) diabetes mellitus. *J Clin Invest* 76: 149-155, 1985.
40. **DeFronzo RA and Tripathy D.** Skeletal muscle insulin resistance is the primary defect in type 2 diabetes. *Diabetes Care* 32 Suppl 2: S157-163, 2009.
41. **Delp MD and Duan C.** Composition and size of type I, IIA, IID/X, and IIB fibers and citrate synthase activity of rat muscle. *J Appl Physiol* 80: 261-270, 1996.
42. **Derave W, Lund S, Holman GD, Wojtaszewski J, Pedersen O, and Richter EA.** Contraction-stimulated muscle glucose transport and GLUT-4 surface content are dependent on glycogen content. *Am J Physiol* 277: E1103-1110, 1999.
43. **Devlin JT and Horton ES.** Effects of prior high-intensity exercise on glucose metabolism in normal and insulin-resistant men. *Diabetes* 34: 973-979, 1985.
44. **Douen AG, Ramlal T, Klip A, Young DA, Cartee GD, and Holloszy JO.** Exercise-induced increase in glucose transporters in plasma membranes of rat skeletal muscle. *Endocrinology* 124: 449-454, 1989.
45. **Douen AG, Ramlal T, Rastogi S, Bilan PJ, Cartee GD, Vranic M, Holloszy JO, and Klip A.** Exercise induces recruitment of the "insulin-responsive glucose transporter". Evidence for distinct intracellular insulin- and exercise-recruitable transporter pools in skeletal muscle. *J Biol Chem* 265: 13427-13430, 1990.

46. **Facchini FS, Hua N, Abbasi F, and Reaven GM.** Insulin resistance as a predictor of age-related diseases. *J Clin Endocrinol Metab* 86: 3574-3578, 2001.
47. **Fisher JS, Gao J, Han DH, Holloszy JO, and Nolte LA.** Activation of AMP kinase enhances sensitivity of muscle glucose transport to insulin. *Am J Physiol Endocrinol Metab* 282: E18-23, 2002.
48. **Ford ES, Williamson DF, and Liu S.** Weight change and diabetes incidence: findings from a national cohort of US adults. *Am J Epidemiol* 146: 214-222, 1997.
49. **Funai K and Cartee GD.** Contraction-stimulated glucose transport in rat skeletal muscle is sustained despite reversal of increased PAS-phosphorylation of AS160 and TBC1D1. *J Appl Physiol* 105: 1788-1795, 2008.
50. **Funai K and Cartee GD.** Inhibition of contraction-stimulated AMP-activated protein kinase inhibits contraction-stimulated increases in PAS-TBC1D1 and glucose transport without altering PAS-AS160 in rat skeletal muscle. *Diabetes* 58: 1096-1104, 2009.
51. **Funai K, Schweitzer GG, Castorena CM, Kanzaki M, and Cartee GD.** In vivo exercise followed by in vitro contraction additively elevates subsequent insulin-stimulated glucose transport by rat skeletal muscle. *Am J Physiol Endocrinol Metab* 298: E999-1010, 2010.
52. **Funai K, Schweitzer GG, Sharma N, Kanzaki M, and Cartee GD.** Increased AS160 phosphorylation, but not TBC1D1 phosphorylation, with increased postexercise insulin sensitivity in rat skeletal muscle. *Am J Physiol Endocrinol Metab* 297: E242-251, 2009.
53. **Gao J, Ren J, Gulve EA, and Holloszy JO.** Additive effect of contractions and insulin on GLUT-4 translocation into the sarcolemma. *J Appl Physiol* 77: 1597-1601, 1994.
54. **Gao J, Sherman WM, McCune SA, and Osei K.** Effects of acute running exercise on whole body insulin action in obese male SHHF/Mcc-facp rats. *J Appl Physiol* 77: 534-541, 1994.
55. **Garetto LP, Richter EA, Goodman MN, and Ruderman NB.** Enhanced muscle glucose metabolism after exercise in the rat: the two phases. *Am J Physiol Endocrinol Metab* 246: E471-475, 1984.
56. **Gribun A, Cheung KL, Huen J, Ortega J, and Houry WA.** Yeast Rvb1 and Rvb2 are ATP-dependent DNA helicases that form a heterohexameric complex. *J Mol Biol* 376: 1320-1333, 2008.
57. **Gual P, Le Marchand-Brustel Y, and Tanti JF.** Positive and negative regulation of insulin signaling through IRS-1 phosphorylation. *Biochimie* 87: 99-109, 2005.
58. **Hamada T, Arias EB, and Cartee GD.** Increased submaximal insulin-stimulated glucose uptake in mouse skeletal muscle after treadmill exercise. *J Appl Physiol* 101: 1368-1376, 2006.
59. **Han DH, Hansen PA, Host HH, and Holloszy JO.** Insulin resistance of muscle glucose transport in rats fed a high-fat diet: a reevaluation. *Diabetes* 46: 1761-1767, 1997.
60. **Han X, Ploug T, and Galbo H.** Effect of diet on insulin- and contraction-mediated glucose transport and uptake in rat muscle. *Am J Physiol* 269: R544-551, 1995.
61. **Hansen PA, Han DH, Nolte LA, Chen M, and Holloszy JO.** DHEA protects against visceral obesity and muscle insulin resistance in rats fed a high-fat diet. *Am J Physiol* 273: R1704-1708, 1997.
62. **Hansen PA, Nolte LA, Chen MM, and Holloszy JO.** Increased GLUT-4 translocation mediates enhanced insulin sensitivity of muscle glucose transport after exercise. *J Appl Physiol* 85: 1218-1222, 1998.
63. **Hardie DG.** Energy sensing by the AMP-activated protein kinase and its effects on muscle metabolism. *Proc Nutr Soc* 70: 92-99, 2011.

64. **Henriksen EJ, Bourey RE, Rodnick KJ, Koranyi L, Permutt MA, and Holloszy JO.** Glucose transporter protein content and glucose transport capacity in rat skeletal muscles. *Am J Physiol* 259: E593-598, 1990.
65. **Herman MA and Kahn BB.** Glucose transport and sensing in the maintenance of glucose homeostasis and metabolic harmony. *J Clin Invest* 116: 1767-1775, 2006.
66. **Hirosumi J, Tuncman G, Chang L, Gorgun CZ, Uysal KT, Maeda K, Karin M, and Hotamisligil GS.** A central role for JNK in obesity and insulin resistance. *Nature* 420: 333-336, 2002.
67. **Holland WL and Summers SA.** Sphingolipids, insulin resistance, and metabolic disease: new insights from in vivo manipulation of sphingolipid metabolism. *Endocr Rev* 29: 381-402, 2008.
68. **Holloszy JO.** Muscle metabolism during exercise. *Arch Phys Med Rehabil* 63: 231-234, 1982.
69. **Holloszy JO and Narahara HT.** Enhanced permeability to sugar associated with muscle contraction. Studies of the role of Ca++. *J Gen Physiol* 50: 551-562, 1967.
70. **Horgan CP and McCaffrey MW.** Rab GTPases and microtubule motors. *Biochem Soc Trans* 39: 1202-1206, 2011.
71. **Howlett KF, Sakamoto K, Hirshman MF, Aschenbach WG, Dow M, White MF, and Goodyear LJ.** Insulin signaling after exercise in insulin receptor substrate-2-deficient mice. *Diabetes* 51: 479-483, 2002.
72. **Hutagalung AH and Novick PJ.** Role of Rab GTPases in membrane traffic and cell physiology. *Physiol Rev* 91: 119-149, 2011.
73. **Ihlemann J, Ploug T, and Galbo H.** Effect of force development on contraction induced glucose transport in fast twitch rat muscle. *Acta Physiol Scand* 171: 439-444, 2001.
74. **Ihlemann J, Ploug T, Hellsten Y, and Galbo H.** Effect of stimulation frequency on contraction-induced glucose transport in rat skeletal muscle. *Am J Physiol Endocrinol Metab* 279: E862-867, 2000.
75. **Ikura T, Ogryzko VV, Grigoriev M, Groisman R, Wang J, Horikoshi M, Scully R, Qin J, and Nakatani Y.** Involvement of the TIP60 histone acetylase complex in DNA repair and apoptosis. *Cell* 102: 463-473, 2000.
76. **Itani SI, Pories WJ, Macdonald KG, and Dohm GL.** Increased protein kinase C theta in skeletal muscle of diabetic patients. *Metabolism* 50: 553-557, 2001.
77. **Ivy JL and Kuo CH.** Regulation of GLUT4 protein and glycogen synthase during muscle glycogen synthesis after exercise. *Acta Physiol Scand* 162: 295-304, 1998.
78. **James DE, Kraegen EW, and Chisholm DJ.** Muscle glucose metabolism in exercising rats: comparison with insulin stimulation. *Am J Physiol* 248: E575-580, 1985.
79. **Jensen TE and Richter EA.** Regulation of glucose and glycogen metabolism during and after exercise. *J Physiol* 590: 1069-1076, 2012.
80. **Jensen TE, Rose AJ, Hellsten Y, Wojtaszewski JF, and Richter EA.** Caffeine-induced Ca(2+) release increases AMPK-dependent glucose uptake in rodent soleus muscle. *Am J Physiol Endocrinol Metab* 293: E286-292, 2007.
81. **Jessen N and Goodyear LJ.** Contraction signaling to glucose transport in skeletal muscle. *J Appl Physiol* 99: 330-337, 2005.
82. **Johannsson E, Jensen J, Gundersen K, Dahl HA, and Bonen A.** Effect of electrical stimulation patterns on glucose transport in rat muscles. *Am J Physiol* 271: R426-431, 1996.

83. **Kane S, Sano H, Liu SC, Asara JM, Lane WS, Garner CC, and Lienhard GE.** A method to identify serine kinase substrates. Akt phosphorylates a novel adipocyte protein with a Rab GTPase-activating protein (GAP) domain. *J Biol Chem* 277: 22115-22118, 2002.
84. **Kanemaki M, Kurokawa Y, Matsu-ura T, Makino Y, Masani A, Okazaki K, Morishita T, and Tamura TA.** TIP49b, a new RuvB-like DNA helicase, is included in a complex together with another RuvB-like DNA helicase, TIP49a. *J Biol Chem* 274: 22437-22444, 1999.
85. **Kawanaka K, Tabata I, Tanaka A, and Higuchi M.** Effects of high-intensity intermittent swimming on glucose transport in rat epitrochlearis muscle. *J Appl Physiol* 84: 1852-1857, 1998.
86. **Kewalramani G, Bilan PJ, and Klip A.** Muscle insulin resistance: assault by lipids, cytokines and local macrophages. *Curr Opin Clin Nutr Metab Care* 13: 382-390, 2010.
87. **Kewalramani G, Fink LN, Asadi F, and Klip A.** Palmitate-activated macrophages confer insulin resistance to muscle cells by a mechanism involving protein kinase C theta and epsilon. *PLoS One* 6: e26947, 2011.
88. **Kien CL, Everingham KI, R DS, Fukagawa NK, and Muoio DM.** Short-term effects of dietary fatty acids on muscle lipid composition and serum acylcarnitine profile in human subjects. *Obesity (Silver Spring)* 19: 305-311, 2011.
89. **Kim JD, McCarter RJ, and Yu BP.** Influence of age, exercise, and dietary restriction on oxidative stress in rats. *Aging (Milano)* 8: 123-129, 1996.
90. **Kim JK, Fillmore JJ, Sunshine MJ, Albrecht B, Higashimori T, Kim DW, Liu ZX, Soos TJ, Cline GW, O'Brien WR, Littman DR, and Shulman GI.** PKC-theta knockout mice are protected from fat-induced insulin resistance. *J Clin Invest* 114: 823-827, 2004.
91. **Kim JK, Wi JK, and Youn JH.** Metabolic impairment precedes insulin resistance in skeletal muscle during high-fat feeding in rats. *Diabetes* 45: 651-658, 1996.
92. **Kim JY, Nolte LA, Hansen PA, Han DH, Ferguson K, Thompson PA, and Holloszy JO.** High-fat diet-induced muscle insulin resistance: relationship to visceral fat mass. *Am J Physiol Regul Integr Comp Physiol* 279: R2057-2065, 2000.
93. **Knowler WC, Barrett-Connor E, Fowler SE, Hamman RF, Lachin JM, Walker EA, and Nathan DM.** Reduction in the incidence of type 2 diabetes with lifestyle intervention or metformin. *N Engl J Med* 346: 393-403, 2002.
94. **Koh HJ, Toyoda T, Fujii N, Jung MM, Rathod A, Middelbeek RJ, Lessard SJ, Treebak JT, Tsuchihara K, Esumi H, Richter EA, Wojtaszewski JF, Hirshman MF, and Goodyear LJ.** Sucrose nonfermenting AMPK-related kinase (SNARK) mediates contraction-stimulated glucose transport in mouse skeletal muscle. *Proc Natl Acad Sci U S A* 107: 15541-15546, 2010.
95. **Kraegen EW, James DE, Storlien LH, Burleigh KM, and Chisholm DJ.** In vivo insulin resistance in individual peripheral tissues of the high fat fed rat: assessment by euglycaemic clamp plus deoxyglucose administration. *Diabetologia* 29: 192-198, 1986.
96. **Kramer HF, Witczak CA, Taylor EB, Fujii N, Hirshman MF, and Goodyear LJ.** AS160 regulates insulin- and contraction-stimulated glucose uptake in mouse skeletal muscle. *J Biol Chem* 281: 31478-31485, 2006.
97. **Lauritzen HP, Galbo H, Toyoda T, and Goodyear LJ.** Kinetics of contraction-induced GLUT4 translocation in skeletal muscle fibers from living mice. *Diabetes* 59: 2134-2144, 2010.
98. **Lavan BE and Lienhard GE.** Insulin signalling and the stimulation of glucose transport. *Biochem Soc Trans* 22: 676-680, 1994.

99. **Lawlor MA and Alessi DR.** PKB/Akt: a key mediator of cell proliferation, survival and insulin responses? *J Cell Sci* 114: 2903-2910, 2001.
100. **Li Y, Soos TJ, Li X, Wu J, Degennaro M, Sun X, Littman DR, Birnbaum MJ, and Polakiewicz RD.** Protein kinase C Theta inhibits insulin signaling by phosphorylating IRS1 at Ser(1101). *J Biol Chem* 279: 45304-45307, 2004.
101. **Liu L, Zhang Y, Chen N, Shi X, Tsang B, and Yu YH.** Upregulation of myocellular DGAT1 augments triglyceride synthesis in skeletal muscle and protects against fat-induced insulin resistance. *J Clin Invest* 117: 1679-1689, 2007.
102. **Liu S, Baracos VE, Quinney HA, and Clandinin MT.** Dietary fat modifies exercise-dependent glucose transport in skeletal muscle. *J Appl Physiol* 80: 1219-1224, 1996.
103. **MacKrell JG and Cartee GD.** A Novel Method to Measure Glucose Uptake and Myosin Heavy Chain Isoform Expression of Single Fibers from Rat Skeletal Muscle. *Diabetes* In Press: Accepted January, 2012.
104. **Mascher H, Andersson H, Nilsson PA, Ekblom B, and Blomstrand E.** Changes in signalling pathways regulating protein synthesis in human muscle in the recovery period after endurance exercise. *Acta Physiol (Oxf)* 191: 67-75, 2007.
105. **McCune SA, Baker PB, and Harold F. Stills J.** SHHF/Mcc-cp Rat: Model of Obesity, Non-insulin-dependent Diabetes, and Congestive Heart Failure. *ILAR Journal V32(3)*, 1990.
106. **Megeney LA, Neufer PD, Dohm GL, Tan MH, Blewett CA, Elder GC, and Bonen A.** Effects of muscle activity and fiber composition on glucose transport and GLUT-4. *Am J Physiol* 264: E583-593, 1993.
107. **Merry TL, Dywer RM, Bradley EA, Rattigan S, and McConell GK.** Local hindlimb antioxidant infusion does not affect muscle glucose uptake during in situ contractions in rat. *J Appl Physiol* 108: 1275-1283, 2010.
108. **Merry TL, Lynch GS, and McConell GK.** Downstream mechanisms of nitric oxide-mediated skeletal muscle glucose uptake during contraction. *Am J Physiol Regul Integr Comp Physiol* 299: R1656-1665, 2010.
109. **Merry TL and McConell GK.** Do reactive oxygen species regulate skeletal muscle glucose uptake during contraction? *Exerc Sport Sci Rev* 40: 102-105, 2012.
110. **Merry TL, Steinberg GR, Lynch GS, and McConell GK.** Skeletal muscle glucose uptake during contraction is regulated by nitric oxide and ROS independently of AMPK. *Am J Physiol Endocrinol Metab* 298: E577-585, 2010.
111. **Merry TL, Wadley GD, Stathis CG, Garnham AP, Rattigan S, Hargreaves M, and McConell GK.** N-Acetylcysteine infusion does not affect glucose disposal during prolonged moderate-intensity exercise in humans. *J Physiol* 588: 1623-1634, 2010.
112. **Mikines KJ, Sonne B, Farrell PA, Tronier B, and Galbo H.** Effect of physical exercise on sensitivity and responsiveness to insulin in humans. *Am J Physiol* 254: E248-259, 1988.
113. **Mizuno K, Tokumasu A, Nakamura A, Hayashi Y, Kojima Y, Kohri K, and Noce T.** Genes associated with the formation of germ cells from embryonic stem cells in cultures containing different glucose concentrations. *Mol Reprod Dev* 73: 437-445, 2006.
114. **Mokdad AH, Ford ES, Bowman BA, Dietz WH, Vinicor F, Bales VS, and Marks JS.** Prevalence of obesity, diabetes, and obesity-related health risk factors, 2001. *JAMA* 289: 76-79, 2003.
115. **Morino K, Petersen KF, and Shulman GI.** Molecular mechanisms of insulin resistance in humans and their potential links with mitochondrial dysfunction. *Diabetes* 55 Suppl 2: S9-S15, 2006.

116. **Moro C, Galgani JE, Luu L, Pasarica M, Mairal A, Bajpeyi S, Schmitz G, Langin D, Liebisch G, and Smith SR.** Influence of gender, obesity, and muscle lipase activity on intramyocellular lipids in sedentary individuals. *J Clin Endocrinol Metab* 94: 3440-3447, 2009.
117. **Muoio DM.** Intramuscular triacylglycerol and insulin resistance: guilty as charged or wrongly accused? *Biochim Biophys Acta* 1801: 281-288, 2010.
118. **Myers MG, Jr., Sun XJ, and White MF.** The IRS-1 signaling system. *Trends Biochem Sci* 19: 289-293, 1994.
119. **Narayan KM, Boyle JP, Thompson TJ, Sorensen SW, and Williamson DF.** Lifetime risk for diabetes mellitus in the United States. *JAMA* 290: 1884-1890, 2003.
120. **Nesher R, Karl IE, and Kipnis DM.** Dissociation of effects of insulin and contraction on glucose transport in rat epitrochlearis muscle. *Am J Physiol* 249: C226-232, 1985.
121. **Oakes ND, Kennedy CJ, Jenkins AB, Laybutt DR, Chisholm DJ, and Kraegen EW.** A new antidiabetic agent, BRL 49653, reduces lipid availability and improves insulin action and glucoregulation in the rat. *Diabetes* 43: 1203-1210, 1994.
122. **Ochiai M and Matsuo T.** Effects of Short-Term Dietary Change from High-Carbohydrate Diet to High-Fat Diet on Storage, Utilization, and Fatty Acid Composition of Rat Muscle Triglyceride during Swimming Exercise. *J Clin Biochem Nutr* 44: 168-177, 2009.
123. **Oliveira AG, Carvalho BM, Tobar N, Ropelle ER, Pauli JR, Bagarolli RA, Guadagnini D, Carvalheira JB, and Saad MJ.** Physical exercise reduces circulating lipopolysaccharide and TLR4 activation and improves insulin signaling in tissues of DIO rats. *Diabetes* 60: 784-796, 2011.
124. **Pal M, Wunderlich CM, Spohn G, Bronneke HS, Schmidt-Supprian M, and Wunderlich FT.** Alteration of JNK-1 signaling in skeletal muscle fails to affect glucose homeostasis and obesity-associated insulin resistance in mice. *PLoS One* 8: e54247, 2013.
125. **Pandorf CE, Caiozzo VJ, Haddad F, and Baldwin KM.** A rationale for SDS-PAGE of MHC isoforms as a gold standard for determining contractile phenotype. *J Appl Physiol* 108: 222-222; author reply 226, 2010.
126. **Pauli JR, Ropelle ER, Cintra DE, Carvalho-Filho MA, Moraes JC, De Souza CT, Velloso LA, Carvalheira JB, and Saad MJ.** Acute physical exercise reverses S-nitrosation of the insulin receptor, insulin receptor substrate 1 and protein kinase B/Akt in diet-induced obese Wistar rats. *J Physiol* 586: 659-671, 2008.
127. **Perseghin G, Price TB, Petersen KF, Roden M, Cline GW, Gerow K, Rothman DL, and Shulman GI.** Increased glucose transport-phosphorylation and muscle glycogen synthesis after exercise training in insulin-resistant subjects. *N Engl J Med* 335: 1357-1362, 1996.
128. **Ploug T, Galbo H, and Richter EA.** Increased muscle glucose uptake during contractions: no need for insulin. *Am J Physiol* 247: E726-731, 1984.
129. **Ploug T, Galbo H, Vinten J, Jorgensen M, and Richter EA.** Kinetics of glucose transport in rat muscle: effects of insulin and contractions. *Am J Physiol* 253: E12-20, 1987.
130. **Rashid S, Pilecka I, Torun A, Olchowik M, Bielinska B, and Miaczynska M.** Endosomal adaptor proteins APPL1 and APPL2 are novel activators of beta-catenin/TCF-mediated transcription. *J Biol Chem* 284: 18115-18128, 2009.
131. **Rattigan S, Dora KA, Tong AC, and Clark MG.** Perfused skeletal muscle contraction and metabolism improved by angiotensin II-mediated vasoconstriction. *Am J Physiol* 271: E96-103, 1996.

132. **Resnick HE, Valsania P, Halter JB, and Lin X.** Relation of weight gain and weight loss on subsequent diabetes risk in overweight adults. *J Epidemiol Community Health* 54: 596-602, 2000.
133. **Richter EA, Garetto LP, Goodman MN, and Ruderman NB.** Enhanced muscle glucose metabolism after exercise: modulation by local factors. *Am J Physiol* 246: E476-482, 1984.
134. **Richter EA, Garetto LP, Goodman MN, and Ruderman NB.** Muscle glucose metabolism following exercise in the rat: increased sensitivity to insulin. *J Clin Invest* 69: 785-793, 1982.
135. **Richter EA, Mikines KJ, Galbo H, and Kiens B.** Effect of exercise on insulin action in human skeletal muscle. *J Appl Physiol* 66: 876-885, 1989.
136. **Richter EA, Nielsen JN, Jorgensen SB, Frosig C, and Wojtaszewski JF.** Signalling to glucose transport in skeletal muscle during exercise. *Acta Physiol Scand* 178: 329-335, 2003.
137. **Richter EA, Ploug T, and Galbo H.** Increased muscle glucose uptake after exercise. No need for insulin during exercise. *Diabetes* 34: 1041-1048, 1985.
138. **Roach WG, Chavez JA, Miinea CP, and Lienhard GE.** Substrate specificity and effect on GLUT4 translocation of the Rab GTPase-activating protein Tbc1d1. *Biochem J* 403: 353-358, 2007.
139. **Rockl KS, Witczak CA, and Goodyear LJ.** Signaling mechanisms in skeletal muscle: acute responses and chronic adaptations to exercise. *IUBMB Life* 60: 145-153, 2008.
140. **Ropelle ER, Pauli JR, Prada PO, de Souza CT, Picardi PK, Faria MC, Cintra DE, Fernandes MF, Flores MB, Velloso LA, Saad MJ, and Carvalheira JB.** Reversal of diet-induced insulin resistance with a single bout of exercise in the rat: the role of PTP1B and IRS-1 serine phosphorylation. *J Physiol* 577: 997-1007, 2006.
141. **Rose AJ and Richter EA.** Skeletal muscle glucose uptake during exercise: how is it regulated? *Physiology (Bethesda)* 20: 260-270, 2005.
142. **Ruggero D and Sonenberg N.** The Akt of translational control. *Oncogene* 24: 7426-7434, 2005.
143. **Sabio G, Kennedy NJ, Cavanagh-Kyros J, Jung DY, Ko HJ, Ong H, Barrett T, Kim JK, and Davis RJ.** Role of muscle c-Jun NH2-terminal kinase 1 in obesity-induced insulin resistance. *Mol Cell Biol* 30: 106-115, 2010.
144. **Saltiel AR and Kahn CR.** Insulin signalling and the regulation of glucose and lipid metabolism. *Nature* 414: 799-806, 2001.
145. **Sandstrom ME, Zhang SJ, Bruton J, Silva JP, Reid MB, Westerblad H, and Katz A.** Role of reactive oxygen species in contraction-mediated glucose transport in mouse skeletal muscle. *J Physiol* 575: 251-262, 2006.
146. **Sano H, Kane S, Sano E, Miinea CP, Asara JM, Lane WS, Garner CW, and Lienhard GE.** Insulin-stimulated phosphorylation of a Rab GTPase-activating protein regulates GLUT4 translocation. *J Biol Chem* 278: 14599-14602, 2003.
147. **Sartelet H, Oligny LL, and Vassal G.** AKT pathway in neuroblastoma and its therapeutic implication. *Expert Rev Anticancer Ther* 8: 757-769, 2008.
148. **Savage DB, Petersen KF, and Shulman GI.** Disordered lipid metabolism and the pathogenesis of insulin resistance. *Physiol Rev* 87: 507-520, 2007.
149. **Schenk S and Horowitz JF.** Acute exercise increases triglyceride synthesis in skeletal muscle and prevents fatty acid-induced insulin resistance. *J Clin Invest* 117: 1690-1698, 2007.

150. **Schenk S, Saberi M, and Olefsky JM.** Insulin sensitivity: modulation by nutrients and inflammation. *J Clin Invest* 118: 2992-3002, 2008.
151. **Schertzer JD, Antonescu CN, Bilan PJ, Jain S, Huang X, Liu Z, Bonen A, and Klip A.** A transgenic mouse model to study glucose transporter 4myc regulation in skeletal muscle. *Endocrinology* 150: 1935-1940, 2009.
152. **Schmitz-Peiffer C, Oakes ND, Browne CL, Kraegen EW, and Biden TJ.** Reversal of chronic alterations of skeletal muscle protein kinase C from fat-fed rats by BRL-49653. *Am J Physiol* 273: E915-921, 1997.
153. **Sen P, Mukherjee S, Ray D, and Raha S.** Involvement of the Akt/PKB signaling pathway with disease processes. *Mol Cell Biochem* 253: 241-246, 2003.
154. **Sharma N, Arias EB, and Cartee GD.** Rapid reversal of insulin-stimulated AS160 phosphorylation in rat skeletal muscle after insulin exposure. *Physiol Res*, 2009.
155. **Sharoff CG, Hagobian TA, Malin SK, Chipkin SR, Yu H, Hirshman MF, Goodyear LJ, and Braun B.** Combining short-term metformin treatment and one bout of exercise does not increase insulin action in insulin-resistant individuals. *Am J Physiol Endocrinol Metab* 298: E815-823, 2010.
156. **Shulman GI, Samuel VT, and Petersen KF.** Lipid-induced insulin resistance: unravelling the mechanism. *Lancet* 375: 2267-2277, 2010.
157. **Song S, Andrikopoulos S, Filippis C, Thorburn AW, Khan D, and Proietto J.** Mechanism of fat-induced hepatic gluconeogenesis: effect of metformin. *Am J Physiol Endocrinol Metab* 281: E275-282, 2001.
158. **Sriwijitkamol A, Coletta DK, Wajcberg E, Balbontin GB, Reyna SM, Barrientes J, Eagan PA, Jenkinson CP, Cersosimo E, DeFronzo RA, Sakamoto K, and Musi N.** Effect of acute exercise on AMPK signaling in skeletal muscle of subjects with type 2 diabetes: a time-course and dose-response study. *Diabetes* 56: 836-848, 2007.
159. **Storlien LH, James DE, Burleigh KM, Chisholm DJ, and Kraegen EW.** Fat feeding causes widespread in vivo insulin resistance, decreased energy expenditure, and obesity in rats. *Am J Physiol* 251: E576-583, 1986.
160. **Summers SA and Birnbaum MJ.** A role for the serine/threonine kinase, Akt, in insulin-stimulated glucose uptake. *Biochem Soc Trans* 25: 981-988, 1997.
161. **Tamemoto H, Kadowaki T, Tobe K, Yagi T, Sakura H, Hayakawa T, Terauchi Y, Ueki K, Kaburagi Y, Satoh S, and et al.** Insulin resistance and growth retardation in mice lacking insulin receptor substrate-1. *Nature* 372: 182-186, 1994.
162. **Tanaka S, Hayashi T, Toyoda T, Hamada T, Shimizu Y, Hirata M, Ebihara K, Masuzaki H, Hosoda K, Fushiki T, and Nakao K.** High-fat diet impairs the effects of a single bout of endurance exercise on glucose transport and insulin sensitivity in rat skeletal muscle. *Metabolism* 56: 1719-1728, 2007.
163. **Taniguchi CM, Emanuelli B, and Kahn CR.** Critical nodes in signalling pathways: insights into insulin action. *Nat Rev Mol Cell Biol* 7: 85-96, 2006.
164. **Thong FS, Derave W, Kiens B, Graham TE, Urso B, Wojtaszewski JF, Hansen BF, and Richter EA.** Caffeine-induced impairment of insulin action but not insulin signaling in human skeletal muscle is reduced by exercise. *Diabetes* 51: 583-590, 2002.
165. **Thong FS and Graham TE.** The putative roles of adenosine in insulin- and exercise-mediated regulation of glucose transport and glycogen metabolism in skeletal muscle. *Can J Appl Physiol* 27: 152-178, 2002.

166. **Treadway JL, James DE, Burcel E, and Ruderman NB.** Effect of exercise on insulin receptor binding and kinase activity in skeletal muscle. *Am J Physiol* 256: E138-144, 1989.
167. **Treebak JT, Birk JB, Rose AJ, Kiens B, Richter EA, and Wojtaszewski JF.** AS160 phosphorylation is associated with activation of alpha2beta2gamma1- but not alpha2beta2gamma3-AMPK trimeric complex in skeletal muscle during exercise in humans. *Am J Physiol Endocrinol Metab* 292: E715-722, 2007.
168. **Treebak JT, Frosig C, Pehmoller C, Chen S, Maarbjerg SJ, Brandt N, MacKintosh C, Zierath JR, Hardie DG, Kiens B, Richter EA, Pilegaard H, and Wojtaszewski JF.** Potential role of TBC1D4 in enhanced post-exercise insulin action in human skeletal muscle. *Diabetologia* 52: 891-900, 2009.
169. **Tuomilehto J, Lindstrom J, Eriksson JG, Valle TT, Hamalainen H, Ilanne-Parikka P, Keinanen-Kiukaanniemi S, Laakso M, Louheranta A, Rastas M, Salminen V, and Uusitupa M.** Prevention of type 2 diabetes mellitus by changes in lifestyle among subjects with impaired glucose tolerance. *N Engl J Med* 344: 1343-1350, 2001.
170. **Turner N, Kowalski GM, Leslie SJ, Risis S, Yang C, Lee-Young RS, Babb JR, Meikle PJ, Lancaster GI, Henstridge DC, White PJ, Kraegen EW, Marette A, Cooney GJ, Febbraio MA, and Bruce CR.** Distinct patterns of tissue-specific lipid accumulation during the induction of insulin resistance in mice by high-fat feeding. *Diabetologia*, 2013.
171. **van den Broek NM, Ciapaite J, De Feyter HM, Houten SM, Wanders RJ, Jeneson JA, Nicolay K, and Prompers JJ.** Increased mitochondrial content rescues in vivo muscle oxidative capacity in long-term high-fat-diet-fed rats. *FASEB J* 24: 1354-1364, 2010.
172. **Vanhaesebroeck B and Alessi DR.** The PI3K-PDK1 connection: more than just a road to PKB. *Biochem J* 346 Pt 3: 561-576, 2000.
173. **Vanhaesebroeck B, Leevers SJ, Panayotou G, and Waterfield MD.** Phosphoinositide 3-kinases: a conserved family of signal transducers. *Trends Biochem Sci* 22: 267-272, 1997.
174. **Wallberg-Henriksson H.** Glucose transport into skeletal muscle. Influence of contractile activity, insulin, catecholamines and diabetes mellitus. *Acta Physiol Scand Suppl* 564: 1-80, 1987.
175. **Wallberg-Henriksson H, Constable SH, Young DA, and Holloszy JO.** Glucose transport into rat skeletal muscle: interaction between exercise and insulin. *J Appl Physiol* 65: 909-913, 1988.
176. **Wang J, Obici S, Morgan K, Barzilai N, Feng Z, and Rossetti L.** Overfeeding rapidly induces leptin and insulin resistance. *Diabetes* 50: 2786-2791, 2001.
177. **Weiske J and Huber O.** The histidine triad protein Hint1 interacts with Pontin and Reptin and inhibits TCF-beta-catenin-mediated transcription. *J Cell Sci* 118: 3117-3129, 2005.
178. **White MF.** Insulin signaling in health and disease. *Science* 302: 1710-1711, 2003.
179. **White MF and Kahn CR.** The insulin signaling system. *J Biol Chem* 269: 1-4, 1994.
180. **Wilson CR, Tran MK, Salazar KL, Young ME, and Taegtmeyer H.** Western diet, but not high fat diet, causes derangements of fatty acid metabolism and contractile dysfunction in the heart of Wistar rats. *Biochem J* 406: 457-467, 2007.
181. **Wojtaszewski JF, Hansen BF, Gade, Kiens B, Markuns JF, Goodyear LJ, and Richter EA.** Insulin signaling and insulin sensitivity after exercise in human skeletal muscle. *Diabetes* 49: 325-331, 2000.
182. **Wojtaszewski JF, Hansen BF, Kiens B, and Richter EA.** Insulin signaling in human skeletal muscle: time course and effect of exercise. *Diabetes* 46: 1775-1781, 1997.

183. **Wojtaszewski JF, Higaki Y, Hirshman MF, Michael MD, Dufresne SD, Kahn CR, and Goodyear LJ.** Exercise modulates postreceptor insulin signaling and glucose transport in muscle-specific insulin receptor knockout mice. *J Clin Invest* 104: 1257-1264, 1999.
184. **Wojtaszewski JF, Lynge J, Jakobsen AB, Goodyear LJ, and Richter EA.** Differential regulation of MAP kinase by contraction and insulin in skeletal muscle: metabolic implications. *Am J Physiol* 277: E724-732, 1999.
185. **Wojtaszewski JF, Nielsen JN, and Richter EA.** Invited review: effect of acute exercise on insulin signaling and action in humans. *J Appl Physiol* 93: 384-392, 2002.
186. **Wright DC, Hucker KA, Holloszy JO, and Han DH.** Ca(2+) and AMPK Both Mediate Stimulation of Glucose Transport by Muscle Contractions. *Diabetes* 53: 330-335, 2004.
187. **Xie X, Chen Y, Xue P, Fan Y, Deng Y, Peng G, Yang F, and Xu T.** RUVBL2, a novel AS160-binding protein, regulates insulin-stimulated GLUT4 translocation. *Cell Res*, 2009.
188. **Xu Y, Rubin BR, Orme CM, Karpikov A, Yu C, Bogan JS, and Toomre DK.** Dual-mode of insulin action controls GLUT4 vesicle exocytosis. *J Cell Biol*, 2011.
189. **Yeh JI, Gulve EA, Rameh L, and Birnbaum MJ.** The effects of wortmannin on rat skeletal muscle. Dissociation of signaling pathways for insulin- and contraction-activated hexose transport. *J Biol Chem* 270: 2107-2111, 1995.
190. **Youngren JF.** Regulation of insulin receptor function. *Cell Mol Life Sci* 64: 873-891, 2007.
191. **Yu C, Chen Y, Cline GW, Zhang D, Zong H, Wang Y, Bergeron R, Kim JK, Cushman SW, Cooney GJ, Atcheson B, White MF, Kraegen EW, and Shulman GI.** Mechanism by which fatty acids inhibit insulin activation of insulin receptor substrate-1 (IRS-1)-associated phosphatidylinositol 3-kinase activity in muscle. *J Biol Chem* 277: 50230-50236, 2002.
192. **Yu CF, Cresswell J, Loffler MG, and Bogan JS.** The glucose transporter 4-regulating protein TUG is essential for highly insulin-responsive glucose uptake in 3T3-L1 adipocytes. *Journal of Biological Chemistry* 282: 7710-7722, 2007.
193. **Zorzano A, Balon TW, Garetto LP, Goodman MN, and Ruderman NB.** Muscle alpha-aminoisobutyric acid transport after exercise: enhanced stimulation by insulin. *Am J Physiol* 248: E546-552, 1985.

Chapter III

Study 1:

Clustering of GLUT4, TUG, and RUVBL2 Protein Levels Correlate with Myosin Heavy Chain Isoform Pattern in Skeletal Muscles, but AS160 and TBC1D1 Levels Do Not

Abstract

Skeletal muscle is a heterogeneous tissue. To further elucidate this heterogeneity, we probed relationships between myosin heavy chain (MHC) isoform composition and abundance of GLUT4 and four other proteins that are established or putative GLUT4 regulators [Akt substrate of 160 kDa (AS160), Tre-2/Bub2/Cdc 16-domain member 1 (TBC1D1), Tethering protein containing an UBX-domain for GLUT4 (TUG) and RuvB-like protein two (RUVBL2)] in 12 skeletal muscles or muscle regions from Wistar rats [adductor longus, extensor digitorum longus, epitrochlearis, gastrocnemius (mixed, red and white), plantaris, soleus, tibialis anterior (red and white), tensor fasciae latae and white vastus lateralis]. Key results were: 1) significant differences found among the muscles (range of muscle expression values) for GLUT4 (2.5-fold), TUG (1.7-fold), RUVBL2 (2.0-fold) and TBC1D1 (2.7-fold), but not AS160; 2) significant positive correlations for pairs of proteins: GLUT4 versus TUG (R=0.699), GLUT4 versus RUVBL2 (R=0.613), TUG versus RUVBL2 (R=0.564), AS160 versus TBC1D1 (R=0.293) and AS160 versus TUG (R=0.246); 3) significant positive correlations for % MHC-I: GLUT4 (R=0.460), TUG (R=0.538) and RUVBL2 (R=0.511); 4) significant positive correlations for % MHC-IIa: GLUT4 (R=0.293) and RUVBL2 (R=0.204); 5) significant negative correlations for

%MHC-IIb versus: GLUT4 (R=-0.642), TUG (R=-0.626) and RUVBL2 (R=-0.692); and 6) neither AS160 nor TBC1D1 significantly correlated with MHC isoforms. In 12 rat muscles, GLUT4 abundance tracked with TUG and RUVBL2 and correlated with MHC isoform expression, but was unrelated to AS160 or TBC1D1. Our working hypothesis is that some of the mechanisms that regulate GLUT4 abundance in rat skeletal muscle also influence TUG and RUVBL2 abundance.

Introduction

Skeletal muscle is a heterogeneous tissue, and different muscles in the same individual can vary greatly with regard to metabolic characteristics, including the capacity for insulin-mediated glucose uptake. Henriksen et al. (19) found that the GLUT4 protein abundance of four different isolated rat skeletal muscles varied by ~4-fold, with the following rank-order: flexor digitorum brevis (FDB) > soleus > extensor digitorum longus (EDL) > epitrochlearis. Based on previously published data for the fiber type compositions (based on myosin ATPase staining) of the FDB (6), epitrochlearis (28), soleus and EDL (2), it was evident that the two muscles that were known to be largely composed of slow-oxidative (SO) or fast-oxidative-glycolytic (FOG) fibers (soleus and FDB, respectively) were characterized by greater GLUT4 abundance compared to the other two muscles that were predominantly composed of fast-glycolytic (FG) fibers (epitrochlearis and EDL). The most comprehensive study to measure both GLUT4 abundance and fiber type composition in multiple rat skeletal muscles was performed by Megeney et al. (27) who evaluated six different muscles or muscle regions and correlated percent fiber type composition of the muscles (determined by ATPase staining in the same six muscles from other rats) with GLUT4 abundance. They found a significant positive correlation with percent of oxidative fibers (SO + FOG) and a significant negative correlation with the percent of FG fibers. We have extended the knowledge from earlier studies by measuring both GLUT4 and fiber type (based on myosin heavy chain isoform, MHC-I, MHC-IIa, MHC-IIb and MHC-IIx expression) in 12 different rat muscles or regions of muscles.

Although GLUT4 is the ultimate mediator of muscle glucose transport capacity, a number of other proteins participate in insulin's regulation of GLUT4 function. Akt substrate of 160 kDa (also known as TBC1D4) and TBC1D1 are two paralog Rab GTPase (GAP) proteins that were recently recognized as key signaling proteins that can control GLUT4 trafficking and

glucose transport (8, 10-11, 33). Taylor et al. (40) reported that the abundance of each of these proteins varied greatly among three mouse skeletal muscles. AS160 protein abundance was ~10-fold greater in the soleus compared to the tibialis anterior (TA) and the EDL. TBC1D1 abundance was much greater for the TA compared to the EDL (~3-fold) and the soleus (~10-fold). They also noted that TBC1D1 expression appeared to track with the MHC-IIx content of these muscles, but they did not quantitatively analyze the relationship of TBC1D1 or AS160 with each other or with MHC isoform expression. The relationship of AS160 and TBC1D1 abundance to each other or to fiber type of rat skeletal muscle has also not been reported.

Xie et al. (43) recently identified RuvB-like protein two (RUVBL2) as a protein that is physically associated with AS160 in 3T3-L1 adipocytes. Genetic depletion of RUVBL2 in 3T3-L1 cells resulted in a decrease in both phosphorylated AS160 and insulin-stimulated glucose uptake. In addition, the epididymal fat pads of obese diabetic KKAy mice compared to normal controls had greatly reduced RUVBL2 expression. The relationship between RUVBL2 abundance and muscle MHC isoform composition has not been reported.

Bogan et al. (4) identified the Tethering protein containing an UBX-domain for GLUT4 (TUG) as a putative GLUT4 tethering protein that functions as part of the system that retains GLUT4 intracellularly in 3T3-L1 cells in the absence of insulin. This model has been further supported by subsequent studies in 3T3-L1 adipocytes (44-45). Under basal conditions (without insulin), TUG is associated with GLUT4 in either L6 myotubes or skeletal muscle of transgenic mice with muscle-specific overexpression of GLUT4*myc* (34). Insulin causes GLUT4 to rapidly disassociate from TUG in both L6 cells and in skeletal muscle from GLUT4*myc* transgenic mice. Although GLUT4 and TUG are known to be binding partners, their relative expression levels in skeletal muscles with diverse MHC composition are unknown.

The first major goal of this study was to extend knowledge about the relationship between MHC isoform composition and the abundance of five proteins (GLUT4, AS160, TBC1D1, RUVBL2 and TUG) that are either established or putative regulators of glucose transport in rat skeletal muscle. The second major goal was to determine if the abundance of any of these proteins were significantly associated with each other. Notable aspects of the experimental design were: 1) the inclusion of a large number of skeletal muscles (12 muscles or regions of muscles) with diverse fiber type compositions; 2) the assessment of relative MHC isoform levels and abundance of GLUT4 and four other proteins (TUG, RUVBL2, TBC1D1 and

AS160) for which very little was known with regard to relative expression by rat skeletal muscles; and 3) immunoblotting for each of the proteins and the determination of relative MHC isoform levels were all performed using the same muscles from the same rats. We hypothesized that: 1) the abundance of each of the 5 proteins would vary among the 12 different muscles; 2) % MHC-I and % MHC-IIa would be positively correlated with GLUT4 and TUG; 3) % MHC-IIb would be negatively correlated with GLUT4 and TUG; 4) GLUT4 would be positively correlated with TUG; 5) % MHC-IIx would be positively correlated with TBC1D1 and negatively correlated with AS160 and RUVBL2; 6) AS160 would be positively correlated with RUVBL2; and 7) TBC1D1 would be negatively correlated with AS160 and RUVBL2.

Methods

Materials

The reagents and apparatus for SDS-PAGE and immunoblotting were purchased from Bio-Rad (Hercules, CA). Bicinchoninic acid protein assay reagent (no. 23227) and West Dura Extended Duration Substrate were from Pierce Biotechnology (Rockford, IL). Anti-AS160 (no. 07-741) was from Millipore (Billerica, MA). Anti-RUVBL2 (no. ab36569) was from Abcam (Cambridge, MA). Anti-TBC1D1 was provided by Dr. Makoto Kanzaki (Tohoku University). Anti-TUG was previously described (4). Anti-GLUT4 was provided by Dr. Samuel Cushman (NIH, Bethesda, MD).

Animal Treatment

Procedures for animal care were approved by the University of Michigan Committee on Use and Care of Animals. Male Wistar rats (150-220 g; Harlan, Indianapolis, IN) were provided with rodent chow (Lab Diet; PMI Nutritional International, Brentwood, MO) and water ad libitum. Rats were anesthetized with an intraperitoneal injection of sodium pentobarbital (50 mg/kg wt). While rats were under deep anesthesia, the following muscles or portions of muscles were dissected out and freeze-clamped: adductor longus (AL), extensor digitorum longus (EDL), epitrochlearis (EPI), mixed gastrocnemius (GAS_M), red gastrocnemius (GAS_R), white gastrocnemius (GAS_W), plantaris (PLAN), soleus (SOL), red tibialis anterior (TA_R), white tibialis anterior (TA_W), tensor fasciae latae (TFL), and white vastus lateralis (VL_W). The deep

red (GAS and TA) and superficial white (GAS, TA and VL) regions of the relevant muscles were identified based on visual inspection and dissected out. The GAS_M was dissected from the muscle's medial head.

Muscle Homogenization

Frozen muscles were weighed, transferred to pre-chilled glass tissue grinding tubes (Kontes, Vineland, NJ), and homogenized in ice-cold lysis buffer (20 mM Tris-HCL, 150 mM NaCl, 1% Triton X-100, 1 mM Na_3VO_4, 1 mM EDTA, 1 mM EGTA, 2.5 mM NaPP, 1 mM β-glycerophosphate, 1 µg/ml leupeptin, 1mM PMSF at 1 ml/muscle) using a glass pestle attached to a motorized homogenizer (Caframo, Wiarton, ON). Homogenates were then rotated at 4°C for 1 h and an aliquot of the homogenate (whole homogenate) was taken for myosin heavy-chain (MHC) analysis prior to being centrifuged (1,000 g for 10 min at 4°C). Portions of the supernatant and the whole homogenate were used to determine protein concentration according to the manufacturer's protocol (Pierce Biotechnology no. 23227). The remaining supernatant was stored at -80°C until further analyzed. A portion of the whole homogenate was immediately used to determine MHC isoform composition as described below.

Relative Abundance of Myosin Heavy Chain Isoforms

Laemmli sample buffer was added to 5 µg of the whole homogenate prior to heating for 10 min at 90°C. Samples where then run at 45 V for 24 h at 4 °C on an 8% acrylamide-bis (50:1), 30% glycerol gel as described by Talmadge and Roy (39). Gels were then trimmed and stained with Coomassie Blue for 1 h while gently rotating, followed by destaining for 3-4 h in 20% methanol and 10% acetic acid solution. MHC bands were quantified using densitometry.

Immunoblotting

Homogenized muscle lysates were boiled for 5-10 min in sodium dodecyl sulfate loading buffer then separated via PAGE and electrophoretically transferred to nitrocellulose membranes. Samples were then rinsed with Tris-buffered saline plus Tween (TBST) (140 mM NaCl, 20 mM Tris base, pH 7.6, and 0.1% Tween), blocked with 5% nonfat dry milk in TBST for 2 h at room temperature, washed 3 x 5 min at room temperature and treated with the appropriate primary antibody (1:1,000 in TBST + 5% BSA) overnight at 4°C. Blots were then washed 6 x 5 min with

TBST, incubated with the secondary antibody, goat anti-rabbit IgG horse horseradish peroxidase conjugate (1:20,000 in TBST + 5% milk) for 1 h at room temperature. They were washed again 6 x 5 min with TBST then 4 x 5 min TBS, and subjected to enhanced chemiluminescence (West Dura Extended Duration Substrate; #34075; Pierce). The chemiluminescence of protein bands on nitrocellulose membranes was quantified using electrically cooled CCD camera technology (Alpha Innotech, San Leandro, CA). The individual values for the samples were normalized to the mean value for all of the samples on the blot.

Statistics

The data used for comparison of protein abundance among the 12 different muscles or muscle regions were analyzed by one-way ANOVA, and the Bonferroni correction was used to identify the source of significant variance for data. If data failed the normality test, the Kruskal-Wallis one-way ANOVA on Ranks and the Tukey post hoc test were used. The nonparametric Spearman Rank Order Correlation (for individual data rather than on mean values for each of the 12 muscles) was used to assess the relationships between abundance of each pair of the proteins studied (e.g., between GLUT4 vs. TUG) and between abundance of each protein and % of each MHC isoform (MHC-I, MHC-IIa, MHC-IIb and MHC-IIx). The statistical analyses were performed using Sigma Plot (San Rafael, CA) version 11.0. Data are expressed as means ± SE. $P \leq 0.05$ was considered to be statistically significant.

Results

Relative Abundance of Myosin Heavy Chain (MHC) Isoforms

The relative abundance (%) of each MHC isoform for the 12 muscles or muscle regions is summarized in Table 3.1 and Figure 3.1.

Relative Protein Abundance

In the 12 muscle or muscle regions studied the relative abundance of GLUT4 differed as follows: SOL was significantly greater ($P<0.05$) than the EDL, EPI, GAS_M, GAS_W, TA_W, TFL, and VL_W; AL was significantly greater ($P<0.05$) than the EPI, GAS_M, GAS_W, TA_W, TFL, and

VL_W; the TA_R, and GAS_R were significantly greater ($P<0.05$) than the EPI, GAS_W, TA_W, and VL_W; PLAN was significantly greater ($P<0.05$) than the EPI, GAS_W, and TA_W; EDL was significantly greater ($P<0.05$) than the EPI and VL_W (Figure 3.2). In the 12 muscles studied the GLUT4 abundance had a range of 2.5-fold (the VL_W had the lowest and the SOL had the highest values).

TUG protein abundance in the AL and SOL was significantly greater ($P<0.05$) than all of the other muscles studied (Figure 3.3). The range of TUG abundance was 1.7-fold (the EPI had the lowest and the SOL had the highest values).

The relative abundance of RUVBL2 in the 12 muscle or muscle regions studied differed as follows: SOL was significantly greater ($P<0.05$) than the EDL, EPI, GAS_W, TA_W, and VL_W; AL was significantly greater ($P<0.05$) than the EDL, GAS_W, TA_W, and VL_W; both PLAN and TFL were significantly greater ($P<0.05$) than TA_W and VL_W; GAS_R was significantly greater ($P<0.05$) than the VL_W (Figure 3.4). The range of RUVBL2 abundance was 2.0-fold (the VL_W had the lowest and the SOL had the highest values).

AS160 protein abundance did not differ significantly among any of the muscles or muscle regions studied (Figure 3.5).

TBC1D1 protein abundance in both the GAS_W and EDL was significantly greater ($P<0.05$) than both the TFL and EPI (Figure 3.6). The GAS_R and GAS_M both had significantly greater ($P<0.05$) TBC1D1 abundance compared to the TFL. The range for TBC1D1 abundance was 2.7-fold (the TFL had the lowest and GAS_R had the highest values).

Correlations

As expected, the % MHC-I values were high for the AL (90%) and SOL (88%). These muscles compared to the other muscle studied were also characterized as having higher values for GLUT4, TUG or RUVBL2. In an earlier study, Megeney et al. (27) evaluated 6 rat skeletal muscles (including the SOL, but not the AL) for correlations between GLUT4 and fiber type. For some comparisons, they identified the SOL as an outlier and excluded the SOL data from the correlation analysis. In the current study, correlations were performed both with and without

exclusion of the AL and SOL data to make it possible to assess the data both with and without the influence of these muscles that have exceptional MHC profiles.

The following pairs of proteins were significantly and positively correlated with each other either with all of the data or with the AL and SOL data excluded: GLUT4 vs. TUG (Figure 3.7A), GLUT4 vs. RUVBL2 (Figure 3.7B), TUG vs. RUVBL2 (Figure 3.7C), AS160 vs. TBC1D1 (Figure 3.7D) and AS160 vs. TUG (Figure 3.7E).

There were significant positive correlations for % MHC-I and the abundance of the following proteins with either all of the data or excluding the AL and SOL data: TUG (Figure 3.8B) and RUVBL2 (Figure 3.8C). % MHC-I vs. GLUT4 was significantly positively correlated only when all of the data were in the analysis (Figure 3.8A).

There were significant positive relationships between % MHC-IIa and the abundance of the following proteins either with all of the data or excluding the AL and SOL data: GLUT4 (Figure 3.9A) and RUVBL2 (Figure 3.9C). TUG was significantly positively correlated with % MHC-IIa only when the AL and SOL data were excluded (Figure 3. 9B).

There were significant negative correlations for % MHC-IIb and the abundance of the following proteins either using all of the data or excluding the AL and SOL data: GLUT4 (Figure 3.10A), TUG (Figure 3.10B), and RUVBL2 (Figure 3.10C).

There was a significant negative correlation between % MHC-IIx and the abundance of TUG using all of the data; however, when the AL and SOL data were excluded, the correlation between % MHC-IIx and TUG was significant, but positive (Figure 3.11B). In addition, when the AL and SOL data were excluded there were significant positive correlations for % MHC-IIx with either GLUT4 (Figure 3.11A) or RUVBL2 (Figure 3.11C).

Neither AS160 nor TBC1D1 significantly correlated with the relative abundance of any of the MHC isoforms based on analysis using either all of the data or excluding the AL and SOL data (Figure 3.12-15).

Discussion

This study provides novel information about five proteins (GLUT4, TUG, RUVBL2, AS160 and TBC1D1) that are either established or putative regulators of glucose transport. The results supported some, but not all of the hypotheses about the relationships of these proteins with each other and with relative MHC isoform expression. The hypotheses that related to GLUT4 and TUG were largely supported: the abundance of both GLUT4 and TUG varied significantly among the muscles that were studied; the % MHC-I abundance was positively correlated to either GLUT4 or TUG; the % MHC-IIb abundance was negatively correlated with either GLUT4 or TUG; and GLUT4 and TUG were positively correlated with each other. As was hypothesized, several of the muscles were significantly different with regard to TBC1D1 abundance. However, none of the other hypotheses related to TBC1D1 or AS160 were supported by the results: AS160 and TBC1D1 were positively rather than negatively correlated with each other; neither TBC1D1 nor AS160 was significantly correlated with the relative abundance of any MHC isoform; and no significant differences were detected for AS160 abundance among the muscles studied. The results also revealed several unanticipated insights about RUVBL2, including significant positive correlations for RUVBL2 with GLUT4, TUG, % MHC-I and % MHC-IIa and a significant negative correlation for RUVBL2 with % MHC-IIb. However, RUVBL2 was not significantly correlated with either AS160 or TBC1D1.

As expected, the 12 different muscles or muscle regions that were studied were diverse with regard to the relative abundance of MHC isoforms. The results for relative MHC isoform abundance were in good agreement with previously published values for the AL, SOL (20), GAS_M (39), GAS_R, GAS_W, EDL (35), EPI (1), PLAN (29), and VL_W (26). The current study was apparently the first to report MHC isoform values for the TFL, TA_R or TA_W from rats.

Previous studies that have assessed the relationship between fiber type composition of skeletal muscle and GLUT4 abundance have relied on histological assessment of myosin ATPase for fiber typing. Measurement of MHC isoform by SDS-PAGE provides important advantages for quantitative analysis of skeletal muscle when compared to fiber type composition based on myosin ATPase activity (30). The rank order for relative values of GLUT4 by the different muscles or muscle regions were similar to the results from several previous publications that evaluated GLUT4 abundance for three or more of the rat skeletal muscles assessed in the current

study, including the SOL, EPI and EDL (19), GAS_R, GAS_W, PLAN, EDL, and SOL (5), GAS_R, GAS_W, PLAN, and SOL (41), TA_R, TA_W, and EDL (21), and SOL, PLAN, EDL, GAS_R and GAS_W (27). Megeney et al. (27) assessed GLUT4 abundance and fiber type composition (using myosin ATPase staining) in rat skeletal muscles. They found a significant positive correlation for % SO + FOG fibers vs. GLUT4, and a significant negative correlation for FG fibers vs. GLUT4. In the current study, there were significant positive correlations for GLUT4 with either % MHC-I or % MHC-IIa vs. GLUT4, and a significant negative correlation for % MHC-IIb vs. GLUT4. The ~2.5-fold range from the lowest to highest values in the current study compares to ranges from ~2- to ~4-fold reported in earlier studies that evaluated several rat skeletal muscles with a range of fiber type compositions (5, 19, 21, 27, 41).

A key outcome of this study was that the relative expression of three proteins (GLUT4, TUG and RUVBL2) clustered together based on comparisons of the muscles that were studied. These results raise the possibility that the expression of the three proteins may be modulated, in part, by shared mechanisms. Skeletal muscle MHC isoform expression is influenced by conditions that alter neuromuscular activity, including spinal cord injury, hindlimb unloading, chronic bed rest, spaceflight, compensatory overloading, chronic electrical stimulation and exercise training (38). Although the MHC isoform expressed by skeletal muscle is unlikely to directly determine GLUT4 expression levels, the abundance of GLUT4 in skeletal muscle has also been reported to be responsive to many of these same interventions. For example, chronic electrical stimulation of skeletal muscle (21, 23) or endurance exercise training (5, 32, 36) can result in an increase in GLUT4 abundance, and denervation can reduce muscle GLUT4 abundance (27). To date, the effects of increased or decreased neuromuscular activity on muscle TUG or RUVBL2 abundance have not been reported, but it seems possible that their expression might also be altered in a manner that is similar to activity-related shifts in GLUT4 abundance.

The significant correlation between TUG and GLUT4 abundance in skeletal muscles was a novel, but not unexpected finding. Because TUG and GLUT4 can physically associate with each other, and because TUG-GLUT4 binding appears to play a role in the subcellular localization of GLUT4, altering the abundance of one of the binding partners may potentially influence the abundance of the other. Consistent with a role for TUG in controlling GLUT4 protein levels, genetic depletion of TUG by siRNA in 3T3-L1 cells resulted in a marked decrease

in GLUT4 protein abundance that appeared to be attributable to greater GLUT4 protein degradation (45). However, the possibility that altered GLUT4 abundance might influence TUG abundance has not been assessed.

RUVBL2 was evaluated because it was recently reported to be physically associated with AS160 in 3T3-L1 adipocytes and because genetic depletion of RUVBL2 in 3T3-L1 cells induced decrements in both phosphorylated AS160 and insulin-stimulated glucose uptake without altering the abundance of Akt or AS160 protein (43). However, RUVBL2 has received much more scrutiny for its roles in the regulation of DNA structure and function. It is a member of the AAA+ (ATPase associated with diverse cellular activities) family of DNA helicases and has been implicated in the response to DNA double-strand breaks and the regulation of gene expression (16). Although RUVBL2 has been shown to have important functions in the nucleus, it is localized in both the cytosol and the nucleus (43). The current study, apparently the first to assess RUVBL2 protein abundance in skeletal muscle, revealed significant positive correlations for RUVBL2 with % MHC-I or MHC-IIa, and a significant negative correlation for RUVBL2 with % MHC-IIb. The causes and functional consequences of these differences in RUVBL2 expression levels are not currently known.

Taylor et al. (40) found a 10-fold range in the relative abundance of TBC1D1 in skeletal muscles from mice, with the rank order of TA > EDL > SOL. TBC1D1 abundance also varied among the rat skeletal muscles evaluated in the current study, with 2.7-fold greater values for GAS_R (highest) vs. TFL (lowest) muscle. TBC1D1 abundance for the rat EDL was very similar to the GAS_R. The TBC1D1 values for the SOL, TA_R and TA_W were intermediate, but not significantly different than the EDL (Figure 3.6). Taylor et al. (40) also measured MHC isoform abundance and noted that TBC1D1 appeared to track with the type MHC-IIx content of the TA, EDL and SOL muscles, although quantitative analysis for this relationship was not reported. However, there was no evidence that TBC1D1 abundance in rat skeletal muscle was related with relative expression of MHC-IIx or with any of the other MHC isoforms. An et al. (15) reported that increasing TBC1D1 expression of mouse TA muscle by ~7-fold did not alter glucose uptake (basal, insulin-stimulated or contraction-stimulated) or abundance of AS160 or GLUT4. The causes and functional consequences of the different levels of TBC1D1 protein abundance in rat skeletal muscles remain to be determined.

AS160 and TBC1D1 have substantial structural similarities and appear to have overlapping functional properties, including the regulation of GLUT4 trafficking in skeletal muscle (8). There were no significant differences for AS160 abundance among the rat skeletal muscles in the current study. Consistent with these results, Gupte et al. (17) found no difference between the EPI and SOL of rats for AS160 abundance. However, the current results are in contrast to substantial muscle-specific differences in the mouse, in which AS160 protein abundance was ~10-fold greater for the SOL compared to TA or EDL muscles (40). Increasing AS160 abundance in mouse TA muscle by ~8-fold (i.e., to levels nearly as great as the endogenously high values found in mouse SOL) did not alter basal or insulin-stimulated glucose uptake or expression of GLUT4 protein (24). However, contraction-stimulated glucose uptake was reduced ~24% with AS160 overexpression compared to empty vector controls (24). Endurance trained rats fed a high fat diet compared to sedentary controls eating the same diet had a small (15%), but significant decrease in muscle AS160 abundance concomitant with a moderately large (50%) increase in muscle GLUT4 protein content (25). Endurance training by lean or obese humans also resulted in elevated muscle GLUT4 protein levels (~20-50%), but in contrast to the results for rats, there were also small (~20-30%) training-induced increases in AS160 abundance (14, 42). Either humans with type 2 diabetes compared to non-diabetic controls (22) or insulin resistant obese Zucker rats compared to lean controls (3) have reduced insulin-mediated phosphorylation of AS160 without differences in AS160 protein abundance in skeletal muscle. Transfection of skeletal muscle of either lean or obese rats with PGC1α induced a significant increase in GLUT4 abundance without concurrent changes in AS160 content (3). There are various mechanisms for regulating AS160 function without large changes in AS160 protein abundance. For example, AS160 is acutely regulated by insulin-induced phosphorylation of key sites and subcellular localization of AS160, and there is also evidence that AS160 function is modulated by its association with other proteins, e.g., 14-3-3 (31) and possibly RUVBL2 (43). Clarification of how muscles differ with regard to these regulatory processes will be needed to fully appreciate AS160's role in determining muscle-related differences for glucose transport with insulin and/or exercise.

The current study evaluated GLUT4 and related proteins in more muscles than previous publications. However, we opted to not include the flexor digitorum brevis (FDB). In our experience (7, 9), other muscles offer advantages compared to the FDB for studying GLUT4,

insulin signaling proteins and glucose uptake. Advantages of the epitrochlearis or soleus vs. FDB include a larger data base of publications for comparing the results, the presence of less connective tissue in the muscle, and relatively greater fold-increases in insulin-mediated glucose uptake.

It is important to interpret the correlations between protein abundance and relative levels of MHC isoforms with care. Obviously, correlations do not prove causality. Furthermore, it is inappropriate to assume that expression of a given protein is uniform in all of the fibers expressing a certain MHC isoform. For example, in pooled single fibers expressing MHC-I collected from sedentary humans, GLUT4 abundance was greater for the fibers taken from the vastus lateralis compared to fibers collected from either the soleus or triceps brachii (12). In addition, hybrid muscle fibers that express more than one MHC isoform can be relatively common in rat skeletal muscles (37). The correlation for a given protein's abundance with the % of MHC isoforms with relatively lower expression (MHC-IIa and MHC-IIx) can be highly influenced by the levels of the more abundant isoforms (MHC-I and MHC-IIb) in the group of muscles being studied. For example, the correlation between MHC-IIx and TUG was significantly negative when all 12 muscles were included in the analysis, but the correlation was significantly positive when the analysis was performed after excluding the muscles with extremely high levels of MHC-I (SOL and AL, which have 0 or 1% MHC-IIx). Nonetheless, careful examination of the correlations between the abundance of a given protein and the relative levels of the MHC isoforms can provide useful insights.

In conclusion, an important result of this study was the identification of a cluster of three proteins (GLUT4, TUG and RUVBL2) that tracked together in the skeletal muscles that were evaluated. GLUT4, TUG and RUVBL2 were each also positively correlated with % MHC-I and inversely correlated with the % MHC-IIb levels. The paralog proteins AS160 and TBC1D1 are 47% identical, share several important functional domains, and are implicated as regulators of glucose transport (40). AS160 and TBC1D1 were positively correlated with each other, but neither of these proteins was significantly correlated with the relative levels of any of the MHC isoforms. Earlier research has clearly documented that altered neuromuscular activation of skeletal muscle can markedly alter GLUT4 protein levels (5, 13, 21, 23, 36). Training effects on TUG and RUVBL2 abundance have apparently not been assessed to date. Given that SOL

compared to EDL muscles from sedentary male Wistar rats have much greater levels of motor unit activation (18), it is notable that the SOL compared to the EDL had significantly greater values for GLUT4, TUG and RUVBL2. Our working hypothesis is that TUG and RUVBL2 protein content in rat skeletal muscle are regulated by mechanisms that, at least in part, are similar to those that control GLUT4 protein abundance and that each is influenced by the level of neuromuscular activation.

Acknowledgments

This research was supported by grants from the National Institutes of Health (DK071771 and AG10026 to G.D.Cartee and DK075772 to J.S. Bogan). I would also like to thank Dr. James G. MacKrell for his assistance with data collection.

Table 3.1 Relative Myosin Heavy Chain Isoform Composition of Rat Skeletal Muscles

	% MHC-I	% MHC-IIa	% MHC-IIb	% MHC-IIx
AL	90 ± 10	3 ± 1	6 ± 2	1 ± 1
EDL	2 ± 1	12 ± 2	57 ± 7	29 ± 3
EPI	8 ± 2	13 ± 2	51 ± 6	28 ± 13
GAS_M	10 ± 3	10 ± 3	59 ± 9	22 ± 3
GAS_R	20 ± 4	17 ± 2	32 ± 5	31 ± 4
GAS_W	1 ± 1	7 ± 2	72 ± 9	20 ± 3
PLAN	4 ± 1	20 ± 2	44 ± 5	32 ± 4
SOL	88 ± 10	12 ± 3	0 ± 0	0 ± 0
TA_R	1 ± 1	19 ± 3	54 ± 7	26 ± 5
TA_W	1 ± 1	4 ± 1	77 ± 9	18 ± 3
TFL	8 ± 3	17 ± 2	42 ± 5	33 ± 4
VL_W	2 ± 1	1 ± 1	86 ± 10	10 ± 2

The myosin heavy chain (MHC) isoforms were separated by SDS-PAGE, gels were stained with Coomassie Blue, and bands quantified by densitometry were expressed as relative values (%) for each of the 12 skeletal muscles or muscle regions: adductor longus (AL), extensor digitorum longus (EDL), epitrochlearis (EPI), mixed gastrocnemius (GAS_M), red gastrocnemius (GAS_R), white gastrocnemius (GAS_W), plantaris (PLAN), soleus (SOL), red tibialis anterior (TA_R), white tibialis anterior (TA_W), tensor fasciae latae (TFL), and white vastus lateralis (VL_W). Values are means ± SE (n=8).

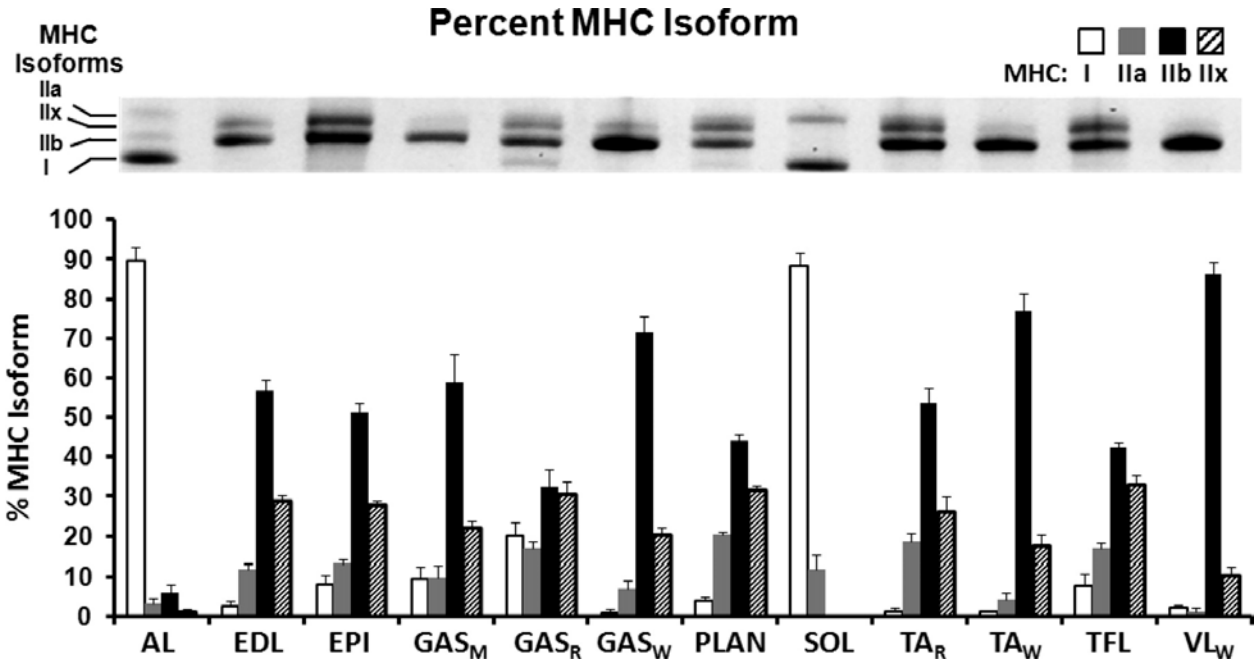

Figure 3.1

Relative abundance (%) of myosin heavy chain (MHC) isoforms in the 12 skeletal muscles or muscle regions. Open bars represent % MHC-I, gray bars represent % MHC-IIa, closed bars represent % MHC-IIb, and hatched bars represent % MHC-IIx. Values are means ±SE; n = 8 for each muscle or muscle region.

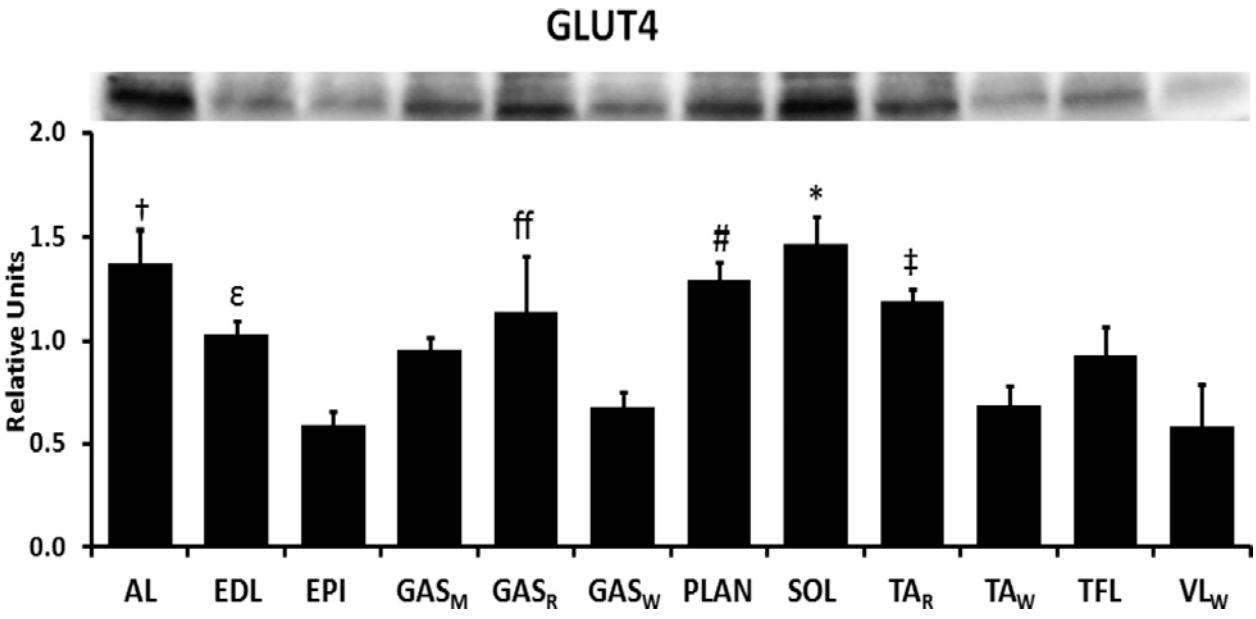

Figure 3.2

Relative GLUT4 protein abundance for 12 muscles or muscle regions. *SOL greater than: EDL, EPI, GAS_M, GAS_W, TA_W, TFL, VL_W ($P<0.05$); †AL greater than: EPI, GAS_M, GAS_W, TA_W, TFL, VL_W ($P<0.05$); $^{\#}$PLAN greater than: EPI, GAS_W, TA_W ($P<0.05$); ‡TA_R greater than: EPI, GAS_W, TA_W ($P<0.05$); ff GAS_R greater than: EPI, GAS_W, TA_W, VL_W; $P<0.05$; $^{\varepsilon}$EDL greater than: EPI, VL_W ($P<0.05$). Values are means ±SE; n = 8 for each muscle or muscle region.

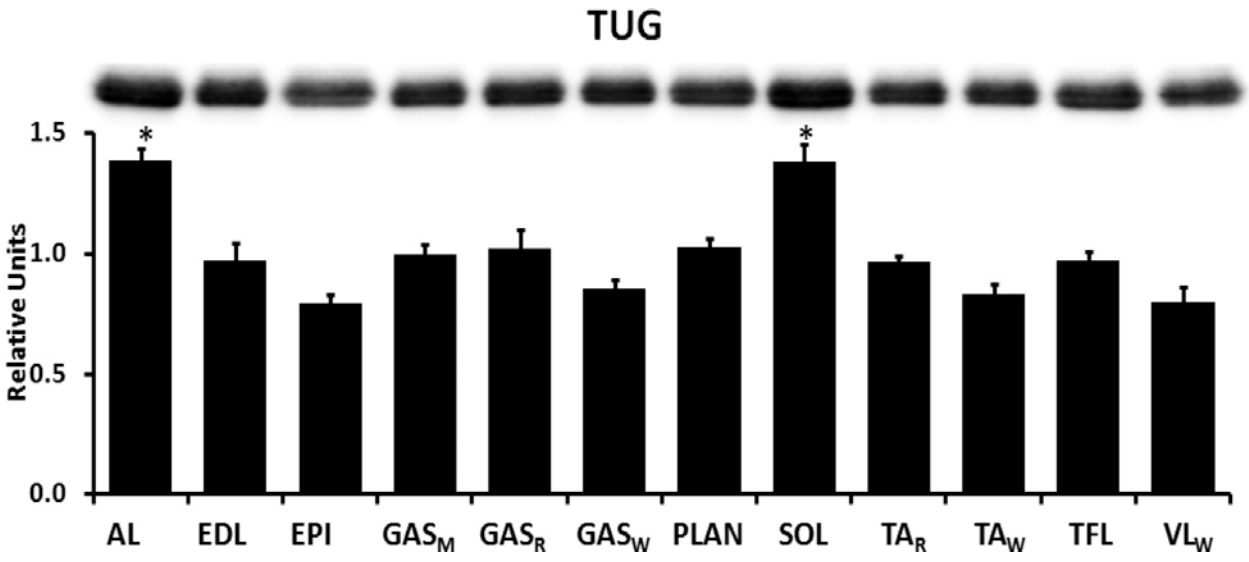

Figure 3.3

Relative TUG protein abundance for 12 muscles or muscle regions. *SOL and AL were greater than: EPI, EDL, VL W, TA_W, GAS_W ($P<0.05$). Values are means ±SE; n = 8 for each muscle or muscle region.

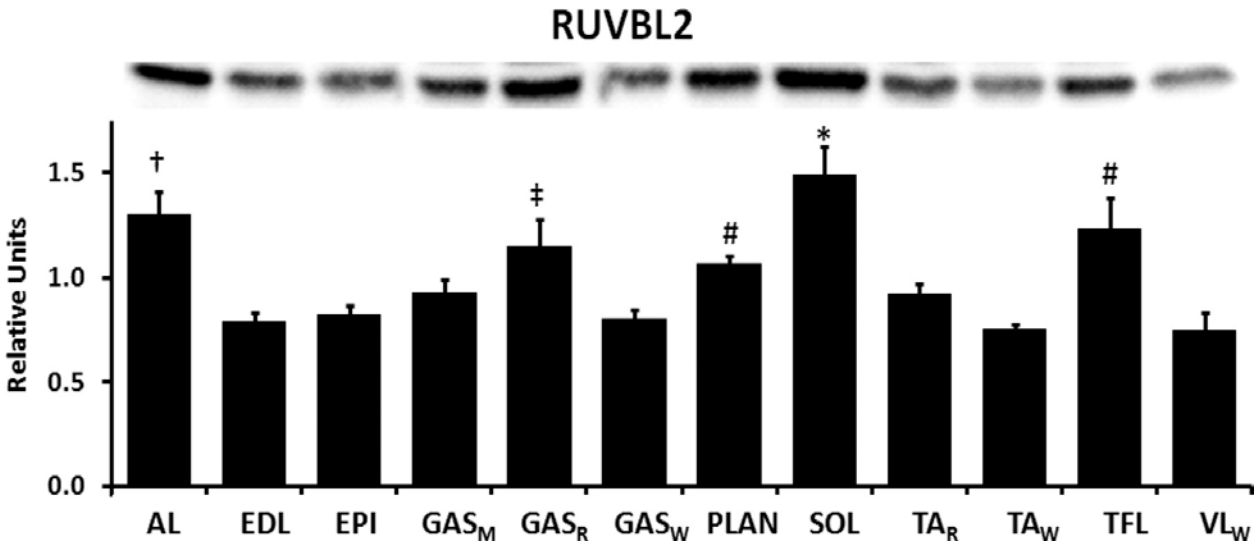

Figure 3.4

Relative RUVBL2 protein abundance for 12 muscles or muscle regions. *SOL greater than: GAS_W, VL_W, TA_W, EDL ($P < 0.05$); †AL greater than: VL_W, TA_W, GAS_W ($P < 0.05$); # TFL and PLAN greater than VL_W and TA_W ($P<0.05$); and ‡ GasR was greater than the VL_W. Values are means ±SE; n = 8 for each muscle or muscle region.

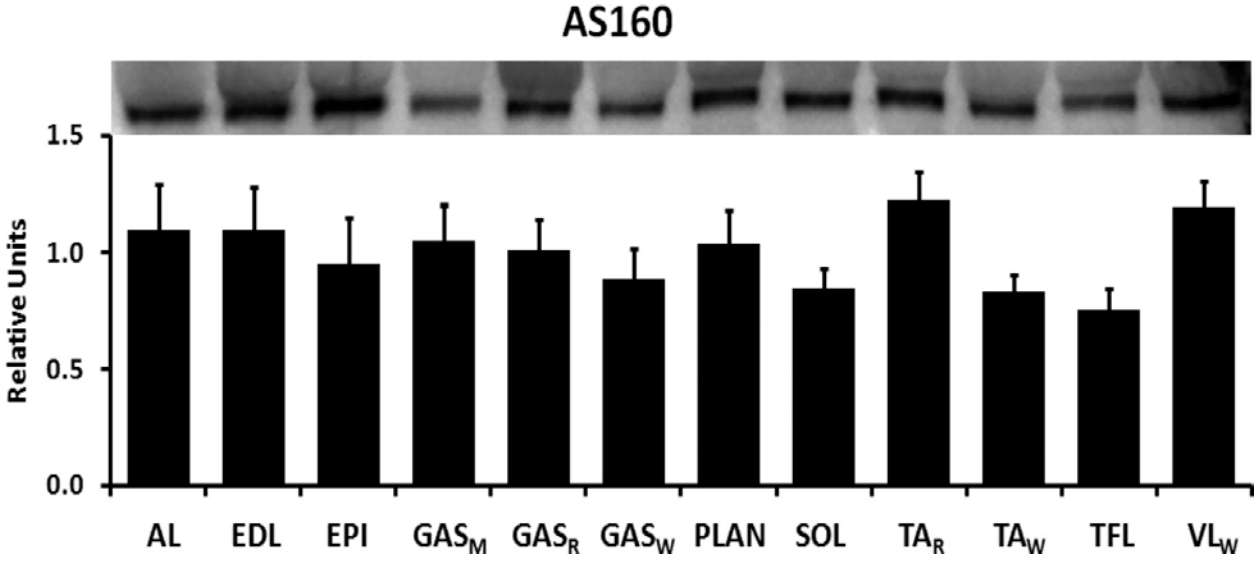

Figure 3.5

Relative AS160 protein abundance for 12 muscles or muscle regions. Values are means ±SE; n = 8 for each muscle or muscle region.

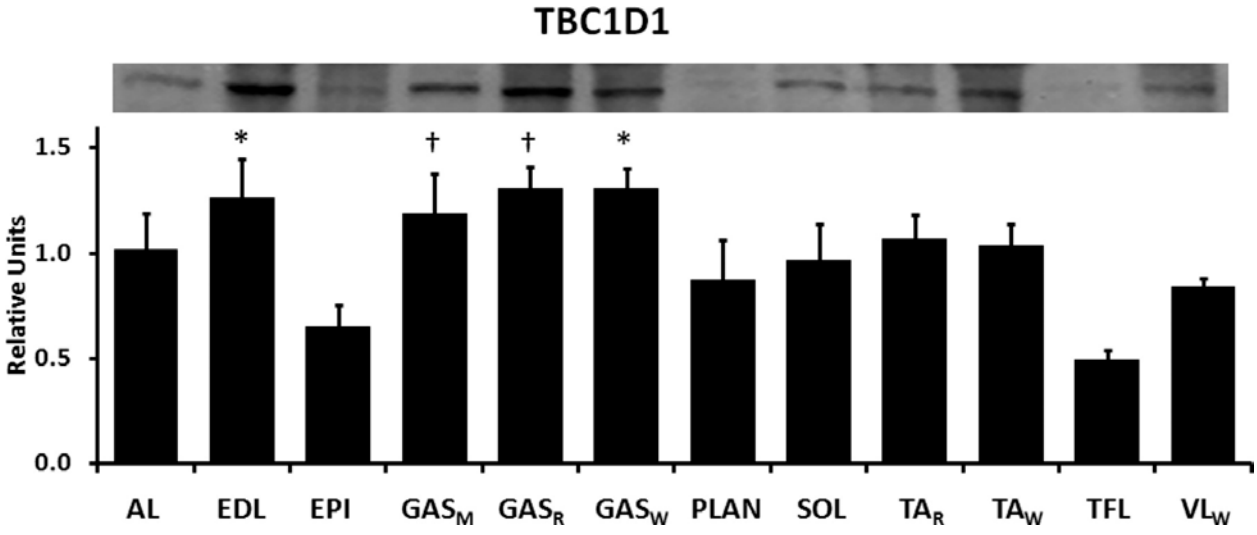

Figure 3.6

Relative TBC1D1 protein abundance for 12 muscles or muscle regions. *GAS_W and EDL are greater than EPI and TFL ($P < 0.05$); †GAS_M and GAS_R are greater than TFL ($P < 0.05$). Values are means ±SE; n = 8 for each muscle or muscle region.

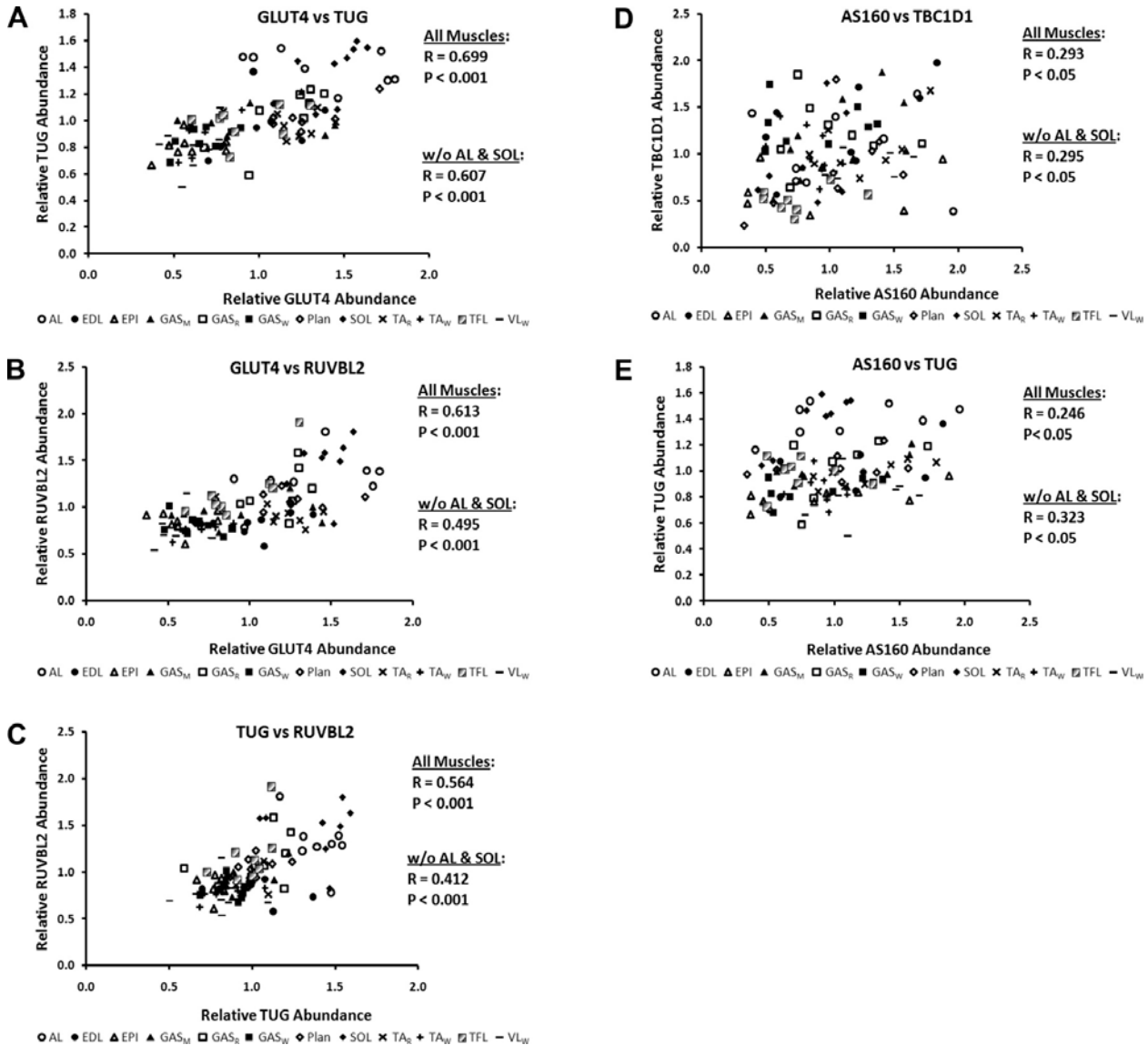

Figure 3.7A-E

Correlations between the following pairs of proteins: A: GLUT4 vs. TUG; B: GLUT4 vs. RUVBL2; C: TUG vs. RUVBL2; D: AS160 vs. TBC1D1; E: AS160 vs. TUG. The symbols represent individual data. For correlations using All Muscles, n = 96. For correlations excluding the AL and SOL data (w/o AL & SOL), n = 80.

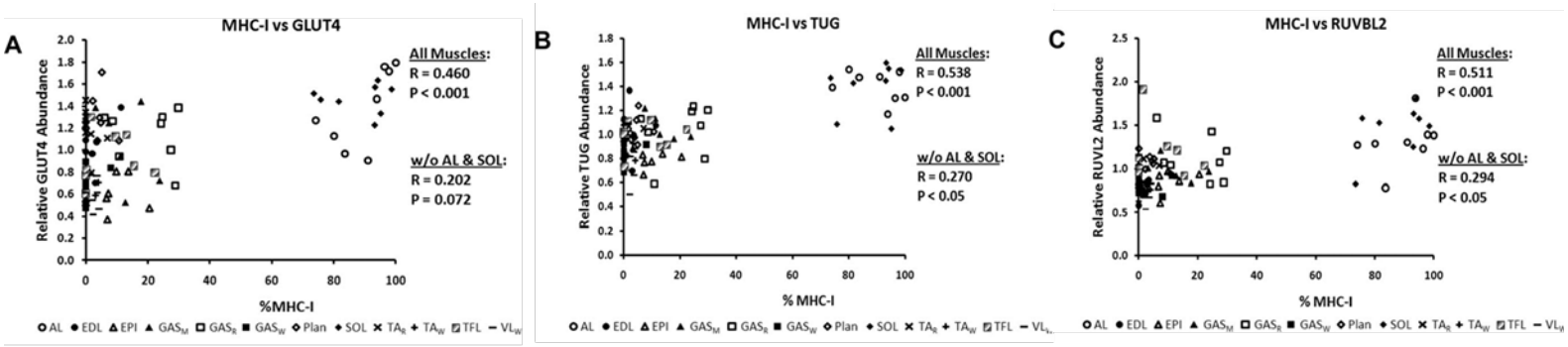

Figure 3.8A-C

Correlations between % MHC-I and the following proteins: A: GLUT4; B: TUG; and C: RUVBL2. The symbols represent individual data. For correlations using All Muscles, n = 96. For correlations excluding the AL and SOL data (w/o AL & SOL), n = 80.

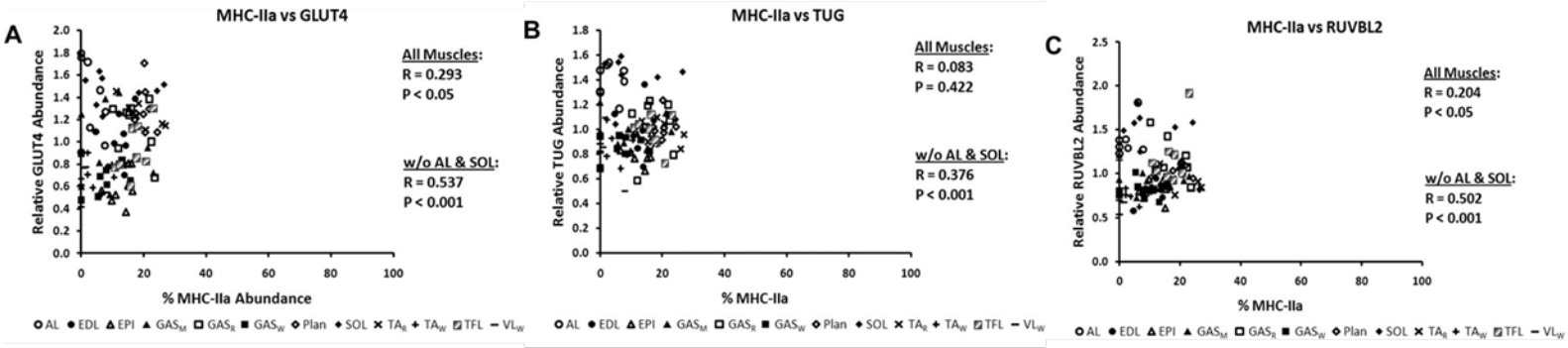

Figure 3.9A-C

Correlations between % MHC-IIa and the following proteins: A: GLUT4; B: TUG; and C: RUVBL2. The symbols represent individual data. For correlations using All Muscles, n = 96. For correlations excluding the AL and SOL data (w/o AL & SOL), n = 80.

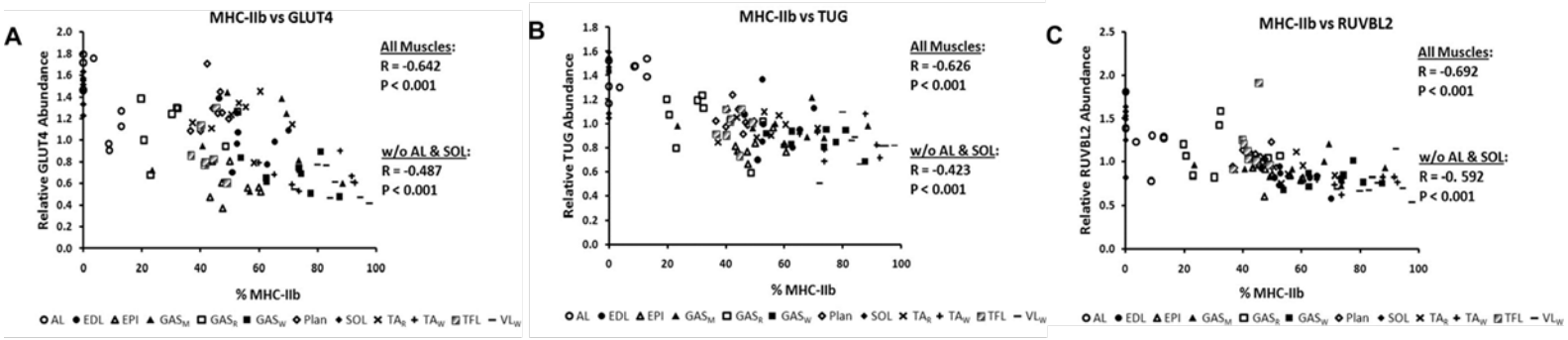

Figure 3.10A-C

Correlations between % MHC-IIb and the following proteins: A: GLUT4; B: TUG; and C: RUVBL2. The symbols represent individual data. For correlations using All Muscles, n = 96. For correlations excluding the AL and SOL data (w/o AL & SOL), n = 80.

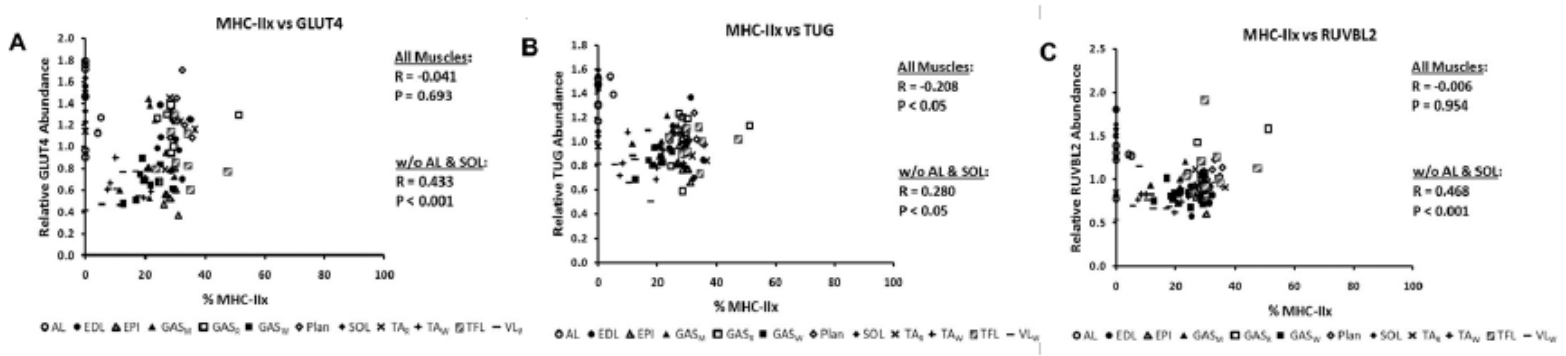

Figure 3.11A-C

Correlation between % MHC-IIx and the following proteins: A: GLUT4; B: TUG; and C: RUVBL2. The symbols represent individual data. For correlations using All Muscles, n = 96. For correlations excluding the AL and SOL data (w/o AL & SOL), n = 80.

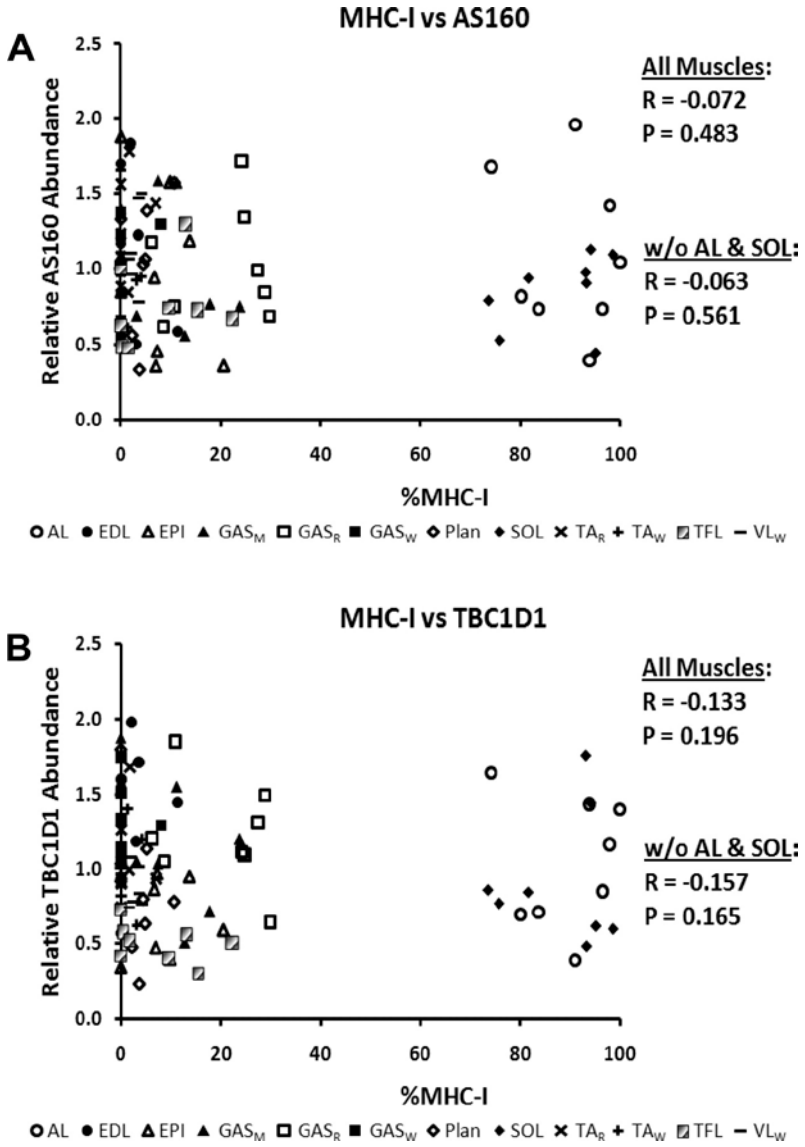

Figure 3.12A-B

Correlations between % MHC-I and the following proteins: A: AS160; and B: TBC1D1. For correlations using All Muscles, n = 96. For correlations excluding the AL and SOL data (w/o AL & SOL), n = 80.

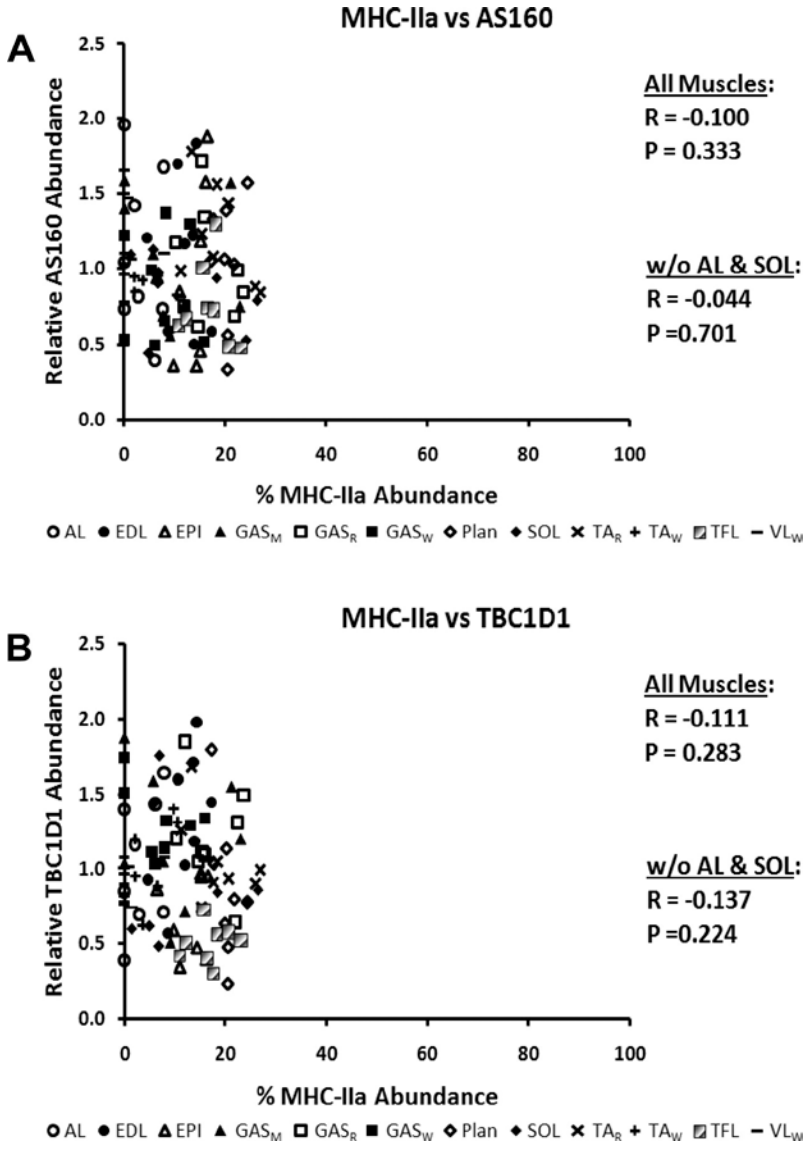

Figure 3.13A- B

Correlations between % MHC-IIa and the following proteins: A: AS160; and B: TBC1D1. For correlations using All Muscles, n = 96. For correlations excluding the AL and SOL data (w/o AL & SOL), n = 80.

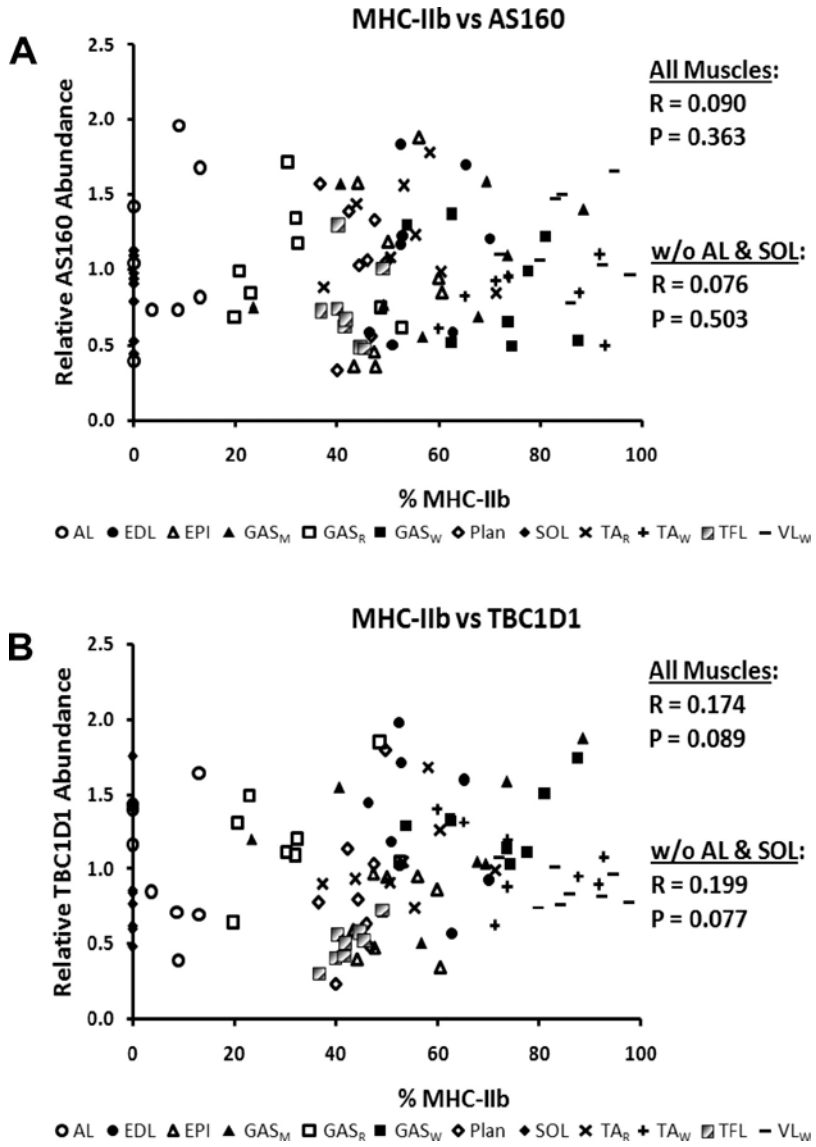

Figure 3.14A-B

Correlations between % MHC-IIb and the following proteins: A: AS160; and B: TBC1D1. For correlations using All Muscles, n = 96. For correlations excluding the AL and SOL data (w/o AL & SOL), n = 80.

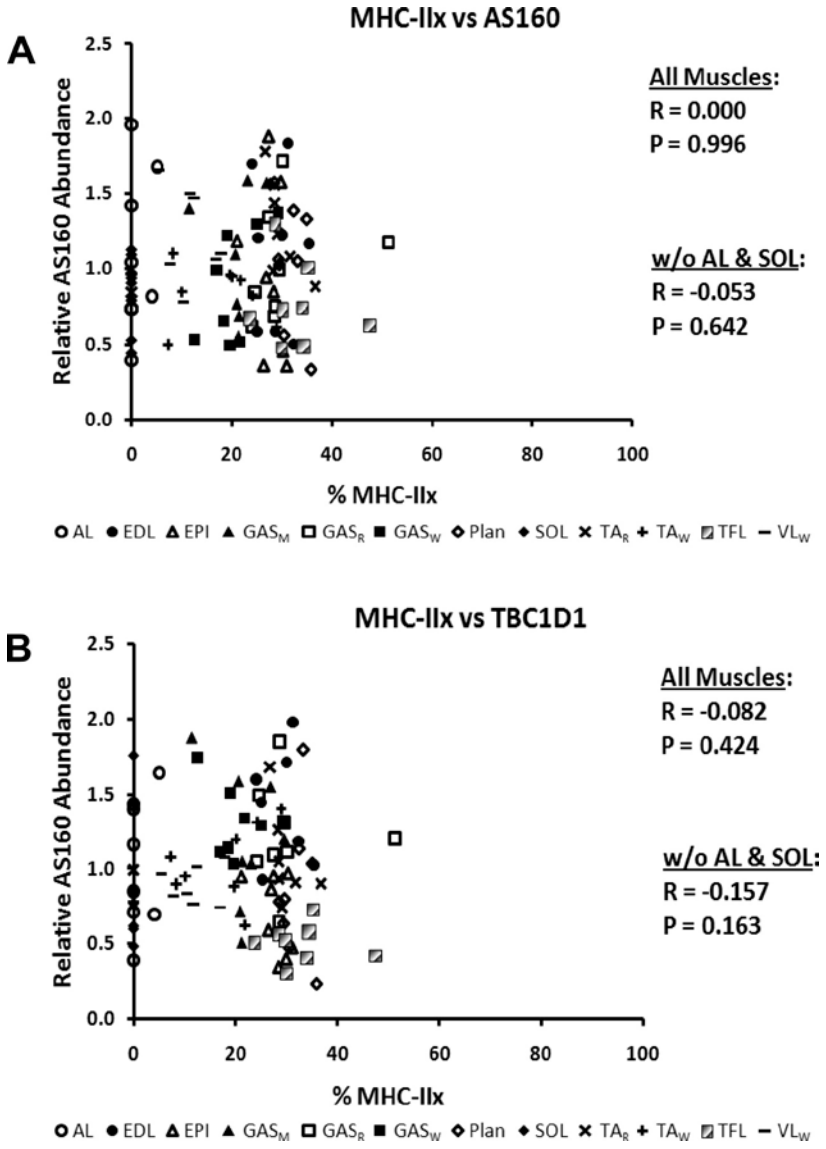

Figure 3.15A-B

Correlations between % MHC-IIx and the following proteins: A) AS160; and B) TBC1D1. For correlations using All Muscles, n = 96. For correlations excluding the AL and SOL data (w/o AL & SOL), n = 80.

References

1. **Allaf O, Goubel F, and Marini JF.** A curve-fitting procedure to explain changes in muscle force-velocity relationship induced by hyperactivity. *J Biomech* 35: 797-802, 2002.
2. **Ariano MA, Armstrong RB, and Edgerton VR.** Hindlimb muscle fiber populations of five mammals. *J Histochem Cytochem* 21: 51-55, 1973.
3. **Benton CR, Holloway GP, Han XX, Yoshida Y, Snook LA, Lally J, Glatz JF, Luiken JJ, Chabowski A, and Bonen A.** Increased levels of peroxisome proliferator-activated receptor gamma, coactivator 1 alpha (PGC-1alpha) improve lipid utilisation, insulin signalling and glucose transport in skeletal muscle of lean and insulin-resistant obese Zucker rats. *Diabetologia* 53: 2008-2019, 2010.
4. **Bogan JS, Hendon N, McKee AE, Tsao TS, and Lodish HF.** Functional cloning of TUG as a regulator of GLUT4 glucose transporter trafficking. *Nature* 425: 727-733, 2003.
5. **Brozinick JT, Jr., Etgen GJ, Jr., Yaspelkis BB, 3rd, Kang HY, and Ivy JL.** Effects of exercise training on muscle GLUT-4 protein content and translocation in obese Zucker rats. *Am J Physiol* 265: E419-427, 1993.
6. **Carlsen RC, Larson DB, and Walsh DA.** A fast-twitch oxidative-glycolytic muscle with a robust inward calcium current. *Can J Physiol Pharmacol* 63: 958-965, 1985.
7. **Cartee GD and Dean DJ.** Glucose transport with brief dietary restriction: heterogenous responses in muscles. *Am J Physiol* 266: E946-952, 1994.
8. **Cartee GD and Funai K.** Exercise and Insulin: Convergence or Divergence at AS160 and TBC1D1? *Exercise and Sport Sciences Reviews* 37: 188-195, 2009.
9. **Cartee GD, Wetter TJ, Guerra AN, and Cox TN.** Decline in muscle insulin-dependent and -independent glucose uptake but not GLUT-4 in 21- vs. 28-day-old rats. *Am J Physiol* 272: E446-452, 1997.
10. **Cartee GD and Wojtaszewski JF.** Role of Akt substrate of 160 kDa in insulin-stimulated and contraction-stimulated glucose transport. *Appl Physiol Nutr Metab* 32: 557-566, 2007.
11. **Chavez JA, Roach WG, Keller SR, Lane WS, and Lienhard GE.** Inhibition of GLUT4 Translocation by Tbc1d1, a Rab GTPase-activating Protein Abundant in Skeletal Muscle, Is Partially Relieved by AMP-activated Protein Kinase Activation. *J Biol Chem* 283: 9187-9195, 2008.
12. **Daugaard JR and Richter EA.** Muscle- and fibre type-specific expression of glucose transporter 4, glycogen synthase and glycogen phosphorylase proteins in human skeletal muscle. *Pflugers Arch* 447: 452-456, 2004.
13. **Daugaard JR and Richter EA.** Relationship between muscle fibre composition, glucose transporter protein 4 and exercise training: possible consequences in non-insulin-dependent diabetes mellitus. *Acta Physiol Scand* 171: 267-276, 2001.
14. **Frosig C, Rose AJ, Treebak JT, Kiens B, Richter EA, and Wojtaszewski JF.** Effects of endurance exercise training on insulin signaling in human skeletal muscle: interactions at the level of phosphatidylinositol 3-kinase, Akt, and AS160. *Diabetes* 56: 2093-2102, 2007.
15. **Funai K, Schweitzer GG, Castorena CM, Kanzaki M, and Cartee GD.** In vivo exercise followed by in vitro contraction additively elevates subsequent insulin-stimulated glucose transport by rat skeletal muscle. *Am J Physiol Endocrinol Metab* 298: E999-1010, 2010.
16. **Gallant P.** Control of transcription by pontin and reptin. *Trends Cell Biol* 17: 187-192, 2007.

17. **Gupte AA, Bomhoff GL, and Geiger PC.** Age-related differences in skeletal muscle insulin signaling: the role of stress kinases and heat shock proteins. *J Appl Physiol* 105: 839-848, 2008.
18. **Hennig R and Lomo T.** Firing patterns of motor units in normal rats. *Nature* 314: 164-166, 1985.
19. **Henriksen EJ, Bourey RE, Rodnick KJ, Koranyi L, Permutt MA, and Holloszy JO.** Glucose transporter protein content and glucose transport capacity in rat skeletal muscles. *Am J Physiol* 259: E593-598, 1990.
20. **Huey KA, Roy RR, Baldwin KM, and Edgerton VR.** Temporal effects of inactivty on myosin heavy chain gene expression in rat slow muscle. *Muscle Nerve* 24: 517-526, 2001.
21. **Johannsson E, McCullagh KJ, Han XX, Fernando PK, Jensen J, Dahl HA, and Bonen A.** Effect of overexpressing GLUT-1 and GLUT-4 on insulin- and contraction-stimulated glucose transport in muscle. *Am J Physiol* 271: E547-555, 1996.
22. **Karlsson HK, Hallsten K, Bjornholm M, Tsuchida H, Chibalin AV, Virtanen KA, Heinonen OJ, Lonnqvist F, Nuutila P, and Zierath JR.** Effects of metformin and rosiglitazone treatment on insulin signaling and glucose uptake in patients with newly diagnosed type 2 diabetes: a randomized controlled study. *Diabetes* 54: 1459-1467, 2005.
23. **Kong X, Manchester J, Salmons S, and Lawrence JC, Jr.** Glucose transporters in single skeletal muscle fibers. Relationship to hexokinase and regulation by contractile activity. *J Biol Chem* 269: 12963-12967, 1994.
24. **Kramer HF, Witczak CA, Taylor EB, Fujii N, Hirshman MF, and Goodyear LJ.** AS160 regulates insulin- and contraction-stimulated glucose uptake in mouse skeletal muscle. *J Biol Chem* 281: 31478-31485, 2006.
25. **Lessard SJ, Rivas DA, Chen ZP, Bonen A, Febbraio MA, Reeder DW, Kemp BE, Yaspelkis BB, 3rd, and Hawley JA.** Tissue-specific effects of rosiglitazone and exercise in the treatment of lipid-induced insulin resistance. *Diabetes* 56: 1856-1864, 2007.
26. **Masuda S, Hayashi T, Hashimoto T, and Taguchi S.** Correlation of dystrophin-glycoprotein complex and focal adhesion complex with myosin heavy chain isoforms in rat skeletal muscle. *Acta Physiol (Oxf)* 195: 483-494, 2009.
27. **Megeney LA, Neufer PD, Dohm GL, Tan MH, Blewett CA, Elder GC, and Bonen A.** Effects of muscle activity and fiber composition on glucose transport and GLUT-4. *Am J Physiol* 264: E583-593, 1993.
28. **Nesher R, Karl IE, Kaiser KE, and Kipnis DM.** Epitrochlearis muscle. I. Mechanical performance, energetics, and fiber composition. *Am J Physiol* 239: E454-460, 1980.
29. **Ogura Y, Naito H, Kakigi R, Akema T, Sugiura T, Katamoto S, and Aoki J.** Different adaptations of alpha-actinin isoforms to exercise training in rat skeletal muscles. *Acta Physiol (Oxf)* 196: 341-349, 2009.
30. **Pandorf CE, Caiozzo VJ, Haddad F, and Baldwin KM.** A rationale for SDS-PAGE of MHC isoforms as a gold standard for determining contractile phenotype. *J Appl Physiol* 108: 222-222; author reply 226, 2010.
31. **Ramm G, Larance M, Guilhaus M, and James DE.** A role for 14-3-3 in insulin-stimulated GLUT4 translocation through its interaction with the RabGAP AS160. *J Biol Chem* 281: 29174-29180, 2006.
32. **Rodnick KJ, Henriksen EJ, James DE, and Holloszy JO.** Exercise training, glucose transporters, and glucose transport in rat skeletal muscles. *Am J Physiol* 262: C9-14, 1992.

33. **Sano H, Kane S, Sano E, Miinea CP, Asara JM, Lane WS, Garner CW, and Lienhard GE.** Insulin-stimulated phosphorylation of a Rab GTPase-activating protein regulates GLUT4 translocation. *J Biol Chem* 278: 14599-14602, 2003.
34. **Schertzer JD, Antonescu CN, Bilan PJ, Jain S, Huang X, Liu Z, Bonen A, and Klip A.** A transgenic mouse model to study glucose transporter 4myc regulation in skeletal muscle. *Endocrinology* 150: 1935-1940, 2009.
35. **Schuenke MD, Reed DW, Kraemer WJ, Staron RS, Volek JS, Hymer WC, Gordon S, and Perry Koziris L.** Effects of 14 days of microgravity on fast hindlimb and diaphragm muscles of the rat. *Eur J Appl Physiol* 106: 885-892, 2009.
36. **Slentz CA, Gulve EA, Rodnick KJ, Henriksen EJ, Youn JH, and Holloszy JO.** Glucose transporters and maximal transport are increased in endurance-trained rat soleus. *J Appl Physiol* 73: 486-492, 1992.
37. **Stephenson GM.** Hybrid skeletal muscle fibres: a rare or common phenomenon? *Clin Exp Pharmacol Physiol* 28: 692-702, 2001.
38. **Talmadge RJ.** Myosin heavy chain isoform expression following reduced neuromuscular activity: potential regulatory mechanisms. *Muscle Nerve* 23: 661-679, 2000.
39. **Talmadge RJ and Roy RR.** Electrophoretic separation of rat skeletal muscle myosin heavy-chain isoforms. *J Appl Physiol* 75: 2337-2340, 1993.
40. **Taylor EB, An D, Kramer HF, Yu H, Fujii NL, Roeckl KS, Bowles N, Hirshman MF, Xie J, Feener EP, and Goodyear LJ.** Discovery of TBC1D1 as an Insulin-, AICAR-, and Contraction-stimulated Signaling Nexus in Mouse Skeletal Muscle. *J Biol Chem* 283: 9787-9796, 2008.
41. **Torgan CE, Etgen GJ, Jr., Kang HY, and Ivy JL.** Fiber type-specific effects of clenbuterol and exercise training on insulin-resistant muscle. *J Appl Physiol* 79: 163-167, 1995.
42. **Vind BF, Pehmoller C, Treebak JT, Birk JB, Hey-Mogensen M, Beck-Nielsen H, Zierath JR, Wojtaszewski JFP, and Hojlund K.** Impaired insulin-induced site-specific phosphorylation of TBC1 domain family, member 4 (TBC1D4) in skeletal muscle of type 2 diabetes patients is restored by endurance exercise-training. *Diabetologia* 54: 157-167, 2011.
43. **Xie X, Chen Y, Xue P, Fan Y, Deng Y, Peng G, Yang F, and Xu T.** RUVBL2, a novel AS160-binding protein, regulates insulin-stimulated GLUT4 translocation. *Cell Res*, 2009.
44. **Xu Y, Rubin BR, Orme CM, Karpikov A, Yu C, Bogan JS, and Toomre DK.** Dual-mode of insulin action controls GLUT4 vesicle exocytosis. *J Cell Biol*, 2011.
45. **Yu CF, Cresswell J, Loffler MG, and Bogan JS.** The glucose transporter 4-regulating protein TUG is essential for highly insulin-responsive glucose uptake in 3T3-L1 adipocytes. *Journal of Biological Chemistry* 282: 7710-7722, 2007.

Chapter IV

Study 2:

Myosin Heavy Chain Isoform Expression, Contraction-stimulated Glucose Uptake and Abundance of Proteins that Regulate Glucose Uptake and Metabolism in Single Skeletal Muscle Fibers

Abstract

Skeletal muscle is a heterogenous tissue, and this diversity is often studied in the context of muscle fiber type profile (myosin heavy chain, MHC, isoform expression). Earlier research using whole skeletal muscles from rats suggested a possible fiber type difference based on the observation of greater contraction-stimulated glucose uptake in the predominantly MHC-IIa flexor digitorum versus the predominantly MHC-IIb epitrochlearis. However, to fully understand skeletal muscle at the cellular level, it is essential to evaluate single muscle fibers. Therefore, the major goals of this study were to determine if there are fiber type-related differences in single fibers for: 1) contraction-stimulated glucose uptake or 2) the abundance of proteins that are established or potential regulators of glucose uptake or metabolism. Paired epitrochlearis muscles isolated from male Wistar rats were either electrically stimulated to contract (*E-Stim*) or served as resting controls (*No-Estim*). Muscles were incubated with [^{3}H]-2-deoxy-d-glucose (2-DG), followed by isolation of ~20-40 single fibers per muscle. MHC isoform and 2-DG uptake were determined for each fiber. Immunoblotting of single fibers was used to determine abundance of several key proteins. *E-Stim* versus *No E-Stim* fibers had

significantly greater ($P < 0.05$) 2-DG uptake among all fiber types that were isolated (MHC-IIa, MHC-IIax, MHC-IIx, MHC-IIxb and MHC-IIb), but contraction-stimulated 2-DG uptake was not significantly different among the fiber types. GLUT4, TUG (tethering protein containing a UBX domain for GLUT4), COX IV (cytochrome C oxidase IV) and filamin C protein levels were significantly greater ($P < 0.05$) in MHC-IIa versus MHC-IIx, MHC-IIxb, MHC-IIb fibers. In addition, TUG and COX IV in MHC-IIax and MHC-IIx fibers exceeded values for MHC-IIxb and MHC-IIb, and GLUT4 levels for MHC-IIax exceeded MHC-IIxb. Abundance values for GLUT4, COX IV, filamin C and TUG determined in single fibers significantly ($P < 0.05$) correlated with each other. No significant fiber type-related differences were found for AS160 (Akt substrate of 160 kDa), glycogen phosphorylase or glyceraldehyde-3-phosphate dehydrogenase abundance. RUVBL2 was not detectable in any of the single fibers evaluated. TBC1D1 was detectable, but not significantly different for MHC-IIb versus MHC-IIxb fibers, and it was undetectable in ~90% of the MHC-IIa, MHC-IIax and MHC-IIx fibers tested. In contrast to previous results for whole muscles with differing fiber type profiles, these data revealed no significant fiber type-related differences for contraction-stimulated glucose uptake by single fibers despite substantial fiber type-related differences in the abundance of several proteins, including GLUT4. Furthermore, the significant and positive correlations found for abundance of GLUT4, COX IV, filamin C and TUG suggest that the abundance of these proteins within individual fibers may be regulated by overlapping mechanisms.

Introduction

Skeletal muscle is a heterogeneous tissue, and different muscles in a single individual can vary greatly with regard to many functional characteristics. For example, the magnitude of the exercise-induced increase in glucose uptake is not uniform across all skeletal muscles (31, 52). Although, the diversity in glucose uptake during *in vivo* exercise is in large part attributable to the levels of muscle recruitment and blood flow, variability in the intrinsic characteristics of the muscles may also influence the capacity for contraction-stimulated glucose uptake. The intrinsic properties of muscle are often evaluated in the context of muscle differences in fiber type composition (e.g., as assessed by the expression of myosin heavy chain, MHC, isoforms), and a common strategy is to compare two or more muscles with differing fiber type profiles.

When the goal is to elucidate the intrinsic properties of the muscle in response to contraction, a useful approach is to study isolated rodent skeletal muscles undergoing electrical stimulation. Henriksen et al. (26) evaluated four different rat skeletal muscles with varying fiber type compositions and reported that the greatest contraction-stimulated glucose uptake was in the flexor digitorum brevis [FDB; 92% type IIa fibers (1, 8)] and the lowest values were in the epitrochlearis [51% type IIb fibers (11)]. These results, which were subsequently confirmed by others (1-2, 29-30), supported the idea that the capacity for contraction-stimulated glucose uptake of type IIa fibers greatly exceeds that of type IIb fibers in rat skeletal muscles. However, several caveats should be considered when interpreting these results.

When comparing two muscles with very different fiber type profiles, it cannot be assumed that fiber type differences account for every functional difference between the muscles. Furthermore, it is important to note that hybrid fibers expressing more than one MHC isoform are common in rat skeletal muscle (6-7, 44, 59), and evaluation of glucose uptake by these hybrid fibers requires analysis at the single fiber level. To fully understand glucose uptake at the cellular level in both hybrid and non-hybrid fibers, it is essential to assess glucose uptake by single fibers. Therefore, we recently developed a novel method that can be used to determine both glucose uptake and fiber type in a single rat skeletal muscle fiber (44). We found that insulin-stimulated glucose uptake was substantially greater for single fibers that expressed the IIa MHC versus the other fiber types that were assessed (IIb, IIx, and IIxb). Insulin and contractile activity can each induce increased glucose uptake secondary to translocation of the GLUT4 glucose transporter protein to the cell surface membranes, but multiple lines of evidence indicate that these two stimuli use distinct mechanisms to achieve this outcome (9-10, 15, 22, 24, 48-49). Quantitative analysis for the effect of contraction on glucose uptake in single fibers of differing fiber types has not been previously reported. Thus, the first major goal of Study 2 was to make direct fiber type comparisons for contraction-stimulated glucose uptake within the same intact rat epitrochlearis muscles (fiber type representative of the entire rat hindlimb), which were incubated *ex vivo* and electrically stimulated to contract prior to single fiber isolation and glucose uptake measurements.

Fiber type composition *per se* is probably not a direct determinant of glucose uptake capacity. It seems more likely that fiber type composition is co-regulated with the direct

determinants of glucose uptake. Contraction-stimulated glucose uptake is ultimately dependent on the GLUT4 glucose transporter, and several studies have demonstrated that differences in fiber type composition in multiple muscles are accompanied by differences in GLUT4 protein abundance (11, 26, 33, 46, 51). For example, we studied twelve muscles or regions of muscles with diverse fiber type profiles and found a negative relationship between GLUT4 abundance and percentage of MHC-IIb abundance (11). Henriksen et al. (26) found that GLUT4 abundance corresponded to the level of glucose uptake by four different muscles that were stimulated by insulin, contractile activity, or both stimuli. Based on these results, they proposed that GLUT4 abundance was "a major determinant for muscle cells to take up glucose." Consistent with this interpretation, Brozinick et al. (5) reported that contraction-stimulated glucose uptake by several muscles in the perfused rat hindlimb was predicted by the muscle's level of GLUT4 abundance. Because previous studies have not evaluated the relationship between fiber type and GLUT4 abundance in intact single fibers from rat skeletal muscle, the second major goal was to determine if GLUT4 abundance differed according to MHC isoform expression in single fibers.

In Study 1 evaluated the relationship between fiber type and abundance of GLUT4 and several proteins that are established or possible regulators of GLUT4 and/or glucose uptake (TUG, AS160, TBC1D1, and RUVBL2) (11). Based on whole tissue analysis of multiple muscles with diverse fiber type profiles, we found that the relative levels of GLUT4, TUG and RUVBL2 appeared to cluster together. However, these observations are not definitive evidence that the expression levels of these proteins are actually tracking together within the same muscle fibers. Therefore, our third major goal was to further investigate the fiber type and protein co-expression patterns for GLUT4, TUG, AS160, TBC1D1 and RUVBL2 at the single fiber level. Finally, we also evaluated in single fibers the abundance of several metabolically relevant proteins in single fibers (cytochrome C oxidase IV, COX IV; glycogen phosphorylase; and glyceraldehyde-3-phosphate dehydrogenase, GAPDH) and filamin C, an actin-binding protein with potential structural and signaling roles (50). The results of this study provided unique insights at the cellular level with regard to fiber type differences in both contraction-stimulated glucose uptake and the expression of several proteins that are relevant to the regulation of glucose uptake, metabolism and other cellular functions.

Methods

Material

The reagents and apparatus for sodium dodecyl sulfate polyacrylamide gel electrophoresis (SDS-PAGE) and Coomassie Brilliant Blue (no. 161-0436) were from Bio-Rad (Hercules, CA). Bicinchoninic acid protein assay reagent (no. 23227) was from Pierce Biotechnology (Rockford, IL). Anti-COX IV (no. 4850) and anti-GAPDH (no. 2118) were from Cell Signaling Technologies (Boston, MA). Anti-AS160 (no. 07-741) and Luminata™ Forte Western Horseradish Peroxidase Substrate (no. WBLUF0100) were from Millipore (Billerica, MA). Anti-RUVBL2 (no. ab36569) was from Abcam (Cambridge, MA). Anti-Glycogen Phosphorylase (GP; no. H00005837-m10) was from Novus Biologicals (Littleton, CO). Anti-Filamin C (no. sc-48496) was from Santa Cruz Biotechnology (Dallas, TX). Anti-TBC1D1 was provided by Dr. Makoto Kanzaki (Tohoku University; Sendai, Japan). Anti-GLUT4 and anti-TUG were provided by Dr. Jonathan Bogan (Yale University; New Haven, CT). Collagenase Type 2 (305 units/mg) was purchased from Worthington Biochemical (no. LS004177, Lakewood, NJ).

Animal Treatment

Procedures for animal care were approved by the University of Michigan Committee on Use and Care of Animals. Male Wistar rats (~8 wk-old; 250-300g; Harlan, Indianapolis, IN) were provided with standard rodent chow and water ad libitum. Rats were fasted the night before the experiment at ~1900. On the morning after the overnight fast (between 0700 and 0900), rats were given an intraperitoneal injection of sodium pentobarbital (50 mg/kg wt). While rats were under deep anesthesia, both epitrochlearis muscles were dissected out, rapidly rinsed in warm (35°C) Krebs-Henseleit buffer (KHB) and transferred to vials for subsequent *ex vivo* incubations.

Muscle Incubations and Electrical Stimulation

Isolated muscles were incubated in vials containing the appropriate media that was gassed from above (95% O_2/5% CO_2) in a water bath (35°C for Steps 1-3 and 5; and Step 4 was on ice) throughout all of the incubation steps. For Step 1 (30 min), both epitrochlearis muscles

from each rat were placed in vials containing 2 mL of Media 1 [KHB supplemented with 8mM glucose]. For Step 2 (10 min), one of the paired muscles was suspended in a 5-ml bath containing two platinum electrodes with one end of the muscle attached to a glass rod and the other end attached to a force transducer (Radnoti, Litchfield, CT). The mounted muscle was incubated in Media 1 and electrically stimulated to contract [*E-Stim*: 0.1 ms twitch, 100 Hz train for 10 s, 1 train/min for 10 min; Grass S48 Stimulator; Grass Instruments, Quincy, MA (19, 23)]. The contralateral muscle, that served as a rested/non-electrically stimulated control (*No E-Stim*), was transferred to a vial containing Media 1. For Step 3 (30 min), all muscles were transferred to vials containing 2 ml of Step 3 Media [KHB supplemented with 0.1% BSA, 0.1 mM 2-deoxyglucose (2-DG; final specific activity of 13.5 mCi/mmol ^{3}H-2-DG) and 9.9 mM mannitol]. For Step 4 (15 min), muscles underwent 3 washes (5 min/wash with shaking at 115 revolutions per min) in ice-cold Wash Media [Ca^{2+}-free KHB supplemented with 0.1% BSA and 8mM glucose, to clear the extracellular space (ECS) of ^{3}H-2-DG (58)]. For Step 5 (60-70 min), muscles were incubated in vials containing Collagenase Media (Wash Media plus 1.5% Type II collagenase) for enzymatic digestion of muscle collagen (collagenase-treated muscles are hereafter referred to as fiber bundles).

Isolation and Processing of Single Fibers for Glucose Uptake and Immunoblotting

After incubation Step 5, fiber bundles were removed from Collagenase Media, washed with Wash Media at room temperature, and placed in a petri-dish containing Isolation Media (Wash Media supplemented with 0.25% Trypan Blue, TB) (44). Under a dissecting microscope (Leica EZ4D; Buffalo Grove, IL), intact single fibers were gently teased away from the fiber bundle using forceps. Only fibers that were not permeable to TB (TB-permeable fibers were very rare) were isolated. Each fiber was imaged using a camera-enabled microscope with Leica Application Suite EZ software after isolation. Fiber dimensions were measured using Image J software. Width (mean value for width measured at 3 locations on each fiber: near the fiber midpoint and approximately halfway between the midpoint and each end of the fiber) and length of each fiber were be used to calculate an estimated volume ($V = \pi r^2 l$; r = radius as determined by half of the width measurement, l = length). After imaging, each fiber was transferred by pipette with 10µl of Isolation Media to a micro-centrifuge tube containing 10µl of lysis buffer (1 ml/muscle; 20 mM Tris-HCL, 150 mM NaCl, 1% Triton X-100, 1 mM Na_3VO_4, 1 mM EDTA, 1

mM EGTA, 2.5 mM NaPP, 1 mM β-glycerophosphate, 1 µg/ml leupeptin, 1mM PMSF), for a total volume of 20 µl. Without disturbing the muscle fiber, a 10µl aliquot of the solution was removed from each fiber's tube and pipetted into a separate tube to serve as Background Media. The Background Media was used to correct for any residual ^{3}H-2-DG from the ECS that had not been eliminated by the three washes of the fiber bundle during Step 4 described above. Lysis buffer (40µl) and 2X Laemmli buffer (50µl) were added to each isolated fiber tube and also to each fiber's corresponding Background Media tube. The tubes were then vortexed and heated to 95-100 ˚C. Samples were then cooled and stored at -20^{o}C until 2-DG uptake and MHC isoform expression were determined.

Fiber Bundle Homogenization and 2-DG Uptake

After isolation of single fibers (~20-40 fibers per fiber bundle), the remainder of each fiber bundle was homogenized in 1ml ice-cold lysis buffer using a glass-on-glass pestle and grinding tubes (Kontes, Vineland, NJ) chilled on ice. Aliquots of fiber bundle homogenates were added to vials containing scintillation cocktail (Research Products International, Mount Prospect, IL) for scintillation counting, and 2-DG accumulation was determined (44). A portion of the homogenate was used to determine protein concentration according to the manufacturer's protocol (Pierce Biotechnology no. 23227), and 2-DG uptake was normalized to protein content (µmol • µg^{-1} protein for fiber bundles) (44).

Single Fiber 2-DG Uptake

An aliquot of each lysed single fiber and its corresponding Background Media were pipetted into separate vials with each containing 10ml of scintillation cocktail. Aliquots of Incubation Step 3 Media (in which muscles had been incubated with ^{3}H-2DG) were added to separate vials containing 10ml of scintillation cocktail. The raw counts obtained from the Background Media were subtracted from the single fiber raw counts (single fiber counts – background counts = corrected single fiber counts). The corrected single fiber counts were then used to determine the single fiber ^{3}H-2DG accumulation which was calculated and normalized to the calculated fiber volume and expressed as nmol • µl^{-1} as previously described (44).

Myosin Heavy Chain (MHC) Isoform Expression

MHC isoforms from aliquots of single fiber lysates were separated and identified by sodium dodecyl sulfate-polyacrylamide gel electrophoresis (SDS-PAGE) essentially as previously described (43-44, 55), with the following minor modifications made to the resolving gel (final reagent concentrations): 6.5% acrylamide-bis (50:1), 30% glycerol gel, 210 mM Tris-HCl (pH 7.4), 105 mM glycine, 0.4% SDS, 19% H_2O, 0.1% ammonium persulfate, 0.05% TEMED. Samples and a MHC isoform standard (6 μg protein of a 3:2 mixture of homogenized rat soleus and extensor digitorum longus muscles containing all four MHC isoforms: I, IIa, IIb, IIx) were run at a constant voltage (40 V) for 1 h (during electrophoresis that was performed in a refrigerator cooled to 4^{o}C, the gel box was placed in a secondary container that was packed with ice) with continuous mixing by a magnetic stir bar inside the electrophoresis apparatus (Mini-PROTEAN® Tetra cell no. 165-8004, Hercules, CA). The use of a secondary container packed in ice and continuous stirring were slight modifications from our original methods with single fibers (44). After 1 h, the power supply was switched from constant voltage mode to constant current mode, with the current setting at the end of the first hour of electrophoresis maintained for the subsequent 23-25 h (with the gel box packed on ice in a refrigerator at 4^{o}C). Gels were subsequently removed and stained with Coomassie Brilliant Blue overnight at room temperature while gently rotating on an orbital shaker. The gels were then destained in 20% methanol and 10% acetic acid solution for 4-6 h while rotating (destaining solution was replaced with fresh solution every 45-60 min). MHC bands were quantified using densitometry (AlphaEase FC, Alpha Innotech, San Leandro, CA).

Immunoblotting

Aliquots of single fiber lysates were to heated to 90˚C for 5-10 min, separated via SDS-PAGE using 4-20% TGX^{TM} gradient gels (Bio-Rad no. 456-1095), and then electrophoretically transferred to nitrocellulose membranes. After transfer, gels were stained in Coomassie Brilliant Blue overnight and then destained the following morning as described above. The Coomassie-stained MHC bands in the gels were quantified by densitometry with these post-transfer MHC band densities served as the loading controls for the subsequently immunoblotted proteins (Alpha Innotech, San Leandro, CA) (34, 43-44). Membranes were then rinsed with Tris-buffered saline (TBS: 140 mM NaCl and 20 mM Tris base, pH 7.6), blocked with 5% nonfat dry

milk in TBS plus tween (TBST: 0.1% tween) for 1 h at room temperature, washed 3 x 5 min at room temperature and incubated with the appropriate primary antibody (with 5% BSA unless otherwise specified by the manufacturer) and rotated on orbital shaker overnight at 4°C. On the following morning membranes were washed 3 x 5 min with TBST, then incubated with the appropriate IgG horseradish peroxidase (HRP) conjugated secondary antibody (1:20,000 in TBST + 5% milk) for 3 h at room temperature. Membranes were then washed again 3 x 5 min with TBST, 3 x 5 min TBS and subjected to enhanced chemiluminescence to visualize protein bands. Protein bands from the membranes were quantified by densitometry (Alpha Innotech, San Leandro, CA). The individual values for samples were normalized to the mean value for all of the samples on the blot, and then divided by the loading control (the post-transfer MHC density determined for the respective sample on Coomassie stained gels) (34).

Statistics

The two-tailed t-test was used for comparison of means between two groups. One-way ANOVA was used for comparisons of means among more than two groups, and the Bonferroni correction was used to identify the source of significant variance for data when appropriate. To determine the effects of fiber type and contraction on glucose uptake, two-way ANOVA and the Bonferroni post-hoc test were used. The nonparametric Spearman rank order correlation for individual data was used to assess the relationships between abundance of each pair of the proteins studied (e.g., between GLUT4 vs. TUG). Data that were not normally distributed were mathematically transformed to achieve normality prior to running the appropriate statistical analysis. Statistical analyses were performed using Sigma Plot (San Rafael, CA) version 11.0. Data were expressed as means ± SE. A P-value < 0.05 was considered statistically significant.

Results

MHC Isoforms

Single muscle fibers isolated from the epitrochlearis muscle expressed five distinct fiber types: MHC-IIa, MHC-IIax, MHC-IIx, MHC-IIxb and MHC-IIb (Figure 4.1). The respective percentages of total isolated single fibers from each of these fiber types were as follows: MHC-

IIxb (~44%), MHC-IIb (~28%), MHC-IIx (~17%), MHC-IIa (~6%) and MHC-IIax (~5%). Consistent with earlier research using the collagenase method to isolate single fibers from rat epitrochlearis muscles (43-44), no MHC-I fibers were found among any of the single fibers that were isolated in the current study.

2-DG Uptake

E-Stim fiber bundles versus *No E-Stim* fiber bundles had significantly greater ($P < 0.01$) contraction-stimulated 2-DG uptake (Figure 4.2). For single fiber 2-DG uptake (Figure 4.3), there were significant main effects of *E-stim* ($P < 0.01$) and fiber type ($P < 0.01$). Within the *No E-Stim* group, 2-DG uptake was significantly greater ($P < 0.01$) for MHC-IIa fibers versus MHC-IIx and MHC-IIxb fibers. Within the *E-Stim* group, 2-DG uptake was not statistically different among the fiber types. For each fiber type, 2-DG uptake was significantly greater ($P < 0.01$) for *E-Stim* fibers versus the corresponding *No E-Stim* fibers.

Relative Protein Abundance

The relative GLUT4 protein abundance differed among the fiber types as follows: MHC-IIa was significantly ($P < 0.05$) greater than MHC-IIx, MHC-IIxb and MHC-IIb; and MHC-IIax was significantly ($P < 0.05$) greater than MHC-IIxb and MHC-IIb (Figure 4.4). In the 5 fiber types that were identified, the GLUT4 abundance ranged by ~4.2-fold (with the lowest values in the MHC-IIb fibers and the highest values in the MHC-IIa fibers).

TUG protein abundance differed among the fiber types as follows: MHC-IIa was significantly ($P < 0.05$) greater than MHC-IIxb and MHC-IIb; and MHC-IIax and MHC-IIx were significantly ($P < 0.05$) greater than MHC-IIxb (Figure 4.5). The range of values for TUG abundance was ~3.1-fold (with the lowest values in the MHC-IIxb and the highest values in the MHC-IIa fibers).

COX IV protein abundance differed among the fiber types as follows: MHC-IIa was significantly ($P < 0.05$) greater than MHC-IIx, MHC-IIxb and MHC-IIb; and MHC-IIax and MHC-IIx were significantly ($P < 0.05$) greater than MHC-IIxb and MHC-IIb (Figure 4.6). The range of values for COX IV abundance was ~7.6-fold (with the lowest values in the MHC-IIxb and the highest values in the MHC-IIa fibers).

Filamin C protein abundance in MHC-IIa fibers was significantly ($P < 0.05$) greater than in MHC-IIx, MHC-IIxb and MHC-IIb fibers (Figure 4.7). The range of values for filamin C abundance was ~5.2-fold (with the lowest values in the MHC-IIb and the highest values in the MHC-IIa fibers)

TBC1D1 protein abundance was assessed by immunoblotting in a total of 75 single fibers (15 single fibers for each of the 5 fiber types), but TBC1D1 was not detectable in every single fiber. TBC1D1 protein was detected in the following numbers of single fibers: MHC-IIa fibers (n = 1), MHC-IIax fibers (n = 1), MHC-IIx (n = 2), MHC-IIxb fibers (n = 11) and MHC-IIb fibers (n = 11). Because TBC1D1 was detectable in only 1 or 2 of the MHC-IIa, MHC-IIax, and MHC-IIx fibers, the statistical analysis was performed only using the values of MHC-IIxb (n = 11) and MHC-IIb (n = 11) fibers for which TBC1D1 was detectable. The relative TBC1D1 protein abundance did not significantly differ between MHC-IIxb and MHC-IIb fibers (Figure 4.8).

The relative protein abundance values for AS160, GP and GAPDH did not significantly differ among any of the 5 fiber types (Figure 4.9 - 4.11).

RUVBL2 protein was not detectable in any of the single fibers that were tested (n = 75 single fibers; 15 per fiber type).

Correlations

Correlation analysis was performed for each pair of proteins that was studied. Significant ($P < 0.05$) correlations were identified between the following pairs: GLUT4 versus TUG (Figure 4.12A), GLUT4 versus COX IV (Figure 4.12B), GLUT4 versus filamin C (Figure 4.12C), filamin C versus COX IV (Figure 4.12D), TUG versus COX IV (Figure 4.12E), TUG versus filamin C (Figure 4.12F), AS160 versus TUG (Figure 4.13A), AS160 versus GP (Figure 4.13B), AS160 versus filamin C (Figure 4.13C), TCB1D1 versus COX IV (Figure 4.13D), GP versus GAPDH (Figure 4.14A), GP versus filamin C (Figure 4.14B) and GAPDH versus filamin C (Figure 4.14C).

Discussion

Single muscle fibers have been extensively studied with regard to their contractile function, but many of their metabolic properties are relatively poorly understood. In this context, the current study significantly advanced the knowledge of muscle's metabolic phenotype at the cellular level by measuring in single fibers: 1) fiber type (based on MHC isoform expression); 2) rate of contraction-stimulated glucose uptake; and 3) abundance of eight proteins that are established or potential regulators of muscle glucose uptake or metabolism. There were no significant differences in contraction-stimulated glucose uptake among the five fiber types that were studied (MHC-IIa, MHC-IIax, MHC-IIx, MHC-IIxb and MHC-IIb) even though these fiber types differed substantially in their abundance of several proteins, including GLUT4. These data revealed valuable new insights that cannot be discerned by conventional approaches using whole tissue analysis.

Two earlier publications assessed contraction effects on glucose uptake of single fibers, but neither included quantitative comparisons between differing fiber types (47, 57). In both studies, 2-deoxyglucose (2-DG) was infused into anesthetized cats in which muscle contractions were induced by electrical stimulation of motor neurons. Toop et al. (57) infused radiolabeled 2-DG into the cats and prepared serial sections of muscle samples. One section was used to histochemically determine if motor units were fast or slow based on myosin adenosine triphosphatase (ATPase) and oxidative enzyme activity. A second section was used for autoradiographic assessment of 2-DG accumulation by individual fibers. Although quantitative values for 2-DG accumulation were not reported, the authors noted that it was their "impression that autoradiographic labeling was less heavy" in the fibers of slow compared to fast motor units. Nemeth et al. (47) infused non-radioactive 2-DG into anesthetized cats concomitant with electrical stimulation of motor neurons. Muscles were subsequently collected and serially sectioned, with one section used for fiber typing by myosin ATPase staining. Individual frozen fibers were then micro-dissected from an adjacent muscle section, and 2-DG-6-phosphate (2-DG6P) content was measured by biochemical analysis. As expected, accumulation of 2-DG6P was much greater in fibers from electrically stimulated motor units compared to non-stimulated controls, but no comparisons of contraction-stimulated glucose uptake were reported for single fibers with different fiber types. To the best of our knowledge, the results from the current study

provided the first quantitative comparison of contraction-stimulated glucose uptake among single fibers with differing fiber types.

It is important to interpret the current data together with earlier research using intact skeletal muscle preparations. Henriksen et al. (26) and others (1-2, 29-30) have previously reported that, based on results from whole skeletal muscles studied *ex vivo*, contraction-stimulated glucose uptake was substantially greater in the FDB (enriched in type IIa fibers) compared to the epitrochlearis (enriched in type IIb fibers) muscles from rats. These results are often cited as evidence that the capacity for contraction-stimulated glucose uptake is greater for IIa versus IIb fibers. However, analysis of muscle tissue has limitations for elucidating differences among fiber types at the cellular level because: 1) no rat muscles have been found to exclusively express a single MHC isoform; 2) no rat muscle has been recognized to be predominantly composed of MHC-IIx fibers; 3) whole tissue analysis cannot determine the glucose uptake of hybrid fibers that express multiple MHC isoforms; 4) many cell types (including vascular, neural, and adipose cells) contribute to glucose uptake by skeletal muscle tissue; and 5) it cannot be assumed that every difference between muscles with divergent fiber type profiles is a direct consequence of differing fiber type. The difference in contraction-stimulated glucose uptake between the FDB and epitrochlearis in earlier research taken together with the lack of significant fiber type differences in contraction-stimulated glucose uptake for MHC-IIa compared to MHC-IIb single fibers provides a notable example of this final caveat.

In contrast to the lack of fiber type differences for glucose uptake by single fibers from muscles that had been stimulated to contract, we previously found substantial fiber type-related differences for insulin-stimulated glucose uptake by single fibers from rat epitrochlearis muscles (43-44). Insulin-stimulated glucose uptake was more than 2-fold greater for MHC-IIa fibers versus fibers expressing each of the other MHC isoforms that were studied, and insulin-stimulated glucose uptake was also greater for MHC-IIxb versus MHC-IIb fibers (44). The results for insulin-stimulated single fibers were consistent with the greater insulin-stimulated glucose uptake that has been found in the whole FDB versus the whole epitrochlearis (26). We also previously reported a significant difference for AICAR-stimulated glucose uptake by single MHC-IIb fibers versus MHC-IIa fibers (MHC-IIb greater than MHC-IIa) (44) which corresponded to the greater AICAR-stimulated glucose uptake that had been observed for the

whole epitrochlearis versus the whole FDB (1). Thus, in single fibers from rat epitrochlearis muscles, fiber type-related effects on glucose uptake capacity are highly stimulus-specific: 1) contraction-stimulated glucose uptake for MHC-IIa fibers is similar to MHC-IIb fibers; 2) insulin-stimulated glucose uptake for MHC-IIa fibers exceeds MHC-IIb fibers; and 3) AICAR-stimulated glucose uptake for MHC-IIa fibers is less than MHC-IIb fibers. These results may be related, at least in part, to differences in the expression patterns of key proteins that play stimulus-specific roles in the activation of glucose transport.

Although the relationship between fiber type and glucose uptake is stimulus-specific, GLUT4 is the glucose transporter protein that is redistributed to the cell surface membranes in response to each of these stimuli, i.e., contraction (39, 42, 49), insulin (17-18, 38, 45, 49) and AICAR (35, 40-41). The greater values for GLUT4 abundance in MHC-IIa versus MHC-IIb fibers may be related to the greater insulin-stimulated glucose uptake in MHC-IIa fibers (43-44), but this begs the question, why does GLUT4 expression not also track with the capacity for glucose uptake in response to either contraction or AICAR? Several lines of evidence support the idea that skeletal muscle has distinct subcellular pools of GLUT4, and that these subsets of GLUT4 vary in their susceptibility to recruitment by different stimuli (14, 18, 37, 49). If this scenario is true, the capacity for contraction-stimulated and AICAR-stimulated glucose transport in a given fiber type may be constrained by the amount of GLUT4 that is allocated to the contraction-susceptible and AICAR-susceptible pools of GLUT4.

The ~4-fold greater GLUT4 abundance in MHC-IIa versus MHC-IIb fibers compares well with the ~4-fold difference in GLUT4 abundance of the FDB versus the epitrochlearis reported by Henriksen et al. (26). This difference can also be compared with Study 1 of my dissertation in which we evaluated 12 different rat skeletal muscles or regions of muscles with wide differences in fiber type composition. Based on analysis of multiple muscles, we found that the mean values for GLUT4 abundance varied by 2.5-fold, the % MHC-IIa fibers was positively correlated with GLUT4 levels, and the % MHC-IIb fibers was negatively correlated with GLUT4 levels (11). The current study was apparently the first to assess single rat fibers for both MHC isoform expression and GLUT4 abundance by immunoblotting. However, Hashimoto et al. (25) studied rat plantaris muscles and performed immunohistochemical analysis of GLUT4 content along with determination of fiber type profiles based on histochemical

analysis (myosin ATPase, succinate dehydrogenase, and α-glycerophosphate dehydrogenase). They reported that the rank order for GLUT4 content was: slow oxidative (SO) fibers exceeded fast-oxidative glycolytic (FOG) which, in turn, exceeded fast glycolytic (FG) fibers, but only the SO versus FG difference achieved statistical significance. Kong et al. (36) studied single fibers from rabbit tibialis anterior muscles and found GLUT4 protein levels measured by immunoblotting were roughly 2 to 3-fold greater on average in FOG fibers (identified on the basis of having high enzymatic activities of both malate dehydrogenase, MDH, and lactate dehydrogenase, LDH) compared to FG fibers (identified by low MDH activity and high LDH activity). Daugaard et al. (16) dissected single fibers from human vastus lateralis muscle biopsies and determined MHC isoform expression (I, IIa and IIx are the MHC isoforms expressed in human muscle). After pooling fibers that expressed the same MHC isoform, they determined GLUT4 abundance by immunoblotting. GLUT4 abundance was ~20% greater for type I compared to MHC-IIa or MHC-IIx fibers, and GLUT4 in the latter fiber types did not differ from each other. When both fiber type and GLUT4 were determined in single fibers of human vastus muscles by immunohistochemical analysis, GLUT4 levels were ~13% greater for type I versus type II fibers (types IIa and IIx were not differentiated). The relative magnitude of differences between fiber types may vary among species, but the use of different methods complicates the comparisons across experiments. Regardless, a unique aspect of the current study was that GLUT4 abundance was determined for hybrid fibers. The results indicated greater GLUT4 content of MHC-IIax fibers compared to either MHC-IIxb or MHC-IIb fibers (but not MHC-IIa or MHC-IIx fibers), and MHC-IIxb fibers were not significantly different from either MHC-IIx or MHC-IIb fibers.

Based on the analysis of multiple rat skeletal muscles of varying fiber type, we previously found that the relative levels of GLUT4, TUG and RUVBL2 expression were clustered together (11). Our current analysis of these same proteins in single fibers extended the earlier results by demonstrating an association between the relative levels of GLUT4 and TUG at the cellular level. These two proteins are known to be binding partners, and their interaction appears to play a role in the subcellular localization of GLUT4 (4). Whereas the GLUT4 and TUG relationship that we observed by tissue analysis was confirmed in single fibers, the results for RUVBL2 in single fibers provided a new perspective for interpreting the results of tissue analysis. We were unable to detect RUVBL2 in single fibers using the same antibody that we

previously used to detect RUVBL2 in whole epitrochlearis muscles. Because these results suggest that RUVBL2 is not highly expressed by type MHC-II fibers, the whole tissue data appear to have been largely attributable to RUVBL2 expression by other cell types (e.g., MHC-I fibers, neurons, adipocytes, vascular cells, or satellite cells, etc.).

It is well known that type IIa fibers are characterized by greater mitochondrial content compared to type IIb fibers (13, 20, 25, 27, 43). The current results for the mitochondrial enzyme COX IV were consistent with these expectations, and they also confirmed our previously reported finding that COX IV abundance differed markedly in single fibers with the highest values in IIa fibers and the lowest values in MHC-IIb fibers (43). Because earlier studies have provided evidence for co-regulation of GLUT4 and COX IV in muscle (3, 28), it was not surprising that there was a relatively high correlation between GLUT4 and COX IV abundance. In view of the relationship between GLUT4 and TUG, the positive association found between COX-IV and TUG abundance was also not unexpected. GLUT4 and COX IV expression levels in skeletal muscle can be increased in response to chronic electrical stimulation of skeletal muscle or endurance exercise training (28, 36), and denervation can lead to reduced GLUT4 and COX IV abundance (12, 46). Although it seems possible that TUG abundance is also responsive to the level of neuromuscular activity, this idea has not yet been experimentally tested.

The relative AS160 protein abundance in single fibers did not differ significantly among the fiber types. This finding corresponds to our earlier results in which AS160 abundance did not correlate with MHC-isoform proportions, and in which no significant differences in AS160 abundance were detected among multiple muscles with wide diversity in fiber type composition (11). We originally became interested in possible fiber type differences in AS160 on the basis of the results of Taylor et al. (56) who reported large differences in AS160 abundance in different skeletal muscles of mice (soleus was ~10-fold greater than the extensor digitorum longus, EDL, and tibialis anterior, TA). They noted that AS160 abundance tracked with the relative content of type MHC-I and MHC-IIa in the three muscles studied (TA: ~47% MHC-IIx, and ~53% MHC-IIb; EDL: ~35% MHC-IIx, and ~65% MHC-IIb; soleus: ~27% MHC-I, ~38% MHC-IIa, ~15% MHC-IIx, and ~20% MHC-IIb). In biopsies from humans, Jensen et al. (32) found AS160 abundance did not differ in muscles that varied in fiber type profile: soleus (71% MHC-I, 27% MHC-IIa, 1% MHC-IIx), gastrocnemius (54% MHC-I, 42% MHC-IIa, 4% MHC-IIx) and vastus

lateralis (47% MHC-I, 50% MHC-IIa, 2% MHC-IIx). There seems to be variability among species for the range of AS160 expression values found in muscles with different fiber type profiles.

The current study also provided new information about the relationship between AS160 and RUVBL2. It has been suggested based on results in adipocytes that RUVBL2 binding to AS160 can regulate insulin-stimulated AS160 phosphorylation and glucose transport (60). However, these proposed roles for RUVBL2 may not apply to type II fibers from rat skeletal muscle which lacked detectable RUVBL2 protein.

Another important new finding was that TBC1D1 was undetectable in most (~91%) of the MHC-IIa, MHC-IIax and MHC-IIx single fibers. In striking contrast, TBC1D1 was detectable in most (~73%) of the MHC-IIb and MHC-IIbx single fibers. Using the same TBC1D1 antibody, we were able to detect TBC1D1 in each of 12 different muscles or muscles regions from rats (11). In the earlier study of multiple muscles, TBC1D1 abundance was not significantly correlated with MHC isoform expression. In the first study that evaluated TBC1D1 abundance in multiple muscles, Taylor et al. (56) reported that TBC1D1 abundance differed by 10-fold among three different skeletal muscles from mice, with the TBC1D1 content of the TA greater than the EDL which was greater than the soleus. They suggested that the level of TBC1D1 corresponded to the relative content of type MHC-IIx in the three muscles studied, but this relationship was not quantitatively analyzed. In contrast to the results for mice, we found no significant difference in TBC1D1 abundance among the TA, EDL and soleus muscles of rats and there was no association between TBC1D1 and the % MHC-IIx fibers (11). Furthermore, the current data indicates TBC1D1 is not highly expressed by single MHC-IIx fibers from rats. Regardless of the possible species differences for TBC1D1 levels in various muscles, there is evidence based on results using whole muscles with high proportions of MHC-IIb fibers from both rats (epitrochlearis) and mice (EDL) that TBC1D1 may participate in the regulation of contraction-stimulated glucose uptake (22, 56). However, the current results for TBC1D1 in MHC-IIa, MHC-IIax, and MHC-IIx fibers suggest some uncertainty about TBC1D1's role for regulating contraction-stimulated glucose uptake in these fiber types of rat skeletal muscle.

Filamin C is an actin-binding protein and Akt substrate that is selectively expressed in skeletal muscle (21, 50, 54). Filamin C is largely found in two different cellular locations in

skeletal muscle: near the sarcolemma in association with the dystrophin-glycoprotein complex and near the Z-line (50). Filamin C's purpose is uncertain, and it may have distinct functions associated with the two locations. Nonetheless, it is notable that the remodeling of actin filaments has potential roles in both spatial localization of signaling proteins and translocation of GLUT4 glucose transporter vesicles (61). Furthermore, we recently found that insulin leads to increased Ser2213 phosphorylation of filamin C in skeletal muscle (53-54). Although there is currently no evidence that directly links filamin C to the regulation of glucose uptake or metabolism, the results for filamin C abundance were novel and interesting. Filamin C abundance was highly fiber type-dependent, the pattern for its expression was similar to the pattern for the expression of GLUT4, TUG and COX IV, and there were significant correlations between the abundance of filamin C and the abundance of each of these proteins. There were also modest, but significant correlations between filamin C abundance and the abundance of glycogen phosphorylase, GAPDH and AS160. The causes and consequences of the fiber type-related expression pattern of filamin C remain to be determined.

Glycogen phosphorylase and GAPDH are enzymes that participate in carbohydrate metabolism. There were no significant differences among the fiber types for abundance of either protein. Because glycogen phosphorylase is essential for the breakdown of glycogen, the current data suggest that any differences in glycogenolysis among the MHC-II fiber types would depend on factors other than large differences in glycogen phosphorylase abundance. There was a modest positive correlation between the abundance of each of these proteins.

In the current study and in the two previous studies in which we evaluated the MHC expression of single fibers in the epitrochlearis (43-44), we did not isolate any MHC-I fibers. The relative abundance of the MHC composition of whole epitrochlearis from male Wistar rats (8% I, 13% IIa, 28% IIx, and 51% IIb) (11), and it is unclear why MHC-I fibers were not found among the many hundreds of single fibers that we have isolated to date. Regardless, we were able to isolate single fibers expressing each of the other MHC isoforms (representing >90% of MHC in the rat epitrochlearis). It should also be noted that we did not identify any MHC-IIax fibers in our previous studies (43-44). Our identification of MHC-IIax fibers in the current study may be the result of slight modifications in the SDS-PAGE procedure (see Methods). The MHC-IIa and MHC-IIx bands of MHC-IIax fibers were apparently not effectively separated in

the original studies, resulting in the classification of these hybrid fibers as either MHC-IIa or MHC-IIx fibers.

For many decades, the concept of muscle fiber types has offered a useful perspective for understanding the heterogeneity that occurs both between and within skeletal muscles. To fully understand this heterogeneity at the cellular level, it is essential to make functional measurements in single fibers. The most important new finding was that contraction-stimulated glucose uptake did not differ significantly among the five MHC-II fiber types that were studied. It remains possible that fiber type-related differences in glucose uptake occur in MHC-II fibers with voluntary exercise *in vivo*, but such differences would likely be primarily dependent factors other than the fibers' intrinsic capacity for contraction-stimulated glucose uptake (e.g., extent of recruitment and blood flow). There were several compelling fiber type-related differences in protein abundance, including differences that were expected based on earlier studies (e.g., GLUT4 and COX IV). The substantial and unanticipated fiber type differences for filamin C abundance provide novel information with implications for the functional roles of this protein. In addition, the lack of detectable RUVBL2 in any of the fiber types that were tested, and the fiber type differences for TBC1D1 have relevance for clarifying the biological purposes of these proteins in muscle. The analysis of single fibers offers unique information and opportunities, but the optimal benefits of this approach require the careful consideration of the knowledge obtained from studying both isolated skeletal muscle preparations and the intact organism.

Acknowledgements

This research was supported by grants from the National Institutes of Health (DK071771 and AG10026 to G. D. Cartee). I would also like to thank Dr. Edward B. Arias and Dr. Naveen Sharma for their assistance with experiments and data collection.

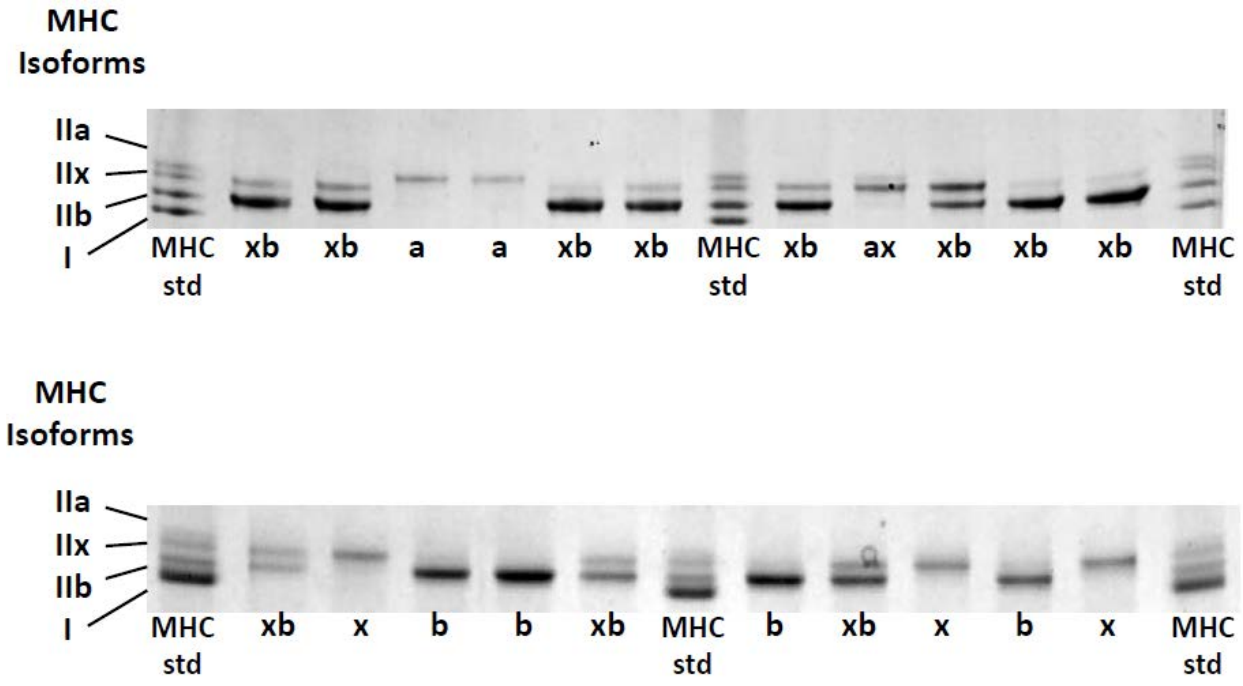

Figure 4.1

Representative Coomassie stained gels showing the fiber types expressed by single fibers isolated from the rat epitrochlearis muscles.

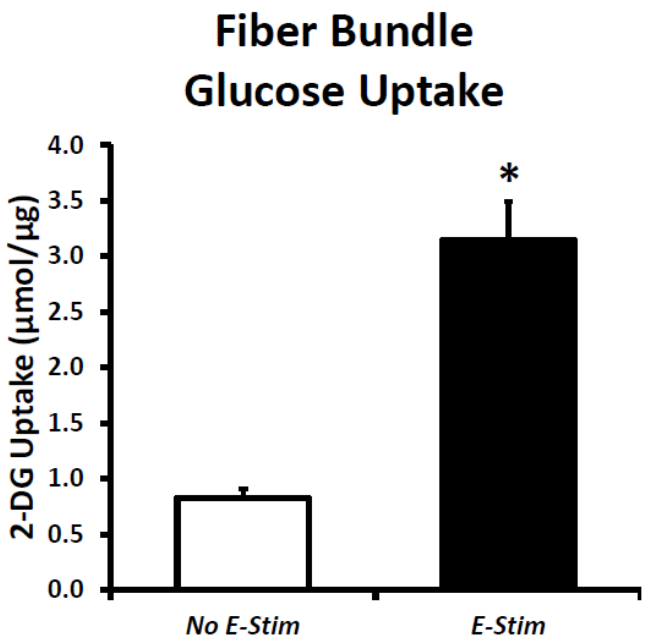

Figure 4.2

Contraction-stimulated 2-DG uptake by fiber bundles. *Indicates significance difference for 2-tailed paired t-test between No E-Stim versus E-Stim ($P < 0.01$; $n = 11$).

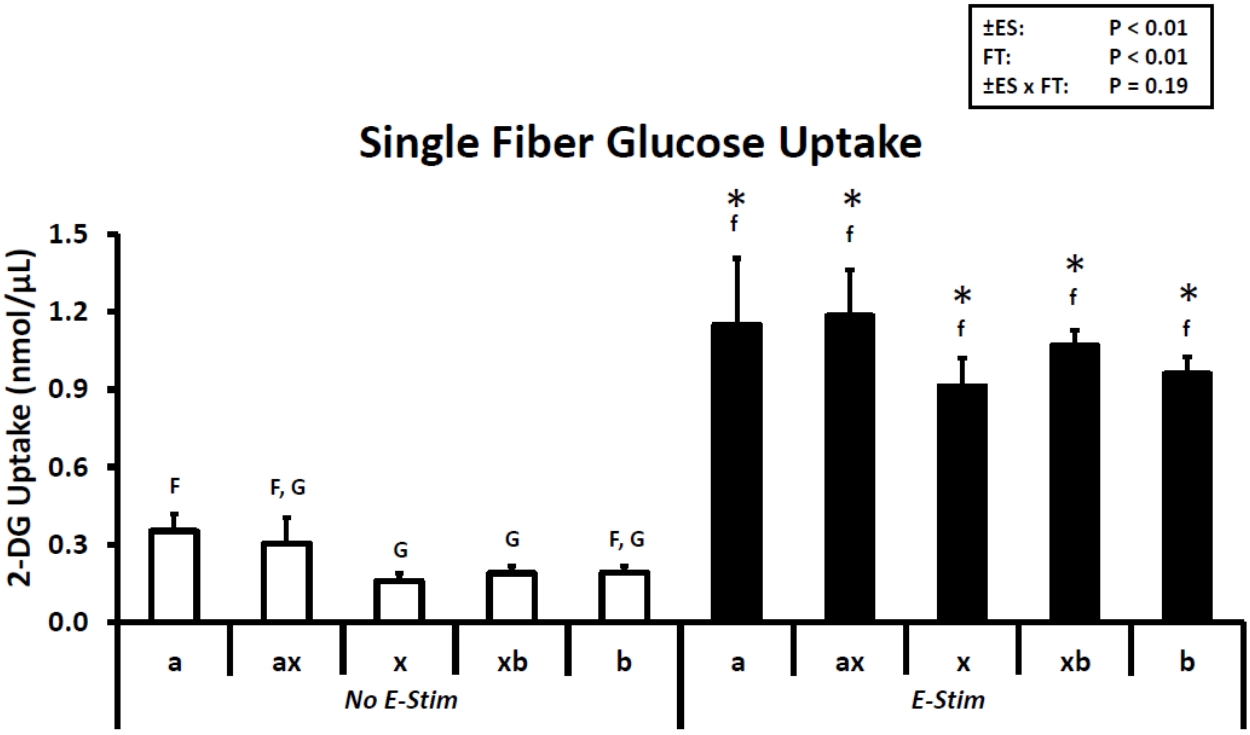

Figure 4.3

Contraction-stimulated 2-DG uptake by single muscle fibers. Box in upper right shows 2-way ANOVA analysis (*No E-Stim* vs. *E-Stim*, ± ES; Fiber Type, FT; Interaction, ± ES x FT). For post-hoc analysis statistical significance ($P < 0.05$) within the *No E-Stim* fibers (open bars) is indicated by uppercase letters, and statistical significance ($P < 0.05$) within the *E-Stim* fibers (filled bars) is indicated by lowercase letters. *Indicates significance difference ($P < 0.05$) for *No E-Stim* vs. *E-Stim* within a given fiber type (e.g., *No E-Stim* MCH-IIa vs. *E-Stim* MHC-IIa). Values are means ± SE with n for *No E-Stim/E-Stim* fibers: MHC-IIa (25/21), MHC-IIax (15/27), MHC-IIx (59/72), MHC-IIxb (157/193) and MHC-IIb (84/136).

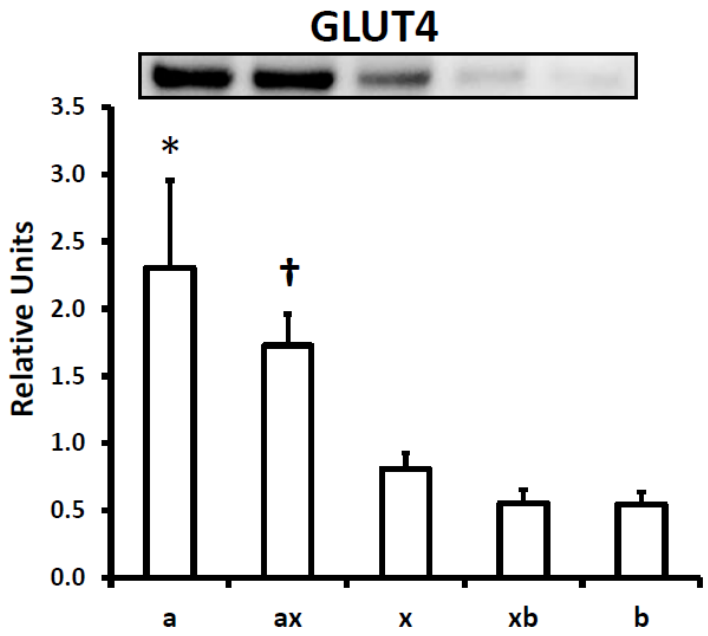

Figure 4.4

Relative GLUT 4 protein abundance for single muscle fibers. *Indicates statistical significance for MHC-IIa vs. MHC-IIx, MHC-IIxb and MHC-IIb ($P < 0.05$). †Indicates statistical significance for MHC-IIax vs. MHC-IIxb and MHC-IIb ($P < 0.05$). Values are means ± SE; n = 10 for each fiber type.

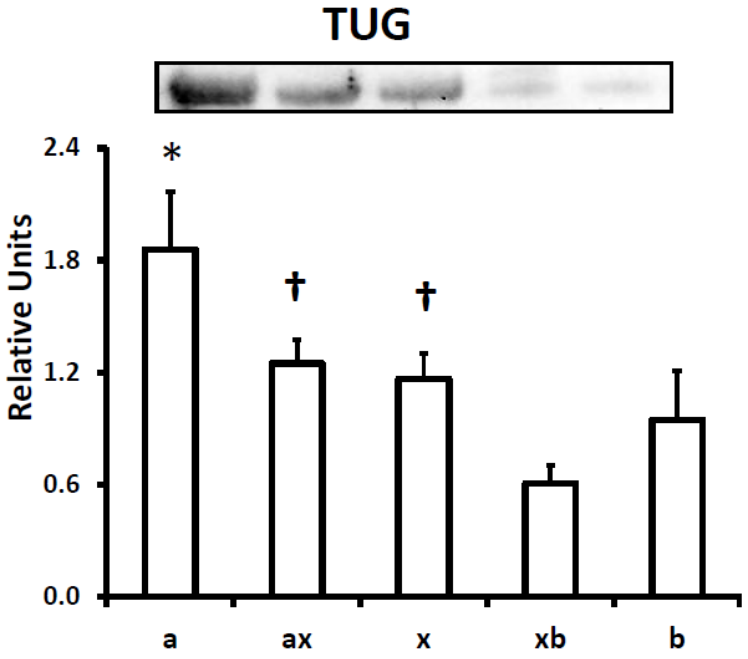

Figure 4.5

Relative TUG protein abundance for single muscle fibers. *Indicates statistical significance for MHC-IIa vs. MHC-IIxb and MHC-IIb ($P < 0.05$). †Indicates statistical significance for MHC-IIax and MHC-IIx vs MHC-IIxb ($P < 0.05$). Values are means ± SE; n = 13 for each fiber type.

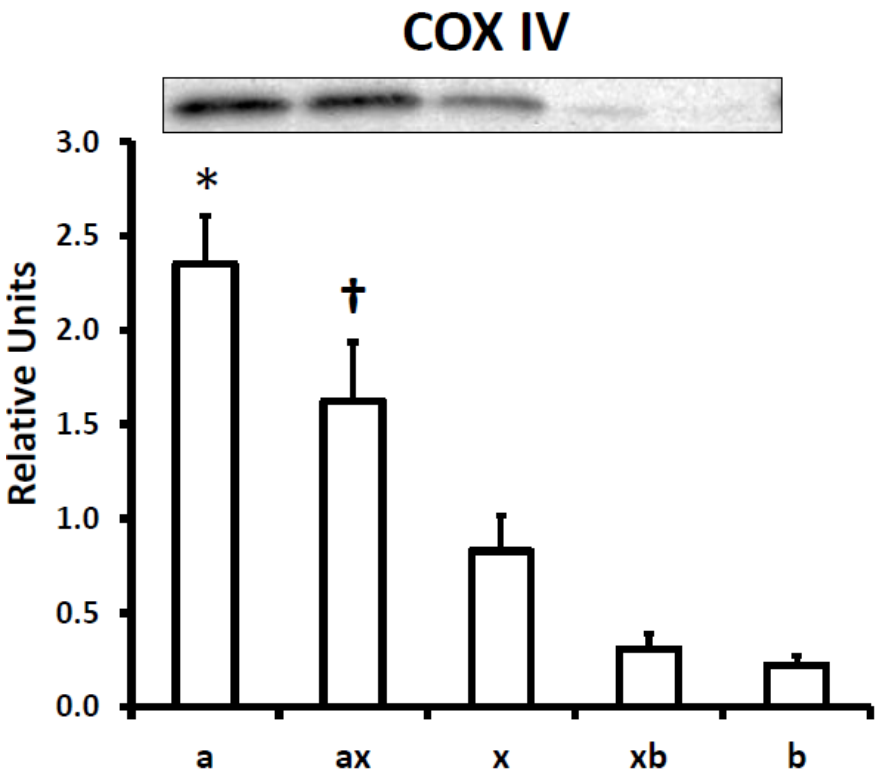

Figure 4.6

Relative COX IV protein abundance for single muscle fibers. *Indicates statistical significance for MHC-IIa vs. MHC-IIx, MHC-IIxb, and MHC-IIb ($P < 0.05$). †Indicates statistical significance for MHC-IIax and MHC-IIx vs MHC-IIxb and MCH-IIb ($P < 0.05$). Values are means ± SE; n = 14 for each fiber type.

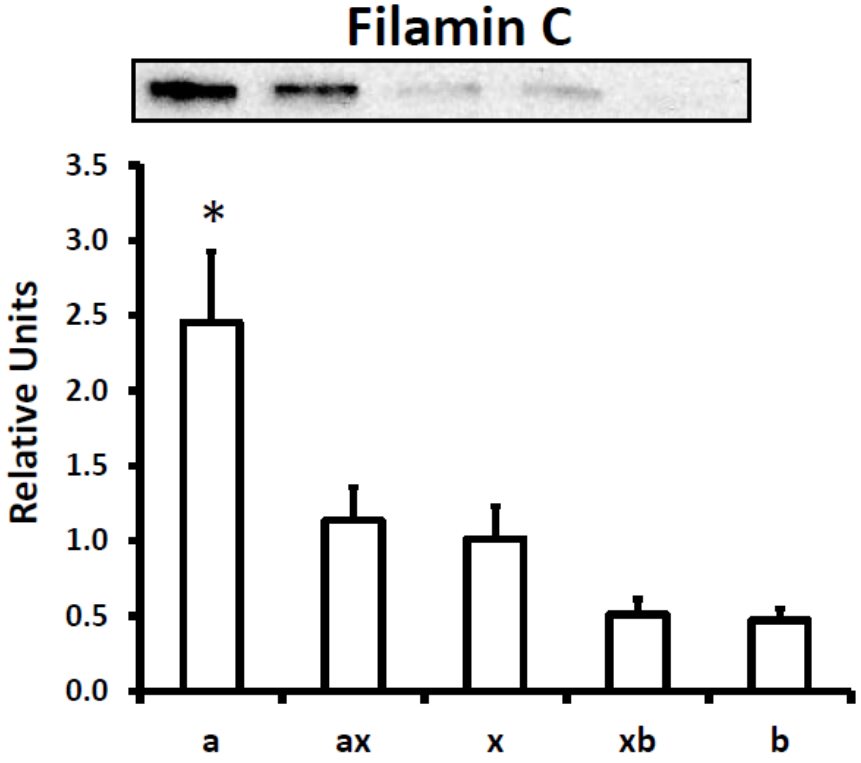

Figure 4.7

Relative filamin C protein abundance for single muscle fibers. *Indicates statistical significance for MHC-IIa vs. MHC-IIx, MHC-IIxb and MHC-IIb ($P < 0.05$). Values are means ± SE; n = 13 for each fiber type.

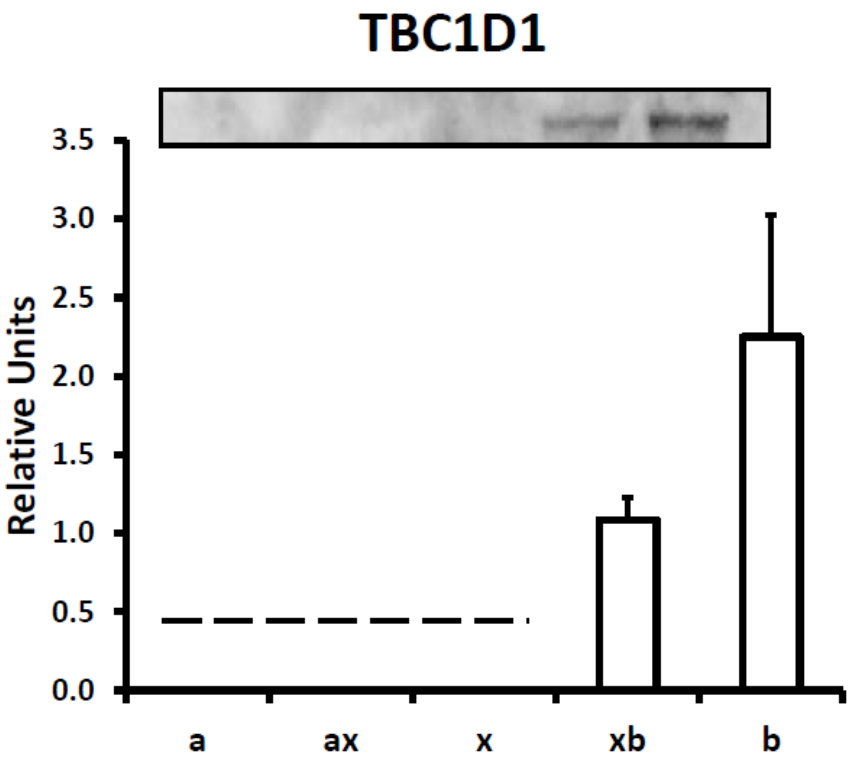

Figure 4.8

Relative TBC1D1 protein abundance for single muscle fibers. Because TBC1D1 was detectable in only 1 to 2 of the MHC-IIa, MHC-IIax, and MHC-IIx fibers, the statistical analysis of TBC1D1 was performed only on the MHC-IIxb fibers and MHC-IIb fibers fibers for which TBC1D1 was detectable. The dashed line for MHC-IIa, MHC-IIax and MHC-IIx fibers indicates that these subgroups were not included in the statistical analysis. Values are means ± SE; n = 11 for each fiber type (MHC-IIxb and MHC-IIb).

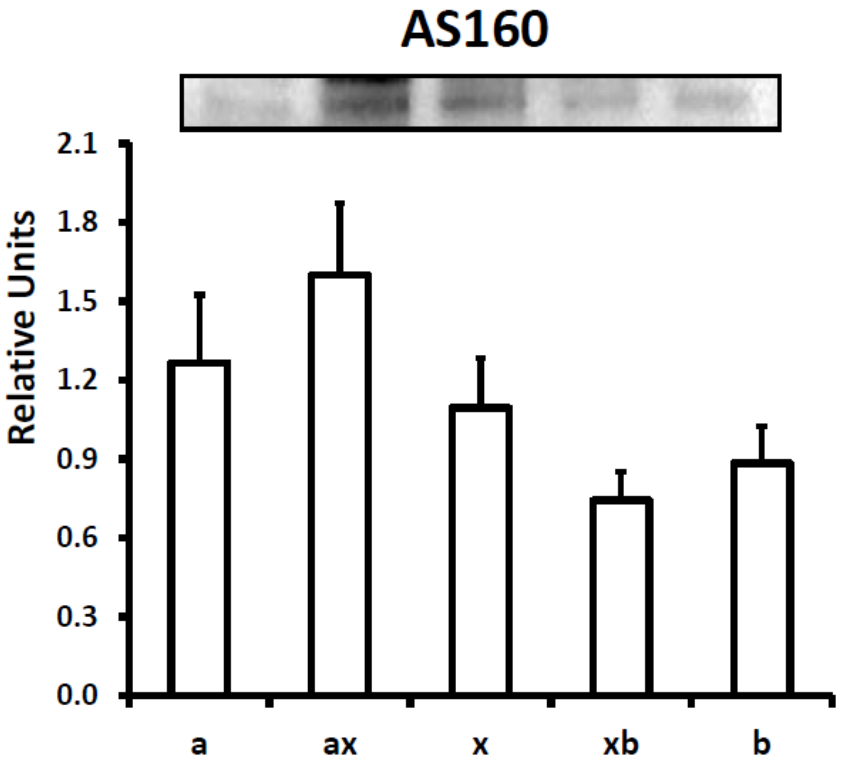

Figure 4.9

Relative AS160 protein abundance for single muscle fibers. Values are means ± SE; n = 13 for each fiber type.

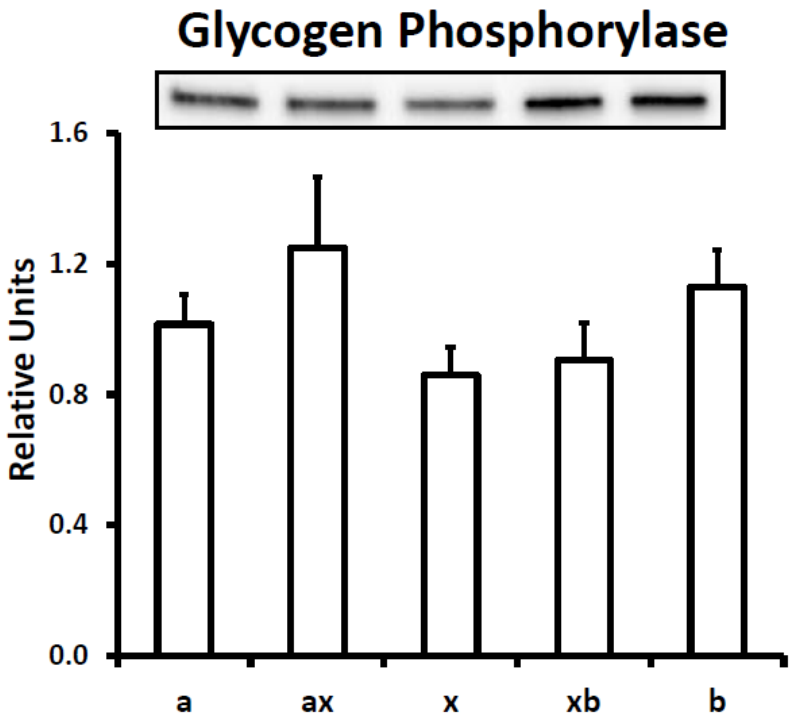

Figure 4.10

Relative Glycogen Phosphorylase protein abundance for single muscle fibers. Values are means ± SE; n = 15 for each fiber type.

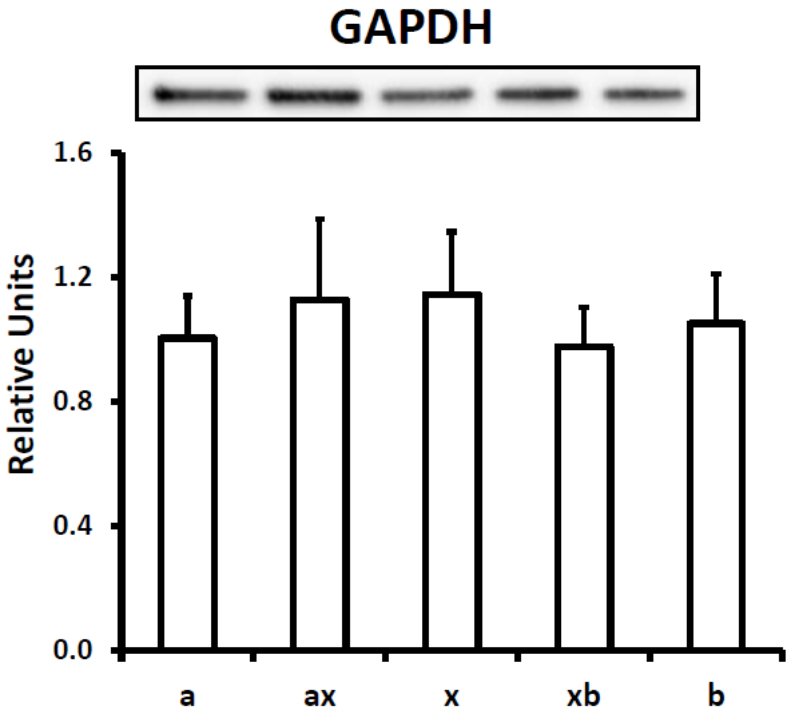

Figure 4.11

Relative GAPDH protein abundance for single muscle fibers. Values are means ± SE; n = 13 for each fiber type.

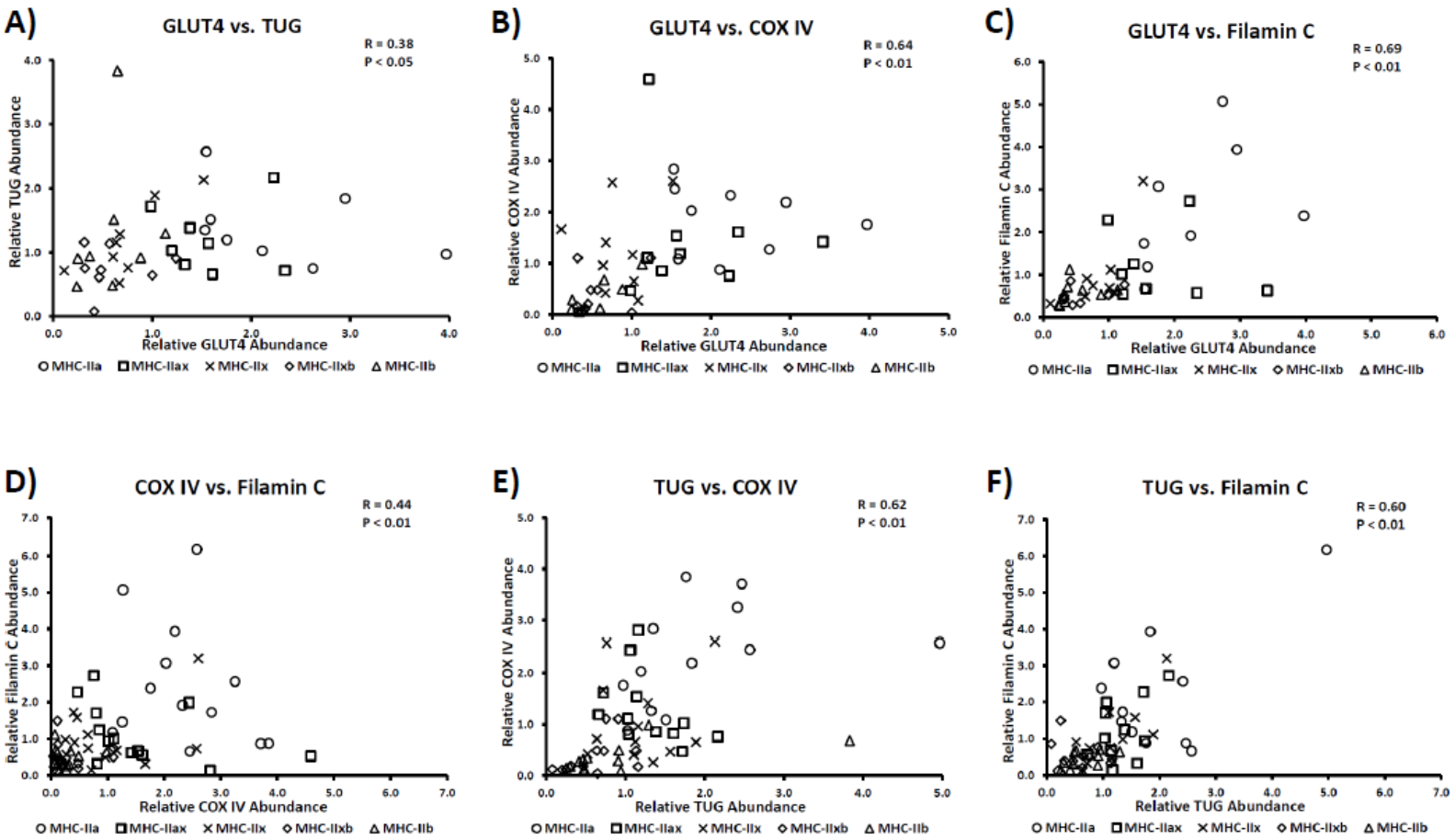

Figure 4.12A-F

Significant correlations. A: GLUT4 vs. TUG, n = 40; B: GLUT4 vs. COX IV, n = 45; C: GLUT4 vs Filamin C, n = 40; D: COX IV vs Filamin C, n = 65; E: TUG vs. COX IV, n = 60; F: TUG vs. Filamin C, n = 55. Each fiber is denoted with an individual symbol.

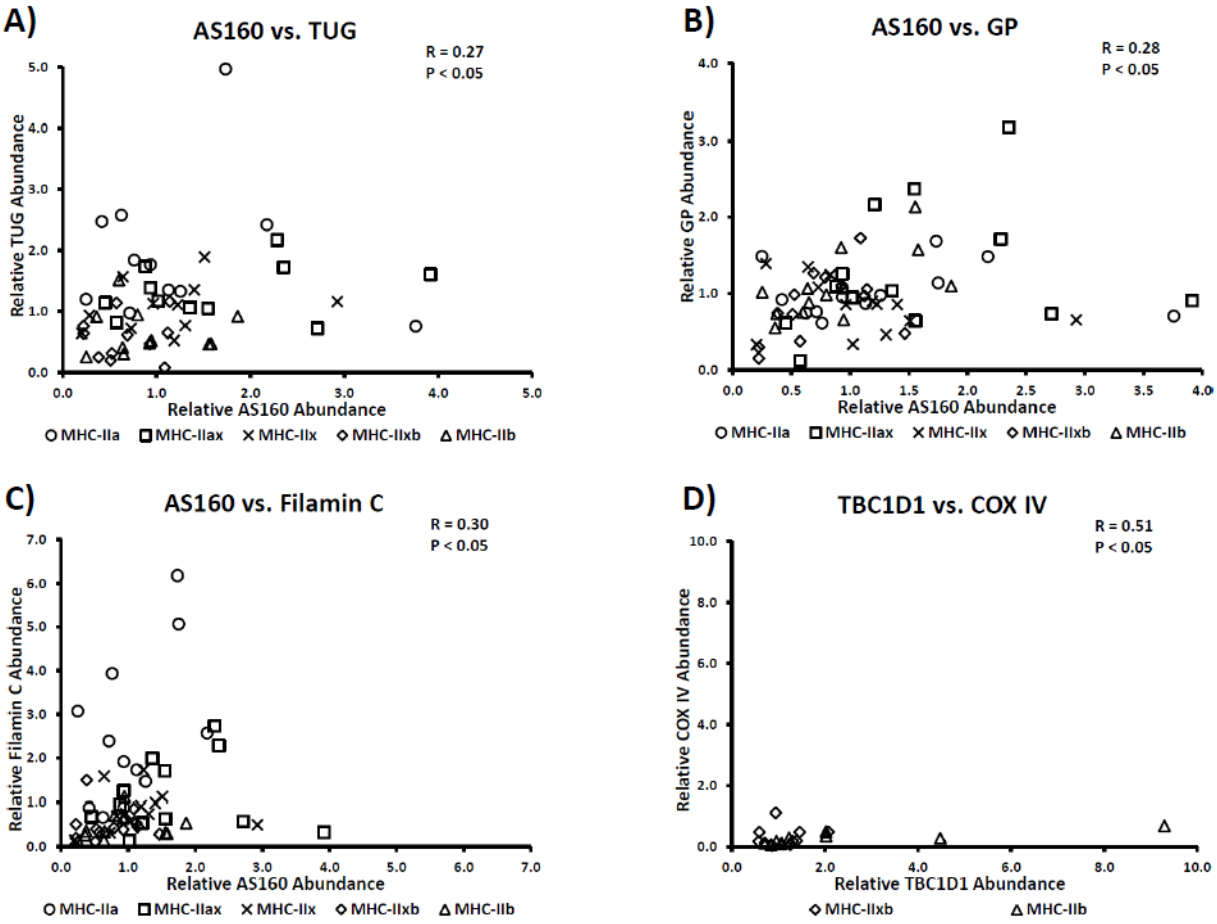

Figure 4.13A-D

Significant correlations. A: AS160 vs. TUG, n = 55; B: AS160 vs. Glycogen Phosphorylase (GP), n = 65; C: AS160 vs. Filamin C, n = 60; D: TCB1D1 vs. COX IV, n = 20. Each fiber is denoted with an individual symbol.

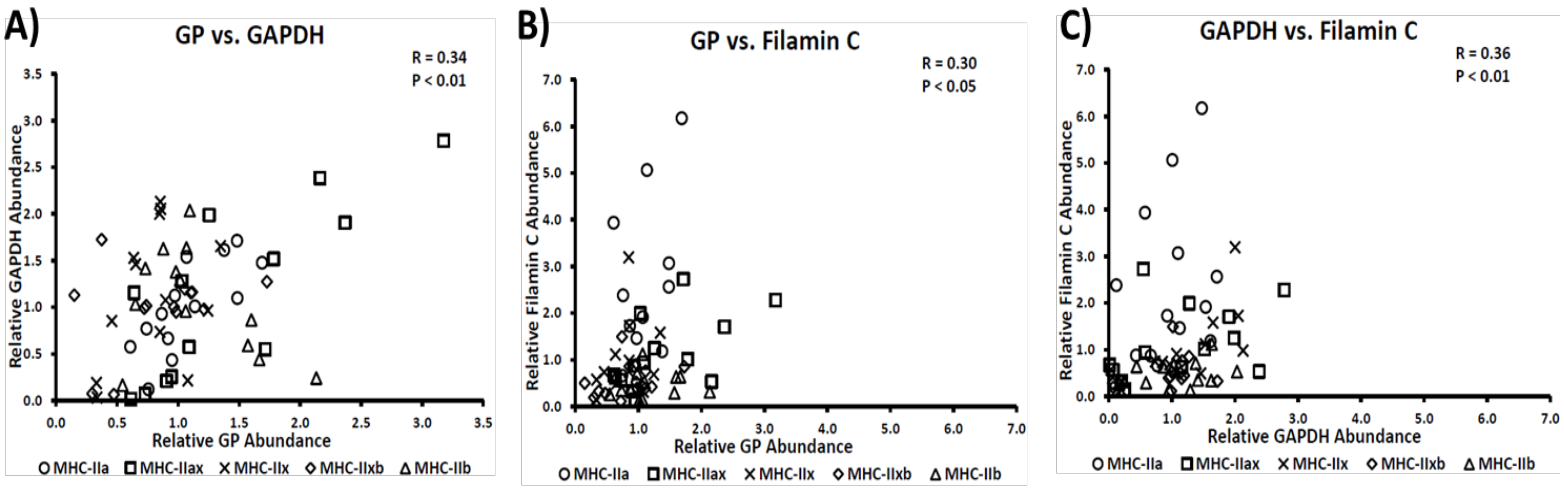

Figure 4.14A-C

Significant correlations. A: Glycogen Phosphorylase (GP) vs. GAPDH, n = 65; B: GP vs. Filamin C, n = 65; C: GAPDH vs. Filamin C, n = 65. Each fiber is denoted with an individual symbol.

References

1. **Ai H, Ihlemann J, Hellsten Y, Lauritzen HP, Hardie DG, Galbo H, and Ploug T.** Effect of fiber type and nutritional state on AICAR- and contraction-stimulated glucose transport in rat muscle. *Am J Physiol Endocrinol Metab* 282: E1291-1300, 2002.
2. **Ai H, Ralston E, Lauritzen HP, Galbo H, and Ploug T.** Disruption of microtubules in rat skeletal muscle does not inhibit insulin- or contraction-stimulated glucose transport. *Am J Physiol Endocrinol Metab* 285: E836-844, 2003.
3. **Benton CR, Nickerson JG, Lally J, Han XX, Holloway GP, Glatz JF, Luiken JJ, Graham TE, Heikkila JJ, and Bonen A.** Modest PGC-1alpha overexpression in muscle in vivo is sufficient to increase insulin sensitivity and palmitate oxidation in subsarcolemmal, not intermyofibrillar, mitochondria. *J Biol Chem* 283: 4228-4240, 2008.
4. **Bogan JS, Hendon N, McKee AE, Tsao TS, and Lodish HF.** Functional cloning of TUG as a regulator of GLUT4 glucose transporter trafficking. *Nature* 425: 727-733, 2003.
5. **Brozinick JT, Jr., Etgen GJ, Jr., Yaspelkis BB, 3rd, Kang HY, and Ivy JL.** Effects of exercise training on muscle GLUT-4 protein content and translocation in obese Zucker rats. *Am J Physiol* 265: E419-427, 1993.
6. **Caiozzo VJ, Baker MJ, Huang K, Chou H, Wu YZ, and Baldwin KM.** Single-fiber myosin heavy chain polymorphism: how many patterns and what proportions? *Am J Physiol Regul Integr Comp Physiol* 285: R570-580, 2003.
7. **Caiozzo VJ, Haddad F, Baker M, McCue S, and Baldwin KM.** MHC polymorphism in rodent plantaris muscle: effects of mechanical overload and hypothyroidism. *Am J Physiol Cell Physiol* 278: C709-717, 2000.
8. **Carlsen RC, Larson DB, and Walsh DA.** A fast-twitch oxidative-glycolytic muscle with a robust inward calcium current. *Can J Physiol Pharmacol* 63: 958-965, 1985.
9. **Cartee GD and Funai K.** Exercise and Insulin: Convergence or Divergence at AS160 and TBC1D1? *Exercise and Sport Sciences Reviews* 37: 188-195, 2009.
10. **Cartee GD and Wojtaszewski JF.** Role of Akt substrate of 160 kDa in insulin-stimulated and contraction-stimulated glucose transport. *Appl Physiol Nutr Metab* 32: 557-566, 2007.
11. **Castorena CM, Mackrell JG, Bogan JS, Kanzaki M, and Cartee GD.** Clustering of GLUT4, TUG and RUVBL2 Protein Levels Correlate with Myosin Heavy Chain Isoform Pattern in Skeletal Muscles, but AS160 and TBC1D1 Levels Do Not. *J Appl Physiol*, 2011.
12. **Chabi B, Adhihetty PJ, O'Leary MF, Menzies KJ, and Hood DA.** Relationship between Sirt1 expression and mitochondrial proteins during conditions of chronic muscle use and disuse. *J Appl Physiol* 107: 1730-1735, 2009.
13. **Chi MM, Hintz CS, Henriksson J, Salmons S, Hellendahl RP, Park JL, Nemeth PM, and Lowry OH.** Chronic stimulation of mammalian muscle: enzyme changes in individual fibers. *Am J Physiol* 251: C633-642, 1986.
14. **Coderre L, Kandror KV, Vallega G, and Pilch PF.** Identification and characterization of an exercise-sensitive pool of glucose transporters in skeletal muscle. *J Biol Chem* 270: 27584-27588, 1995.
15. **Constable SH, Favier RJ, Cartee GD, Young DA, and Holloszy JO.** Muscle glucose transport: interactions of in vitro contractions, insulin, and exercise. *J Appl Physiol* 64: 2329-2332, 1988.

16. **Daugaard JR, Nielsen JN, Kristiansen S, Andersen JL, Hargreaves M, and Richter EA.** Fiber type-specific expression of GLUT4 in human skeletal muscle: influence of exercise training. *Diabetes* 49: 1092-1095, 2000.
17. **Douen AG, Ramlal T, Klip A, Young DA, Cartee GD, and Holloszy JO.** Exercise-induced increase in glucose transporters in plasma membranes of rat skeletal muscle. *Endocrinology* 124: 449-454, 1989.
18. **Douen AG, Ramlal T, Rastogi S, Bilan PJ, Cartee GD, Vranic M, Holloszy JO, and Klip A.** Exercise induces recruitment of the "insulin-responsive glucose transporter". Evidence for distinct intracellular insulin- and exercise-recruitable transporter pools in skeletal muscle. *J Biol Chem* 265: 13427-13430, 1990.
19. **Dumke CL, Kim J, Arias EB, and Cartee GD.** Role of kallikrein-kininogen system in insulin-stimulated glucose transport after muscle contractions. *J Appl Physiol* 92: 657-664, 2002.
20. **Fitts RH, Brimmer CJ, Heywood-Cooksey A, and Timmerman RJ.** Single muscle fiber enzyme shifts with hindlimb suspension and immobilization. *Am J Physiol* 256: C1082-1091, 1989.
21. **Fujita M, Mitsuhashi H, Isogai S, Nakata T, Kawakami A, Nonaka I, Noguchi S, Hayashi YK, Nishino I, and Kudo A.** Filamin C plays an essential role in the maintenance of the structural integrity of cardiac and skeletal muscles, revealed by the medaka mutant zacro. *Dev Biol* 361: 79-89, 2012.
22. **Funai K and Cartee GD.** Inhibition of contraction-stimulated AMP-activated protein kinase inhibits contraction-stimulated increases in PAS-TBC1D1 and glucose transport without altering PAS-AS160 in rat skeletal muscle. *Diabetes* 58: 1096-1104, 2009.
23. **Funai K, Schweitzer GG, Castorena CM, Kanzaki M, and Cartee GD.** In vivo exercise followed by in vitro contraction additively elevates subsequent insulin-stimulated glucose transport by rat skeletal muscle. *Am J Physiol Endocrinol Metab* 298: E999-1010, 2010.
24. **Gao J, Ren J, Gulve EA, and Holloszy JO.** Additive effect of contractions and insulin on GLUT-4 translocation into the sarcolemma. *J Appl Physiol* 77: 1597-1601, 1994.
25. **Hashimoto T, Masuda S, Taguchi S, and Brooks GA.** Immunohistochemical analysis of MCT1, MCT2 and MCT4 expression in rat plantaris muscle. *J Physiol* 567: 121-129, 2005.
26. **Henriksen EJ, Bourey RE, Rodnick KJ, Koranyi L, Permutt MA, and Holloszy JO.** Glucose transporter protein content and glucose transport capacity in rat skeletal muscles. *Am J Physiol* 259: E593-598, 1990.
27. **Hintz CS, Lowry CV, Kaiser KK, McKee D, and Lowry OH.** Enzyme levels in individual rat muscle fibers. *Am J Physiol* 239: C58-65, 1980.
28. **Holloszy JO.** Regulation by exercise of skeletal muscle content of mitochondria and GLUT4. *J Physiol Pharmacol* 59 Suppl 7: 5-18, 2008.
29. **Ihlemann J, Ploug T, and Galbo H.** Effect of force development on contraction induced glucose transport in fast twitch rat muscle. *Acta Physiol Scand* 171: 439-444, 2001.
30. **Ihlemann J, Ploug T, Hellsten Y, and Galbo H.** Effect of stimulation frequency on contraction-induced glucose transport in rat skeletal muscle. *Am J Physiol Endocrinol Metab* 279: E862-867, 2000.
31. **James DE, Kraegen EW, and Chisholm DJ.** Muscle glucose metabolism in exercising rats: comparison with insulin stimulation. *Am J Physiol* 248: E575-580, 1985.
32. **Jensen TE, Leutert R, Rasmussen ST, Mouatt JR, Christiansen ML, Jensen BR, and Richter EA.** EMG-normalised kinase activation during exercise is higher in human gastrocnemius compared to soleus muscle. *PLoS One* 7: e31054, 2012.

33. **Kern M, Wells JA, Stephens JM, Elton CW, Friedman JE, Tapscott EB, Pekala PH, and Dohm GL.** Insulin responsiveness in skeletal muscle is determined by glucose transporter (Glut4) protein level. *Biochem J* 270: 397-400, 1990.
34. **Koh HJ, Toyoda T, Fujii N, Jung MM, Rathod A, Middelbeek RJ, Lessard SJ, Treebak JT, Tsuchihara K, Esumi H, Richter EA, Wojtaszewski JF, Hirshman MF, and Goodyear LJ.** Sucrose nonfermenting AMPK-related kinase (SNARK) mediates contraction-stimulated glucose transport in mouse skeletal muscle. *Proc Natl Acad Sci U S A* 107: 15541-15546, 2010.
35. **Koistinen HA, Galuska D, Chibalin AV, Yang J, Zierath JR, Holman GD, and Wallberg-Henriksson H.** 5-amino-imidazole carboxamide riboside increases glucose transport and cell-surface GLUT4 content in skeletal muscle from subjects with type 2 diabetes. *Diabetes* 52: 1066-1072, 2003.
36. **Kong X, Manchester J, Salmons S, and Lawrence JC, Jr.** Glucose transporters in single skeletal muscle fibers. Relationship to hexokinase and regulation by contractile activity. *J Biol Chem* 269: 12963-12967, 1994.
37. **Lauritzen HP.** Insulin- and contraction-induced glucose transporter 4 traffic in muscle: insights from a novel imaging approach. *Exerc Sport Sci Rev* 41: 77-86, 2013.
38. **Lauritzen HP, Galbo H, Brandauer J, Goodyear LJ, and Ploug T.** Large GLUT4 vesicles are stationary while locally and reversibly depleted during transient insulin stimulation of skeletal muscle of living mice: imaging analysis of GLUT4-enhanced green fluorescent protein vesicle dynamics. *Diabetes* 57: 315-324, 2008.
39. **Lauritzen HP, Galbo H, Toyoda T, and Goodyear LJ.** Kinetics of contraction-induced GLUT4 translocation in skeletal muscle fibers from living mice. *Diabetes* 59: 2134-2144, 2010.
40. **Lemieux K, Konrad D, Klip A, and Marette A.** The AMP-activated protein kinase activator AICAR does not induce GLUT4 translocation to transverse tubules but stimulates glucose uptake and p38 mitogen-activated protein kinases alpha and beta in skeletal muscle. *Faseb J* 17: 1658-1665, 2003.
41. **Li J, Hu X, Selvakumar P, Russell IR, Cushman SW, Holman GD, and Young LH.** Role of the Nitric Oxide Pathway in AMPK-mediated Glucose Uptake and GLUT4 Translocation in Heart Muscle. *Am J Physiol Endocrinol Metab*, 2004.
42. **Lund S, Holman GD, Schmitz O, and Pedersen O.** Contraction stimulates translocation of glucose transporter GLUT4 in skeletal muscle through a mechanism distinct from that of insulin. *Proc Natl Acad Sci U S A* 92: 5817-5821, 1995.
43. **Mackrell JG, Arias EB, and Cartee GD.** Fiber type-specific differences in glucose uptake by single fibers from skeletal muscles of 9- and 25-month-old rats. *J Gerontol A Biol Sci Med Sci* 67: 1286-1294, 2012.
44. **MacKrell JG and Cartee GD.** A Novel Method to Measure Glucose Uptake and Myosin Heavy Chain Isoform Expression of Single Fibers from Rat Skeletal Muscle. *Diabetes* In Press: Accepted January, 2012.
45. **Marette A, Burdett E, Douen A, Vranic M, and Klip A.** Insulin induces the translocation of GLUT4 from a unique intracellular organelle to transverse tubules in rat skeletal muscle. *Diabetes* 41: 1562-1569, 1992.
46. **Megeney LA, Neufer PD, Dohm GL, Tan MH, Blewett CA, Elder GC, and Bonen A.** Effects of muscle activity and fiber composition on glucose transport and GLUT-4. *Am J Physiol* 264: E583-593, 1993.

47. **Nemeth PM, Norris BJ, Lowry OH, Gordon DA, Enoka RM, and Stuart DG.** Activation of muscle fibers in individual motor units revealed by 2-deoxyglucose-6-phosphate. *J Neurosci* 8: 3959-3966, 1988.
48. **Nesher R, Karl IE, and Kipnis DM.** Dissociation of effects of insulin and contraction on glucose transport in rat epitrochlearis muscle. *Am J Physiol* 249: C226-232, 1985.
49. **Ploug T, van Deurs B, Ai H, Cushman SW, and Ralston E.** Analysis of GLUT4 distribution in whole skeletal muscle fibers: identification of distinct storage compartments that are recruited by insulin and muscle contractions. *J Cell Biol* 142: 1429-1446, 1998.
50. **Razinia Z, Makela T, Ylanne J, and Calderwood DA.** Filamins in mechanosensing and signaling. *Annu Rev Biophys* 41: 227-246, 2012.
51. **Richardson JM, Balon TW, Treadway JL, and Pessin JE.** Differential regulation of glucose transporter activity and expression in red and white skeletal muscle. *J Biol Chem* 266: 12690-12694, 1991.
52. **Richter EA, Ploug T, and Galbo H.** Increased muscle glucose uptake after exercise. No need for insulin during exercise. *Diabetes* 34: 1041-1048, 1985.
53. **Sequea DA, Sharma N, Arias EB, and Cartee GD.** Greater filamin C, GSK3alpha, and GSK3beta serine phosphorylation in insulin-stimulated isolated skeletal muscles of calorie restricted 24 month-old rats. *Mech Ageing Dev* 134: 60-63, 2013.
54. **Sharma N, Arias EB, Sequea DA, and Cartee GD.** Preventing the calorie restriction-induced increase in insulin-stimulated Akt2 phosphorylation eliminates calorie restriction's effect on glucose uptake in skeletal muscle. *Biochim Biophys Acta* 1822: 1735-1740, 2012.
55. **Talmadge RJ and Roy RR.** Electrophoretic separation of rat skeletal muscle myosin heavy-chain isoforms. *J Appl Physiol* 75: 2337-2340, 1993.
56. **Taylor EB, An D, Kramer HF, Yu H, Fujii NL, Roeckl KS, Bowles N, Hirshman MF, Xie J, Feener EP, and Goodyear LJ.** Discovery of TBC1D1 as an Insulin-, AICAR-, and Contraction-stimulated Signaling Nexus in Mouse Skeletal Muscle. *J Biol Chem* 283: 9787-9796, 2008.
57. **Toop J, Burke RE, Dum RP, O'Donovan MJ, and Smith CB.** 2-deoxyglucose autoradiography of single motor units: labeling of individual acutely active muscle fibers. *J Neurosci Methods* 5: 283-289, 1982.
58. **Wang C.** Insulin-stimulated glucose uptake in rat diaphragm during postnatal development: lack of correlation with the number of insulin receptors and of intracellular glucose transporters. *Proceedings of the National Academy of Sciences of the United States of America* 82: 3621-3625, 1985.
59. **Wu YZ, Baker MJ, Crumley RL, and Caiozzo VJ.** Single-fiber myosin heavy-chain isoform composition of rodent laryngeal muscle: modulation by thyroid hormone. *Arch Otolaryngol Head Neck Surg* 126: 874-880, 2000.
60. **Xie X, Chen Y, Xue P, Fan Y, Deng Y, Peng G, Yang F, and Xu T.** RUVBL2, a novel AS160-binding protein, regulates insulin-stimulated GLUT4 translocation. *Cell Res*, 2009.
61. **Zaid H, Antonescu CN, Randhawa VK, and Klip A.** Insulin action on glucose transporters through molecular switches, tracks and tethers. *Biochem J* 413: 201-215, 2008.

Chapter V

Study 3:

Acute Exercise Effects on Insulin Signaling and Insulin-Stimulated Glucose Uptake in Isolated Skeletal Muscle from Rats Fed either Low Fat or High Fat Diet

Abstract

Previous studies demonstrated that acute exercise by rats with normal insulin sensitivity can lead to increased insulin-stimulated glucose uptake of skeletal muscle concomitant with increased phosphorylation of Akt Substrate of 160 kDa on Thr642 and Ser588 ($pAS160^{Thr642}$ and $pAS160^{Ser588}$) compared to sedentary control values. Because little is known about mechanisms for exercise effects on insulin sensitivity in insulin-resistant muscle, our goal was to assess exercise effects on insulin-stimulated glucose uptake, $pAS160^{Thr642}$ and $pAS160^{Ser588}$ in muscles from rats fed normal rodent chow (14% kcal fat, low fat diet, LFD) or a high fat diet (60% kcal fat, HFD, for 2wk). Half of the rats from each diet group were sedentary (LFD SED and HFD SED), and the others performed 2h of swim-exercise. Exercise rats were studied either immediately post-exercise (LFD IPEX and HFD IPEX) or 3h post-exercise (LFD 3hPEX and HFD 3hPEX). For IPEX rats, one epitrochlearis muscle was immediately frozen for determination of glycogen and phosphorylation of AMP-activated protein kinase (AMPK) and Akt substrate of 160 kDa (AS160), and the contralateral muscle was incubated with ^{3}H-2-deoxyglucose (2-DG) with no insulin. For 3hPEX rats, paired epitrochlearis muscles were incubated with 2-DG ±100μU/mL insulin. At each time-point (IPEX and 3hPEX) for muscles

from both LFD IPEX and HFD IPEX rats, insulin-independent 2-DG uptake was increased ($P < 0.05$) compared to the respective sedentary controls, and muscle insulin-independent 2-DG uptake was not different for LFD versus HFD groups in either sedentary or exercised rats. IPEX versus Sedentary controls had reduced muscle glycogen and increased phosphorylation of AMPK and AS160, and none of these IPEX-effects differed between diet groups. Muscles from HFD SED versus LFD SED rats had lower ($P < 0.05$) insulin-stimulated 2-DG uptake. For both LFD 3hPEX and HFD 3hPEX groups, muscle insulin-stimulated 2-DG uptake was increased ($P < 0.05$) compared to their respective Sedentary controls, but muscle insulin-stimulated 2-DG uptake was lower ($P < 0.05$) for HFD 3hPEX versus LFD 3hPEX rats. HFD did not significantly alter insulin-stimulated insulin receptor phosphorylation, or phosphatidylinositol-3-kinase associated with insulin receptor substrate-1 (IRS-1), Akt^{Ser473} phosphorylation or Akt activity of insulin-stimulated muscles, but there was a main effect of diet ($P < 0.05$) on for Akt^{Thr308} phosphorylation (LFD > HFD). For insulin-stimulated muscles from LFD 3hPEX rats, greater 2-DG uptake was accompanied by increased ($P < 0.05$) $pAS160^{Thr642}$ and $pAS160^{Ser588}$. For insulin-stimulated muscles from HFD 3hPEX versus HFD Sedentary rats, greater 2-DG uptake was accompanied by increased $pAS160^{Ser588}$, but $pAS160^{Ser588}$ values were significantly lower in the HFD 3hPEX versus LFD 3hPEX rats ($P < 0.05$). In addition, in neither diet-group was the exercised-induced improvement in insulin-stimulated 2-DG uptake by muscle accompanied by: significant improvements in proximal insulin signaling, reduced serine phosphorylation of IRS-1, decreased c-Jun N-terminal Kinase phosphorylation or reductions in diacylglycerols or ceramides. For triacylglycerols, there was a main effect of diet ($P < 0.05$, HFD > LFD) for 18:0, 18:1 (n-9), 20:2, and for LFD 3hPEX versus LFD SED muscles 20:1 was significantly lower ($P < 0.05$). For acyl-CoA, there was a main effect of exercise ($P < 0.05$) for acyl-CoA-16:0 (Sedentary > 3hPEX), and for HFD 3hPEX versus HFD SED muscles acyl-CoA-16:0 was significantly lower ($P < 0.05$). These results indicate that exercise can enhance insulin-stimulated 2-DG uptake of muscles from either LFD or HFD rats concomitant with enhanced pAS160. In addition, these observations implicate the greater pAS160 in the LFD 3hPEX versus HFD 3hPEX group as a possible mechanism for the greater insulin-stimulated 2-DG uptake in muscles from LFD 3hPEX rats.

Introduction

A single exercise bout is an effective stimulus for increasing insulin-stimulated glucose transport in skeletal muscle of humans (38, 61, 63, 68) or rodents (2, 10, 12, 19-20, 38, 45, 53) with normal insulin sensitivity prior to exercise. Following acute exercise by lean rats (28) or humans (61) with normal insulin sensitivity, the improved insulin-stimulated glucose transport is secondary to enhanced recruitment of the GLUT4 glucose transporter to the cell surface. However, the precise mechanism for the greater insulin-mediated GLUT4 translocation is unknown. Numerous studies of healthy humans or rats have found that the greater insulin sensitivity following exercise is not due to improved proximal insulin signaling [e.g., insulin binding to its receptor (4-5, 69), insulin receptor (IR) tyrosine kinase activity (60, 62, 65), insulin receptor substrate-1 tyrosine phosphorylation ($pIRS\text{-}1^{Tyr}$) (28-29), phosphatidylinositol-3-kinase associated with insulin receptor substrate-1 (IRS-1-PI3K) (15, 17, 66-67), or activation of Akt (2, 18, 20, 25, 65)].

The lack of evidence for exercise to elevate the activation of proximal insulin signaling events suggest that exercise may act on more distal signaling processes. In humans or rats the distal insulin signaling protein called Akt Substrate at 160 kDa (AS160; also known as TBC1D4) has been proposed as a possible regulator for the post-exercise increase in insulin sensitivity (2, 9, 19-20). AS160 is a Rab-GTPase protein that is phosphorylated in response to insulin, thereby inhibiting its GTPase activity and allowing for GLUT4 vesicles to translocate to the cell surface (11, 34, 49, 51). During the hours following acute exercise, the elevated AS160 phosphorylation has repeatedly been shown to be sustained (2, 19-20, 56, 63). In addition, evidence suggests that AS160's sustained phosphorylation tracks with the post-exercise increase in insulin-stimulated glucose transport under conditions in which the dietary protocol was altered after exercise (i.e., with or without refeeding a rat chow with a high carbohydrate content) (20).

Insulin resistance associated with high fat feeding is attributable to the reduced ability of insulin to stimulate GLUT4 translocation to the cell surface rather than reduced total GLUT4 abundance (26, 35, 47). Insulin resistance has been reported to be associated with increased muscle levels of lipid metabolites (including acyl-CoA, ceramides and diacylglycerol, DAG), that can increase the activity of serine kinases, including Protein Kinase C-Theta (PKC-θ) and c-Jun N-terminal Kinase (JNK) (6, 14, 48, 52, 55, 57). These serine kinases have been implicated

in increased serine phosphorylation of insulin receptor substrate-1 (pIRS-1^{Ser}) on inhibitory sites (pIRS-1^{Ser307} and pIRS-1^{Ser1101}), leading to reduced downstream signaling steps resulting in reduced Akt activation.

A single bout of exercise can also improve insulin-stimulated glucose uptake in skeletal muscle of insulin resistant humans (7, 16, 44, 54) or rats (3, 21, 36, 41, 46, 59). It is not clear if exercise induces this benefit in both healthy and insulin resistant individuals via the same mechanism. In rats fed a high fat diet (HFD), the limited data available suggest that the improved insulin sensitivity following acute exercise is associated with enhanced proximal signaling secondary to reduced JNK phosphorylation (pJNK) and pIRS-1^{Ser307} (41, 46). However, results from these studies should be interpreted with caution because insulin signaling measurements were obtained only with a supraphysiological insulin dose (41, 46). Furthermore, a similar study by the same group reported improved insulin signaling (increased IRS-1^{Tyr} and Akt phosphorylation, pAkt) in HFD rats after exercise in the absence of reduced pJNK or pIRS-1^{Ser307} (43).

For Study 3 healthy insulin sensitive rats (eating standard chow; low fat diet, LFD) and rats fed a HFD (for two weeks to induce insulin resistance) were evaluated for several potential mechanisms that may be important for the post-exercise increase in insulin-stimulated glucose transport by skeletal muscle. The first major goal for Study 3 was to investigate the mechanism (measurements of proximal insulin signaling and AS160 phosphorylation) for the exercise induced improvements for insulin-stimulated glucose uptake by skeletal muscle from insulin sensitive and insulin resistant rats. The second major goal was to identify possible changes in GLUT4, AS160, TBC1D1, TUG, RUVBL2 and muscle fiber type following 2 weeks of high fat feeding. The third major goal was to determine the effects of acute exercise on putative mediators of insulin resistance [lipid metabolites (acyl-CoA,DAG, ceramide), pJNK and pIRS-1^{Ser307} and pIRS-1^{Ser1101}] in muscles from insulin sensitive and insulin resistant rats.

Methods

Materials

The reagents and apparatus for sodium dodecyl sulfate-polyacrylamide gel electrophoresis (SDS-PAGE) and immunoblotting were from Bio-Rad (Hercules, CA). Bicinchoninic acid protein assay reagent (no. 23227) and Pierce reversible protein stain (Memcode) kit for nitrocellulose membranes (no. 24580) were from Pierce Biotechnology (Rockford, IL). Anti-AS160 (no. ABS54), anti-GLUT4 (no. CBL243), anti-IRS-1 (no. 06-248), anti-PI3K (no. 06-195), Akt1/PKBα Immunoprecipitation-Kinase Assay Kit (17-188), anti-Akt/PH domain clone SKB1 (no. 05-591), Akt substrate peptide (no. 12-340), protein G agarose beads (no. 16-266), MILLIPLEX $_{MAP}$ Cell Signaling Buffer and Detection Kit (no. 48-602), MILLIPLEX MAP Akt/mTOR Phosphoprotein Panel (no. 48-611; Akt^{Ser473}; glycogen synthase beta, GSKβ^{Ser9}; insulin receptor, IR$^{Tyr1162/1163}$; IRS-1^{Ser307}; and tuberous sclerosis 2, TSC2^{Ser939}), MILLIPLEX MAP Phospho JNK/SAPK$^{Thr183/Tyr185}$ (no. 46-613) and Luminata^{TM} Forte Western Horseradish Peroxidase Substrate (no. WBLUF0100) were from Millipore (Billerica, MA). Anti-RUVBL2 (no. ab36569) was from Abcam (Cambridge, MA). Anti-pAkt^{Thr308} (no. 9275), anti-Akt (no. 9272), anti-FoxO1 (Forkhead box protein O1; no. 2880), anti-pFoxO1^{Thr24} (no. 9464), anti-PRAS40 (Proline-rich Akt substrate of 40 kDa; no. 2691), anti-pPRAS40^{Thr246} (no. 2997), anti-GSK3β (no. 9315), anti-JNK (no. 9252) and anti-TSC2 (no. 3612) were from Cell Signaling Technologies (Boston, MA). Phospho-AS160^{Thr642} (no. 3028 P1) was from Symansis Limited (Auckland, New Zealand). Anti-Insulin Receptor-β (no. sc-20739) was from Santa Cruz Biotechnology. Anti-TUG was provided by Dr. Jonathan Bogan (Yale University; New Haven, CT). Insulin ELISA (no. 80-INSRT-E01) was from Alpco Diagnostics (Salem, NH).

Animal Treatment

Procedures for animal care were approved by the University of Michigan Committee on Use and Care of Animals. Male Wistar rats (6 wk old; initial body weight ~200-250g; Harlan, Indianapolis, IN) were individually housed, separated into two groups and provided with either standard rodent chow (Low Fat Diet; LFD: 14% kcal fat, 58% kcal CHO, 28% kcal protein; Lab Diet no. 5001, PMI Nutritional International, Brentwood, MO) or high fat diet [HFD: 60% kcal fat, 20% kcal CHO, 20% kcal protein; Research Diets (no.D12492), New Brunswick, NJ] and

water ad libitum for 2 weeks. After two weeks of the diet intervention, rats were fasted the night before the experiment at ~1900. On the morning after the overnight fast, rats from both diet groups (LFD and HFD) either remained sedentary or performed an acute exercise bout. Beginning at ~0600, exercised rats swam in a barrel filled with water (35°C) to a depth of ~45 cm (6 rats/barrel, 3 rats from each diet group) for 4 × 30 min bouts, with a 5 min rest period between each bout (19). Immediately after completing the exercise protocol (IPEX), some rats were anesthetized (intraperitoneal injection of sodium pentobarbital, 50 mg/kg wt), and epitrochlearis muscles were dissected out. One muscle was used to measure insulin-independent glucose uptake, and the contralateral muscle was immediately frozen for subsequent determination of glycogen concentration, pAMPK and pAS160. The remaining exercising rats were dried and returned to their cages without access to food for 3h, at which time blood was sampled from the tail vein from both time-matched sedentary controls (LFD sedentary or HFD Sedentary) and exercised rats 3 hours post-exercise (LFD 3hPEX or HFD 3hPEX) to determine blood glucose (via Accu-Chek Aviva glucometer, Roche, Indianapolis, IN) and plasma insulin concentration (via Alpco ELISA). Homeostatic model assessment of insulin resistance (HOMA-IR) was calculated: [plasma glucose (mg/dL) x plasma insulin (μUnits/mL)] ÷ 405. Rats were then anesthetized, and their epitrochlearis muscles were dissected out to measure insulin-independent and insulin-dependent glucose uptake. Sedentary rats from each diet group were anesthetized at times coinciding with the IPEX and 3hPEX groups. While rats were under deep anesthesia both epitrochlearis muscles were dissected out, rapidly rinsed in warm (35°C) Krebs-Henseleit buffer (KHB) and transferred to vials for subsequent *ex vivo* incubations.

Muscle Incubations

Isolated epitrochlearis muscles underwent two incubation steps. During both incubation steps, vials containing the appropriate media were continuously shaken and gassed (95% O_2/5% CO_2) in a heated (35°C) water bath. For insulin-independent glucose uptake, epitrochlearis muscles were rapidly dissected out IPEX. One muscle from the IPEX groups and their time-matched SED controls underwent a 2-step incubation procedure. Step 1 IPEX incubation (10 min) was as follows: IPEX muscles were incubated in vial containing 2 ml of Media 1 [Krebs-Henseleit buffer supplemented with 0.1% bovine serum albumin (KHB/BSA), 2 mM sodium pyruvate, and 6 mM mannitol]. Step 2 IPEX incubation (20 min) was a follows: IPEX muscles

were then transferred to a second vial containing 2 ml of Media 2 [(KHB/BSA solution, the same insulin concentration as in Step 1), 1 mM 2-deoxyglucose (2-DG; final specific activity of 2.25 mCi/mmol ^{3}H-2-DG), and 9 mM mannitol (final specific activity of 0.022 mCi/mmol ^{14}C-mannitol)]. Insulin-independent and insulin-dependent glucose uptake were measured in paired epitrochlearis muscles from other rats at 3hPEX along with time-matched SED controls. Step 1 3hPEX incubation (30 min) was as follows: 3hPEX contralateral muscles were placed in vials containing 2 mL of Media 1 with either 0 nM or 0.6 nM insulin. Step 2 3hPEX incubation (20 min) was as follows: muscles were then transferred to a second vial containing 2 ml of Media 2 and the same insulin concentration as in Step 1. Following Step 2 incubations, all muscles were rapidly blotted on filter paper (moistened with ice-cold KHB), trimmed, freeze-clamped using aluminum tongs cooled in liquid nitrogen and stored at −80°C until later processing and analysis.

Muscle Homogenization

Frozen muscles used for glucose uptake and immunoblotting were weighed and then homogenized in ice-cold lysis buffer (1 ml/muscle; 20 mM Tris-HCL, 150 mM NaCl, 1% Triton X-100, 1 mM Na_3VO_4, 1 mM EDTA, 1 mM EGTA, 2.5 mM NaPP, 1 mM β-glycerophosphate, 1 µg/ml leupeptin, 1mM PMSF at 1 ml/muscle) using a TissueLyser II homogenizer (Qiagen Inc, Valencia, CA). Homogenates were rotated at 4°C for 1 h prior to being centrifuged (10,000 g for 10 min at 4°C). The supernatant was used to determine protein concentration according to the manufacturer's protocol (Pierce Biotechnology no. 23227). The remaining supernatant was stored at -80°C until further analysis.

Glucose Uptake

Aliquots of the supernatants from muscles processed for glucose uptake were added to vials containing scintillation cocktail (Research Products International, Mount Prospect, IL), and ^{3}H and ^{14}C disintegrations per minute were measured by a scintillation counter (Perkin Elmer, Waltham, MA). These values were used to determine 2-DG uptake as previously described (8, 27).

Immunoblotting

Appropriate volumes of the muscle lysate for equal protein concentration were boiled for 5-10 min in SDS-loading buffer, separated via SDS-PAGE (poly acrilamide gel electrophoresis) and then electrophoretically transferred to nitrocellulose membranes. Membranes were rinsed with Tris-buffered saline plus Tween (TBST; 140 mM NaCl, 20 mM Tris base, pH 7.6, and 0.1% Tween), blocked with 5% nonfat dry milk in TBST for 2 h at room temperature, washed 3 x 5 min at room temperature and treated with the appropriate primary antibody (in TBST with 5% BSA unless otherwise specified by the manufacturer) overnight at 4°C. Blots were washed 3 x 5 min with TBST, incubated with the appropriate secondary antibody IgG horseradish peroxidase (in TBST + 5% milk) for 1 h at room temperature. Equal protein loading was confirmed using MemCode (1). They were then washed again 3 x 5 min with TBST, 4 x 5 min TBS and subjected to enhanced chemiluminescence to visualize protein bands. Protein bands were quantified by densitometry (Alpha Innotech, San Leandro, CA). The individual values for the samples were normalized to the mean value for all of the samples on the membrane.

IRS-1–PI3K Association

For evaluation of PI3K associated with IRS-1, 400 μg of protein from each sample was combined with 3 μg of anti-IRS-1 antibody and rotated overnight (4°C). The following morning protein G-agarose beads were washed three times with lysis buffer, resupended in lysis buffer (50% slurry) and 100 μl of 50% slurry mix of protein G-agarose beads were added to the sample/antibody mix and rotated 2 h at 4°C. Protein G-agarose beads were isolated by centrifugation (4,000 *g* at 4°C for 1 min) and washed three times in lysis buffer. Antigens were eluted from the beads with 45 μl of 2× SDS loading buffer and were boiled for 5 min before SDS-PAGE and immunoblotted with anti-PI3K, as described above.

Akt Activity Measurement

Akt activity was determined according to the manufacturer's protocol. Briefly, protein G-agarose beads were rotated overnight with anti-Akt/PH domain clone SKB1. The antibody/protein G-agarose mixture was combined with 500 μg of protein from each sample and rotated for 2 h at 4°C. The antigen/antibody/protein G-agarose complex was combined with Akt substrate peptide and [γ-^{32}P]ATP (final concentration of 1 μCi/μl) and shaken at room

temperature for 60 min. The complex was then centrifuged (4,000 *g* for 1 min), and 40 µl of supernatant was collected and transferred to phosphocellulose paper. After washes (3 times with 1.5% phosphoric acid and once with acetone), the phosphocellulose paper was transferred to a vial containing scintillation cocktail for scintillation counting. The individual values for the samples were normalized to the mean value of the raw counts for all of the samples per assay group. An assay group consisted of paired epitrochlearis muscles (previously incubated with insulin or with no insulin) from each diet and exercise group (i.e., LFD Sedentary, HFD Sedentary, LFD 3hPEX and HFD 3hPEX).

Multiplex Analysis

Two multiplex assays were used to assure MAPmate bead compatibility. In the first multiplex assay, muscle homogenates were used to determine the phosphorylation status of the Akt/mTOR signaling axis (Akt^{Ser473}, $GSK\beta^{Ser9}$, $IR^{Tyr1162/1163}$, $IRS\text{-}1^{Ser307}$ and $TSC2^{Ser939}$). In a second Luminex assay, muscle homogenates were used to determine amount of $pJNK/SAPK^{Thr183/Tyr185}$. Analysis was performed by the Luminex L200 instrument (Luminex, Austin, TX), and data were analyzed by xPONENT software (Luminex).

TAG, DAG & Ceramide Analysis

The Lipidomics Core of the University of Michigan Molecular Phenotyping Core performed lipid extraction and triacylglycerol (TAG), DAG and ceramide analysis from muscles in non-incubated epitrochlearis muscles. Briefly, TAG and DAG were isolated via thin layer chromatography and then analyzed by gas chromatography (GC) using a flame ionization detector (39). Ceramides were extracted and analyzed via high-performance liquid chromatography (HPLC) and tandem mass spectrometry (MS/MS), and quantified by ESI-MRM-MS (electronspray ionization-magnetic resonance microscopy-mass spectrometry) on a tandem quadrupole mass spectrometer (30). The individual values of samples were normalized to the mean value for all of the samples from the LFD Sedentary rats.

MHC analysis

Non-incubated muscles were homogenized in pre-chilled glass tissue-grinding tubes (Kontes, Vineland, NJ) containing cold lysis buffer and protein concentrations were determined for whole homagenate. Laemmli sample buffer (2×) was then added to 5 μg of the whole homogenate prior to boiling for 10 min. Samples where then loaded on to gels modified from (13, 37, 58) for SDS-PAGE [Final reagent concentrations for separating gel: 6.5% acrylamide-bis (50:1), 30% glycerol, 210 mM Tris-HCl (pH 7.4), 105 mM glycine, 0.4% SDS, 19% H_20, 0.1% ammonium persulfate, 0.05% TEMED]. Samples and a MHC isoform standard (6 μg protein of a 3:2 mixture of homogenized rat soleus and extensor digitorum longus muscles containing all four MHC isoforms: I, IIa, IIb, IIx) were run at a constant voltage (50 V) for 1 h (during electrophoresis that was performed in a refrigerator cooled to 4^{o}C, the gel box was placed in a secondary container that was packed with ice) with continuous mixing by a magnetic stir bar inside the electrophoresis apparatus (Mini-PROTEAN® Tetra cell no. 165-8004, Hercules, CA). The use of a secondary container packed in ice and continuous. After 1 h, the power supply was switched from constant voltage mode to constant current mode, with the current setting at the end of the first hour of electrophoresis maintained for the subsequent 23-25 h (with the gel box packed on ice in a refrigerator at 4^{o}C). Gels were subsequently removed and stained with Coomassie Brilliant Blue overnight at room temperature while gently rotating on an orbital shaker. The gels were then destained in 20% methanol and 10% acetic acid solution for 4-6 h while rotating (destaining solution was replaced with fresh solution every 45-60 min). MHC bands were quantified using densitometry (AlphaEase FC, Alpha Innotech, San Leandro, CA).

Muscle Glycogen

Muscles used for measurement of glycogen were weighed and then homogenized in ice-cold perchloric acid (0.3 M). An aliquot of the homogenate was used to determine muscle glycogen concentration by the amyloglucosidase method (42).

Statistics

Two-way ANOVA analysis was used to compare means among more than two groups, and the Tukey post-hoc test was used to identify the source of significant variance. Data that

were not normally distributed were mathematically transformed to achieve normality prior to running the appropriate statistical analysis. Statistical analyses were performed using Sigma Plot (San Rafael, CA) version 11.0. Data were expressed as means ± SE. A P-value < 0.05 was considered statistically significant. Two-tailed t-test analysis was used for comparison of means between two groups.

Results

Myosin heavy chain isoform expression

After two weeks of diet intervention, fiber type of the epitrochlearis was not significantly altered (Table 1).

Body Mass, Epididymal Mass, Epidymal/Body Mass Ratio, and Estimated Caloric Intake.

After the two week diet intervention, body mass ($P < 0.01$), epididymal fat pad mass ($P < 0.01$; Figure 5.1) and epididymal/body mass ratio (8.36 ± 0.26 vs. 5.84 ± 0.14 mg/g; $P < 0.01$) were greater for the HFD versus LFD group. Estimated caloric intake (based on the product of food intake, g, and caloric density, kcal/g, of each diet) of LFD rats (85.00 ± 1.70 kcal/d) significantly lower ($P <0.01$) than values for HFD rats (93.43 ± 2.00 kcal/d).

IPEX: Muscle 2-DG Uptake and Glycogen

For insulin-independent 2-DG uptake by isolated epitrochlearis muscles (Figure 5.2A), there was significantly main effect of exercise (IPEX > Sedentary; $P < 0.01$). Post-hoc analysis indicated significantly greater ($P < 0.05$) insulin-independent 2-DG uptake from muscles of IPEX versus sedentary rats within each diet group. Insulin-independent 2-DG uptake did not differ between diet groups for either sedentary or IPEX rats.

For muscle glycogen (Figure 5.2B), there was a significant main effect of exercise (Sedentary > IPEX; $P < 0.01$). Post-hoc analysis indicated significantly lower ($P < 0.05$) muscles glycogen for IPEX versus sedentary rats within each diet group. Muscle glycogen did not differ between diet groups for either sedentary or IPEX rats.

IPEX: Muscle Immunoblotting

There were no significant effects of diet or exercise on total abundance of AMPK and AS160 at IPEX (Figure 5.3).

For pAMPK (Figure 5.4A), there was a significant main effect of exercise (IPEX > Sedentary; $P < 0.05$). Post-hoc analysis indicated that pAMPK was significant greater ($P < 0.05$) for IPEX versus sedentary rats within each diet groups. The pAMPK did not differ between diet groups for either sedentary or IPEX muscles.

For $pAS160^{Thr642}$ (Figure 5.4B), there was a significant main effect of exercise (IPEX > Sedentary; $P < 0.05$). Post-hoc analysis indicated that pAS160 was significantly greater ($P < 0.05$) for IPEX versus sedentary rats within each diet group. There was no significant diet effect on $pAS160^{Thr642}$ in either the sedentary or the IPEX muscles. For $pAS160^{Ser588}$ (Figure 5.4C), was a significant main effect of exercise (IPEX > Sedentary; $P < 0.05$), but the post-hoc analysis did not reveal any significant differences.

3hPEX: Plasma Glucose and Insulin

For plasma glucose (Figure 5.5A), there was a significant main effect of exercise (Sedentary > 3hPEX; $P < 0.01$) and a significant interaction between diet and exercise ($P < 0.05$). Post-hoc analysis revealed that plasma glucose was significantly greater ($P < 0.05$) for Sedentary HFD versus Sedentary LFD rats, but this diet-related difference in glucose was eliminated at 3hPEX. For both LFD and HFD groups, plasma glucose was significantly lower ($P < 0.05$) at 3hPEX versus sedentary controls.

For plasma insulin (Figure 5.5B), there were significant main effects of both diet (HFD > LFD; $P < 0.01$) and exercise (Sedentary > 3hPEX; $P < 0.01$). In the sedentary groups, HFD versus LFD rats had significantly greater ($P < 0.05$) plasma insulin, but in the 3hPEX groups, plasma insulin was not different between diet groups. In the HFD groups, plasma insulin for 3hPEX versus sedentary rats was significantly reduced ($P < 0.05$).

For HOMA-IR (Figure 5.5C), there was a significant main effect of diet (HFD > LFD; $P < 0.01$) and exercise (Sedentary > 3hPEX; $P < 0.01$). In the sedentary groups, HFD versus LFD rats had significantly greater ($P < 0.05$) HOMA-IR, but in the 3hPEX cohorts HOMA-IR did not

differ between diets. For both LFD and HFD groups, HOMA-IR for 3hPEX versus sedentary was significantly reduced ($P < 0.05$).

3hPEX: Muscle 2-DG Uptake

For 2-DG uptake in muscles incubated without insulin (Figure 5.6A), there was a significant main effect of exercise (3hPEX > Sedentary; $P < 0.05$), and post-hoc analysis indicated that insulin-independent 2-DG values were significantly greater ($P < 0.05$) for muscles from 3hPEX versus SED rats in the LFD group. No significant diet-related differences in insulin-independent 2-DG uptake were identified.

For 2-DG uptake in muscles incubated with insulin (Figure 5.6B), there were significant main effects of both diet (LFD > HFD; $P < 0.01$) and exercise (3hPEX > Sedentary; $P < 0.01$). Post-hoc analysis revealed that 2-DG uptake with insulin was significantly ($P < 0.05$) greater for muscles from LFD 3hPEX rats versus all other groups. In the HFD groups, post-hoc analysis indicated that 2-DG uptake with insulin was significantly greater ($P < 0.05$) for muscles from 3hPEX versus SED rats. For delta-insulin (with insulin – no insulin = delta-insulin) 2-DG uptake (Figure 5.5B), there were significant main effects of both diet (LFD > HFD; $P < 0.01$) and exercise (Sedentary < 3hPEX; $P < 0.01$). Post-hoc analysis demonstrated that delta-insulin 2-DG uptake for LFD 3hPEX rats was significantly greater ($P < 0.05$) than all other groups. Post-hoc analysis also indicated that in the sedentary groups, delta-insulin glucose uptake was significantly greater ($P <0.05$) for LFD versus HFD rats. In addition, delta-insulin 2-DG uptake for HFD-3hPEX rats exceeded HFD-SED rats ($P < 0.05$), but these values did not significantly differ for HFD-3hPEX versus LFD-SED rats.

3hPEX: Muscle Immunoblotting

Neither diet nor exercise significantly altered the total abundance of Akt, AS160, GLUT4, TUG, RUVBL2, TBC1D1, GSK3β, PRAS40, JNK, IR, or IRS-1 (Figure 5.7). For total FoxO1 (n = 8 per group) there were significant main effects of exercise (3hPEX > Sedentary; $P < 0.05$) for either muscles incubated with no insulin (LFD Sedentary = 0.52 ± 0.11; HFD Sedentary = 0.42 ± 0.09; LFD 3hPEX = 1.19 ± 0.34; and HFD 3hPEX = 0.80 ± 0.13) or muscles incubated with insulin (LFD Sedentary = 0.66 ± 0.17; HFD Sedentary = 0.93 ± 0.34; LFD 3hPEX = 1.92 ± 0.40; and HFD 3hPEX = 1.57 ± 0.29). For muscles incubated in the absence of insulin, post-hoc

analysis revealed that HFD 3hPEX versus HFD Sedentary values were significantly greater ($P < 0.05$). For insulin-treated muscles, post-hoc analysis revealed that LFD 3hPEX versus LFD Sedentary values were significantly greater ($P < 0.05$).

Neither diet nor exercise significantly altered phosphorylation of the insulin receptor ($pIR^{Tyr1162/1163}$; Figure 5.8A), delta-insulin $pIR^{Tyr1162/1163}$; Figure 5.8B), IRS-1–PI3K association regardless of insulin concentration (Figure 5.8C) or delta-insulin IRS-1–PI3K (Figure 5.8C).

Neither diet nor exercise significantly altered $pAkt^{Thr308}$ for muscles without insulin (Figure 5.9A). For delta-insulin $pAkt^{Thr308}$ (Figure 5.9B), there was a significant main effect of diet (LFD > HFD; $P < 0.05$), but no further significance was revealed by post-hoc analysis. There were no significant effects of either diet or exercise on either $pAkt^{Ser473}$ (Figures 5.9C) or Akt activity (Figures 5.9E) regardless of insulin concentration, delta-insulin $pAkt^{Ser473}$ (Figures 5.9D) or delta-insulin Akt activity (Figures 5.9 F).

For $pAS160^{Thr642}$ (Figure 5.10A), there was a significant main effect of exercise in muscles incubated without insulin (Sedentary < 3hPEX; $P < 0.05$), and post-hoc analysis indicated that for LFD groups, 3hPEX values were greater than Sedentary values ($P < 0.05$). For $pAS160^{Thr642}$ in muscles with insulin, there was a significant main effect of diet (LFD > HFD; $P < 0.01$), and post-hoc analysis revealed that for 3hPEX groups, LFD values were greater than HFD values. For delta-insulin $pAS160^{Thr642}$ (Figure 5.10B), there was a significant main effect of diet (LFD > HFD; $P < 0.05$), and post-hoc analysis indicated that for 3hPEX groups, LFD values exceeded HFD values ($P < 0.05$).

For $pAS160^{Ser588}$ (Figure 5.10C), muscles incubated without insulin there was a significant main effect of diet (LFD > HFD; $P < 0.05$), and post-hoc analysis indicated that within sedentary groups, the LFD values were greater than HFD values ($P < 0.05$). For $pAS160^{Ser588}$ muscles incubated with insulin, there were significant main effects of both diet (LFD > HFD; $P < 0.01$) and exercise (3hPEX > Sedentary; $P < 0.01$). Post-hoc analysis of muscles incubated with insulin indicated that $pAS160^{Ser588}$ for the LFD 3hPEX group was greater than all other groups ($P < 0.05$), $pAS160^{Ser588}$ for the HFD SED group was significantly lower than all other groups ($P < 0.05$), and $pAS160^{Ser588}$ values from LFD SED and HFD 3hPEX were not significantly different. For delta-insulin $pAS160^{Ser588}$ (Figure 5.10D), there were

significant main effects of both diet (LFD > HFD; $P < 0.01$) and exercise (Sedentary < 3hPEX; $P < 0.01$), and post-hoc analysis indicated that values from the LFD 3hPEX group significantly exceeded all other groups ($P < 0.05$).

For pFoxO1^{Thr24} in muscles incubated without insulin (Figure 5.11A), there were no significant differences. For pFoxO1^{Thr24} muscles incubated with insulin, there were significant main effects of both diet (LFD > HFD; $P < 0.01$) and exercise (Sedentary < 3hPEX; $P < 0.01$). Post-hoc analysis of pFoxO1^{Thr24} in muscles incubated with insulin indicated that LFD 3hPEX values were significantly greater than all other groups ($P<0.05$). Post-hoc analysis further revealed that in the HFD groups, 3hPEX values exceeded sedentary values ($P<0.05$). For delta-insulin pFoxO1^{Thr24} (Figure 5.11B), there were significant main effects of both diet (LFD > HFD; $P < 0.05$) and exercise (Sedentary < 3hPEX; $P < 0.01$). Post-hoc analysis indicated that delta-insulin pFoxO1^{Thr24} for LFD 3hPEX values were significantly greater than all other groups ($P < 0.05$), and HFD 3hPEX values exceed HFD sedentary values ($P<0.05$).

For pPRAS40^{Thr246} (Figure 5.11C) in muscles incubated without insulin, there were no significant differences. For pPRAS40^{Thr246} muscles incubated with insulin, there was a significant main effect of diet (LFD > HFD; $P < 0.01$), and post-hoc analysis revealed that LFD 3hPEX values exceeded LFD sedentary values ($P<0.05$). For delta-insulin pPRAS40^{Thr246} (Figure 5.11D), there was a significant main effect of exercise (Sedentary < 3hPEX, $P < 0.05$), and post-hoc analysis indicated that LFD 3hPEX values exceeded LFD Sedentary values ($P < 0.05$).

Neither diet nor exercise significantly altered either pGSK3β^{Ser9} or pTSC2^{Ser939} regardless of insulin concentration (Figures 5.12A-D).

For pIRS-1^{Ser1101} (Figure 5.13A), muscles incubated without insulin had a significant main effect of exercise (3hPEX > Sedentary; $P < 0.01$). Post-hoc analysis revealed HFD 3hPEX values exceeded HFD Sedentary values ($P < 0.05$). For muscles incubated with insulin, there was a significant main effect of diet on pIRS-1^{Ser1101} (LFD > HFD; $P < 0.05$), but post-hoc analysis did not reveal any further differences among the groups.

For pIRS-1^{Ser307} (Figure 5.13B), there were no significant differences among muscles incubated without insulin, but there was a significant main effect of exercise (3hPEX >

Sedentary; $P < 0.05$) in muscles incubated with insulin, but post-hoc analysis did not reveal any further differences among the groups.

Neither diet nor exercise altered pJNK in muscles regardless of insulin concentration (Figure 5.13C).

Lipid Metabolites

There were significant main effects of diet (LFD < HFD; $P < 0.05$) for muscle TAG 18:0, 18:1 (n-9), and 20:2 (Figure 5.14), but post-hoc analysis did not reveal any further differences among them. For TAG 20:1, there was a significant main effect of exercise (Sedentary > 3hPEX; $P < 0.01$), and post-hoc analysis indicated that LFD sedentary values exceeded LFD 3hPEX values ($P < 0.05$).

Muscle acyl CoA 16:0 had a significant main effect of exercise (Sedentary < 3hPEX; $P < 0.01$; Figure 5.15), and post-hoc analysis indicated that HFD Sedentary values exceeded HFD 3hPEX values.

Muscle DAG 20:4 had a significant interaction between diet and exercise (Figure 5.16), and post-hoc analysis indicated that HFD 3hPEX values exceeded HFD Sedentary values ($P < 0.05$).

Neither diet nor exercise significantly altered the level of any ceramide species (Figure 5.17).

Discussion

The current study investigated the mechanisms by which acute exercise improves insulin-stimulated glucose uptake in both insulin sensitive and insulin resistant rat skeletal muscles. The most important results included: 1) each of the key metabolic and signaling outcomes determined for muscles IPEX (insulin-independent glucose uptake, glycogen, $pAMPK^{Thr172}$, $pAS160^{Thr642}$, and $pAS160^{Ser588}$) was indistinguishable in LFD versus HFD rats; 2) skeletal muscles from Sedentary HFD versus Sedentary LFD rats exhibited modest, but significant insulin resistance for glucose uptake accompanied by modest, but significant deficit in

pAS160^{Ser588}; 3) skeletal muscles from LFD rats at 3hPEX versus Sedentary LFD rats were characterized by substantially elevated insulin-stimulated glucose uptake concomitant with significantly increased phosphorylation of AS160 (both pAS160^{Thr642} and pAS160^{Ser588} determined for muscles incubated either with or without insulin as well as the delta-insulin for pAS160^{Ser588}) in the absence of significant changes in proximal insulin signaling steps; 4) skeletal muscles from HFD rats at 3hPEX had insulin-stimulated glucose uptake values that exceeded the Sedentary HFD group and were not different from Sedentary LFD group, but were significantly less than the LFD 3hPEX group; 5) the improvement in insulin-stimulated glucose uptake of muscles from HFD rats at 3hPEX was accompanied by elimination of the diet-induced deficit in pAS160^{Ser588}, but neither pAS160^{Ser588} nor pAS160^{Thr642} of the HFD 3hPEX group attained values as great as the LFD 3hPEX group; 6) the improved in insulin-stimulated glucose uptake in muscle may also be associated with the exercised-induce reduction in acyl-CoA 16:0; and 7) the improved insulin-stimulated glucose uptake by muscles from both LFD and HFD rats at 3hPEX were not accompanied by significant reductions in a number of possible mediators of muscle insulin resistance, including DAG and ceramides concentrations, pIRS1^{Ser307}, pIRS1^{Ser1101}, and pJNK^{Ser73}.

A single session of exercise is known to increase insulin-stimulated glucose uptake by skeletal muscle in healthy rats (2, 10, 12, 19-20, 24, 38, 45, 53) and humans (38, 61, 63, 68). Consistent with previous findings for LFD rats, the improved insulin-mediated glucose uptake by muscles from 3hPEX versus sedentary rats occurred concomitant with increased pAS160^{Thr642}, both with and without insulin, despite unaltered proximal insulin signaling (insulin receptor phosphorylation, IRS-1–PI3K association, Akt phosphorylation or Akt activity). These results for proximal insulin signaling are consistent with those of Wojtaszewski et al. (65-66) who demonstrated that insulin-stimulated glucose disposal after acute exercise by humans occurs without improvement in proximal insulin signaling steps (including Akt phosphorylation). The current results also confirm the findings from several of our previous studies that have reported a sustained increase in pAS160^{Thr642} both with and without insulin several hours post-exercise in the absence of an increase in the calculated delta-insulin pAS160^{Thr642} (19-20, 53). Treebak et al. (63) also found greater pAS160 in muscles from healthy humans after a single session of exercise. In the current study, pAS160^{Ser588} of muscles without insulin was not increased, but both pAS160^{Ser558} in muscles incubated with insulin and delta-insulin on pAS160^{Ser588} were

significantly elevated in the 3hPEX LFD group. The results of both the current and earlier studies demonstrate that acute exercise by healthy rats induces greater pAS160 on Ser588 and Thr642, the phosphomotifs that appear to be most important for regulating insulin-stimulated glucose transport (51). Although greater pAS160 has not yet been proven to be directly responsible for increased skeletal muscle insulin sensitivity in the hours after exercise, enhanced pAS160 is a leading candidate for the mechanism accounting for this benefit of exercise in healthy individuals.

For insulin resistant rats (3, 21, 36, 41, 46, 59) and humans (7, 16, 44, 54), a single session of exercise has also been shown to be an effective stimulus for improving insulin-stimulated glucose uptake. However, surprisingly few studies have addressed the mechanisms for this improvement. In the current study, neither HFD nor acute exercise altered the total GLUT4 abundance. Previous studies suggested that a single exercise session can correct some of the defects in proximal insulin signaling of insulin resistant muscle stimulated with a supraphysiologic insulin dose (41, 43, 46). In contrast the current results indicate that exercise did not induce increases in proximal signaling with a physiologic insulin dose in muscles from HFD rats at 3hPEX compared to HFD Sedentary rats. The current study also provided the first information about the effect of a single exercise session on insulin-stimulated AS160 phosphorylation in insulin resistant skeletal muscle. The insulin resistance for glucose uptake by muscle in the HFD Sedentary rats versus LFD Sedentary rats was accompanied by reduced phosphorylation of $AS160^{Ser588}$. In the HFD 3hPEX versus HFD sedentary rats, $pAS160^{Ser588}$ with insulin was significantly increased, and these values were restored to levels similar to the values in muscles from Sedentary LFD rats. The elimination of diet-related decrement in $pAS160^{Ser588}$ of insulin-stimulated muscles from HFD 3hPEX versus Sedentary LFD rats occurred concomitant with elimination of the diet-related decrease in insulin-stimulated glucose uptake for muscles in the 3hPEX HFD group. The current data provide novel evidence that improved $pAS160^{Ser588}$ in muscle may be important for the mechanism by which exercise can normalize insulin-stimulated glucose uptake by previously insulin resistant muscle.

Notable aspects of the experimental design of the current study were the comparison of the magnitude of exercise's effects on insulin-stimulated glucose uptake in muscles with normal versus defective insulin sensitivity and the investigation of the possibility that distinct

mechanisms may account for exercise-induced improvements of insulin-stimulated glucose uptake in insulin sensitive versus insulin resistant muscles. Even though the metabolic effects of exercise determined IPEX were indistinguishable for LFD and HFD rats, the muscles from LFD 3hPEX versus HFD 3hPEX rats reached a significantly greater level of insulin-mediated glucose uptake. Thus, muscles from insulin resistant rats appeared to have a limited capacity for exercise-induced improvements in insulin-stimulated glucose uptake. Careful examination of the published literature on insulin sensitivity after acute exercise by insulin resistant rats or humans reveals a similar outcome has been previously reported (3, 7, 16, 21, 36, 44, 46). However, earlier research did not identify the reason that exercise does not result in equal insulin-stimulated glucose uptake for normal and insulin resistant individuals. Results of the current study indicate that the difference was not attributable to post-exercise differences in several key events of proximal insulin signaling. Rather, this diet-related difference in insulin-stimulated glucose uptake at 3hPEX was accompanied by differences in the extent of exercise effects on pAS160. In the HFD cohort, exercise significantly improved delta-insulin for pAS160^{Ser588}, but the delta-insulin values for both pAS160^{Ser588} and pAS160^{Thr642} of HFD rats at 3hPEX failed to attain values as great as the LFD rats at 3hPEX. The results of the current study in normal and insulin resistant rats, and results from previous studies of normal rats (2, 19-20, 53) demonstrate that the level of skeletal muscle insulin-stimulated glucose uptake consistently tracks with the extent of post-exercise effects on elevated pAS160.

The specific processes causing greater insulin sensitivity in skeletal muscles after a single session of exercise remains unknown for both normal and insulin resistant rats. It has been suggested that prior exercise might improve insulin sensitivity by reducing muscle levels of various lipid metabolites that are implicated in insulin resistance. There were no significant exercise effects on muscle concentrations of DAG or ceramides in either diet group at 3hPEX. These results are consistent with the observation that, regardless of diet, exercise did not lower muscle levels of pJNK^{Ser73}, pIRS1^{Ser307}, or pIRS1^{Ser1101} which have been linked to insulin resistance (3, 7, 27, 30, 34-35). Although there was a significant main effect of exercise for lower muscle TAG 20:1 concentration, skeletal muscle TAG is not generally considered to be direct mediator of insulin resistance (19-20, 31). However, acyl CoA-16:0 was significantly reduced by exercise, and these levels at 3hPEX were quite similar between the two diet groups. Elevated levels of long-chain acyl-CoA have been shown to be associated with skeletal muscle

insulin resistance (23, 31, 33), and reduced long-chain acyl-CoAs levels in skeletal muscle associated with acute exercise have been shown to correlate with improved insulin-stimulated glucose uptake (40). In this context, it seems possible that the exercise effect on acyl-CoA-16:0 played a role in the improved insulin sensitivity, but the similarity in values for the LFD and HFD groups at 3hPEX indicates that another mechanism accounts for the differences between diet groups for insulin-stimulated glucose uptake after exercise.

The molecular events that account for exercise-related increases in pAS160 remain to be identified. Funai et al. (20) previously demonstrated that prior exercise did not lead to greater phosphorylation of TBC1D1 (a paralog of AS160) in skeletal muscle. This result led to the question, is the greater phosphorylation of AS160 observed several hours after acute exercise represent a unique outcome or is a long-lasting effect of prior exercise evident for the phosphorylation of other Akt substrates in skeletal muscle? In the current study, there was not a increase in phosphorylation of either pTSC2^{Ser939} or pGSK3^{Ser9} on Akt-phosphomotifs, but we identified two other Akt substrates, FoxO1 and PRAS40, that were characterized by elevated insulin-mediated phosphorylation in the hours following exercise. Neither of these proteins are known to regulate skeletal muscle glucose transport, so it seems unlikely that elevated pFoxO1 or pPRAS40 directly account for the post-exercise enhancement of insulin-stimulated glucose uptake at 3hPEX. However, it is possible that prior exercise favors greater phosphorylation of AS160, FoxO1 and PRAS40 via a common mechanism. The lack of detectable exercise-induced changes in key proximal signaling events in the LFD rats raises the possibility that exercise influences the *in vivo* activity of specific kinases and/or phosphatases by mechanisms that are not evident using conventional assays (e.g., by altering protein localization, inducing post-translational modifications other than the phosphorylation sites tested, altering protein-protein binding, etc.).

It should be noted that there was a significant effect of exercise for total FoxO1 abundance. Interestingly the exercise-related differences in total FoxO1 followed a pattern that was quite similar to the pattern for exercise effects on pFoxO1 values. A key characteristic of FoxO1 is that following phosphorylation, FoxO1 translocates from the nucleus to the cytosol (22, 64). It seems likely that the exercise-related increase in FoxO1 abundance reflects the fact that the centrifugation protocol would be expected to precipitate the nuclear fraction, and the

detergents used would not be expected to solubilize the nuclear proteins. It would be worthwhile for future experiments to assess the influence of exercise on subcellular localization of FoxO1 and other signaling proteins.

Sedentary HFD versus Sedentary LFD rats had significantly greater HOMA-IR values, indicating whole body insulin resistance. Under fasting conditions when insulin concentrations are low, skeletal muscle glucose uptake is also low, and HOMA-IR values are more indicative of insulin ability to regulate hepatic glucose production. Earlier research has documented that short term high fat feeding can induce hepatic insulin resistance (32, 50), and it seems likely that in addition to the modest insulin resistance that was found for skeletal muscle in the current study, hepatic insulin resistance contributed to the significantly elevated plasma glucose and insulin levels in the Sedentary HFD rats. HOMA-IR values were significantly reduced for each group of rats at 3hPEX compared to their respective sedentary diet group, and HOMA-IR values for HFD 3hPEX versus LFD 3hPEX rats were not significantly different from each other. The greater insulin-stimulated glucose uptake by skeletal muscle would be expected to play an important role in improved whole body insulin sensitivity after exercise under conditions of elevated insulin. However, it seems possible that exercise effects on hepatic glucose production may help explain the lack of significant differences in HOMA-IR for HFD compared to LFD rats at 3hPEX, but future research will be necessary to determine if this speculation is true.

Improved insulin sensitivity of skeletal muscle is a major health-related benefit of physical activity. The specific underlying mechanisms accounting for this effect are poorly understood, especially for insulin resistant individuals, but the current study provided new insights by evaluating exercise effects on muscle glucose uptake and key signaling steps, including pAS160, in both normal and insulin resistant rats. The results implicate greater pAS160 for exercise benefits on insulin sensitivity in muscle of both groups. Furthermore, the inability of the HFD group to attain insulin-stimulated glucose uptake values equal to the LFD group post-exercise was accompanied with a similar deficit in the ability of acute exercise to enhance pAS160. The current results do not prove a causal relationship between the persistent exercise effect on pAS160 and insulin sensitivity. Nonetheless, the consistency of the relationship between pAS160 and post-exercise insulin sensitivity along with the crucial role of pAS160 for insulin-stimulated glucose transport have led to our working hypothesis that

enhanced pAS160 is important for the improved insulin-stimulated glucose uptake after acute exercise in both normal and insulin resistant muscle. We further hypothesize that the failure of the HFD 3hPEX group to achieve insulin-mediated glucose uptake equal to the LFD 3hPEX group is linked to a lesser exercise-effect on pAS160 in the muscles from the HFD rats. Future research should focus on identifying the specific processes that lead to greater pAS160 after exercise, elucidating the explanation for the lack of the full exercise effect on pAS160 in insulin resistant individuals, and determining the extent to which greater pAS160 is causally linked to the level of increased insulin-stimulated glucose uptake after exercise.

Acknowledgments

This research was supported by grants from the National Institutes of Health (DK071771 and AG10026 to G. D. Cartee). I would also like to thank Dr. Edward B. Arias, Dr. Naveen Sharma and Justin Kang for their assistance with experiments and data collection.

Table 5.1 Relative Myosin Heavy Chain Isoform Composition of Rat Epitrochlearis Muscle

	LFD	**HFD**
MHC-I %	4 ± 1	5 ± 2
MHC-IIa %	9 ± 1	9 ± 1
MHC-IIx %	31 ± 4	27 ± 3
MHC-IIb %	57 ± 6	59 ± 5

The myosin heavy chain (MHC) isoforms were separated by SDS-PAGE, gels were stained with Coomassie blue, and bands quantified by densitometry were expressed as relative values (%) for the epitrochlearis muscles from LFD and HFD fed rats (n = 8 per group). Values are means ± SEM.

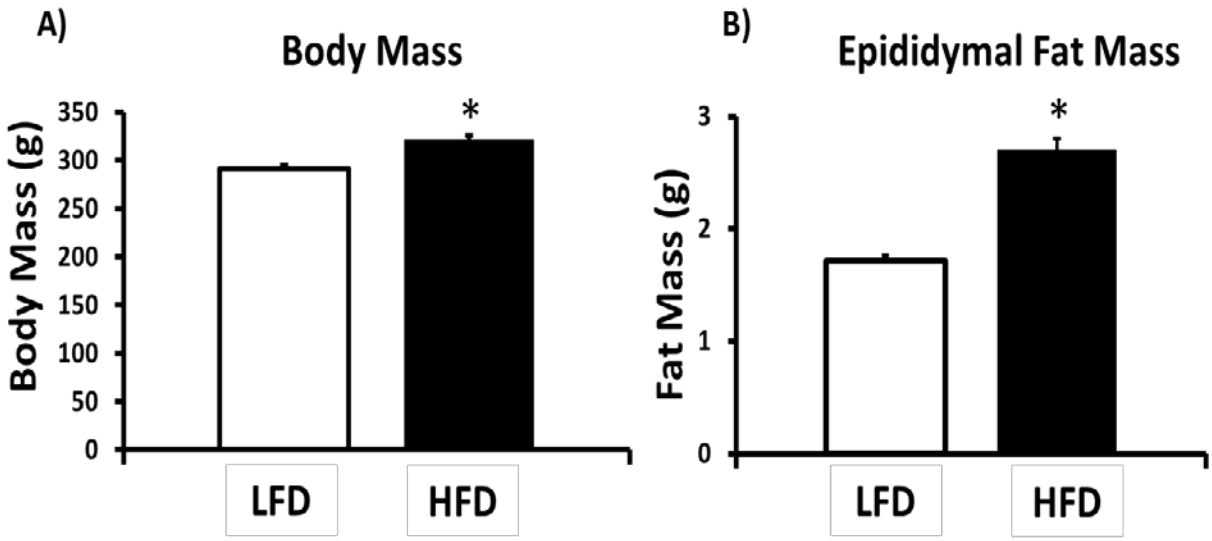

Figure 5.1

A: Body mass. B: Epididymal fat mass. *P < 0.01, Low Fat Diet (LFD) versus High Fat Diet (HFD). Data were analyzed by two-tailed t-test. Values are means ± SEM; n = 36 per diet group.

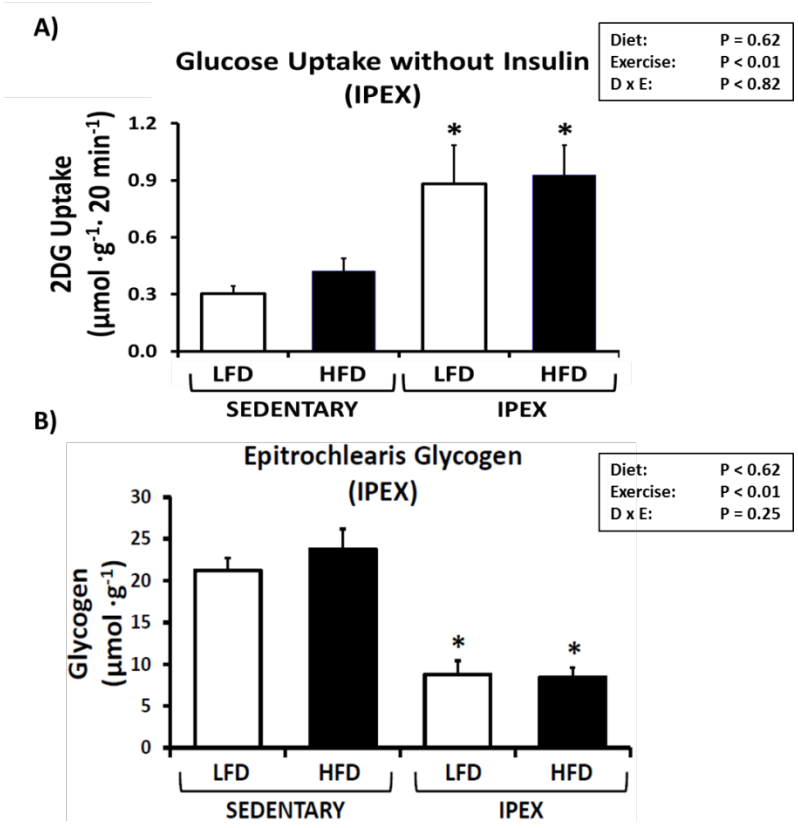

Figure 5.2

A: 2-Deoxyglucose (2-DG) uptake (without insulin) in epitrochlearis muscles of time-matched sedentary and immediately post-exercise (IPEX) rats. B: Glycogen of epitrochlearis muscles from Sedentary and IPEX rats. Data were analyzed by two-way ANOVA. Diet, main effect of diet; Exercise, main effect of exercise; D x E, interaction between Diet and Exercise. Post-hoc analysis was performed to identify the source of significant variance. *P < 0.05, IPEX versus Sedentary within the same diet group (e.g., LFD IPEX vs. LFD Sedentary, etc.). Values are means ± SEM; n = 4-6 per group.

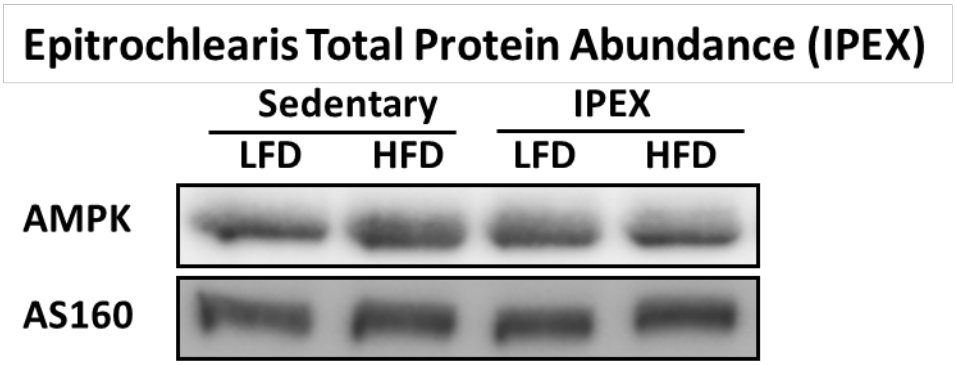

Figure 5.3

Total protein abundance for immediately post-exercise (IPEX) epitrochlearis muscles. Representative total protein immunoblots for proteins for which abundance was not altered by diet or exercise.

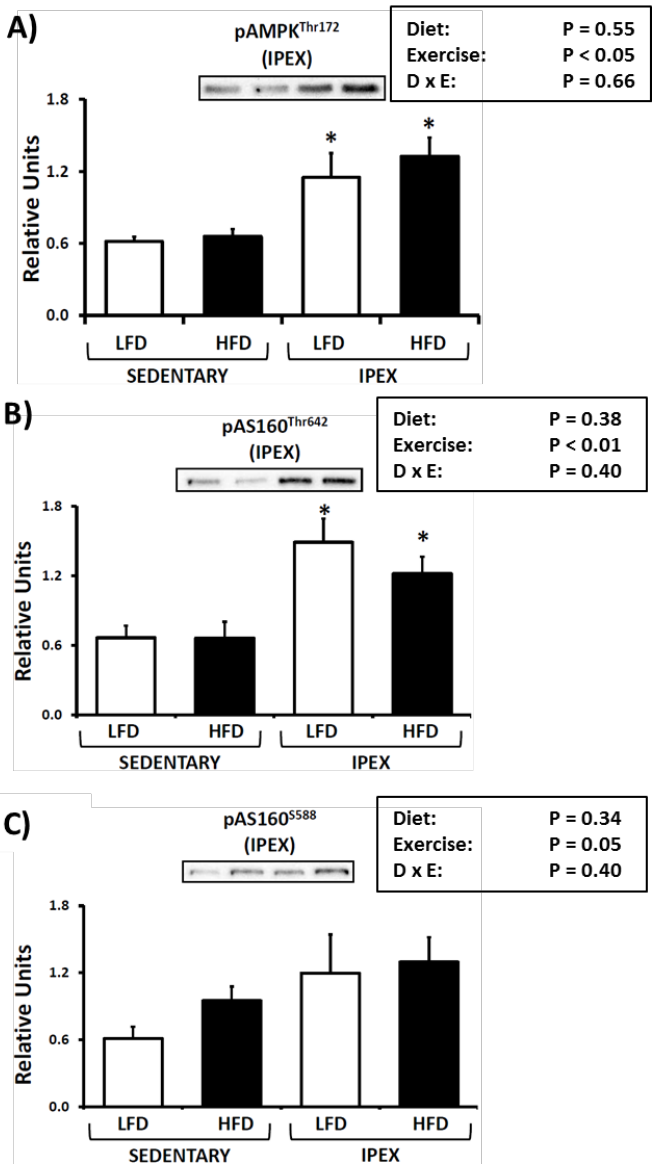

Figure 5.4

Immediately post-exercise (IPEX) measurements for A: pAMPK^{Thr172}; B: pAS160^{Thr642}; and C: pAS160^{Ser588}. Measurements made in epitrochlearis muscles (without insulin) from time-matched sedentary and IPEX rats. Data were analyzed by two-way ANOVA. Diet, main effect of diet; Exercise, main effect of exercise; D x E, interaction between diet and exercise. Post-hoc analysis was performed to identify the source of significant variance. *P < 0.05 for IPEX versus Sedentary within a given diet group (e.g., LFD IPEX vs. LFD Sedentary, etc.). Values are means ± SEM; n = 4-6 per group.

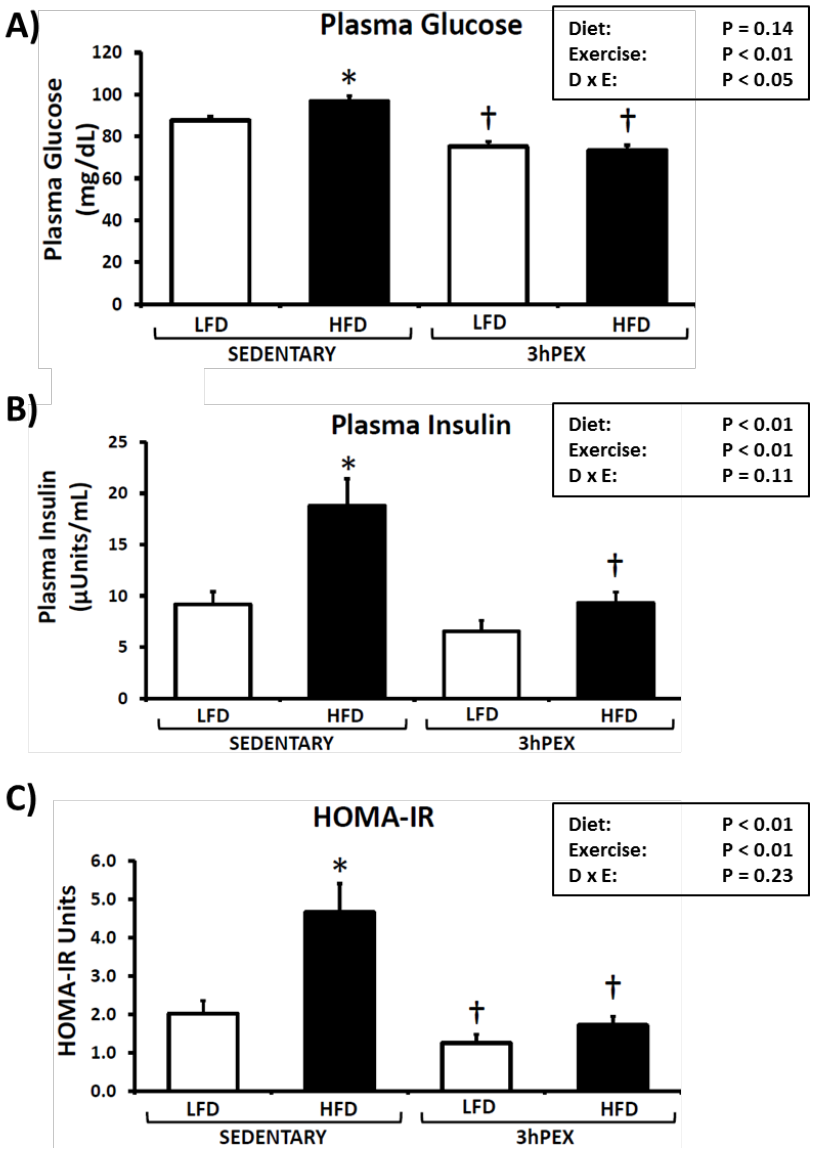

Figure 5.5

A: Plasma Glucose. B: Plasma Insulin. C: HOMA-IR. Data were analyzed by two-way ANOVA. Plasma was obtained from rats at 3h postexercise, 3hPEX, and time-matched Sedentary controls. Diet, main effect of diet; Exercise, main effect of exercise; D x E, interaction between diet and exercise. Post-hoc analysis was performed to identify the source of significant variance. *$P < 0.05$, LFD versus HFD, within Sedentary. †$P < 0.05$, for 3hPEX versus Sedentary within a given diet group (e.g., LFD 3hPEX vs. LFD Sedentary, etc.). Values are means ± SEM; n = 36 per group.

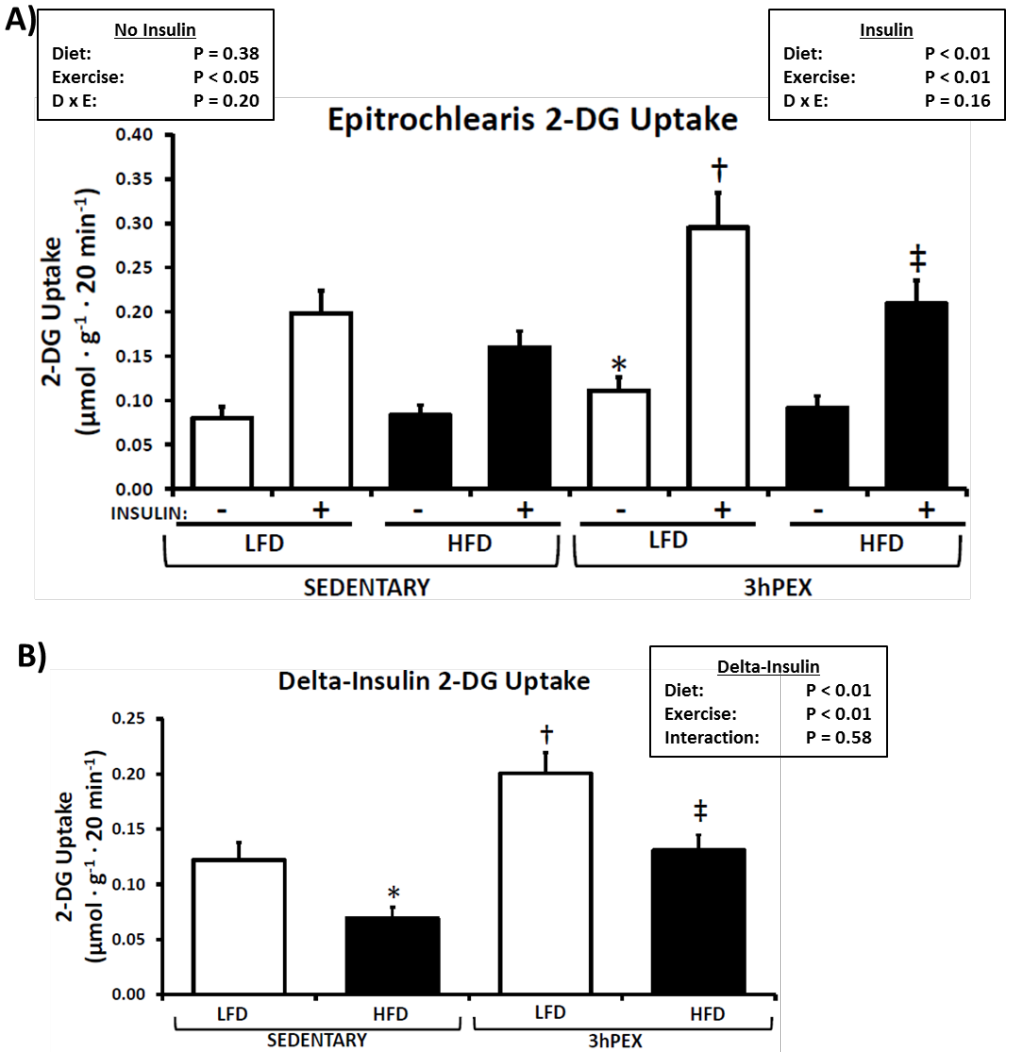

Figure 5.6

A: 2-Deoxyglucose (2-DG) uptake measured in paired epitrochlearis muscles without or with insulin 3h post-exercise (3hPEX). Data were analyzed by two-way ANOVA within each insulin level. Diet, main effect of diet; Exercise, main effect of exercise; D x E, interaction between Diet and Exercise. Post-hoc analysis was performed to identify the source of significant variance. *P < 0.05, for Sedentary versus 3hPEX, within LFD. †P < 0.05 for LFD 3hPEX with insulin versus all other with insulin groups. ‡P < 0.05, for glucose uptake with insulin within HFD, Sedentary versus 3hPEX. Values are means ± SEM; n = 19-24. B: 2-DG uptake delta-insulin values. Data were analyzed by two-way ANOVA within each insulin level. Post-hoc analysis was performed to identify the source of significant variance. *P < 0.05, for LFD versus HFD within Sedentary. †P < 0.05, for LFD 3hPEX versus all other with insulin groups. ‡P < 0.05; for Sedentary versus 3hPEX within HFD. Values are means ± SEM; n = 17-22 per group.

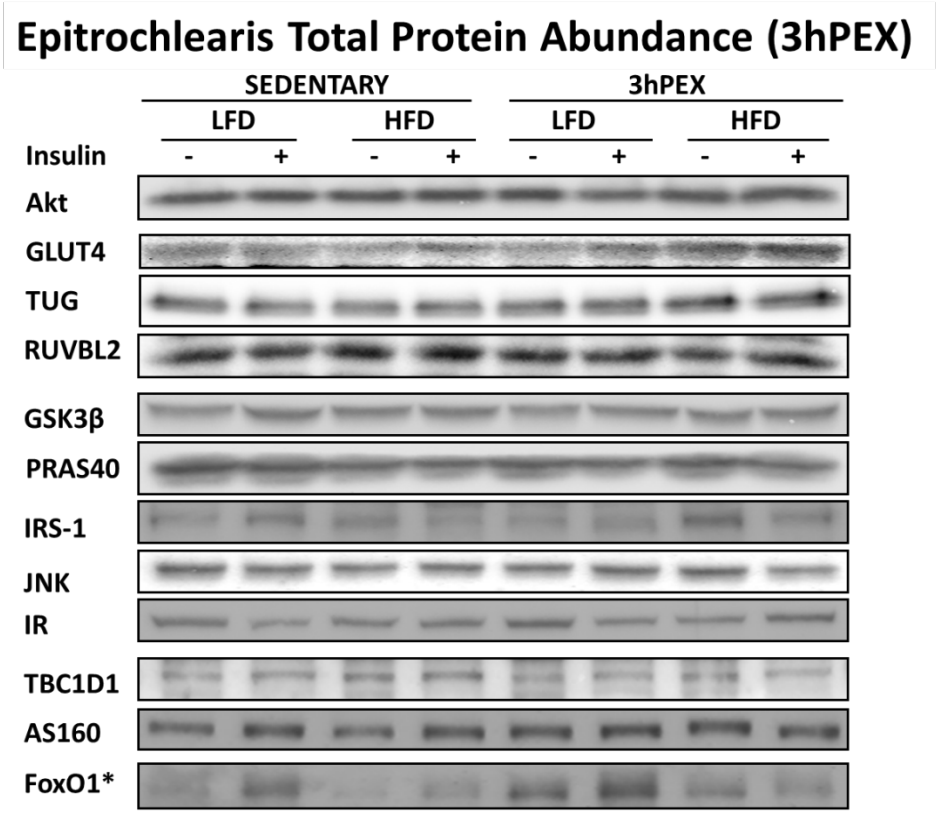

Figure 5.7

Representative total protein abundance for 3h post-exercise (3hPEX) muscles. Total FoxO1 protein was the only protein that was found to be significantly altered by exercise or diet. *FoxO1 (n = 8 per group) there were significant main effects of exercise (3hPEX > Sedentary; $P < 0.05$) for either muscles incubated with no insulin (LFD Sedentary = 0.52 ± 0.11; HFD Sedentary = 0.42 ± 0.09; LFD 3hPEX = 1.19 ± 0.34; and HFD 3hPEX = 0.80 ± 0.13) or muscles incubated with insulin (LFD Sedentary = 0.66 ± 0.17; HFD Sedentary = 0.93 ± 0.34; LFD 3hPEX = 1.92 ± 0.40; and HFD 3hPEX = 1.57 ± 0.29). For muscles incubated in the absence of insulin for FoxO1, post-hoc analysis revealed that HFD 3hPEX versus HFD Sedentary values were significantly greater ($P < 0.05$). For insulin-treated muscles, post-hoc analysis revealed that LFD 3hPEX versus LFD Sedentary values were significantly greater ($P < 0.05$).

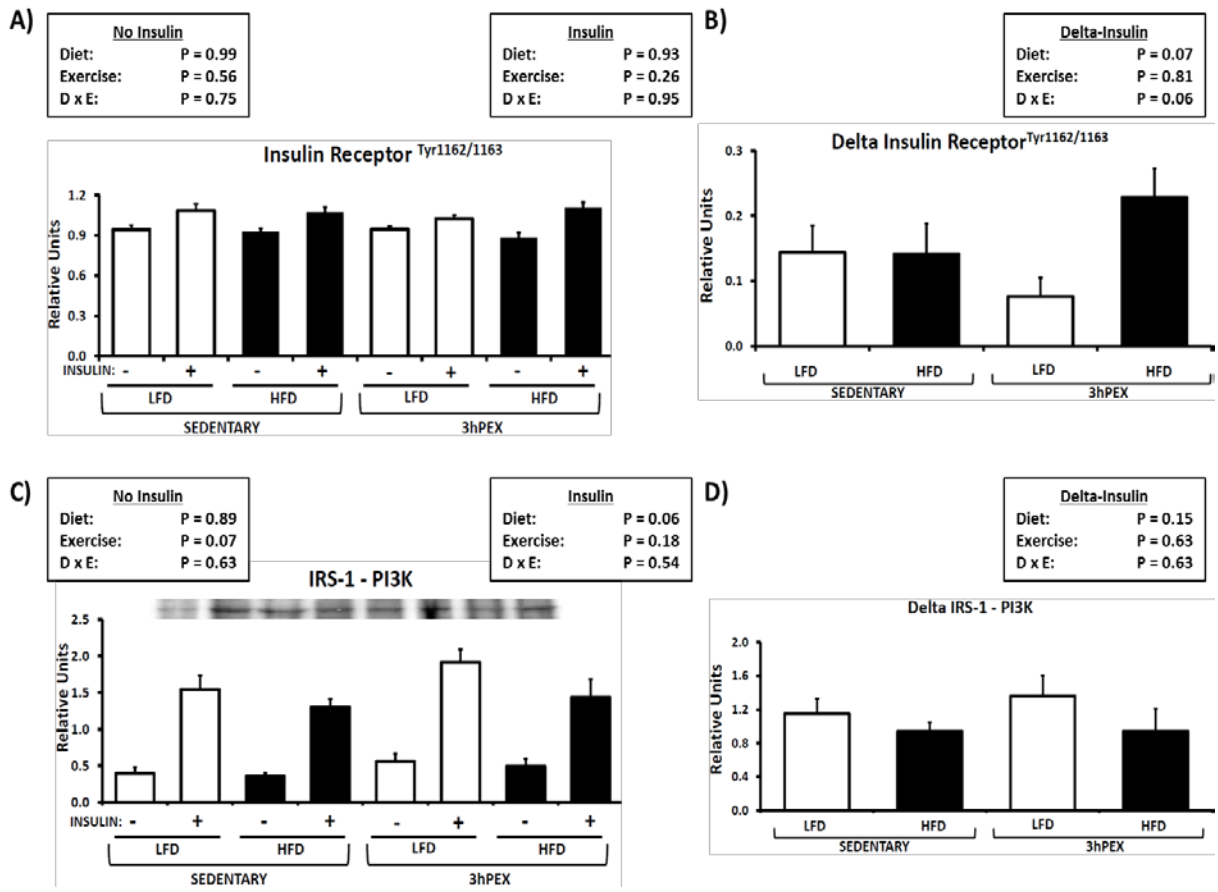

Figure 5.8

A: Insulin Receptor$^{Tyr1162/1163}$ phosphorylation measured in paired epitrochlearis muscles 3hPEX. Data were analyzed by two-way ANOVA within each insulin level. Diet, main effect of diet; Exercise, main effect of exercise; D x E, interaction between Diet and Exercise. Values are means ± SEM; n = 19-20 per group. B: Insulin Receptor$^{Tyr1162/1163}$ delta-insulin values. Data were analyzed by two-way ANOVA within each insulin level. Values are means ± SEM; n = 19-20 per group. C: IRS-1-PI3K association measured in paired epitrochlearis muscles 3hPEX. Data were analyzed by two-way ANOVA within each insulin level. Values are means ± SEM; n = 8 per group. D: IRS-1 – PI3K association delta-insulin values. Data were analyzed by two-way ANOVA within each insulin level. Values are means ± SEM; n = 8 per group.

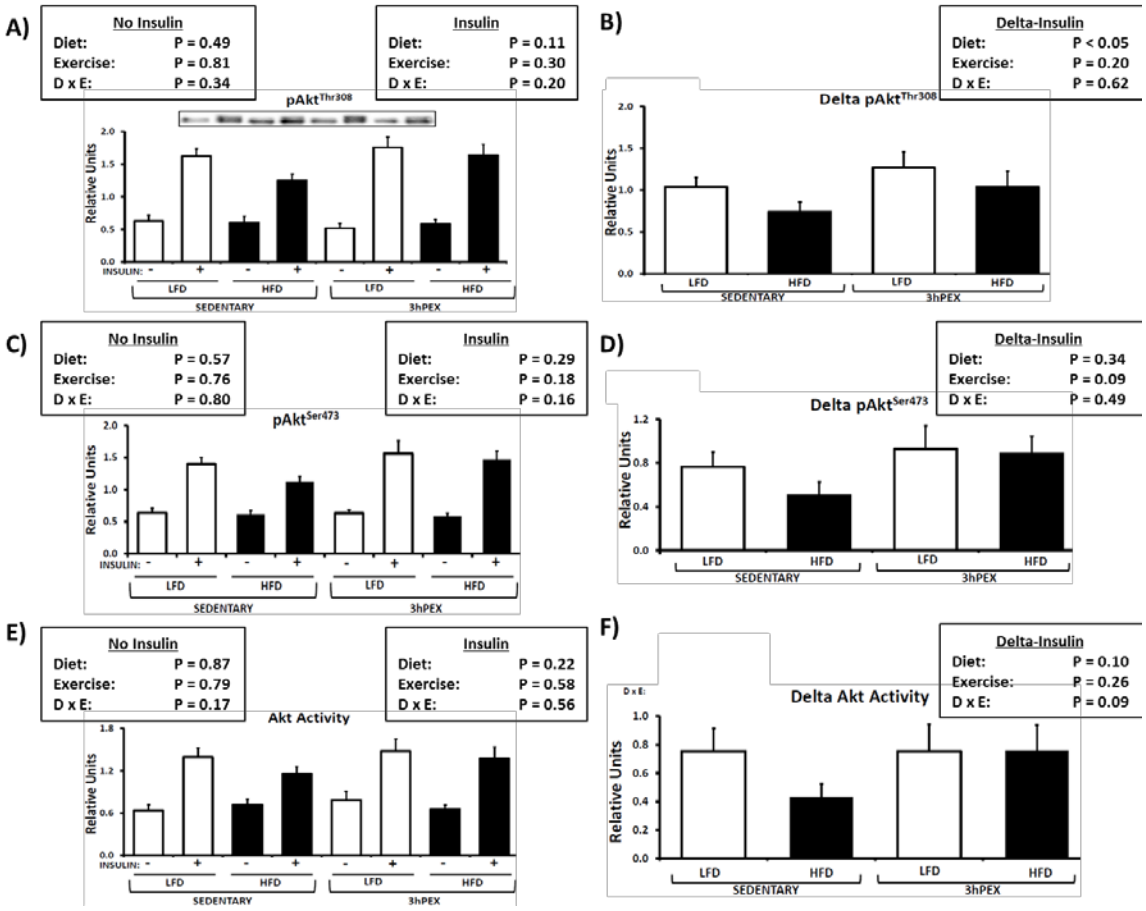

Figure 5.9

A: Akt Thr308 phosphorylation (Akt^{Thr308}) measured in paired epitrochlearis muscles 3hPEX. Data were analyzed by two-way ANOVA within each insulin level. Diet, main effect of diet; Exercise, main effect of exercise; D x E, interaction between Diet and Exercise. Values are means ± SEM; n = 22-26 per group. B: $pAkt^{Thr308}$ delta-insulin values. Data were analyzed by two-way ANOVA within each insulin level. Post-hoc analysis was performed to identify the source of significant variance. Values are means ± SEM; n = 22-25 per group. C: Akt Ser473 phosphorylation ($pAkt^{Ser473}$) measured in paired epitrochlearis muscles 3hPEX. Data were analyzed by two-way ANOVA within each insulin level. Values are means ± SEM; n = 19-20 per group. D: $pAkt^{Ser473}$ delta-insulin values. Data were analyzed by two-way ANOVA within each insulin level. Values are means ± SEM; n = 19-20 per group. E: Akt activity measured in paired epitrochlearis muscles 3hPEX. Data were analyzed by two-way ANOVA within each insulin level. Values are means ± SEM; n = 19-20 per group. F: Akt activity delta-insulin values. Data were analyzed by two-way ANOVA within each insulin level. Values are means ± SEM; n = 18-21 per group.

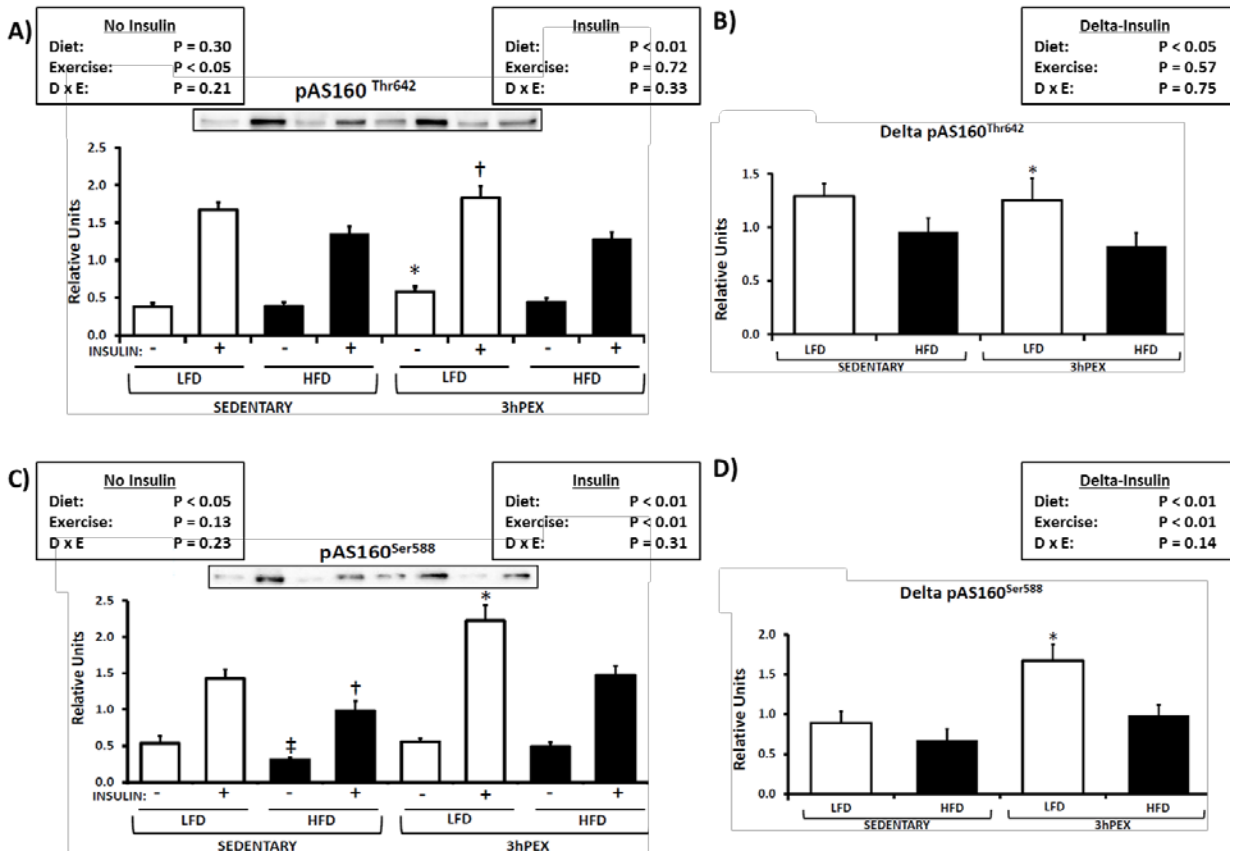

Figure 5.10

A: Akt Subtrate at 160 kDa Thr 642 phosphorylation (pAS160^{Thr642}) measured in paired epitrochlearis muscles 3h post-exercise (3hPEX). Data were analyzed by two-way ANOVA within each insulin level. Diet, main effect of diet; Exercise, main effect of exercise; D x E, interaction between Diet and Exercise. Post-hoc analysis was performed to identify the source of significant variance. *P < 0.05, for Sedentary versus 3hPEX with no insulin within LFD. †P < 0.05, for LFD versus HFD with insulin within 3hPEX. Values are means ± SEM; n = 13-16 per group. B: pAS160^{Thr642} delta-insulin values. Data were analyzed by two-way ANOVA within each insulin level. Post-hoc analysis was performed to identify the source of significant variance. *P < 0.05, for LFD versus HFD within 3hPEX. Values are means ± SEM; n = 13-16 per group. C: Akt Subtrate at 160 kDa Ser 588 phosphorylation (pAS160^{Ser588}) measured in paired epitrochlearis muscles 3hPEX. Data were analyzed by two-way ANOVA within each insulin level. Post-hoc analysis was performed to identify the source of significant variance. ‡P < 0.05, for LFD versus HFD within Sedentary. *P < 0.05, LFD 3hPEX is greater than all other with insulin groups. †P < 0.05, Sedentary HFD is less than all other with insulin groups. Values are means ± SEM; n = 13-16 per group. D: pAS160^{Ser588} delta-insulin values. Data were analyzed by two-way ANOVA within each insulin level. Post-hoc analysis was performed to identify the source of significant variance. *P < 0.05, LFD 3hPEX is greater than all other with insulin groups. Values are means ± SEM; n = 13-16 per group.

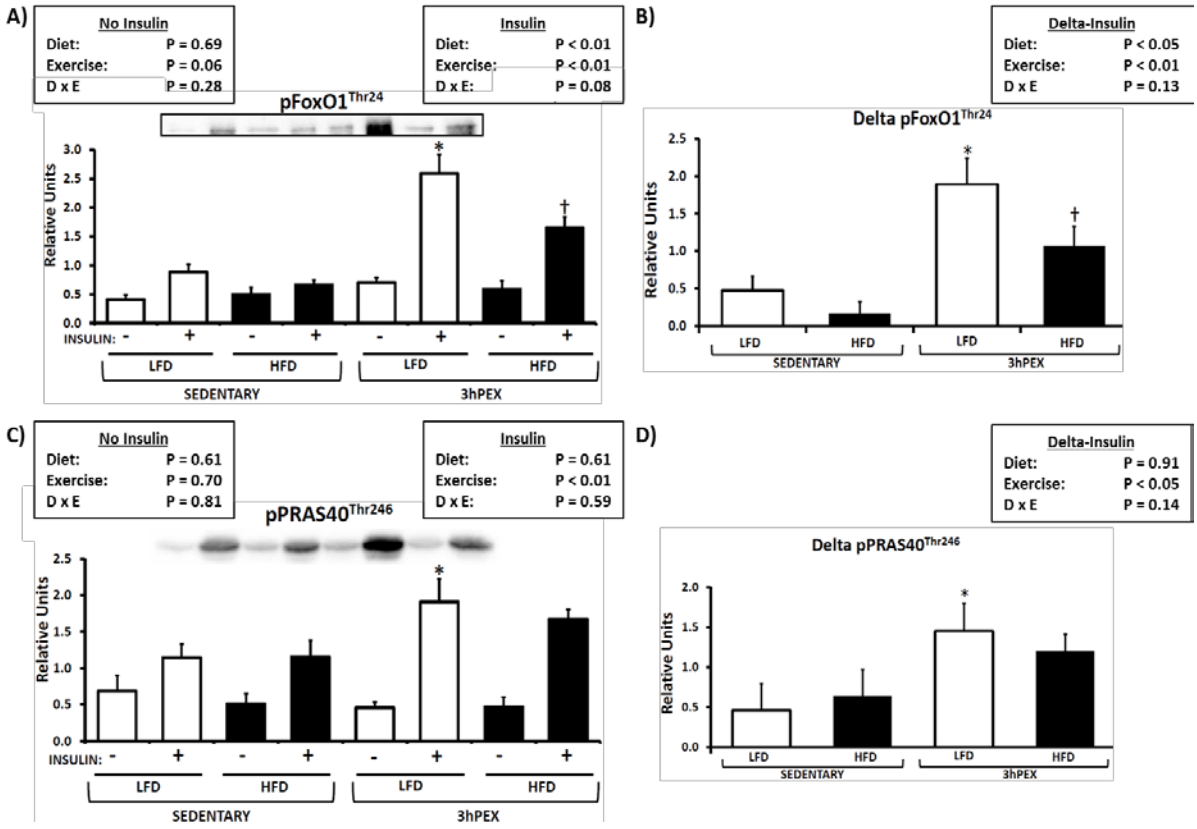

Figure 5.11

A: pFoxO1^{Thr24} measured in paired epitrochlearis muscles 3h post-exercise (3hPEX). Data were analyzed by two-way ANOVA within each insulin level. Diet, main effect of diet; Exercise, main effect of exercise; D x E, interaction between Diet and Exercise. Post-hoc analysis was performed to identify the source of significant variance. *P < 0.05, for LFD 3hPEX versus all other groups with insulin. †P < 0.05, for Sedentary versus 3hPEX with insulin within HFD. Values are means ± SEM; n = 8 per group. B: pFoxO1^{Thr24} delta-insulin values. Data were analyzed by two-way ANOVA within each insulin level. Post-hoc analysis was performed to identify the source of significant variance. *P < 0.05, LFD 3hPEX versus all other groups. †P < 0.05, for Sedentary versus 3hPEX with insulin within HFD. Values are means ± SEM; n = 8 per group. C: pPRAS40^{Thr246} measured in paired epitrochlearis muscles 3hPEX. Data were analyzed by two-way ANOVA within each insulin level. Post-hoc analysis was performed to identify the source of significant variance. *P < 0.05, for Sedentary versus 3hPEX with insulin within LFD. Values are means ± SEM; n = 8 per group. D: pPRAS40^{Thr246} delta-insulin values. Data were analyzed by two-way ANOVA within each insulin level. Post-hoc analysis was performed to identify the source of significant variance. *P < 0.05, for Sedentary versus 3hPEX with insulin within LFD. Vales are means ± SEM; n = 8 per group.

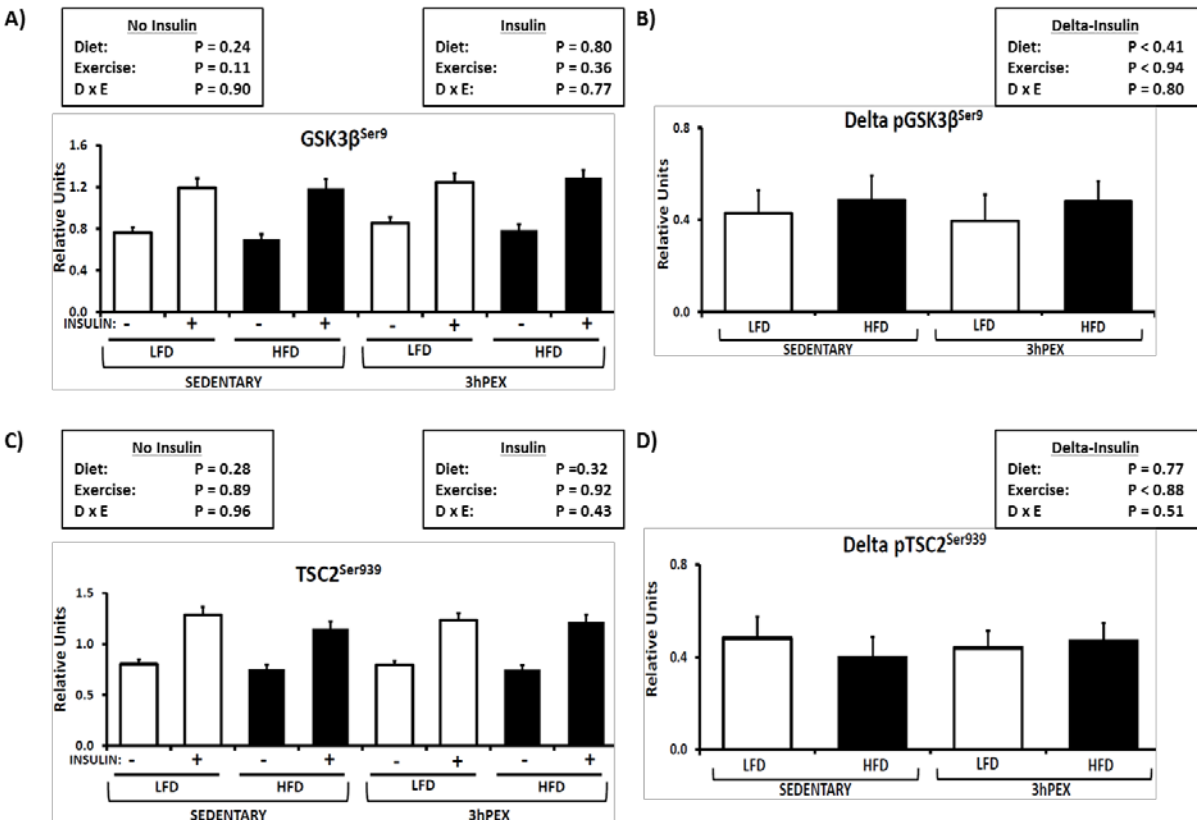

Figure 5.12

A: pGSK3β^{Ser9} measured in paired epitrochlearis muscles 3hPEX. Data were analyzed by two-way ANOVA within each insulin level. Diet, main effect of diet; Exercise, main effect of exercise; D x E, interaction between Diet and Exercise. Values are means ± SEM; n= 19-20. B: pGSK3β^{Ser9} delta-Insulin values measured 3hPEX. Data were analyzed by two-way ANOVA within each insulin level. Values are means ± SEM; n= 19-20. C: pTSC2^{Ser939} measured in paired epitrochlearis muscles 3hPEX. Data were analyzed by two-way ANOVA within each insulin level. Values are means ± SEM; n= 19-20. D: pTSC2^{Ser939} delta-Insulin values measured 3hPEX. Data were analyzed by two-way ANOVA within each insulin level. Values are means ± SEM; n= 19-20.

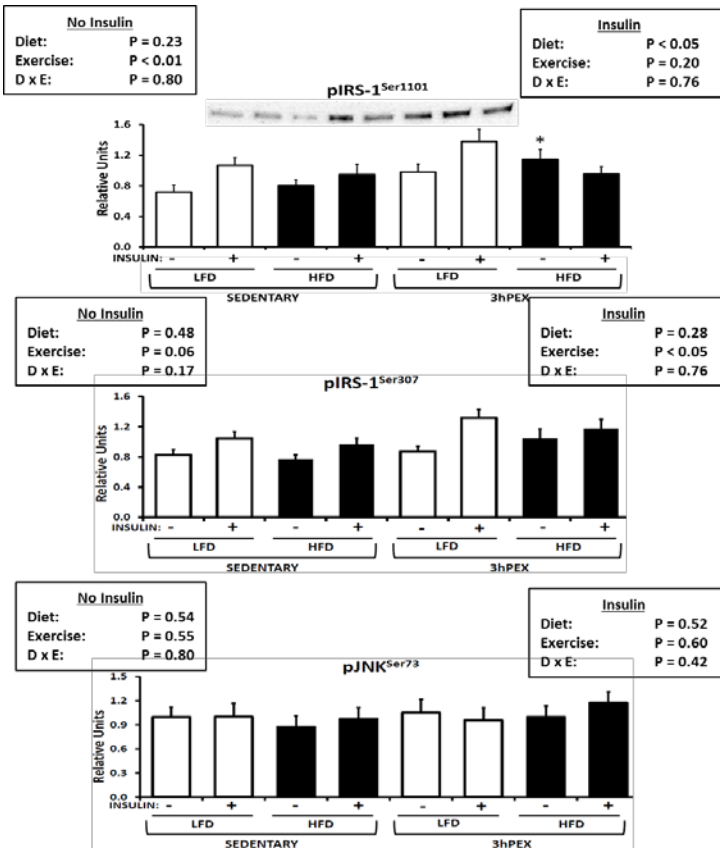

Figure 5.13

A: Insulin receptor substrate 1 Ser1101 phosphorylation (pIRS-1^{Ser1101}) measured in paired epitrochlearis muscles 3hPEX. Data were analyzed by two-way ANOVA within each insulin level. Diet, main effect of diet; Exercise, main effect of exercise; D x E, interaction between Diet and Exercise. Tukey post-hoc analysis was performed to identify the source of significant variance. *P < 0.05, for Sedentary versus 3hPEX without insulin within HFD. Values are means ± SEM; n = 20. B: Insulin receptor substrate 1 Ser307 phosphorylation (IRS-1^{Ser307}) measured in paired epitrochlearis muscles 3hPEX. Data were analyzed by two-way ANOVA within each insulin level. Tukey post-hoc analysis was performed to identify the source of significant variance. Values are means ± SEM; n = 19-20. C: c-Jun N-terminal kinase Ser73 phosphorylation (pJNK^{Ser73}) measured in paired epitrochlearis muscles 3hPEX. Data were analyzed by two-way ANOVA within each insulin level. Values are means ± SEM; n = 11-12.

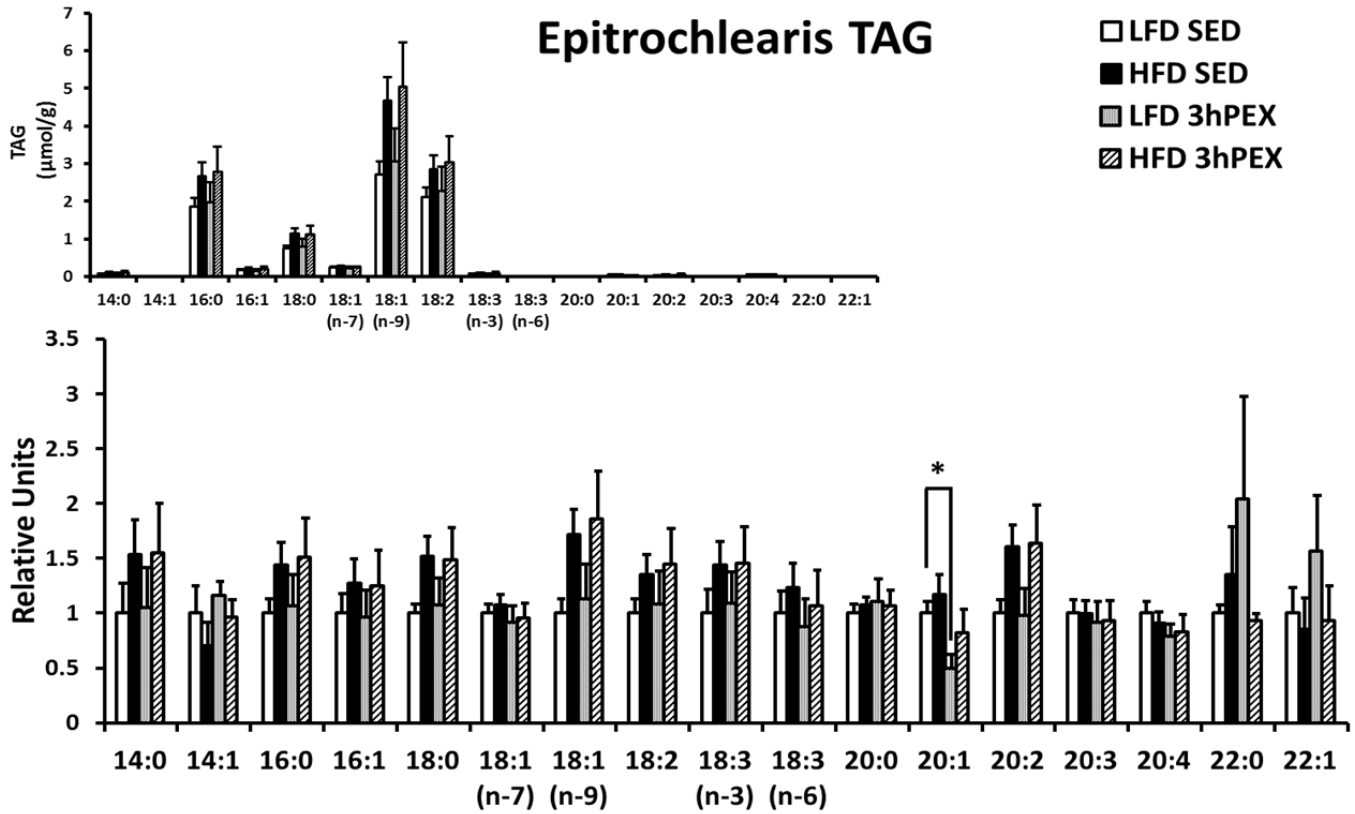

ANOVA	14:0	14:1	16:0	16:1	18:0	18:1 (n-7)	18:1 (n-9)	18:2	18:3 (n-3)	18:3 (n-6)	20:0	20:1	20:2	20:3	20:4	22:0	22:1
Diet	0.31	0.74	0.11	0.27	0.04*	0.65	0.02*	0.73	0.15	0.41	0.9	0.10	0.02*	0.96	0.84	0.48	0.28
Exercise	0.71	0.07	0.79	0.91	0.93	0.41	0.66	0.17	0.85	0.58	0.73	0.01*	0.97	0.64	0.24	0.56	0.37
D x E	0.87	0.8	0.99	0.98	0.81	0.88	0.98	0.98	0.89	0.93	0.67	0.20	0.92	0.95	0.61	0.18	0.50

Figure 5.14

Epitrochlearis muscle triacylglycerides (TAG) 3hPEX. Values are expressed relative to the LFD Sedentary (SED) group for each lipid species. Data were analyzed by two-way ANOVA within each insulin level. Diet, main effect of diet; Exercise, main effect of exercise; D x E, interaction between Diet and Exercise. Tukey post-hoc analysis was performed to identify the source of significant variance. *$P < 0.05$, Sedentary versus 3hPEX within LFD. The Inset in upper left shows the absolute concentrations (µmol/g) for the TAG species. Values are means ± SEM; n = 5-9 per group.

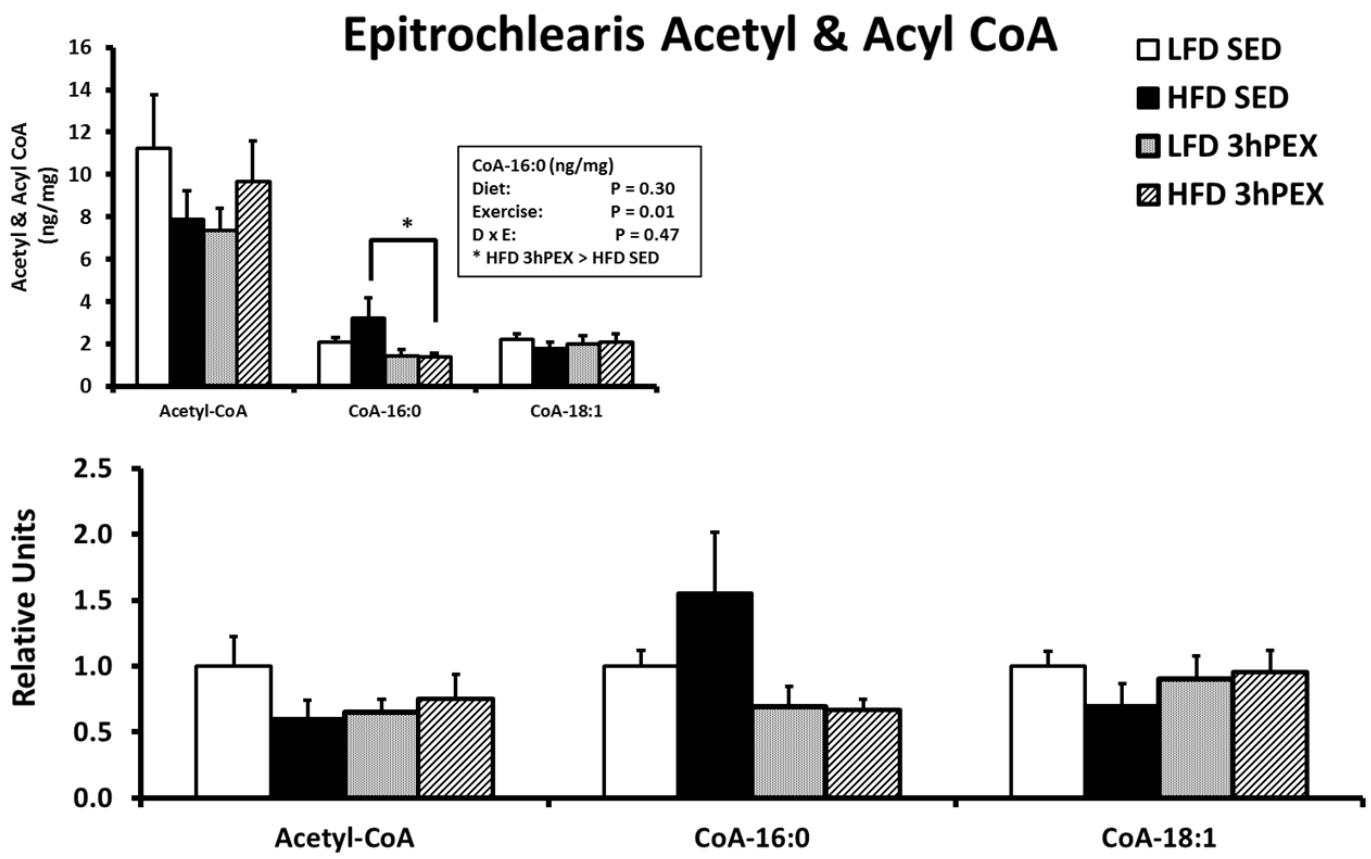

ANOVA	Acetyl	16:0	18:1
Diet	0.32	0.30	0.70
Exercise	0.39	0.01*	0.19
D x E	0.053	0.47	0.50

Figure 5.15

Epitrochlearis muscle acetyl and acyl CoA 3hPEX. Values are expressed relative to the LFD Sedentary (SED) group for each lipid species. Data were analyzed by two-way ANOVA within each insulin level. Diet, main effect of diet; Exercise, main effect of exercise; D x E, interaction between Diet and Exercise. Tukey post-hoc analysis was performed to identify the source of significant variance. *$P < 0.05$, Sedentary versus 3hPEX within HFD. Values are means ± SEM; n= 5-9 per group. The Inset in upper left shows the absolute concentrations (ng/mg) for the acetyl and acyl CoA species.

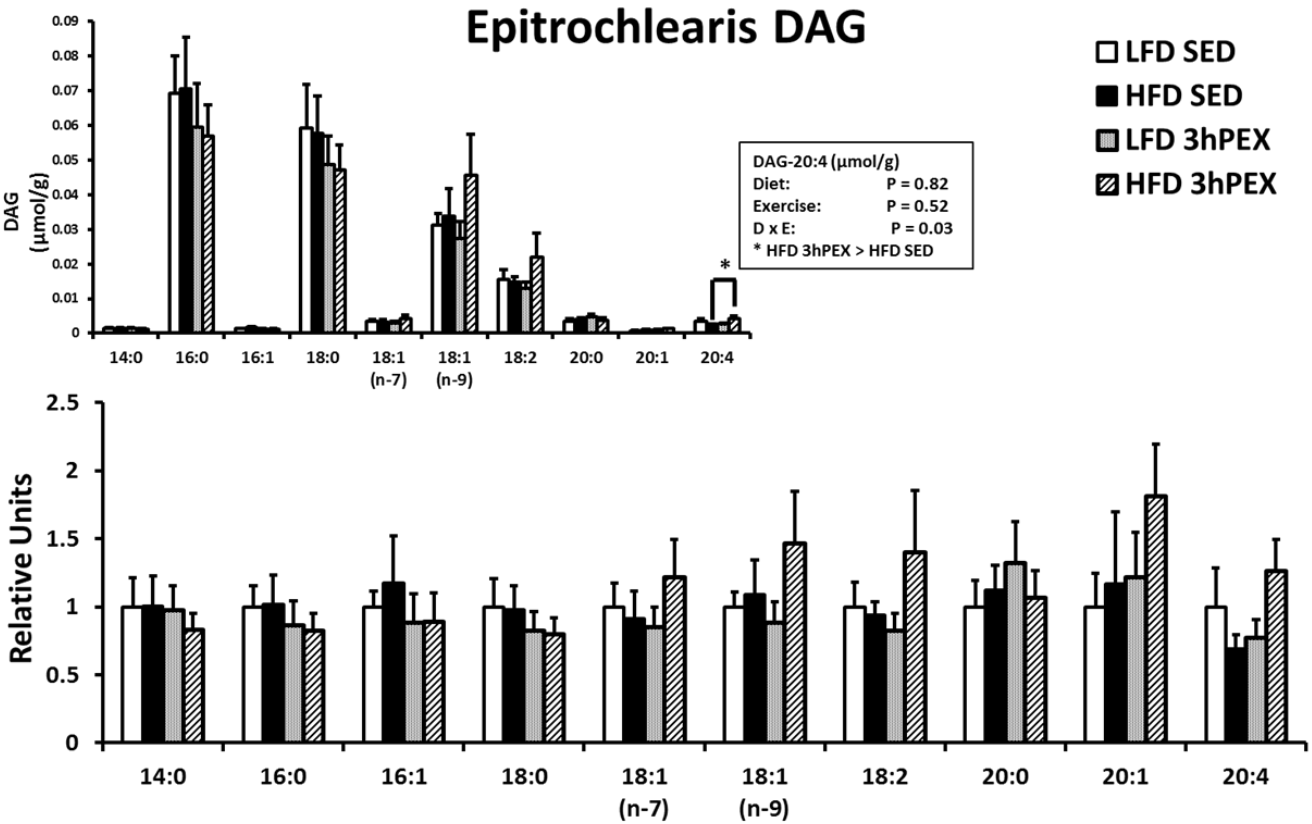

ANOVA	14:0	16:0	16:1	18:0	18:1 (n-7)	18:1 (n-9)	18:2	20:0	20:1	20:4
Diet	0.72	0.96	0.97	0.88	0.79	0.37	0.33	0.77	0.34	0.65
Exericse	0.60	0.35	0.27	0.28	0.79	0.94	0.99	0.58	0.28	0.39
D x E	0.70	0.88	0.79	0.99	0.23	0.24	0.31	0.41	0.59	0.052

Figure 5.16

Epitrochlearis muscle diacylglycerides (DAG) 3hPEX. Values are expressed relative to the LFD Sedentary (SED) group for each lipid species. Data were analyzed by two-way ANOVA within each insulin level. Diet, main effect of diet; Exercise, main effect of exercise; D x E, interaction between Diet and Exercise. Tukey post-hoc analysis was performed to identify the source of significant variance. *$P < 0.05$, Sedentary versus 3hPEX within HFD. Inset in upper left shows the absolute concentrations for the DAG species. Values are means ± SEM, n = 5-9 per group.

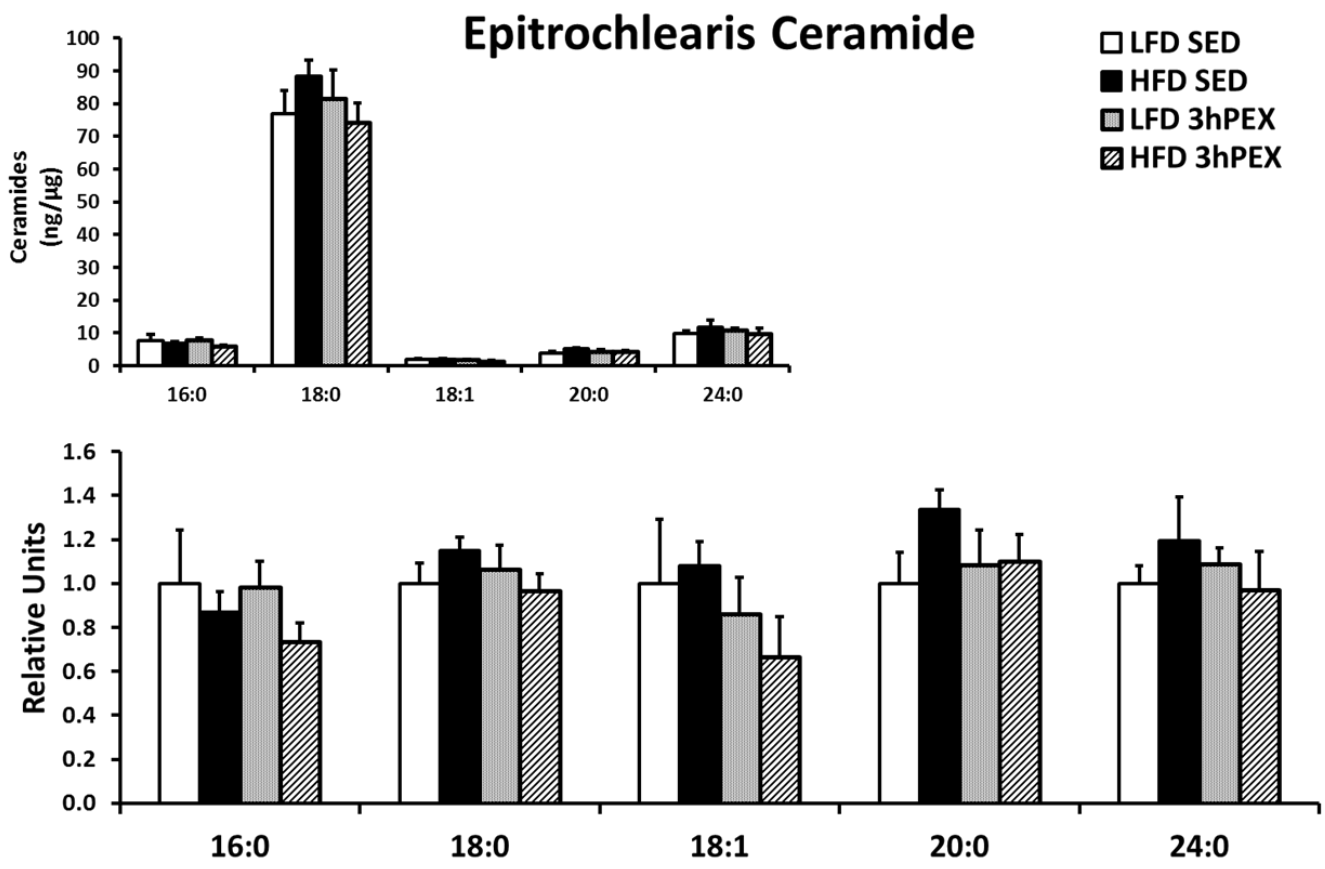

ANOVA	16:0	18:0	18:1	20:0	24:0
Diet	0.74	0.53	0.17	0.09	0.85
Exercise	0.88	0.52	0.91	0.60	0.59
D x E	0.43	0.32	0.61	0.46	0.25

Figure 5.17

Epitrochlearis muscle ceramides 3hPEX. Values are expressed relative to the LFD Sedentary (SED) group for each lipid species. Data were analyzed by two-way ANOVA within each insulin level. Diet, main effect of diet; Exercise, main effect of exercise; D x E, interaction between Diet and Exercise. The Inset in upper left shows the absolute concentrations (ng/µg) for the ceramide species. Values are means ± SEM; n = 5-9 per group.

References

1. **Antharavally BS, Carter B, Bell PA, and Krishna Mallia A.** A high-affinity reversible protein stain for Western blots. *Anal Biochem* 329: 276-280, 2004.
2. **Arias EB, Kim J, Funai K, and Cartee GD.** Prior exercise increases phosphorylation of Akt substrate of 160 kDa (AS160) in rat skeletal muscle. *Am J Physiol Endocrinol Metab* 292: E1191-1200, 2007.
3. **Betts JJ, Sherman WM, Reed MJ, and Gao JP.** Duration of improved muscle glucose uptake after acute exercise in obese Zucker rats. *Obes Res* 1: 295-302, 1993.
4. **Bonen A, Tan MH, Clune P, and Kirby RL.** Effects of exercise on insulin binding to human muscle. *Am J Physiol* 248: E403-408, 1985.
5. **Bonen A, Tan MH, and Watson-Wright WM.** Effects of exercise on insulin binding and glucose metabolism in muscle. *Can J Physiol Pharmacol* 62: 1500-1504, 1984.
6. **Bruce CR, Hoy AJ, Turner N, Watt MJ, Allen TL, Carpenter K, Cooney GJ, Febbraio MA, and Kraegen EW.** Overexpression of carnitine palmitoyltransferase-1 in skeletal muscle is sufficient to enhance fatty acid oxidation and improve high-fat diet-induced insulin resistance. *Diabetes* 58: 550-558, 2009.
7. **Burstein R, Epstein Y, Shapiro Y, Charuzi I, and Karnieli E.** Effect of an acute bout of exercise on glucose disposal in human obesity. *J Appl Physiol* 69: 299-304, 1990.
8. **Cartee GD and Bohn EE.** Growth hormone reduces glucose transport but not GLUT-1 or GLUT-4 in adult and old rats. *Am J Physiol* 268: E902-909, 1995.
9. **Cartee GD and Funai K.** Exercise and Insulin: Convergence or Divergence at AS160 and TBC1D1? *Exercise and Sport Sciences Reviews* 37: 188-195, 2009.
10. **Cartee GD and Holloszy JO.** Exercise increases susceptibility of muscle glucose transport to activation by various stimuli. *Am J Physiol* 258: E390-393, 1990.
11. **Cartee GD and Wojtaszewski JF.** Role of Akt substrate of 160 kDa in insulin-stimulated and contraction-stimulated glucose transport. *Appl Physiol Nutr Metab* 32: 557-566, 2007.
12. **Cartee GD, Young DA, Sleeper MD, Zierath J, Wallberg-Henriksson H, and Holloszy JO.** Prolonged increase in insulin-stimulated glucose transport in muscle after exercise. *Am J Physiol* 256: E494-499, 1989.
13. **Castorena CM, Mackrell JG, Bogan JS, Kanzaki M, and Cartee GD.** Clustering of GLUT4, TUG and RUVBL2 Protein Levels Correlate with Myosin Heavy Chain Isoform Pattern in Skeletal Muscles, but AS160 and TBC1D1 Levels Do Not. *J Appl Physiol*, 2011.
14. **Copps KD and White MF.** Regulation of insulin sensitivity by serine/threonine phosphorylation of insulin receptor substrate proteins IRS1 and IRS2. *Diabetologia* 55: 2565-2582, 2012.
15. **Cusi K, Maezono K, Osman A, Pendergrass M, Patti ME, Pratipanawatr T, DeFronzo RA, Kahn CR, and Mandarino LJ.** Insulin resistance differentially affects the PI 3-kinase- and MAP kinase-mediated signaling in human muscle. *J Clin Invest* 105: 311-320, 2000.
16. **Devlin JT and Horton ES.** Effects of prior high-intensity exercise on glucose metabolism in normal and insulin-resistant men. *Diabetes* 34: 973-979, 1985.
17. **Douen AG, Ramlal T, Klip A, Young DA, Cartee GD, and Holloszy JO.** Exercise-induced increase in glucose transporters in plasma membranes of rat skeletal muscle. *Endocrinology* 124: 449-454, 1989.

18. **Fisher JS, Gao J, Han DH, Holloszy JO, and Nolte LA.** Activation of AMP kinase enhances sensitivity of muscle glucose transport to insulin. *Am J Physiol Endocrinol Metab* 282: E18-23, 2002.
19. **Funai K, Schweitzer GG, Castorena CM, Kanzaki M, and Cartee GD.** In vivo exercise followed by in vitro contraction additively elevates subsequent insulin-stimulated glucose transport by rat skeletal muscle. *Am J Physiol Endocrinol Metab* 298: E999-1010, 2010.
20. **Funai K, Schweitzer GG, Sharma N, Kanzaki M, and Cartee GD.** Increased AS160 phosphorylation, but not TBC1D1 phosphorylation, with increased postexercise insulin sensitivity in rat skeletal muscle. *Am J Physiol Endocrinol Metab* 297: E242-251, 2009.
21. **Gao J, Sherman WM, McCune SA, and Osei K.** Effects of acute running exercise on whole body insulin action in obese male SHHF/Mcc-facp rats. *J Appl Physiol* 77: 534-541, 1994.
22. **Gross DN, Wan M, and Birnbaum MJ.** The role of FOXO in the regulation of metabolism. *Curr Diab Rep* 9: 208-214, 2009.
23. **Gulli RA, Tishinsky JM, MacDonald T, Robinson LE, Wright DC, and Dyck DJ.** Exercise restores insulin, but not adiponectin, response in skeletal muscle of high-fat fed rodents. *Am J Physiol Regul Integr Comp Physiol* 303: R1062-1070, 2012.
24. **Gulve EA, Cartee GD, Zierath JR, Corpus VM, and Holloszy JO.** Reversal of enhanced muscle glucose transport after exercise: roles of insulin and glucose. *Am J Physiol* 259: E685-691, 1990.
25. **Hamada T, Arias EB, and Cartee GD.** Increased submaximal insulin-stimulated glucose uptake in mouse skeletal muscle after treadmill exercise. *J Appl Physiol* 101: 1368-1376, 2006.
26. **Han DH, Hansen PA, Host HH, and Holloszy JO.** Insulin resistance of muscle glucose transport in rats fed a high-fat diet: a reevaluation. *Diabetes* 46: 1761-1767, 1997.
27. **Hansen PA, Gulve EA, and Holloszy JO.** Suitability of 2-deoxyglucose for in vitro measurement of glucose transport activity in skeletal muscle. *J Appl Physiol* 76: 979-985, 1994.
28. **Hansen PA, Nolte LA, Chen MM, and Holloszy JO.** Increased GLUT-4 translocation mediates enhanced insulin sensitivity of muscle glucose transport after exercise. *J Appl Physiol* 85: 1218-1222, 1998.
29. **Howlett KF, Sakamoto K, Hirshman MF, Aschenbach WG, Dow M, White MF, and Goodyear LJ.** Insulin signaling after exercise in insulin receptor substrate-2-deficient mice. *Diabetes* 51: 479-483, 2002.
30. **Kasumov T, Huang H, Chung YM, Zhang R, McCullough AJ, and Kirwan JP.** Quantification of ceramide species in biological samples by liquid chromatography electrospray ionization tandem mass spectrometry. *Anal Biochem* 401: 154-161, 2010.
31. **Kiens B.** Skeletal muscle lipid metabolism in exercise and insulin resistance. *Physiol Rev* 86: 205-243, 2006.
32. **Kraegen EW, Clark PW, Jenkins AB, Daley EA, Chisholm DJ, and Storlien LH.** Development of muscle insulin resistance after liver insulin resistance in high-fat-fed rats. *Diabetes* 40: 1397-1403, 1991.
33. **Kraegen EW and Cooney GJ.** Free fatty acids and skeletal muscle insulin resistance. *Curr Opin Lipidol* 19: 235-241, 2008.
34. **Kramer HF, Witczak CA, Taylor EB, Fujii N, Hirshman MF, and Goodyear LJ.** AS160 regulates insulin- and contraction-stimulated glucose uptake in mouse skeletal muscle. *J Biol Chem* 281: 31478-31485, 2006.

35. **Kusunoki M, Storlien LH, MacDessi J, Oakes ND, Kennedy C, Chisholm DJ, and Kraegen EW.** Muscle glucose uptake during and after exercise is normal in insulin-resistant rats. *Am J Physiol* 264: E167-172, 1993.
36. **Liu S, Baracos VE, Quinney HA, and Clandinin MT.** Dietary fat modifies exercise-dependent glucose transport in skeletal muscle. *J Appl Physiol* 80: 1219-1224, 1996.
37. **MacKrell JG and Cartee GD.** A Novel Method to Measure Glucose Uptake and Myosin Heavy Chain Isoform Expression of Single Fibers from Rat Skeletal Muscle. *Diabetes* In Press: Accepted January, 2012.
38. **Mikines KJ, Sonne B, Farrell PA, Tronier B, and Galbo H.** Effect of physical exercise on sensitivity and responsiveness to insulin in humans. *Am J Physiol* 254: E248-259, 1988.
39. **Morrison WR and Smith LM.** Preparation of Fatty Acid Methyl Esters and Dimethylacetals from Lipids with Boron Fluoride--Methanol. *J Lipid Res* 5: 600-608, 1964.
40. **Oakes ND, Bell KS, Furler SM, Camilleri S, Saha AK, Ruderman NB, Chisholm DJ, and Kraegen EW.** Diet-induced muscle insulin resistance in rats is ameliorated by acute dietary lipid withdrawal or a single bout of exercise: parallel relationship between insulin stimulation of glucose uptake and suppression of long-chain fatty acyl-CoA. *Diabetes* 46: 2022-2028, 1997.
41. **Oliveira AG, Carvalho BM, Tobar N, Ropelle ER, Pauli JR, Bagarolli RA, Guadagnini D, Carvalheira JB, and Saad MJ.** Physical exercise reduces circulating lipopolysaccharide and TLR4 activation and improves insulin signaling in tissues of DIO rats. *Diabetes* 60: 784-796, 2011.
42. **Passonneau JV and Lauderdale VR.** A comparison of three methods of glycogen measurement in tissues. *Anal Biochem* 60: 405-412, 1974.
43. **Pauli JR, Ropelle ER, Cintra DE, Carvalho-Filho MA, Moraes JC, De Souza CT, Velloso LA, Carvalheira JB, and Saad MJ.** Acute physical exercise reverses S-nitrosation of the insulin receptor, insulin receptor substrate 1 and protein kinase B/Akt in diet-induced obese Wistar rats. *J Physiol* 586: 659-671, 2008.
44. **Perseghin G, Price TB, Petersen KF, Roden M, Cline GW, Gerow K, Rothman DL, and Shulman GI.** Increased glucose transport-phosphorylation and muscle glycogen synthesis after exercise training in insulin-resistant subjects. *N Engl J Med* 335: 1357-1362, 1996.
45. **Richter EA, Garetto LP, Goodman MN, and Ruderman NB.** Muscle glucose metabolism following exercise in the rat: increased sensitivity to insulin. *J Clin Invest* 69: 785-793, 1982.
46. **Ropelle ER, Pauli JR, Prada PO, de Souza CT, Picardi PK, Faria MC, Cintra DE, Fernandes MF, Flores MB, Velloso LA, Saad MJ, and Carvalheira JB.** Reversal of diet-induced insulin resistance with a single bout of exercise in the rat: the role of PTP1B and IRS-1 serine phosphorylation. *J Physiol* 577: 997-1007, 2006.
47. **Rosholt MN, King PA, and Horton ES.** High-fat diet reduces glucose transporter responses to both insulin and exercise. *Am J Physiol* 266: R95-101, 1994.
48. **Ruvolo PP.** Intracellular signal transduction pathways activated by ceramide and its metabolites. *Pharmacol Res* 47: 383-392, 2003.
49. **Sakamoto K and Holman GD.** Emerging role for AS160/TBC1D4 and TBC1D1 in the regulation of GLUT4 traffic. *Am J Physiol Endocrinol Metab* 295: E29-37, 2008.
50. **Samuel VT, Liu ZX, Qu X, Elder BD, Bilz S, Befroy D, Romanelli AJ, and Shulman GI.** Mechanism of hepatic insulin resistance in non-alcoholic fatty liver disease. *J Biol Chem* 279: 32345-32353, 2004.

51. **Sano H, Kane S, Sano E, Miinea CP, Asara JM, Lane WS, Garner CW, and Lienhard GE.** Insulin-stimulated phosphorylation of a Rab GTPase-activating protein regulates GLUT4 translocation. *J Biol Chem* 278: 14599-14602, 2003.
52. **Savage DB, Petersen KF, and Shulman GI.** Disordered lipid metabolism and the pathogenesis of insulin resistance. *Physiol Rev* 87: 507-520, 2007.
53. **Schweitzer GG, Arias EB, and Cartee GD.** Sustained postexercise increases in AS160 Thr642 and Ser588 phosphorylation in skeletal muscle without sustained increases in kinase phosphorylation. *J Appl Physiol* 113: 1852-1861, 2012.
54. **Sharoff CG, Hagobian TA, Malin SK, Chipkin SR, Yu H, Hirshman MF, Goodyear LJ, and Braun B.** Combining short-term metformin treatment and one bout of exercise does not increase insulin action in insulin-resistant individuals. *Am J Physiol Endocrinol Metab* 298: E815-823, 2010.
55. **Shulman GI, Samuel VT, and Petersen KF.** Lipid-induced insulin resistance: unravelling the mechanism. *Lancet* 375: 2267-2277, 2010.
56. **Sriwijitkamol A, Coletta DK, Wajcberg E, Balbontin GB, Reyna SM, Barrientes J, Eagan PA, Jenkinson CP, Cersosimo E, DeFronzo RA, Sakamoto K, and Musi N.** Effect of acute exercise on AMPK signaling in skeletal muscle of subjects with type 2 diabetes: a time-course and dose-response study. *Diabetes* 56: 836-848, 2007.
57. **Summers SA, Garza LA, Zhou H, and Birnbaum MJ.** Regulation of insulin-stimulated glucose transporter GLUT4 translocation and Akt kinase activity by ceramide. *Mol Cell Biol* 18: 5457-5464, 1998.
58. **Talmadge RJ and Roy RR.** Electrophoretic separation of rat skeletal muscle myosin heavy-chain isoforms. *J Appl Physiol* 75: 2337-2340, 1993.
59. **Tanaka S, Hayashi T, Toyoda T, Hamada T, Shimizu Y, Hirata M, Ebihara K, Masuzaki H, Hosoda K, Fushiki T, and Nakao K.** High-fat diet impairs the effects of a single bout of endurance exercise on glucose transport and insulin sensitivity in rat skeletal muscle. *Metabolism* 56: 1719-1728, 2007.
60. **Thong FS, Derave W, Kiens B, Graham TE, Urso B, Wojtaszewski JF, Hansen BF, and Richter EA.** Caffeine-induced impairment of insulin action but not insulin signaling in human skeletal muscle is reduced by exercise. *Diabetes* 51: 583-590, 2002.
61. **Thorell A, Hirshman MF, Nygren J, Jorfeldt L, Wojtaszewski JF, Dufresne SD, Horton ES, Ljungqvist O, and Goodyear LJ.** Exercise and insulin cause GLUT-4 translocation in human skeletal muscle. *Am J Physiol* 277: E733-741, 1999.
62. **Treadway JL, James DE, Burcel E, and Ruderman NB.** Effect of exercise on insulin receptor binding and kinase activity in skeletal muscle. *Am J Physiol* 256: E138-144, 1989.
63. **Treebak JT, Frosig C, Pehmoller C, Chen S, Maarbjerg SJ, Brandt N, MacKintosh C, Zierath JR, Hardie DG, Kiens B, Richter EA, Pilegaard H, and Wojtaszewski JF.** Potential role of TBC1D4 in enhanced post-exercise insulin action in human skeletal muscle. *Diabetologia* 52: 891-900, 2009.
64. **Tzivion G, Dobson M, and Ramakrishnan G.** FoxO transcription factors; Regulation by AKT and 14-3-3 proteins. *Biochim Biophys Acta* 1813: 1938-1945, 2011.
65. **Wojtaszewski JF, Hansen BF, Gade, Kiens B, Markuns JF, Goodyear LJ, and Richter EA.** Insulin signaling and insulin sensitivity after exercise in human skeletal muscle. *Diabetes* 49: 325-331, 2000.
66. **Wojtaszewski JF, Hansen BF, Kiens B, and Richter EA.** Insulin signaling in human skeletal muscle: time course and effect of exercise. *Diabetes* 46: 1775-1781, 1997.

67. **Wojtaszewski JF, Higaki Y, Hirshman MF, Michael MD, Dufresne SD, Kahn CR, and Goodyear LJ.** Exercise modulates postreceptor insulin signaling and glucose transport in muscle-specific insulin receptor knockout mice. *J Clin Invest* 104: 1257-1264, 1999.
68. **Wojtaszewski JF, Nielsen JN, and Richter EA.** Invited review: effect of acute exercise on insulin signaling and action in humans. *J Appl Physiol* 93: 384-392, 2002.
69. **Zorzano A, Balon TW, Garetto LP, Goodman MN, and Ruderman NB.** Muscle alpha-aminoisobutyric acid transport after exercise: enhanced stimulation by insulin. *Am J Physiol* 248: E546-552, 1985.

Chapter VI

Discussion

The dissertation included three independent, but related studies that aimed to further the understanding of the mechanisms regulating skeletal muscle glucose transport. This chapter of the dissertation will: 1) summarize the major goals and new results from each of the three studies, 2) provide a unified perspective of some of the key findings of the research that were included in either two or all three of the studies, 3) propose some future directions for research that are based on the results of this dissertation, and 4) offer overall conclusions.

Summary of Major Goals and Results for Studies 1 to 3

Study 1: *Clustering of GLUT4, TUG, and RUVBL2 Protein Levels Correlate with Myosin Heavy Chain Isoform Pattern in Skeletal Muscles, but AS160 and TBC1D1 Levels Do Not*

Because skeletal muscle is a heterogeneous tissue, it is important to understand differences among various muscles in addition to differences within the various fiber types found in a given muscle. Muscle fiber type (myosin heavy chain, MHC, expression) has previously been shown to be associated with differences in protein expression (17, 26, 32, 34, 39), insulin-stimulated glucose transport (16, 21), and contraction-stimulated glucose uptake (1-2, 17, 20-21) of whole muscles. Therefore, the first major goal for Study 1 was to extend the knowledge about the relationship between MHC isoform composition and the abundance of GLUT4 and four

proteins [AS160 (Akt substrate at 160 kDa), TBC1D1 (Tre-2/Bub2/Cdc 16-domain member 1), TUG (tethering protein containing a UBX domain for GLUT4) and RUVBL2 (RuvB like protein two)] that are established or potential regulators of glucose transport in rat skeletal muscle. The second major goal of Study 1 was to determine if the abundance of any of these proteins are significantly correlated with each other.

An important result of Study 1 was the identification of a cluster of three proteins (GLUT4, TUG and RUVBL2) that tracked together in the skeletal muscles that were evaluated. GLUT4, TUG and RUVBL2 were each also positively correlated with % MHC-I and inversely correlated with the % MHC-IIb levels. AS160 and TBC1D1 were positively correlated with each other, but neither of these proteins was significantly correlated with the relative levels of any of the MHC isoforms. Earlier research has clearly documented that altered neuromuscular activation of skeletal muscle can markedly alter GLUT4 protein levels (6, 11, 23, 28, 46). Training effects on TUG and RUVBL2 abundance have apparently not been assessed to date. Given that soleus (SOL) compared to extensor digitorum longus (EDL) muscles from sedentary male Wistar rats have much greater levels of motor unit activation (16), it is notable that the SOL compared to the EDL had significantly greater values for GLUT4, TUG and RUVBL2. Our working hypothesis is that TUG and RUVBL2 protein content in rat skeletal muscle are regulated by mechanisms that, at least in part, are similar to those that control GLUT4 protein abundance and that each is influenced by the level of neuromuscular activation. Although AS160 and TBC1D1 have been shown to regulate GLUT4 translocation (8, 24, 42-43), data from this study suggested that the relative abundance of AS160 and TBC1D1 may not be regulated via similar mechanisms as GLUT4, TUG and RUVBL2.

Study 2: *Myosin Heavy Chain Isoform Expression, Contraction-stimulated Glucose Uptake and Abundance of Proteins that Regulate Glucose Uptake and Metabolism in Single Skeletal Muscle Fibers*

The first major goal for Study 2 was to measure contraction-stimulated glucose uptake (independent of insulin) in single muscle fibers that had been characterized by fiber type (MHC

isoform expression), so that fiber type-related comparisons for contraction-stimulated glucose uptake was possible within the same muscle. The second major goal of Study 2 was to test if the abundance of any of the proteins that had been evaluated at the whole muscle level in Study 1 (GLUT4, TUG, AS160, TBC1D1, and RUVBL2) differed according to fiber type when evaluated at the single fiber level. The third major goal of Study 2 was to determine if there were significant correlations in the abundance of any of these proteins with each other or with several other metabolically relevant proteins (Cytochrome C oxidase IV, COX IV; glycogen phosphorylase; glyceraldehyde-3-phosphate dehydrogenase, GAPDH; and filamin C).

The most important new finding from Study 2 was that contraction-stimulated glucose uptake did not differ significantly among the five MHC-II fiber types that were studied in rat epitrochlearis muscles. It remains possible that fiber type-related differences in glucose uptake occur in MHC-II fibers with voluntary exercise *in vivo*, but such differences would likely be primarily dependent on factors other than the fibers' intrinsic capacity for contraction-stimulated glucose uptake (e.g., extent of recruitment and/or blood flow). There were several compelling fiber type-related differences in protein abundance, including differences that were expected based on earlier studies for GLUT4, TUG and COX IV (MHC-IIa > MCH-IIax > MHC-IIx > MHC-IIxb > MHC-IIb) (9, 17, 34). The substantial and unanticipated fiber type differences for filamin C abundance (MHC-IIa > MCH-IIax > MHC-IIx > MHC-IIxb > MHC-IIb) provided novel information with implications for the functional roles of this actin-binding protein. In addition, the lack of detectable RUVBL2 in any of the fiber types that were tested, and the fiber type differences for TBC1D1 (only consistently detected in MHC-IIxb and MHC-IIb fibers) have relevance for clarifying the biological functions of these proteins in different muscle fiber types. The analysis of single fibers offers unique information and opportunities, but the optimal benefits of this approach require that the single fiber results be evaluated with careful consideration of the knowledge obtained from studying both isolated skeletal muscle preparations and the intact organism.

Study 3: *Acute Exercise Effects on Insulin Signaling and Insulin-Stimulated Glucose Uptake in Isolated Skeletal Muscle from Rats Fed either Low Fat or High Fat Diet*

The first major goal for Study 3 was to measure key insulin signaling processes (including phosphorylation of Akt, pAkt; and AS160, pAS160) to test potential mechanisms for the exercise-induced improvements for insulin-stimulated glucose uptake by skeletal muscle from both insulin sensitive and insulin resistant rats. The second major goal of Study 3 was to determine if a high fat diet would induce changes in muscle fiber type composition or in the abundance of GLUT4, AS160, TBC1D1, TUG, or RUVBL2. The third major goal of Study 3 was to determine the effects of acute exercise on putative mediators of insulin resistance: lipid metabolites (acyl-CoA; diacylglycerol, DAG; ceramide), phosphorylation of the serine kinase c-Jun N-terminal (pJNK) and serine phosphorylation of insulin receptor substrate-1 (pIRS-1^{Ser})].

The most important results for Study 3 included: 1) each of the key metabolic and signaling outcomes determined for muscles IPEX (insulin-independent glucose uptake, glycogen, pAMPK^{Thr172}, pAS160^{Thr642}, and pAS160^{Ser588}) was indistinguishable in LFD versus HFD rats; 2) skeletal muscles from HFD Sedentary versus LFD Sedentary rats exhibited modest, but significant insulin resistance for glucose uptake accompanied by modest, but significant deficits in key insulin signaling steps that regulate glucose uptake (delta-insulin pAkt^{Thr308}, pAS160^{Ser588}, delta-insulin pAS160^{Thr642} and delta-insulin pAS160^{Ser588}); 3) skeletal muscles from LFD 3hPEX versus LFD Sedentary rats were characterized by substantially elevated insulin-stimulated glucose uptake concomitant with significantly increased phosphorylation of AS160 (both pAS160^{Thr642} and pAS160^{Ser588} determined for muscles incubated either with or without insulin as well as the delta-insulin for pAS160^{Ser588}) in the absence of significant exercise-induced changes in proximal insulin signaling steps; 4) skeletal muscles from HFD rats at 3hPEX had insulin-stimulated glucose uptake values that exceeded the Sedentary HFD group and were not different from Sedentary LFD group, but were significantly less than the LFD 3hPEX group; 5) the improvement in insulin-stimulated glucose uptake of muscles from HFD rats at 3hPEX was accompanied by elimination of the diet-induced deficit in pAS160^{Ser588}, but neither pAS160^{Ser588} nor pAS160^{Thr642} of the HFD 3hPEX group attained values as great as the LFD 3hPEX group; 6) the improved insulin-stimulated glucose uptake in muscle may also be associated with the exercised induce reduction in acyl-CoA 16:0; and 7) the improved insulin-stimulated glucose uptake by muscles from both LFD and HFD rats at 3hPEX were not accompanied by significant reductions in a number of possible mediators of muscle insulin resistance, including DAG and ceramides concentrations, pIRS1^{Ser307}, pIRS1^{Ser1101}, and

pJNK^{Ser73} (and within Sedentary groups none of these possible mediators of insulin resistance differed between the diet groups).

The reproducible relationship between pAS160 and post-exercise insulin-stimulated glucose uptake in this study and in earlier research (3, 13-14, 45) along with the crucial role of pAS160 for insulin-stimulated glucose transport have led to our working hypothesis that enhanced pAS160 is important for the improved insulin-stimulated glucose uptake after acute exercise in both normal and insulin resistant muscle. We further hypothesize that the failure of the HFD 3hPEX group to achieve insulin-mediated glucose uptake equal to the LFD 3hPEX group is linked to a lesser exercise-effect on pAS160 in the muscles from the HFD rats.

A Unified Perspective of Some of the Key Outcomes from Studies 1 to 3

Prior to Study 1, a common viewpoint was that GLUT4 protein abundance was greater in muscles that were enriched with MHC-I and MHC-IIa fibers versus muscles enriched with MHC-IIb fibers. However, this interpretation was based on studies using a limited number of muscles, and these earlier studies did not fiber type the muscles themselves and/or used subjective fiber typing methods that did not allow for the identification of all four MHC isoforms that are expressed in rat skeletal muscle (17, 34). Study 1 is the most comprehensive study of the relationship between GLUT4 abundance and fiber type in rat skeletal muscle. Results from Study 2 revealed that in single muscle fibers there was a fiber type-dependent relationship for GLUT4 abundance that was consistent with the fiber type-dependent relationship found in whole muscle results from Study 1. It was previously suggested that the capacity for contraction-stimulated glucose uptake by skeletal muscle was dependent on the total abundance of GLUT4, and that both glucose uptake capacity and GLUT4 were related to fiber type (17). However, in single fibers characterized by fiber type, despite ~4-fold range in GLUT4 abundance, contraction-stimulated glucose uptake was not different among the fiber types. Additionally, results from Study 3 indicated that skeletal muscle insulin resistance associated with two weeks of high fat feeding was not due to reduced GLUT4 abundance. Previously published research along with the current study using the isolated single muscle fibers from the epitrochlearis have shown: 1) insulin-stimulated glucose uptake was greater in MHC-IIa versus MHC-IIb fibers (33); 2) AICAR stimulated glucose uptake was greater in MHC-IIb versus MHC-IIa fibers (33); and 3) contraction-stimulated glucose uptake did not track with GLUT4 abundance. Therefore,

these data suggest that the capacity for glucose transport in response to various stimuli is stimulus-specific rather than being uniformly dependent on GLUT4 abundance. The fiber type capacity for contraction-stimulated glucose uptake seems likely to be related to the contraction-specific mechanisms that regulate GLUT4 translocation. Earlier studies in muscle tissue provided evidence for distinct "pools" of GLUT4 in skeletal muscle that selectively respond to different stimuli (i.e. contraction regulated GLUT4 pools and insulin regulated GLUT4 pools) (36-37). It may be that size and/or regulation of the contraction-regulated GLUT4 pool is similar among fiber types (accounting for the lack of a difference for contraction-stimulated glucose uptake among fibers), but the size and/or regulation of the insulin-regulated GLUT4 pool varies among fiber types (accounting for the difference for insulin-stimulated glucose uptake among fibers). However, this hypothesis is speculative, and further research is necessary to verify this possibility.

Prior to the studies included in this dissertation, most of the knowledge of TUG was based on results in adipocytes. This dissertation provided novel information regarding the abundance of TUG in skeletal muscle. These studies were the first to show that: 1) the abundance to TUG tracks with fiber type at both the whole muscle and single fiber level; 2) the abundance of TUG versus GLUT4 are highly correlated at the whole muscle and single fiber level; and 3) the abundance of GLUT4 or TUG was not altered by two weeks of a HFD. These findings, together with previously published data suggesting that GLUT4 and TUG physically associate with each other in skeletal muscle (44), are consistent with the idea that TUG may influence GLUT4 localization in muscle. Furthermore, the positive relationship between the protein abundance of TUG and GLUT4 suggests that their abundance may be regulated by similar mechanisms. Data from fat cells has indicated that reducing the abundance of TUG via shRNA knockdown also resulted in reduced GLUT4 abundance (56). It would be interesting to determine if in skeletal muscle interventions that alter GLUT4 abundance (e.g., physiologic interventions: exercise training, denervation, etc.; or genetic interventions: GLUT4 overexpression or knockdown) have similar effects on TUG abundance and vice-versa. Because TUG was discovered using a screen intended to identify insulin responsive proteins that physically associate with GLUT4 (4), it was not entirely surprising that in adipocytes the association between TUG and GLUT4 was shown to be is reduced in response to insulin allowing for GLUT4 translocation. However, it is not known if contraction also disrupts the

TUG-GLUT4 association. If in skeletal muscle, the TUG-GLUT4 association is only regulated by insulin and not regulated by contraction, this would provide useful insight that may account for the lack of a relationship between GLUT4 and contraction-stimulated glucose uptake by single muscle fibers. In other words, a highly speculative idea is that there may be specific TUG isoforms or "TUG-like" proteins that restrain GLUT4 to intracellular sites, and that are only responsive to specific stimuli (i.e., contraction or insulin), and the function of contraction-responsive "TUG-like" proteins may not vary among type II fiber types.

Data from earlier studies using fats cells suggested that the relative abundance of RUVBL2 was associated with the level of insulin-stimulated glucose uptake and pAS160 (55). However, prior to the research in this dissertation, little was known regarding RUVBL2 abundance in skeletal muscle. Results from Study 1 suggested that the relative abundance of RUVBL2 may be related to skeletal muscle fiber type, and RUVBL2's abundance was found to be highly correlated with GLUT4 and TUG. However, RUVBL2 abundance did not correlate with abundance of AS160, its putative binding partner, in skeletal muscle. Interestingly in Study 2, RUVLB2 was not detected in any of the single muscle fibers that were analyzed by immunoblotting. In Study 3, epitrochlearis muscles from insulin resistant rats did not have altered RUVBL2 abundance despite having reduced insulin-stimulated glucose uptake and pAS160. Previous studies using fat cells suggested that reductions in RUVBL2 protein abundance were associated with insulin resistance via reduced AS160 phosphorylation (55). The lack of detectable RUVBL2 in single skeletal muscle cells and the lack of a change in RUVBL2 abundance in insulin resistant muscle raise the possibility that the reported relationship of RUVBL2 abundance and insulin resistance in fat cells may not apply to skeletal muscle under conditions of mild insulin resistance. Therefore, RUVBL2 seems to be an unlikely candidate to influence the observed skeletal muscle insulin resistance following high fat diet or improved insulin-stimulated glucose uptake after exercise in either insulin sensitive or insulin resistant rats.

Prior to this dissertation, the relationship between AS160 abundance and fiber type in rat skeletal muscle had not been studied. Additionally, although numerous studies have investigated the role of pAS160 in the improved skeletal muscle insulin sensitivity following acute exercise in insulin sensitive muscle, the role of pAS160 in exercise effects on glucose uptake had not been examined in insulin resistant muscles. AS160 protein abundance was found to not significantly

differ among 12 muscles or regions of muscles of widely varying fiber type, and this lack of a fiber type difference was confirmed at the cellular level. Thus, these data suggest that the total abundance of AS160 may not be a major determining factor for glucose transport in rat skeletal muscle. This interpretation is supported by the previous observations that insulin-stimulated glucose uptake is much greater for single MHC-IIA versus single MHC-IIB fibers (33), ~8-fold overexpression of AS160 in mouse skeletal muscle did not alter insulin-stimulated glucose uptake (31), diabetic rats have impaired insulin-mediated increases in pAS160 without changes in AS160 abundance (7, 10), pAS160 was reduced without differences in AS160 abundance in skeletal muscle of insulin resistant humans (50), and diabetic humans have normal total AS160 expression but reduced insulin-stimulated pAS160 (25). There are two studies that have investigated effect of whole body deletion of AS160 in mice (7, 54). AS160 knockouts had whole body insulin resistance. However, in isolated skeletal muscle from AS160 deficient mice, the soleus had reduced insulin-stimulated glucose uptake, but insulin-stimulated glucose uptake by the EDL was normal. To interpret these results, it is important to recognize that unlike rat skeletal muscle, in mouse skeletal muscle AS160 abundance is ~10-fold greater in the soleus versus the EDL (49). Therefore, deletion of AS160 in a skeletal muscle in which AS160 is highly abundant, such as the soleus, may have a greater effect on insulin-mediated glucose transport compared with muscles in which AS160 is in low abundance, such as the EDL. It should also be noted that the deletion of AS160 in the soleus also resulted in a significant reduction in GLUT4 (GLUT4 abundance was not altered by AS160 deletion in the EDL). Therefore, the reduced insulin-stimulated glucose uptake by the soleus is likely to be at least partly due to differences in GLUT4. The explanation for the lack of a close relationship between AS160 abundance and glucose uptake in studies from rats (7, 10) and humans (25) is uncertain. However, AS160 is a Rab GAP protein, Rab GAPs can have multiple cellular functions (18-19), and it is possible that only a portion of the AS160 expressed in a muscle cell is functionally relevant for regulating glucose transport. Regardless, the level of insulin-stimulated pAS160 does seem to be related to the level of insulin-stimulated glucose transport. For muscles from HFD Sedentary versus LFD Sedentary rats, both insulin-stimulated glucose uptake and pAS160 were reduced. For muscles from both LFD 3hPEX and HFD 3hPEX rats, both insulin-stimulated glucose and pAS160 were increased compared to their respective sedentary controls. For HFD 3hPEX versus LFD 3hPEX muscles, both insulin-stimulated glucose uptake and pAS160 were

not elevated to the same level. Although the mechanisms remains unknown, these findings support the idea that the level of pAS160 consistently tracks with skeletal muscle insulin sensitivity following acute exercise. It is unclear why HFD feeding resulted in a blunted exercise response to insulin for pAS160, but these data suggest that mechanisms for improved skeletal muscle insulin sensitivity following acute exercise are not identical for insulin sensitive versus insulin resistant rats.

Similar to AS160, the relationship between muscle fiber type and TBC1D1 abundance had not been studied in rat skeletal muscle prior to this dissertation. In contrast to earlier data from mice (49), there was not an inverse relationship for the relative abundance of TBC1D1 versus AS160, the differences in TBC1D1 protein abundance among various muscles or regions of muscles were much smaller in rats (2.7-fold range among 12 rat muscles evaluated in Study 2) compared to the earlier study (49) in mice (10-fold range among 3 mouse muscles), and TBC1D1 abundance was not related to fiber type in rat muscles. Unexpectedly, TBC1D1 was only consistently detectable in MHC-IIxb and MHC-IIb fibers (i.e., TBC1D1 was not consistently detected in MHC-IIa, MHC-IIax, or MHC-IIx fibers). It is possible that TBC1D1 is important for regulating contraction-stimulated glucose uptake in MHC-IIxb and MHC-IIb fibers and less important in MHC-IIa, MHC-IIax, or MHC-IIx fibers. However, further analysis is necessary before this conclusion could be made. It is also possible that the abundance of TBC1D1 in MHC-IIa, MHC-IIax, and MHC-IIx fibers may fall just below the detectable range, and a small amount of TBC1D1 may be sufficient for it to be functionally significant. It would be interesting to determine if pooling multiple fibers in which TBC1D1 was not detectable, such as MHC-IIa fibers, would allow for TBC1D1 to be detected. If this approach was successful, then estimations could be made between the relative abundance of TBC1D1 in MHC-IIa, MHC-IIax, and MHC-IIx fibers with MHC-IIxb and MHC-IIb fibers.

A common theme throughout this dissertation was the exploration of the functional importance of skeletal muscle fiber type. Fiber typing was performed by the identification of MHC isoform expression. However, there are various methods for determining fiber type (i.e., visual inspection to determine the “redness” or “whiteness” of a muscle, histochemical staining, contractile properties, etc.). Fiber typing by MHC isoform expression was selected because it can be used for single fibers, it is an objective measurement of a functionally relevant protein, it

is reproducible and it has been described as the gold standard for determining fiber type (5). Therefore, it is important to note that fiber type was used as a means to categorize both whole muscles and single muscle fibers, so it is possible to compare results from whole muscle with results from single fibers. Single fiber analysis for Study 2 reinforced findings from whole muscle analysis performed in Study 1 (i.e., GLUT4 and TUG abundance tracks with fiber type and AS160 abundance was not related to fiber type). However, Study 2 also revealed many interesting findings that could only be identified by single fiber analysis: 1) contraction-stimulated glucose uptake did not differ among fiber types; 2) TBC1D1 was only consistently detectable in MHC-IIxb and MHC-IIb fibers; 3) RUVBL2 was readily detected in muscle tissue, but not detectable in single type II muscle fibers (likely more highly expressed in other cell types within muscle); and 4) the epitrochlearis has a large proportion (~61%) of hybrid fibers. Although data from Study 2 provided novel information, these results only allow for interpretations based on total protein abundance in relation to fiber type because the current method does not allow phosphorylation measurements to be made (i.e., the isolation of single fibers appears to influence the phosphorylation status of fibers; unpublished results). Other approaches (e.g., immunohistochemistry), will be needed to evaluate protein phosphorylation at the level of single fibers. Finally, several caveats for the single fiber results should be acknowledged, including that type I (slow-twitch) fibers were not evaluated because they were not isolated by the collagenase method, and it remains to be established if the single fiber results for the epitrochlearis are generalizable to single fibers in other muscles.

Determination of total protein abundance is important, but protein function is also influenced by many other factors. Protein abundance is certainly not the only determinant of AS160 function. For Studies 1, 2 and 3 AS160 total abundance did not differ among 12 different muscles of varying fiber type, did not differ among 5 different fibers types in muscle cells, and did not differ in response to HFD, acute exercise, or insulin. However, Study 3 emphasized the role of pAS160 and showed the degree by which pAS160 tracked with glucose uptake. This was evident by the results showing that insulin-simulated glucose uptake by skeletal muscle and the level of pAS160 followed the same stepwise relationship: HFD SED < HFD 3hPEX = LFD SED < LFD 3hPEX. Although these results for pAS160 and insulin-stimulated glucose uptake coincide with previous findings (3, 7, 10, 13-14, 25, 45), it should be noted that additional post-translational modifications may play a role in the regulation of AS160 and glucose uptake. For

example, it was recently shown that TBC1D3 (a paralog of AS160) localization with the plasma membrane was associated with greater palmitoylation (27). It is not known if AS160 is regulated by palmitoylation, but an interesting result from Study 3 indicated that there was a trend for elevated palmitoyl-CoA in muscles from HFD fed rats (possibly associated with the muscle insulin resistance), and following acute exercise there was a main effect of exercise (3hPEX < Sedentary) for the level of palmitoyl-CoA, with HFD 3hPEX muscles having significantly reduced palmitoyl-CoA. Similar to TBC1D3, localization of AS160 may also be influenced by palmitoylation. However, this theory has not yet been tested. Additionally, it cannot be ruled out that AS160 localization and/or activity may be regulated by other post-translational modifications (e.g., methylation, acetylation, etc.), protein-protein interactions [e.g., binding to 14-3-3 proteins (15, 38)], or allosteric interactions with small molecules. Further research is necessary to investigate these and other possibilities to fully understand the role of AS160 in regulating glucose transport.

Future Directions

The combined findings from Studies 1, 2 and 3 have provided valuable insight for future directions for understanding skeletal muscle glucose transport. Because skeletal muscle accounts for the greatest proportion of insulin-stimulated glucose transport and the prevalence of obesity associated insulin resistance and diabetes continues to rise, future studies focusing on understanding the mechanism for improved skeletal muscle insulin sensitivity after acute exercise are of primary importance.

Studies have shown that glucose uptake by rat skeletal muscle tissue in response to a physiologic insulin dose is greater in muscles or regions of muscles rich in oxidative fibers (enriched with MHC-I and IIa fibers) compared with muscles or regions of muscles rich in glycolytic fibers (enriched with MHC-IIb and IIx fibers) (12, 22, 29-30, 40-41). It seems possible that alterations in muscle glucose uptake with various interventions (e.g., exercise or diet) may differ according to fiber type. Studies using hyperinsulinemic-euglycemic clamp with a physiologic insulin dose following HFD feeding indicate that muscles or muscle regions with a large percentage of oxidative fibers were more susceptible to the reduced insulin-stimulated glucose uptake (25% to 45% decrease with HFD) (29-30, 48). However, muscles or regions of muscles with a high percentage of glycolytic fibers appeared to be less susceptible to the diet-

induced reductions in insulin-stimulated glucose uptake (0% to 25% decrease with HFD). Following acute exercise by insulin sensitive rats, apparently only the classic study by Richter et al. (41) has reported insulin-stimulated glucose uptake in different muscles or regions of muscles of varying fiber type. Exercised versus sedentary controls had approximately a two-fold increase in insulin-stimulated glucose uptake in the perfused hindlimb with a physiologic insulin dose with large and significant increases in insulin-stimulated glucose uptake in the red gastrocnemius (rich in MHC-I and MHC-IIa fibers). In contrast, the white gastrocnemius (rich in MHC-IIb and MHC-IIx fibers) from exercise versus sedentary rats had a non-significant trend for increased insulin-stimulated glucose uptake, and no evidence for an exercise-induced increase in insulin-stimulated glucose uptake in the soleus (rich in MHC-I fibers). Apparently, only Oakes et al. have reported insulin-stimulated glucose uptake using a physiologic insulin dose in different muscles or regions of muscles of varying fiber type following a single exercise bout by rats fed a HFD (35). Prior exercise significantly improved insulin-stimulated glucose uptake in both the red quadriceps (rich in MHC-I and MHC-IIa fibers) and white quadriceps (rich in MHC-IIb and MHC-IIx fibers), contrary to findings from healthy LFD fed rats (41). Additionally, the relative increase after exercise in insulin-stimulated glucose uptake was greater in the muscle region with a higher percentage of glycolytic fibers versus the muscle region with a higher percentage of oxidative fibers. Taking together the data from Richter et. al. (41) for insulin sensitive rats and Oakes et al. (35), for rats fed a HFD the exercised-induced improvements in insulin-stimulated uptake may differ based on both diet and muscle fiber type. However, comparisons of data from two different research groups using different exercise protocols, different methods for measuring glucose uptake and different muscles (gastrocnemius versus quadriceps) should be made with caution. Therefore, it would be informative for these comparisons between rats fed LFD versus HFD to be made utilizing the same exercise protocol, with identical methods for measuring glucose uptake by single fibers with differing fiber types from the epitrochlearis. For Study 3, two weeks of high fat feeding was sufficient to induce mild insulin resistance in isolated skeletal muscle. Also, a single session of exercise improved insulin-stimulated glucose uptake in epitrochlearis muscles from both HFD and LFD fed rats, but the muscles from HFD 3hPEX versus LFD 3hPEX rats did not attain equal levels of insulin-stimulated glucose uptake. One hypotheses is that the mild insulin resistance in the epitrochlearis muscles from HFD fed rats was due to a greater degree of insulin resistance in the oxidative fibers (e.g., MHC-IIa) versus

glycolytic fibers (e.g., MHC-IIb), and following acute exercise the more insulin resistant fibers had an impaired exercise response. In order to test this hypothesis it would be ideal to utilize the single fiber method from Study 2, to measure the effects of acute exercise on insulin-stimulated glucose uptake in single muscle fibers from epitrochlearis isolated from LFD and HFD fed rats that either remained sedentary or performed a single session of exercise.

Prior to Study 3, AS160 was the only direct Akt substrate that had been identified to have increased phosphorylation in skeletal muscle in the hours following acute exercise. As a result, exercised induced improvements for skeletal muscle insulin-stimulated glucose uptake and the associated increase in AS160 phosphorylation have been extensively studied (3, 13-14, 45, 47, 51). However, the mechanism that allows for the greater insulin-stimulated AS160 phosphorylation in muscle following acute exercise remains unknown. In Study 3, FoxO1 and PRAS40 were identified as additional proteins that are also direct Akt substrates that have increased phosphorylation with insulin-treatment several hours after a single session of exercise. Therefore, it seems logical to investigate additional similarities among AS160, FoxO1 and PRAS40 to elucidate the possible mechanisms that account for the improved skeletal muscle insulin sensitivity following acute exercise. The most obvious candidate for the greater insulin-stimulated phosphorylation of these three proteins would be changes in the balance between activity for their kinases and/or phosphatases. For insulin sensitive models, Akt does not have greater activity following acute exercise, which is the primary insulin regulated kinase for AS160, FoxO1 (52) and PRAS40 (53). Other known AS160 kinases, such as AMPK (AMPK acitvatied protein kinase), RSK (ribosomal S6 kinase) and SGK1 (Serine/threonine-protein kinase) have also been shown to not have increased insulin-stimulated phosphorylation hours after a single exercise bout (45). Following exercise, it is possible that AS160, FoxO1 and PRAS40 localize to a similar intracellular region that increases their susceptibility for phosphorylation and/or reduces their susceptibility for dephosphorylation. One key characteristic of FoxO1 is that following phosphorylation by Akt, FoxO1 translocates from the nucleus to the cytosol. However, it is not known if exercise results in greater FoxO1 translocation from the nucleus to the cytosol, possibly making FoxO1 more susceptible to phosphorylation by Akt in response to insulin. Therefore, a reasonable starting point would be to determine via immunohistochemistry if the cellular localization for AS160, FoxO1 and PRAS40 in skeletal muscle is altered during the hours following acute exercise. If the results did in fact

show that exercise leads to the redistribution of AS160, FoxO1, and PRAS40, it would then be interesting to perform follow-up studies to identify the causes for this redistribution.

Overall Conclusions

Factors that influence skeletal muscle glucose uptake were the focus of this project because skeletal muscle plays a major role in the regulation of whole body glucose homeostasis. Isolated skeletal muscle was studied to analyze the intrinsic properties of muscle with respect to insulin-independent glucose uptake in response to *ex vivo* contraction, and insulin-dependent glucose uptake by muscle from insulin sensitive and insulin resistant rats following acute exercise. The most important functional results from these studies were: 1) contraction-stimulated glucose uptake did not differ among MHC-II fibers isolated from the rat epitrochlearis; and 2) improved insulin-stimulated glucose uptake by insulin resistant muscles following acute exercise was associated with greater pAS160. Data from Studies 1 and 2 further confirmed the relationship between fiber type and GLUT4 abundance, showing that the GLUT4 expression pattern for single muscle fibers was consistent with whole muscle analysis. Therefore, a reasonable hypothesis would have been that the capacity for contraction-stimulated glucose uptake by single muscle fibers would track with the relative abundance of GLUT4 within a given fiber type. However, contraction-stimulated glucose uptake was not different among any of the fiber types measured. Therefore, it appears that the capacity of contraction-stimulated glucose uptake is not determined by GLUT4 abundance, and further research is needed to identify the factors that determine contraction-stimulated glucose uptake. For Study 3, insulin resistant muscles were found to have improved insulin-mediated glucose uptake following acute exercise and was associated with increased pAS160. Additionally, it appeared that the improved insulin-stimulated pAS160 following acute exercise by insulin sensitive and insulin resistant rats occurred via different mechanisms. Short-term high fat feeding was not only sufficient to induce skeletal muscle insulin resistance, but it was also sufficient to alter the exercised induced improvements for insulin-stimulated glucose uptake by muscle. In conclusion, this dissertation provided novel information regarding the effects of *ex vivo* contraction and *in vivo* exercise on glucose uptake by skeletal muscle. These results lay the

foundation for future experiments to fully understand the mechanisms that regulate skeletal muscle glucose transport.

References

1. **Ai H, Ihlemann J, Hellsten Y, Lauritzen HP, Hardie DG, Galbo H, and Ploug T.** Effect of fiber type and nutritional state on AICAR- and contraction-stimulated glucose transport in rat muscle. *Am J Physiol Endocrinol Metab* 282: E1291-1300, 2002.
2. **Ai H, Ralston E, Lauritzen HP, Galbo H, and Ploug T.** Disruption of microtubules in rat skeletal muscle does not inhibit insulin- or contraction-stimulated glucose transport. *Am J Physiol Endocrinol Metab* 285: E836-844, 2003.
3. **Arias EB, Kim J, Funai K, and Cartee GD.** Prior exercise increases phosphorylation of Akt substrate of 160 kDa (AS160) in rat skeletal muscle. *Am J Physiol Endocrinol Metab* 292: E1191-1200, 2007.
4. **Bogan JS, Hendon N, McKee AE, Tsao TS, and Lodish HF.** Functional cloning of TUG as a regulator of GLUT4 glucose transporter trafficking. *Nature* 425: 727-733, 2003.
5. **Booth FW, Laye MJ, and Spangenburg EE.** Gold standards for scientists who are conducting animal-based exercise studies. *J Appl Physiol* 108: 219-221, 2010.
6. **Brozinick JT, Jr., Etgen GJ, Jr., Yaspelkis BB, 3rd, Kang HY, and Ivy JL.** Effects of exercise training on muscle GLUT-4 protein content and translocation in obese Zucker rats. *Am J Physiol* 265: E419-427, 1993.
7. **Cao S, Li B, Yi X, Chang B, Zhu B, Lian Z, Zhang Z, Zhao G, Liu H, and Zhang H.** Effects of exercise on AMPK signaling and downstream components to PI3K in rat with type 2 diabetes. *PLoS One* 7: e51709, 2012.
8. **Cartee GD and Funai K.** Exercise and Insulin: Convergence or Divergence at AS160 and TBC1D1? *Exercise and Sport Sciences Reviews* 37: 188-195, 2009.
9. **Castorena CM, Mackrell JG, Bogan JS, Kanzaki M, and Cartee GD.** Clustering of GLUT4, TUG and RUVBL2 Protein Levels Correlate with Myosin Heavy Chain Isoform Pattern in Skeletal Muscles, but AS160 and TBC1D1 Levels Do Not. *J Appl Physiol*, 2011.
10. **Chen YC, Lee SD, Kuo CH, and Ho LT.** The effects of altitude training on the AMPK-related glucose transport pathway in the red skeletal muscle of both lean and obese Zucker rats. *High Alt Med Biol* 12: 371-378, 2011.
11. **Daugaard JR and Richter EA.** Relationship between muscle fibre composition, glucose transporter protein 4 and exercise training: possible consequences in non-insulin-dependent diabetes mellitus. *Acta Physiol Scand* 171: 267-276, 2001.
12. **Delp MD and Duan C.** Composition and size of type I, IIA, IID/X, and IIB fibers and citrate synthase activity of rat muscle. *J Appl Physiol* 80: 261-270, 1996.
13. **Funai K, Schweitzer GG, Castorena CM, Kanzaki M, and Cartee GD.** In vivo exercise followed by in vitro contraction additively elevates subsequent insulin-stimulated glucose transport by rat skeletal muscle. *Am J Physiol Endocrinol Metab* 298: E999-1010, 2010.
14. **Funai K, Schweitzer GG, Sharma N, Kanzaki M, and Cartee GD.** Increased AS160 phosphorylation, but not TBC1D1 phosphorylation, with increased postexercise insulin sensitivity in rat skeletal muscle. *Am J Physiol Endocrinol Metab* 297: E242-251, 2009.

15. **Geraghty KM, Chen S, Harthill JE, Ibrahim AF, Toth R, Morrice NA, Vandermoere F, Moorhead GB, Hardie DG, and MacKintosh C.** Regulation of multisite phosphorylation and 14-3-3 binding of AS160 in response to IGF-1, EGF, PMA and AICAR. *Biochem J* 407: 231-241, 2007.
16. **Hennig R and Lomo T.** Firing patterns of motor units in normal rats. *Nature* 314: 164-166, 1985.
17. **Henriksen EJ, Bourey RE, Rodnick KJ, Koranyi L, Permutt MA, and Holloszy JO.** Glucose transporter protein content and glucose transport capacity in rat skeletal muscles. *Am J Physiol* 259: E593-598, 1990.
18. **Horgan CP and McCaffrey MW.** Rab GTPases and microtubule motors. *Biochem Soc Trans* 39: 1202-1206, 2011.
19. **Hutagalung AH and Novick PJ.** Role of Rab GTPases in membrane traffic and cell physiology. *Physiol Rev* 91: 119-149, 2011.
20. **Ihlemann J, Ploug T, and Galbo H.** Effect of force development on contraction induced glucose transport in fast twitch rat muscle. *Acta Physiol Scand* 171: 439-444, 2001.
21. **Ihlemann J, Ploug T, Hellsten Y, and Galbo H.** Effect of stimulation frequency on contraction-induced glucose transport in rat skeletal muscle. *Am J Physiol Endocrinol Metab* 279: E862-867, 2000.
22. **James DE, Jenkins AB, and Kraegen EW.** Heterogeneity of insulin action in individual muscles in vivo: euglycemic clamp studies in rats. *Am J Physiol* 248: E567-574, 1985.
23. **Johannsson E, McCullagh KJ, Han XX, Fernando PK, Jensen J, Dahl HA, and Bonen A.** Effect of overexpressing GLUT-1 and GLUT-4 on insulin- and contraction-stimulated glucose transport in muscle. *Am J Physiol* 271: E547-555, 1996.
24. **Kane S, Sano H, Liu SC, Asara JM, Lane WS, Garner CC, and Lienhard GE.** A method to identify serine kinase substrates. Akt phosphorylates a novel adipocyte protein with a Rab GTPase-activating protein (GAP) domain. *J Biol Chem* 277: 22115-22118, 2002.
25. **Karlsson HK, Zierath JR, Kane S, Krook A, Lienhard GE, and Wallberg-Henriksson H.** Insulin-Stimulated Phosphorylation of the Akt Substrate AS160 Is Impaired in Skeletal Muscle of Type 2 Diabetic Subjects. *Diabetes* 54: 1692-1697, 2005.
26. **Kern M, Wells JA, Stephens JM, Elton CW, Friedman JE, Tapscott EB, Pekala PH, and Dohm GL.** Insulin responsiveness in skeletal muscle is determined by glucose transporter (Glut4) protein level. *Biochem J* 270: 397-400, 1990.
27. **Kong C, Lange JJ, Samovski D, Su X, Liu J, Sundaresan S, and Stahl PD.** Ubiquitination and degradation of the hominoid-specific oncoprotein TBC1D3 is regulated by protein palmitoylation. *Biochem Biophys Res Commun* 434: 388-393, 2013.
28. **Kong X, Manchester J, Salmons S, and Lawrence JC, Jr.** Glucose transporters in single skeletal muscle fibers. Relationship to hexokinase and regulation by contractile activity. *J Biol Chem* 269: 12963-12967, 1994.
29. **Kraegen EW, James DE, Storlien LH, Burleigh KM, and Chisholm DJ.** In vivo insulin resistance in individual peripheral tissues of the high fat fed rat: assessment by euglycaemic clamp plus deoxyglucose administration. *Diabetologia* 29: 192-198, 1986.
30. **Kraegen EW, Storlien LH, Jenkins AB, and James DE.** Chronic exercise compensates for insulin resistance induced by a high-fat diet in rats. *Am J Physiol* 256: E242-249, 1989.
31. **Kramer HF, Witczak CA, Taylor EB, Fujii N, Hirshman MF, and Goodyear LJ.** AS160 regulates insulin- and contraction-stimulated glucose uptake in mouse skeletal muscle. *J Biol Chem* 281: 31478-31485, 2006.

32. **Mackrell JG, Arias EB, and Cartee GD.** Fiber type-specific differences in glucose uptake by single fibers from skeletal muscles of 9- and 25-month-old rats. *J Gerontol A Biol Sci Med Sci* 67: 1286-1294, 2012.
33. **MacKrell JG and Cartee GD.** A Novel Method to Measure Glucose Uptake and Myosin Heavy Chain Isoform Expression of Single Fibers from Rat Skeletal Muscle. *Diabetes* In Press: Accepted January, 2012.
34. **Megeney LA, Neufer PD, Dohm GL, Tan MH, Blewett CA, Elder GC, and Bonen A.** Effects of muscle activity and fiber composition on glucose transport and GLUT-4. *Am J Physiol* 264: E583-593, 1993.
35. **Oakes ND, Bell KS, Furler SM, Camilleri S, Saha AK, Ruderman NB, Chisholm DJ, and Kraegen EW.** Diet-induced muscle insulin resistance in rats is ameliorated by acute dietary lipid withdrawal or a single bout of exercise: parallel relationship between insulin stimulation of glucose uptake and suppression of long-chain fatty acyl-CoA. *Diabetes* 46: 2022-2028, 1997.
36. **Ploug T and Ralston E.** Exploring the whereabouts of GLUT4 in skeletal muscle (review). *Mol Membr Biol* 19: 39-49, 2002.
37. **Ploug T, van Deurs B, Ai H, Cushman SW, and Ralston E.** Analysis of GLUT4 distribution in whole skeletal muscle fibers: identification of distinct storage compartments that are recruited by insulin and muscle contractions. *J Cell Biol* 142: 1429-1446, 1998.
38. **Ramm G, Larance M, Guilhaus M, and James DE.** A role for 14-3-3 in insulin-stimulated GLUT4 translocation through its interaction with the RabGAP AS160. *J Biol Chem* 281: 29174-29180, 2006.
39. **Richardson JM, Balon TW, Treadway JL, and Pessin JE.** Differential regulation of glucose transporter activity and expression in red and white skeletal muscle. *J Biol Chem* 266: 12690-12694, 1991.
40. **Richter EA, Garetto LP, Goodman MN, and Ruderman NB.** Enhanced muscle glucose metabolism after exercise: modulation by local factors. *Am J Physiol Endocrinol Metab* 246: E476-482, 1984.
41. **Richter EA, Garetto LP, Goodman MN, and Ruderman NB.** Muscle glucose metabolism following exercise in the rat: increased sensitivity to insulin. *J Clin Invest* 69: 785-793, 1982.
42. **Sakamoto K and Holman GD.** Emerging role for AS160/TBC1D4 and TBC1D1 in the regulation of GLUT4 traffic. *Am J Physiol Endocrinol Metab* 295: E29-37, 2008.
43. **Sano H, Kane S, Sano E, Miinea CP, Asara JM, Lane WS, Garner CW, and Lienhard GE.** Insulin-stimulated phosphorylation of a Rab GTPase-activating protein regulates GLUT4 translocation. *J Biol Chem* 278: 14599-14602, 2003.
44. **Schertzer JD, Antonescu CN, Bilan PJ, Jain S, Huang X, Liu Z, Bonen A, and Klip A.** A transgenic mouse model to study glucose transporter 4myc regulation in skeletal muscle. *Endocrinology* 150: 1935-1940, 2009.
45. **Schweitzer GG, Arias EB, and Cartee GD.** Sustained postexercise increases in AS160 Thr642 and Ser588 phosphorylation in skeletal muscle without sustained increases in kinase phosphorylation. *J Appl Physiol* 113: 1852-1861, 2012.
46. **Slentz CA, Gulve EA, Rodnick KJ, Henriksen EJ, Youn JH, and Holloszy JO.** Glucose transporters and maximal transport are increased in endurance-trained rat soleus. *J Appl Physiol* 73: 486-492, 1992.
47. **Sriwijitkamol A, Coletta DK, Wajcberg E, Balbontin GB, Reyna SM, Barrientes J, Eagan PA, Jenkinson CP, Cersosimo E, DeFronzo RA, Sakamoto K, and Musi N.** Effect of

acute exercise on AMPK signaling in skeletal muscle of subjects with type 2 diabetes: a time-course and dose-response study. *Diabetes* 56: 836-848, 2007.
48. **Storlien LH, James DE, Burleigh KM, Chisholm DJ, and Kraegen EW.** Fat feeding causes widespread in vivo insulin resistance, decreased energy expenditure, and obesity in rats. *Am J Physiol* 251: E576-583, 1986.
49. **Taylor EB, An D, Kramer HF, Yu H, Fujii NL, Roeckl KS, Bowles N, Hirshman MF, Xie J, Feener EP, and Goodyear LJ.** Discovery of TBC1D1 as an insulin-, AICAR-, and contraction-stimulated signaling nexus in mouse skeletal muscle. *J Biol Chem* 283: 9787-9796, 2008.
50. **Tonks KT, Ng Y, Miller S, Coster AC, Samocha-Bonet D, Iseli TJ, Xu A, Patrick E, Yang JY, Junutula JR, Modrusan Z, Kolumam G, Stockli J, Chisholm DJ, James DE, and Greenfield JR.** Impaired Akt phosphorylation in insulin-resistant human muscle is accompanied by selective and heterogeneous downstream defects. *Diabetologia* 56: 875-885, 2013.
51. **Treebak JT, Frosig C, Pehmoller C, Chen S, Maarbjerg SJ, Brandt N, MacKintosh C, Zierath JR, Hardie DG, Kiens B, Richter EA, Pilegaard H, and Wojtaszewski JF.** Potential role of TBC1D4 in enhanced post-exercise insulin action in human skeletal muscle. *Diabetologia* 52: 891-900, 2009.
52. **Tzivion G, Dobson M, and Ramakrishnan G.** FoxO transcription factors; Regulation by AKT and 14-3-3 proteins. *Biochim Biophys Acta* 1813: 1938-1945, 2011.
53. **Wang H, Zhang Q, Wen Q, Zheng Y, Lazarovici P, Jiang H, Lin J, and Zheng W.** Proline-rich Akt substrate of 40kDa (PRAS40): a novel downstream target of PI3k/Akt signaling pathway. *Cell Signal* 24: 17-24, 2012.
54. **Wang HY, Ducommun S, Quan C, Xie B, Li M, Wasserman DH, Sakamoto K, Mackintosh C, and Chen S.** AS160 deficiency causes whole-body insulin resistance via composite effects in multiple tissues. *Biochem J* 449: 479-489, 2013.
55. **Xie X, Chen Y, Xue P, Fan Y, Deng Y, Peng G, Yang F, and Xu T.** RUVBL2, a novel AS160-binding protein, regulates insulin-stimulated GLUT4 translocation. *Cell Res*, 2009.
56. **Yu CF, Cresswell J, Loffler MG, and Bogan JS.** The glucose transporter 4-regulating protein TUG is essential for highly insulin-responsive glucose uptake in 3T3-L1 adipocytes. *Journal of Biological Chemistry* 282: 7710-7722, 2007.

Appendix I: Study 2

This section contains additional figures for data collected from Study 2 that were not included in Chapter IV.

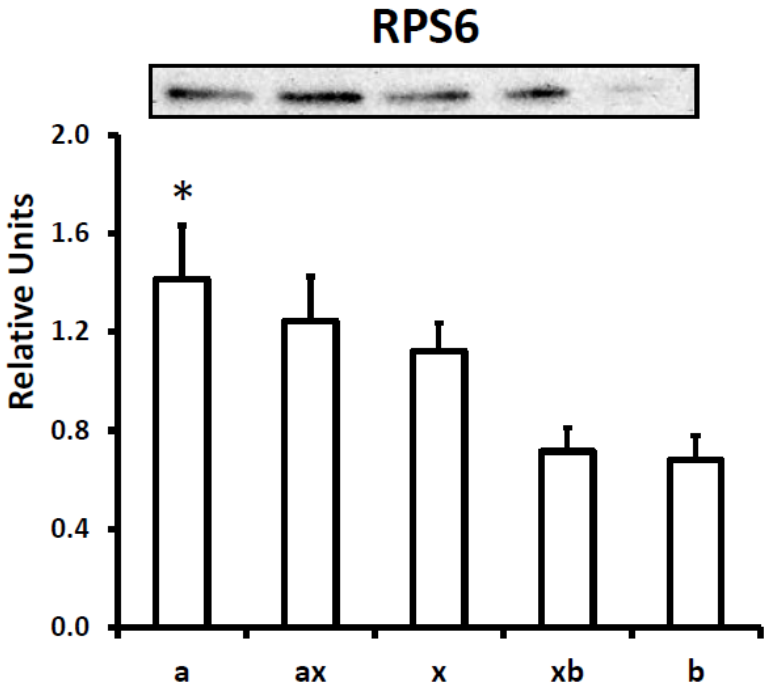

Figure A-I 4.1

Relative RPS6 protein abundance for single muscle fibers. *Indicates statistical significance for MHC-IIa vs. MHC-IIb ($P < 0.05$). Values are means ± SE; n = 15 for each fiber type.

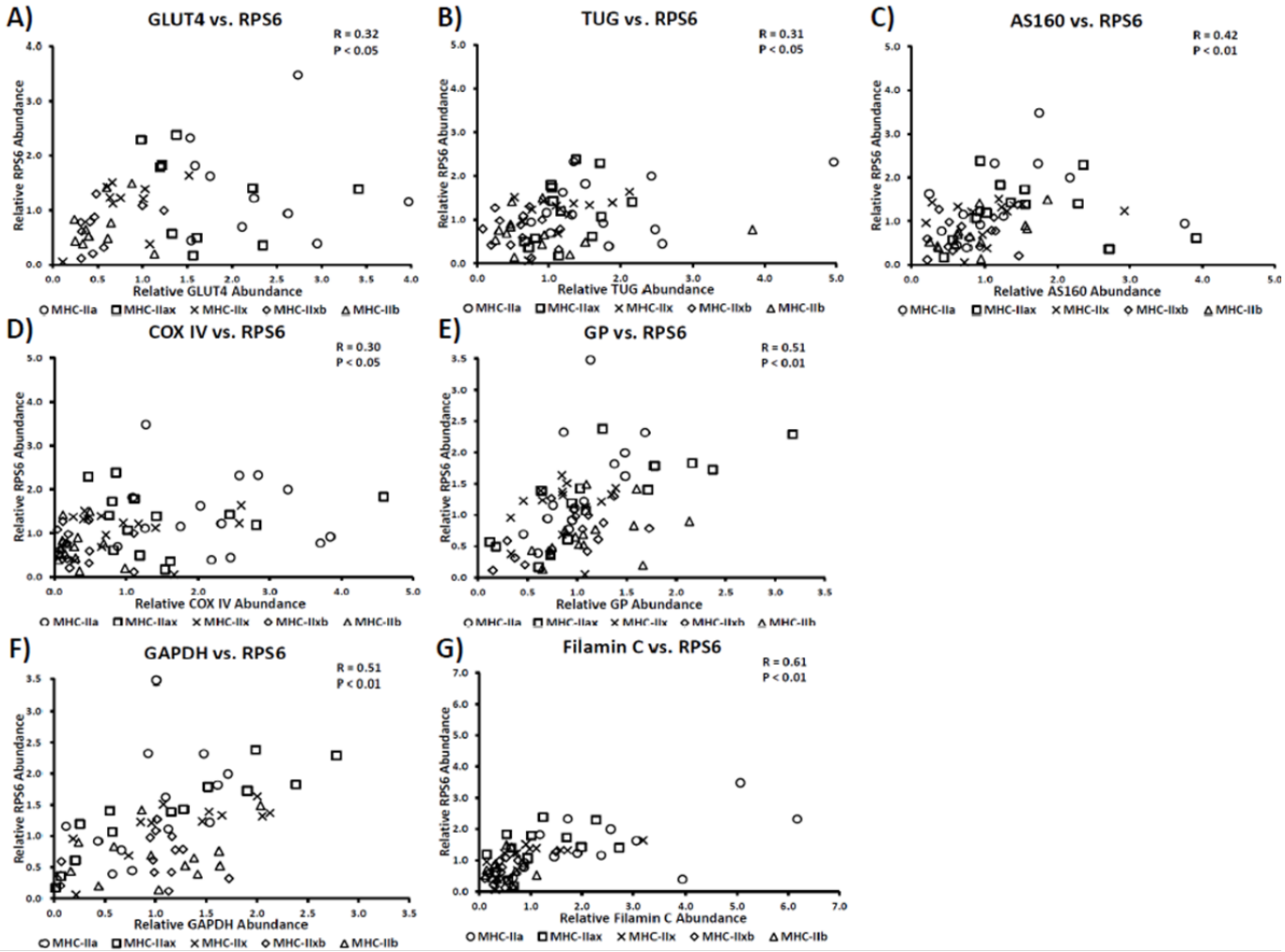

Figure A-I 4.2A-G

Significant correlations among proteins that correlated with RPS6. A: GLUT4 vs. RPS6, n = 50; B: TUG vs. RPS6, n = 65; C: AS160 vs. RPS6, n = 65; D: COX IV vs. RPS6, n = 70; E: Glycogen Phosphorylase (GP) vs. RPS6, n = 75; F: GAPDH vs. RPS6, n = 65; G: Filiman C vs. RPS6, n = 65. The symbols represent individual data.

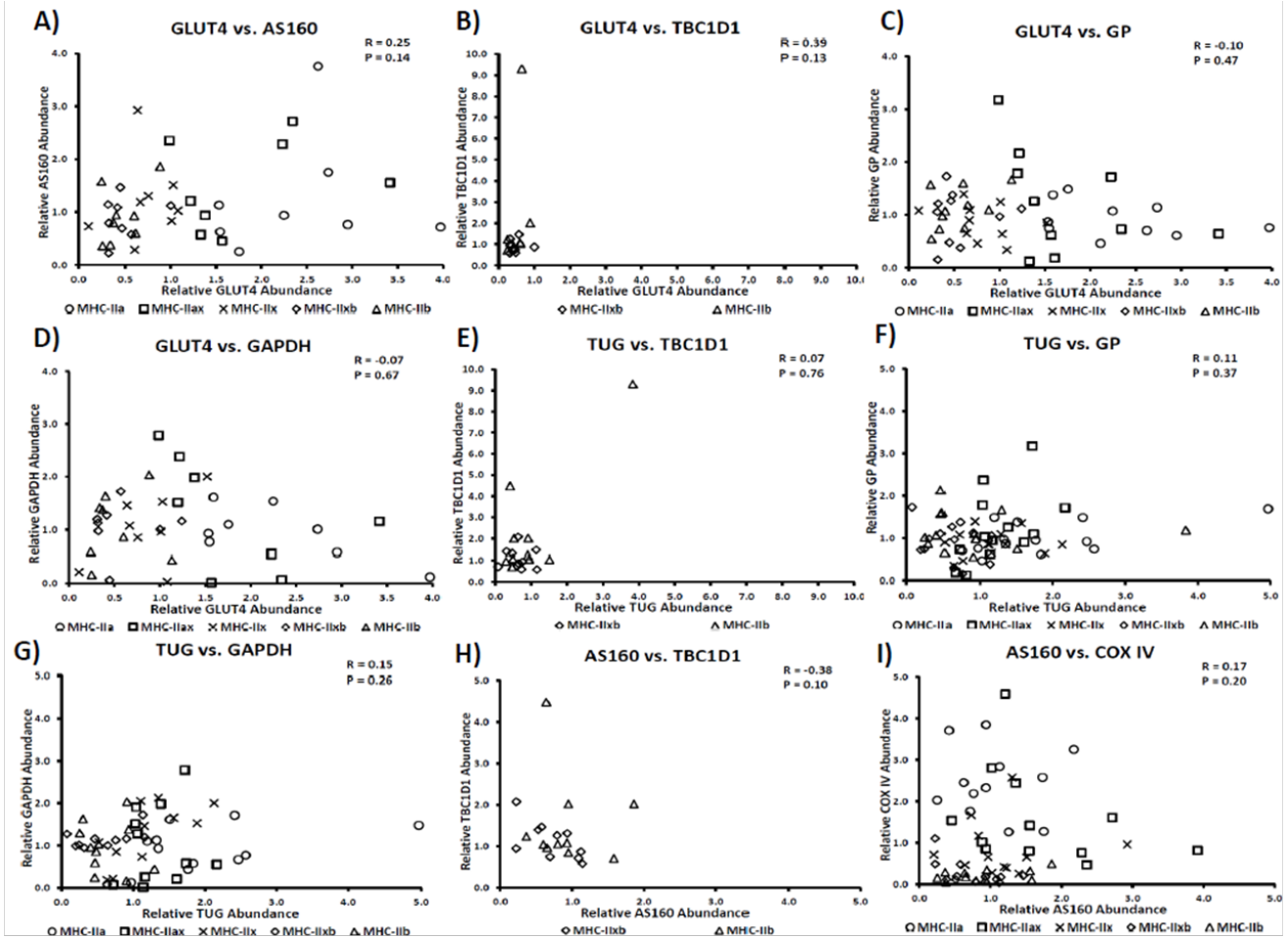

Figure A-I 4.3A-I

Correlations among proteins that did not achieve statistical significance. A: GLUT4 vs. AS160, n = 40; B: GLUT4 vs. TBC1D1, n = 16; C: GLUT4 vs. Glycogen Phosphorylase (GP), n = 50; D: GLUT4 vs. GAPDH, n = 40; E: TUG vs. TBC1D1, n =20; F: TUG vs. GP, n = 65; G: TUG vs. GAPDH, n = 55; H: AS160 vs. TBC1D1, n = 20; I: AS160 vs. COX IV, n = 60. The symbols represent individual data.

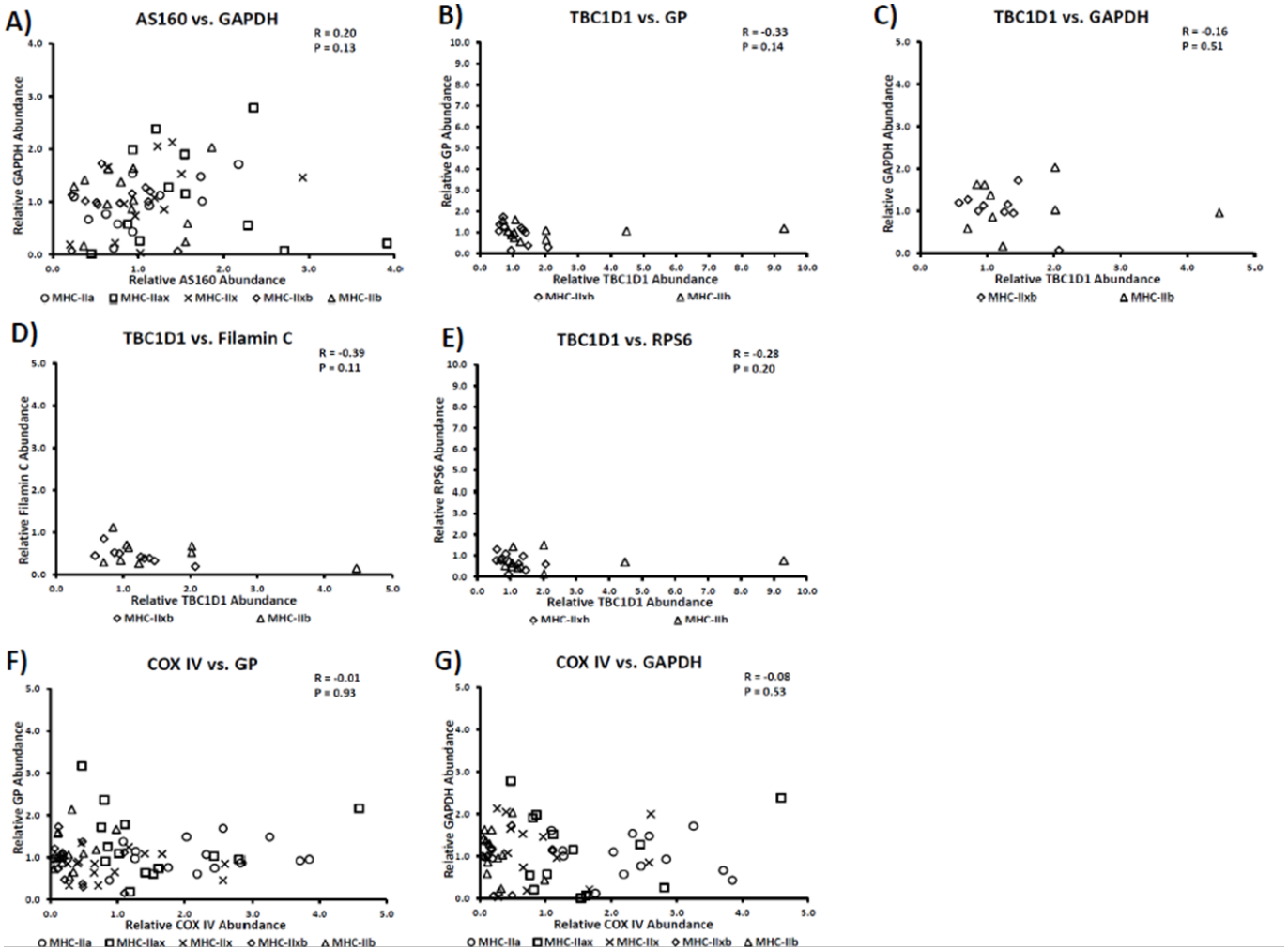

Figure A-I 4.3A-G

Correlations among proteins that did not achieve statistical significance. A: AS160 vs. GAPDH, n = 60; B: TBC1D1 vs. Glycogen Phosphorylase (GP), n = 22; C: TBC1D1 vs. GAPDH, n = 18; D: TBC1D1 vs. Filamin C, n = 18; E: TBC1D1 vs. RPS6, n = 22; F: COX IV vs. GP, n = 70; G: COX IV vs. GAPDH, n = 65 . The symbols represent individual data.

Appendix II: Study 3

This section contains additional information and figures for data collected from Study 3 that were not included in Chapter IV

Lab Diet 5001 (low fat diet; LFD)

Protein	Value		Fat	Value		Carbohydrates	Value
Arginine	1.41%		Cholesterol	200 ppm		Starch	31.90%
Cystine	0.31%		Linoleic Acid	1.22%		Glucose	0.22%
Glycine	1.21%		Linolenic Acid	0.10%		Fructose	0.30%
Histidine	0.57%		Arachidonic Acid	<0.01%		Sucrose	3.70%
Isoleucine	1.14%		Omega-3 Fatty Acids	0.19%		Lactose	2.01%
Leucine	1.83%		Total Saturated Fatty Acids	1.56%		Total	48.70%
Lysine	1.41%		Total Monosaturated Fatty Acids	1.60%			
Methionine	0.67%		Fat	10.70%			
Phenylalanine	1.04%						
Tyrosine	0.71%						
Threonine	0.91%						
Tryptophan	0.29%						
Valine	1.17%						
Serine	1.19%						
Aspartic Acid	2.81%						
Glutamic Acid	4.37%						
Alanine	1.43%						
Proline	1.49%						
Taurine	0.02%						
Protein	23.90%						

Lab Diet 5001 (low fat diet; LFD) Continued

Minerals	Value		Vitamins	Value
Ash	7%		Carotene	2.3 ppm
Calcium	0.95%		Vitamin K (as menadione)	1.3 ppm
Phosphorus	0.66%		Thiamin Hydrochloride	16 ppm
Phosphorus (non-phytate)	0.39%		Riboflavin	4.5 ppm
Potassium	1.18%		Niacin	120 ppm
Magnesium	0.21%		Pantothenic Acid	24 ppm
Sulfur	0.36%		Choline Chloride	2250 ppm
Sodium	0.40%		Folic Acid	7.1 ppm
Chlorine	0.67%		Pyridoxine	6.0 ppm
Fluorine	16 ppm		Biotin	0.30 ppm
Iron	270 ppm		B12	50 mcg/kg
Zinc	79 ppm		Vitamin A	15 IU/g
Manganese	70 ppm		Vitamin D3	4.5 IU/g
Copper	13 ppm		Vitamin E	42 IU/kg
Cobalt	0.90 ppm		Ascorbic Acid	---
Iodine	1.0 ppm			
Chromium	1.2 ppm			
Selenium	0.30 ppm			

Fiber	Value
Fiber (Crude)	5.10%
Neutral Detergent Fiber	15.60%
Acid Detergent Fiber	6.70%

Calories	Value
Protein	28.51%
Fat	13.50%
Carbohydrates	58.00%
Physiological Fuel Value	**3.36 kcal/g**

Research Diets D12492 (high fat diet; HFD)

Ingredient	g	kcal
Casein, 80 Mesh	200	800
L-Cystine	3	12
Corn Starch	0	0
Maltodextrin 10	125	500
Sucrose	68.8	275.2
Cellulose, BW 200	50	0
Soybean Oil	25	225
Lard*	245	2205
Mineral Mix, S10026	10	0
DiCalcium Phosphate	13	0
Calcium Carbonate	5.5	0
Potassium Citrate, 1 H2O	16.5	0
Vitamin Mix, V10001	10	40
Choline Bitartrate	2	0
FD&C Blue Dye #1	0.005	0
Total	773.85	4057

Macronutrient	g%	kcal%
Protein	26.2	20
Carbohydrate	26.3	20
Fat	34.9	60
Total kcal/g	**5.24**	

Typical analysis of cholesterol in lard = 0.95 mg/g
Cholesterol (mg)/4057 kcal = 232.8
Cholesterol (mg)/kg = 300.8

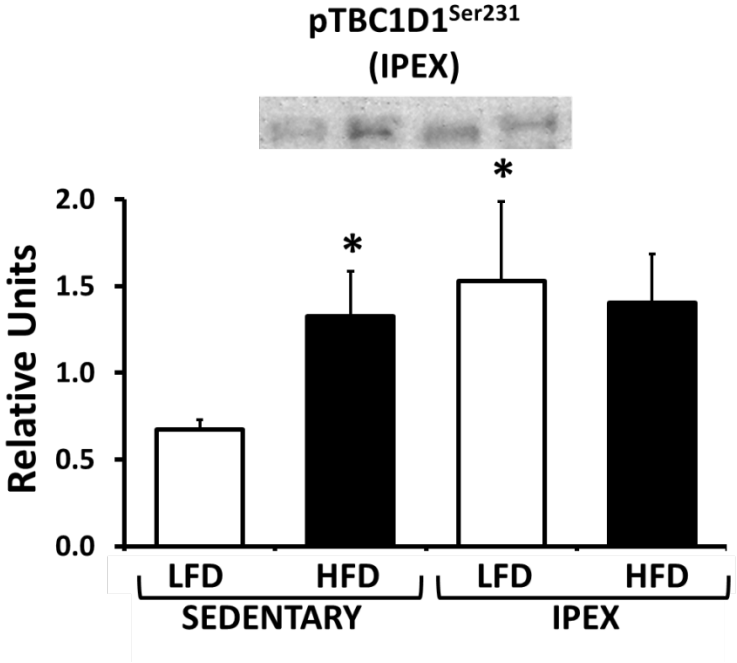

Figure A-II 5.1

IPEX measurements for TBC1D1 Ser231 phosphorylation (pTBC1D1^{Ser231}). Measurements made in epitrochlearis muscles (without insulin) from time-matched sedentary and IPEX rats. Data were analyzed by two-way ANOVA. Diet, main effect of diet; Exercise, main effect of exercise; D x E, interaction between Diet and Exercise. Tukey post-hoc analysis was performed to identify the source of significant variance. *$P < 0.05$ greater than LFD Sedentary. Values are means ± SEM; n = 4-6 per group.

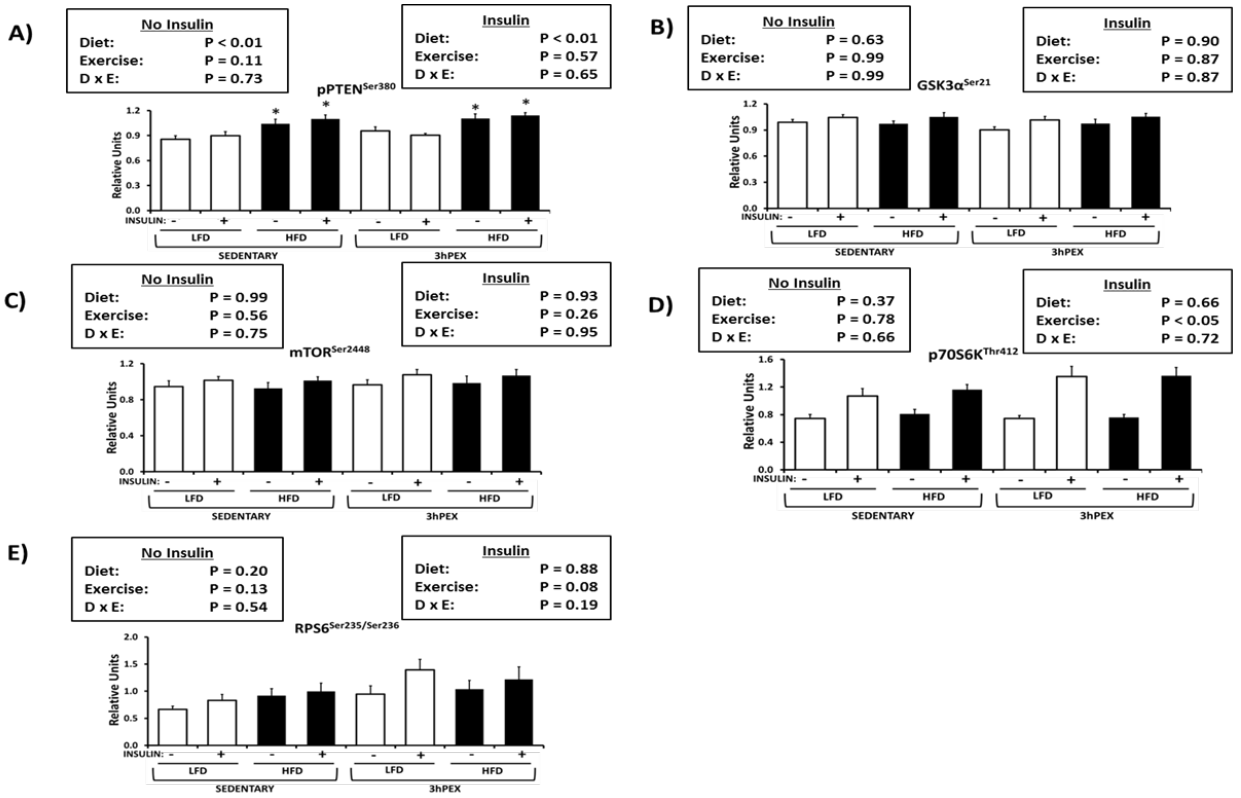

Figure A5.2

A: Phosphatase and tensin homologue deleted on chromosome ten Ser380 phosphorylation ($pPTEN^{Ser380}$) measured in paired epitrochlearis muscles 3hPEX. Data were analyzed by two-way ANOVA within each insulin level. Diet, main effect of diet; Exercise, main effect of exercise; D x E, interaction between Diet and Exercise. Post-hoc analysis was performed to identify the source of significant variance. *P < 0.05 HFD greater than LFD within same activity group and insulin treatment (e.g., HFD SED no insulin > LFD SED no insulin). Values are means ± SEM; n= 19-20. B: $GSK3\alpha^{Ser21}$ measured in paired epitrochlearis muscles 3hPEX. Data were analyzed by two-way ANOVA within each insulin level. Values are means ± SEM; n= 19-20. C: Mammalian target of rapamycin Ser2448($mTOR^{Ser2448}$) measured in paired epitrochlearis muscles 3hPEX. Data were analyzed by two-way ANOVA within each insulin level. Values are means ± SEM; n= 19-20. D: $p70S6K^{Thr412}$ measured in paired epitrochlearis muscles 3hPEX. Data were analyzed by two-way ANOVA within each insulin level. Post-hoc analysis was performed to identify the source of significant variance. Values are means ± SEM; n= 19-20. E: Ribosomal Protein S6 phosphorylated on Ser235/236 ($RPS6^{Ser235/236}$) measured in paired epitrochlearis muscles 3hPEX. Data were analyzed by two-way ANOVA within each insulin level. Values are means ± SEM; n= 19-20.

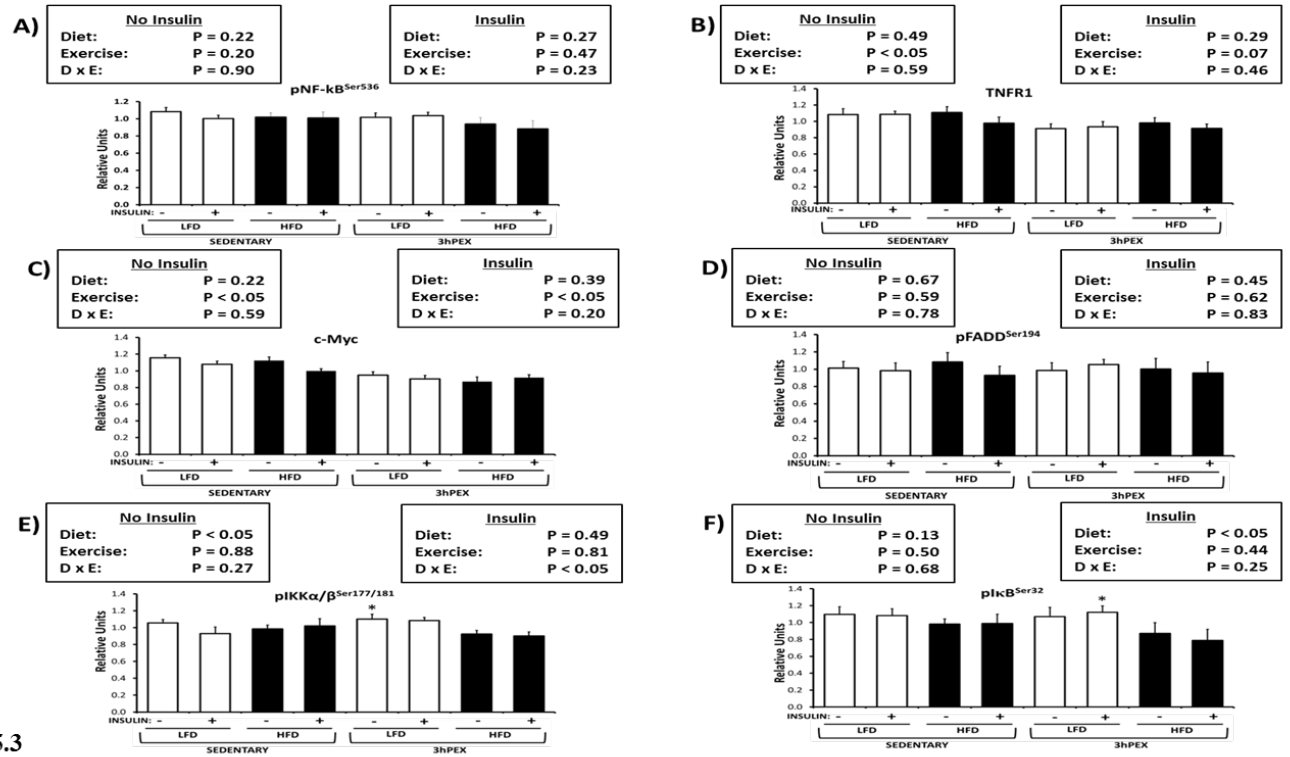

Figure A5.3

A: Nuclear factor kappa beta phosphorylated on Ser536 (pNF-κB^{Ser536}) measured in paired epitrochlearis muscles 3hPEX. Data were analyzed by two-way ANOVA within each insulin level. Diet, main effect of diet; Exercise, main effect of exercise; D x E, interaction between Diet and Exercise. Values are means ± SEM; n= 10. B: Tumor necrosis factor receptor one (TNFR1) measured in paired epitrochlearis muscles 3hPEX. Data were analyzed by two-way ANOVA within each insulin level. Post-hoc analysis was performed to identify the source of significant variance. Values are means ± SEM; n= 10. C: (c-Myc) measured in paired epitrochlearis muscles 3hPEX. Data were analyzed by two-way ANOVA within each insulin level. Post-hoc analysis was performed to identify the source of significant variance. Values are means ± SEM; n= 10. D: Fas-associated death domain phosphorylated on Ser194 (pFADD^{Ser194}) measured in paired epitrochlearis muscles 3hPEX. Data were analyzed by two-way ANOVA within each insulin level. Values are means ± SEM; n= 10. E: (pIKKα/β$^{Ser177/181}$) measured in paired epitrochlearis muscles 3hPEX. Data were analyzed by two-way ANOVA within each insulin level. Post-hoc analysis was performed to identify the source of significant variance. *P < 0.05 LFD greater than HFD with no insulin in exercise group. Values are means ± SEM; n= 10. F: (pIκB^{Ser32}) measured in paired epitrochlearis muscles 3hPEX. Data were analyzed by two-way ANOVA within each insulin level. Tukey post-hoc analysis was performed to identify the source of significant variance. *P < 0.05 LFD greater than HFD with insulin in exercise group. Values are means ± SEM; n= 10.

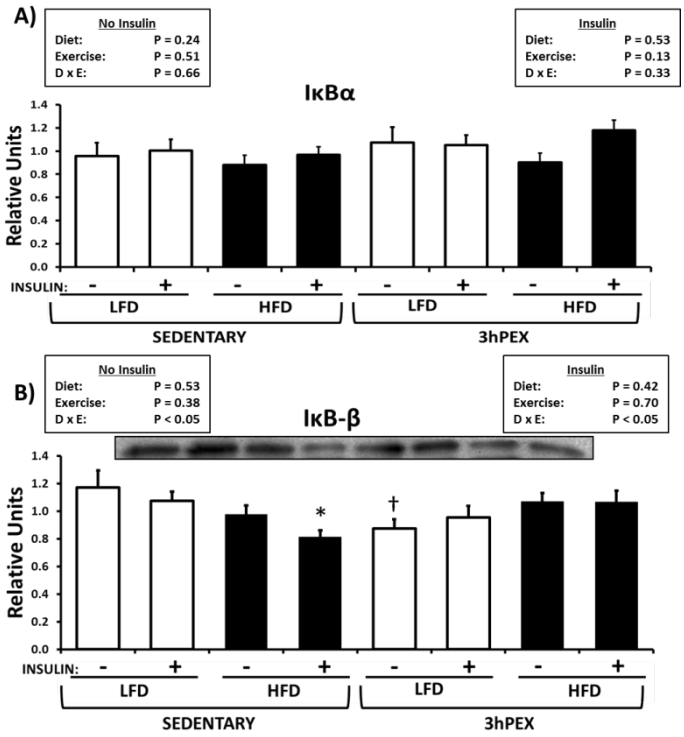

Figure A-II 5.4

A: IκB-α measured in paired epitrochlearis muscles 3hPEX. Data were analyzed by two-way ANOVA within each insulin level. Diet, main effect of diet; Exercise, main effect of exercise; D x E, interaction between Diet and Exercise. Values are means ± SEM; n= 11. B: IκB-β measured in paired epitrochlearis muscles 3hPEX. Data were analyzed by two-way ANOVA within each insulin level. Tukey post-hoc analysis was performed to identify the source of significant variance. *P < 0.05 HFD Sedentary is less than LFD Sedentary and HFD 3hPEX. †P < 0.05 LFD 3hPEX is less than LFD Sedentary are Values are means ± SEM; n= 19-20.

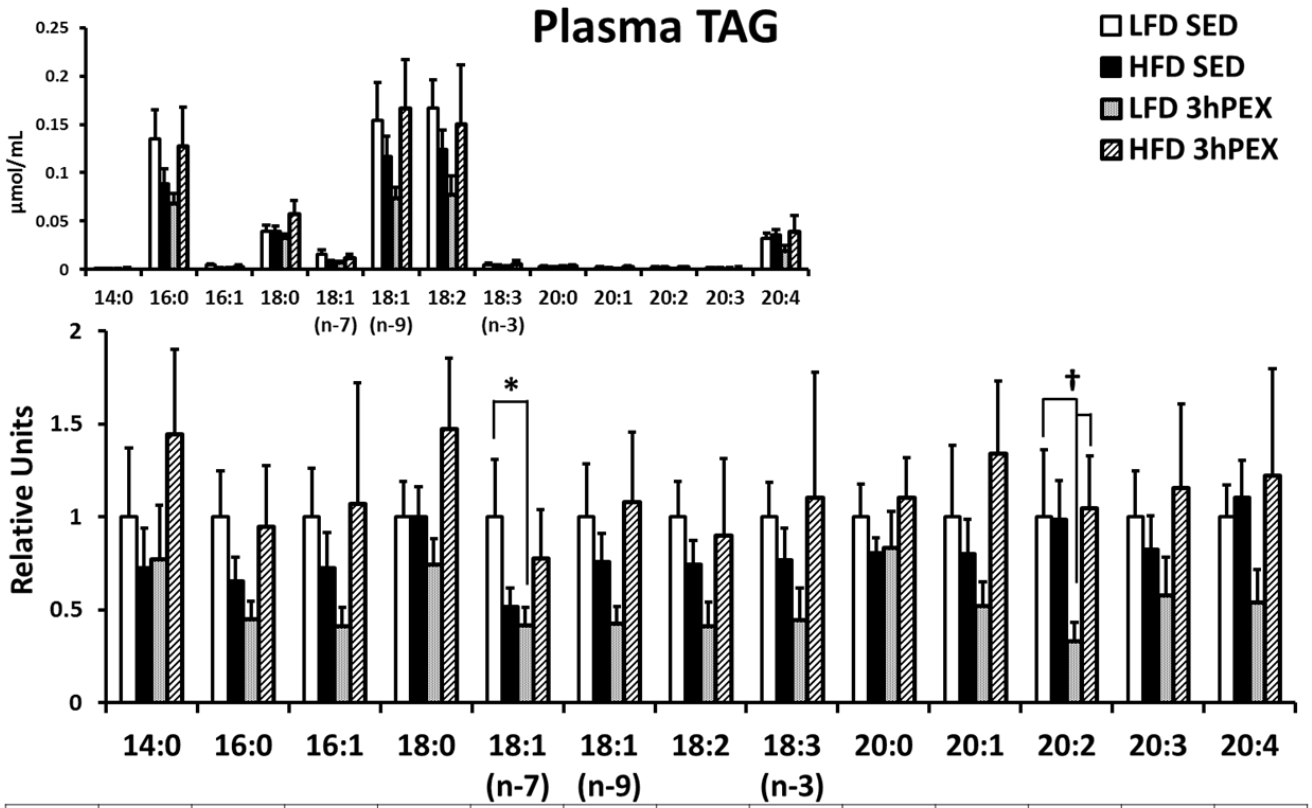

ANOVA	14:0	16:0	16:1	18:0	18:1 (n-7)	18:1 (n-9)	18:2	18:3 (n-3)	20:0	20:1	20:2	20:3	20:4
Diet	0.87	0.97	0.55	0.22	0.57	0.40	0.87	0.69	0.85	0.28	0.04*	0.72	0.25
Exercise	0.75	0.40	0.32	0.66	0.40	0.34	0.34	0.67	0.68	0.79	0.11	0.76	0.65
D x E	0.13	0.08	0.16	0.23	0.04*	0.07	0.07	0.17	0.45	0.07	0.14	0.28	0.41

Figure A-II 5.5

Plasma triacylglycerol (TAG) 3hPEX. Values are expressed relative to the LFD Sedentary (SED) group for each lipid species. Data were analyzed by two-way ANOVA within each insulin level. Diet, main effect of diet; Exercise, main effect of exercise; D x E, interaction between Diet and Exercise. Post-hoc analysis was performed to identify the source of significant variance. *P < 0.05, LFD Sedentary versus LFD 3hPEX. †P <0.05, LFD Sedentary and HFD 3hPEX versus LFD 3hPEX. The Inset in upper left shows the absolute concentrations (µmol/mL) for the TAG species. Values are means ± SEM; n = 5-9 per group.

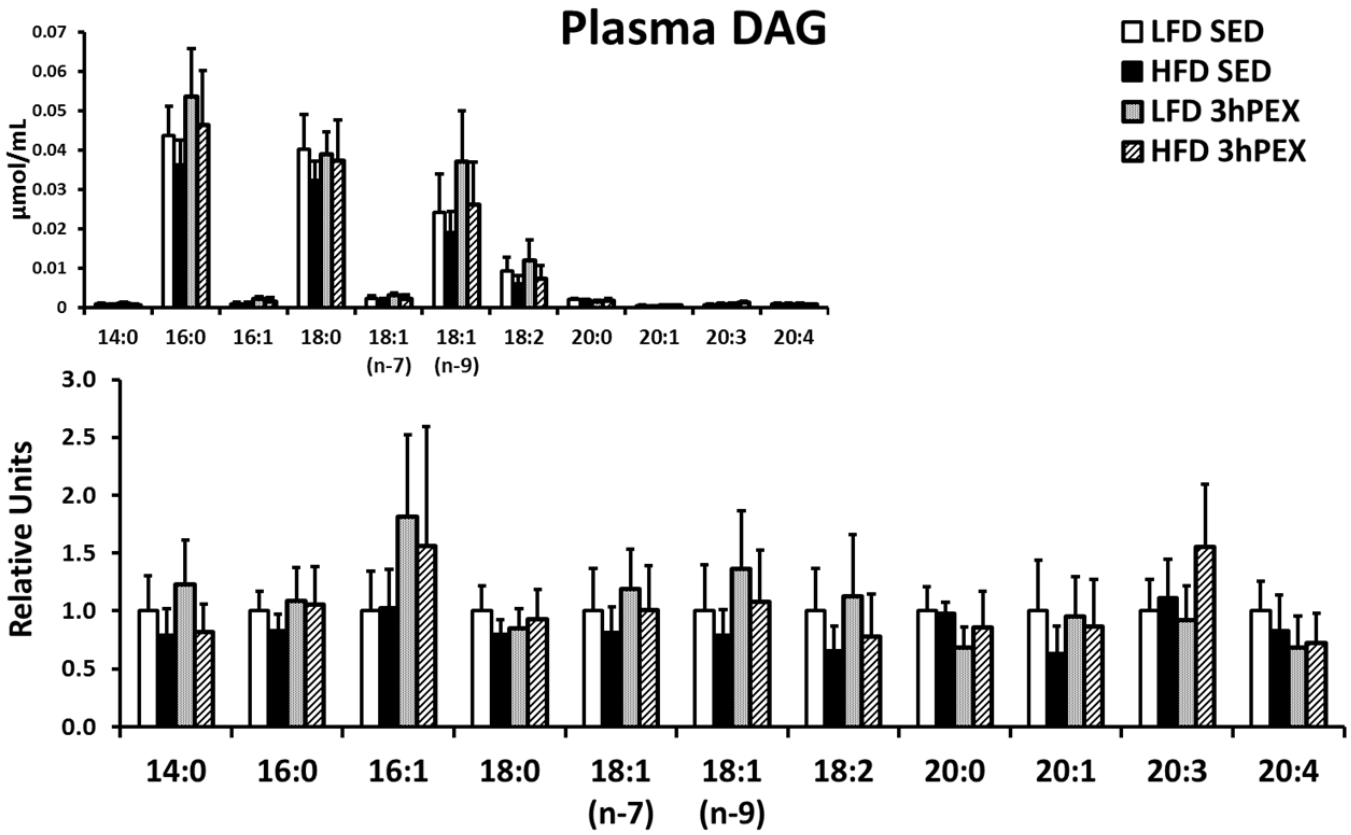

ANOVA	14:0	16:0	16:1	18:0	18:1 (n-7)	18:1 (n-9)	18:2	20:0	20:1	20:3	20:4
Diet	0.04*	0.49	0.97	0.55	0.53	0.06	0.32	0.99	0.57	0.31	0.51
Exercise	0.30	0.34	0.03*	0.81	0.68	0.42	0.99	0.09	0.95	0.62	0.32
D x E	0.79	0.99	0.81	0.68	0.89	0.58	0.99	0.68	0.39	0.36	0.78

Figure A-II 5.6

Plasma diacylglycerol (DAG) 3hPEX. Values are expressed relative to the LFD Sedentary (SED) group for each lipid species. Data were analyzed by two-way ANOVA within each insulin level. Diet, main effect of diet; Exercise, main effect of exercise; D x E, interaction between Diet and Exercise. Tukey post-hoc analysis was performed to identify the source of significant variance. Inset in upper left shows the absolute concentrations (µmol/mL) for the DAG species. Values are means ± SEM, n = 5-9 per group.

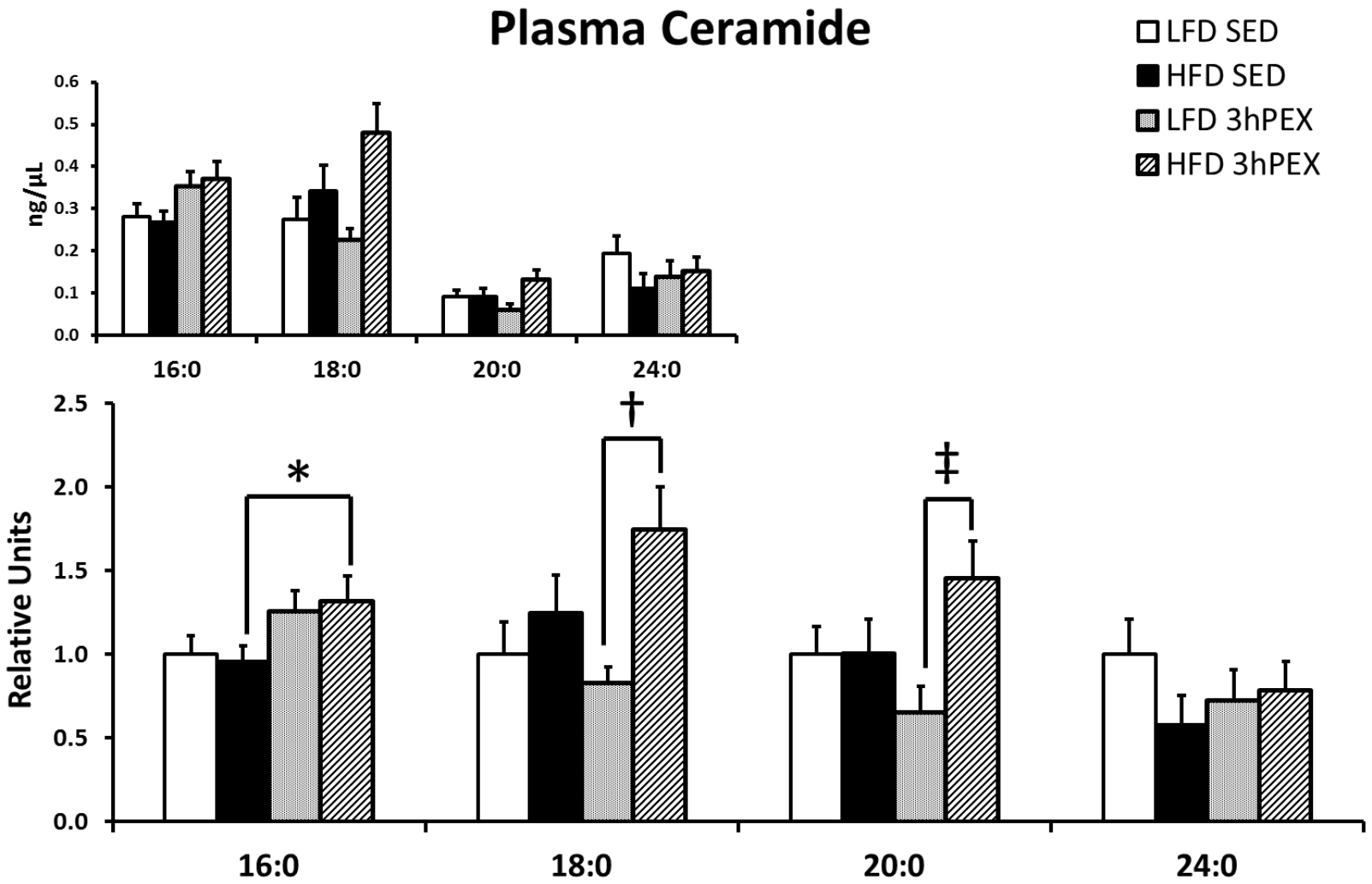

ANOVA	16:0	18:0	20:0	24:0
Diet	0.97	0.01*	0.04*	0.34
Exercise	0.02*	0.44	0.79	0.86
D x E	0.78	0.11	0.04*	0.20